Developing Specifications for Using Recycled Asphalt Pavement as Base, Subbase or General Fill Materials

Final Report

Florida Tech

www.fit.edu • (321) 674-7555

March 1, 2001

Paul J. Cosentino, Ph.D., P.E., Principal Investigator
Edward H. Kalajian, Ph.D., P.E., Co-Principal Investigator

Submitted to:
Robert K. Ho, Ph.D., P.E.
State Soils Materials Engineer,
State Materials Office
Florida Department of Transportation
2006 N.E. Waldo Rd., Gainesville, Florida 32309-8901
(352) 337-3206 • SunCom: 642-1206 • Fax: (352) 334-1648
Contract Number BB-892

Executive Summary

Developing Specifications for Using Recycled Asphalt Pavement as Base, Subbase, or General Fill Materials

by

Paul J. Cosentino, Ph.D., P.E.
Edward H. Kalajian Ph.D., P.E.

Reclaimed Asphalt Pavement (RAP) stockpiles in Florida have been growing due to rehabilitation of the state's roadways. At this time the major use for RAP is as an aggregate in Hot Mix Asphalt (HMA) production. The application of RAP as a Florida Department of Transportation (FDOT) approved base course, subbase, and subgrade has been hindered due to low reported laboratory LBR tests.

A thorough laboratory and field investigation was conducted to evaluate the basic engineering behavior of RAP and to analyze its field performance. The lab studies focused on evaluating the Limerock Bearing Ratio performance of RAP and developing a database of the elementary geotechnical strength parameters such as friction, cohesion and elastic modulus.

An initial lab study enabled LBR characteristics to be evaluated using several compaction techniques. RAP for this portion of the work was taken from a stockpile of material that was not processed after milling from the pavement surface. Proctor energies were used to determine the moisture-density

characteristics and LBR behavior. Standard, modified and double modified Proctor energies were used on RAP stored at 35 ^{o}F, 70 ^{o}F and 120 ^{o}F.

RAP was classified as a well-graded sand or gravel, with a top size of 1.5 inch. Measured asphalt content, specific gravity and absorption values were 6.73±0.14 %, 2.27 and 2.57±0.31 %. The moisture-density behavior did not follow traditional Proctor behavior. The resulting curves did not display a well-defined peak. Samples tested at 70 ^{o}F had densities from 97.2 to 118.5 pcf and LBR values from 8 to 81. Samples compacted at 120 ^{o}F rendered higher LBR values than those compacted at 35 ^{o}F and 70 ^{o}F.

A second lab study again involved LBR testing, however, the compaction processes were varied to include vibratory, static and a modified Marshall processes. Although, the vibratory compaction did not increase the LBR values, the static and modified Marshall compaction processes did. The modified Marchall resulted in LBR's of twice that of the Proctor methods, while static methods yielded LBR's over 100 under very high pressures.

During a third lab study, the basic geotechnical properties of friction, cohesion and elastic modulus were evaluated for RAP subjected to two post-milling processes. The equipment used in these processes was the more commonly used hammermill crusher and the specialty tubgrinder. The hammermill and tubgrinder RAP were characterized based on gradation, asphalt content, and triaxial shear properties. A total of 60 samples were compacted and then stored for three time durations (10, 20, and 30 days), and at three temperatures, 75°F, 100°F, and 125°F (23.9°C, 37.8°C and 51.6°C). Testing was also conducted on material stored for zero days after compaction. Triaxial shear tests were performed on RAP samples compacted using modified Proctor energy at a target moisture content of 6%.

Hammermill RAP classified as a well-graded sand and tubgrinder RAP classified as poorly-graded sand. Tubgrinder RAP contained more coarse sand sized material than the hammermill RAP. Forty percent of both materials were contained within the grain size range specified by the ASTM "Standard Specification for Graded Aggregate Material for Bases or Subbases for Highways or Airports." The measured asphalt content of the hammermill and tubgrinder RAP was 5.80±0.13% and 5.47±0.04%, respectively. The average dry densities for the hammermill and tubgrinder RAP were 117.7 pcf (18.3 kN/m^3) and 121.1 pcf (18.9 KN/m^3) respectively. Tubgrinder RAP was denser, withstood higher stresses and was stiffer than hammermill RAP.

Increasing storage temperature from 75°F (23.9°C) to 100°F (37.8°C) increases the maximum principal stress at failure, stiffness, and the cohesion. Increasing the temperature further to 125°F (51.7°C) did not increase the maximum principal stress at failure, stiffness or cohesion. The triaxial properties of RAP are not affected by the duration of storage time. The angle of friction ranged from 37 and 40 degrees, and did not vary with post milling process, storage temperature or storage time.

The engineering properties of RAP proved to be desirable. They provide a sound basis to establish RAP as an accepted structural fill, or as a base or subbase course in roadway construction.

A field site was constructed in layers 12-, 24- and 36-inches thick of post-milled RAP and a control section of cemented coquina. RAP was compacted with a vibratory roller at two compaction energies, one matching the energy applied to the cemented coquina and a second to evaluate the higher compactive efforts. The site was constructed over a compacted silty sand.

The purpose of the field work was to: 1) subject the RAP to environmental conditions that could not be replicated in a laboratory, 2) study the strength-deformations characteristics of RAP exposed to the environment, 3) recommend alternatives to Limerock Bearing Ratio (LBR) testing and 4) to aid in the development of FDOT Specifications for using this material as a base, subbase or general highway fill.

Nuclear Density tests, LBR tests, Cone Penetrometer tests (CPT), Automatic Dynamic Cone Penetrometer (ADCP) tests, and Falling Weight Deflectometer (FWD) tests were performed at bi-monthly intervals for one year. Thermocouple and Vemco temperature probes were used at varying times during this investigation to record daily high temperatures.

As was evident in the laboratory studies, the field strength of RAP was highly dependent on temperature. It increased and decreased during the cooler spring and warmer summer testing cycles respectively.

Initial LBR results for RAP averaged 16 but increased to an average of 51 within two months. RAP LBR values of 40 were attained within two months and sustained in 82% of subsequent tests. RAP LBR values exceeding 100 were recorded during the cooler months but could not be sustained during the warmer months.

There is a linear correlation between the Impulse Stiffness Modulus (ISM) determined from the FWD, the predicted modulus of elasticity, E_s, from the CPT point resistance and LBR values. The ISM-LBR correlation is the strongest of the three, although all three correlations were considered strong. FWD testing proved to be very reliable, quick, and accurate. During this study, the FWD recorded nine times more data than the LBR in one-third of the time.

Based on the results of this study, RAP has potential to be used as a subbase or subgrade, but did not display evidence that it could be used as an FDOT-approved base course.

Acknowledgements

This work was completed under FDOT contract number BB – 892. The authors would like to acknowledge the following people for their invaluable guidance and help in the completion of this study.

Dr. Robert K.H. Ho and Dr. David Horhota of the Florida Department of Transportation, Thank you for your support throughout the entire project.

Ron Lewis, Rick Venick, Tim Blanton, Todd Britton, and David Benefield (FDOT, State Materials Office) – Thank you for your sharing your expertise and guidance in the testing of the field site.

Pam Jones, Vice President of APAC Florida Inc., MacAsphalt Division – Thank you for providing equipment, labor, material and your expertise in constructing the field site. With out your help, this study would have been considerably more difficult.

The following Florida Tech students, specifically Nathan Tarbox, Bruce Doig, Anthony Call, Dacks Rodriquez, Wilbur Mathurin, Stephen Medeiros, Jose Andrade, and Pisake Larpisal.

1.Introduction

1.1 Background

1.1.1 Definition and History

Pavement reclamation has become a preferred method for pavement rehabilitation in Florida. Rather than remove the road in its entirety, critical areas are removed to a specified depth. Benefits of pavement reclamation include savings in repair costs and maintenance and increases in overall lifespan of the road.

Pavement reclamation can be divided into two methods; milling and full depth removal. Milling entails grinding and removing the top few inches of the asphalt. Full depth removal requires the extraction of the asphalt and base course. A by-product of both of these processes is Reclaimed Asphalt Pavement (RAP).

One of the primary uses of RAP is as an aggregate in Hot Mix Asphalt (HMA) production. According to Federal Highway Administration estimates, 33% of all RAP is re-used in HMA production. In Florida, approximately 75% of all RAP is used in HMA production (Road and Bridges 1999). This, however, was before Florida adopted the SUPERPAVE (Superior Performing Asphalt Pavements) design mix in 1998. Prior to SUPERPAVE implementation, HMA mixtures included an average of 50% RAP. After SUPERPAVE was implemented, the percent mixture of RAP decreased to 35% (TR News 1996).

Florida Department of Transportation (FDOT) has instituted many programs over the years to use available and appropriate recycled materials. Recycling RAP into the Hot Mix Asphalt (HMA) mix became popular in the 1970's when the Arab oil embargo was in effect and when milling machinery

technology became advanced. At that time there were 75 projects using RAP in hot, cold and in-place mixes sponsored by the federal government (Ciesielski, 1995). From 1979 to 1994, 22 million metric tons of RAP were recycled into FDOT projects, saving $188 million in materials and preventing RAP surpluses from developing around the state (Smith, 1996).

In the mid 1980's, nearly every state had developed specifications for the use of RAP as a partial aggregate substitute in HMA. Allowable percentages of RAP in HMA depend on aggregate size, source, and type of mixing plant being used (Ciesielski, 1995). The Florida legislature acknowledged the magnitude of the waste disposal problem in 1988 Senate Bill 1192 (codified as section 336.044 of the Florida Statues) and required the FDOT to investigate uses for waste materials in construction and maintenance projects (Smith, 1996).

1.1.2 Current use of RAP

It is difficult to determine exact numbers for recycling of asphalt pavement materials because the last survey was conducted in the mid nineties. Jason Harrington, Federal Highway Administration (FHWA) pavement engineer, estimates that in the United States there are 90 million tons of RAP being milled every year and between 80 to 90% of this is being reused in roadways. This means that approximately 18 million tons of RAP are not being used in HMA mixes. This is enough material to build an 8-inch base under a four-lane highway with 12-foot lanes for over 2000 miles. Mr. Harrington stated that any material not reused into the HMA mix is not being dumped but is being used as aggregate in unpaved parking lots and rural county roads. There are 36 states performing research on RAP and although RAP's predominant application is recycling into asphalt paving mixes, ten states are studying RAP for use in highway base and subbase applications (Collins, & Ciesielski, 1994).

1.1.3 Advantages

The advantages of using RAP in pavement reclamation include the following:

- Economics – Savings in the costs of material, energy, disposal, and in the general construction procedure.
- Disposal Capacity – Increased usage rates of RAP decrease the need to stockpile the material.
- Availability for Construction – Reconstruction of a road or highway is very slow and tedious. Delivery of new material to the site adds to traffic and safety concerns. Natural aggregate is not always available close to the project site. Also, sensitive subgrades are exposed to inclement weather for an indefinite period of time (Holmes, 1991). RAP can be obtained at the site, processed and used on the same site.
- Environmental Concerns – Quarrying of new natural resources continues to erode the landscape. The amount of base and subbase material in respective quarries and borrow pits is of a finite supply, which directly affects the environment. Recycling conserves these natural resources (Papp, Maher, & Bennert, 1998).
- Pavement Thickness – Milling pavements, rather than just overlaying existing pavement, maintains overpass clearances to satisfy clearances under existing structures. Also, increased thickness in pavements causes a change in site topography, creating problems with the water drainage of the pavements (Prokopy, 1995).

1.2 Base and Subbase Applications

1.2.1 Definition

The base course layer is below the surface layer of the pavement. It is usually composed of crushed stone or other stabilized materials. The base is critical to the pavement system as it is the primary load carrying mechanism. Base failures are not easily repairable, very costly and usually result in the pavement having to be completely rebuilt (Huang, 1993). Below the base is the subbase course layer. It usually consists of a material, which may have a different grain size distribution than that of the base. This minimizes cost because less expensive materials can be used to construct the subbase over the subgrade (Huang, 1993).

1.2.2 Conventional Aggregates used in Florida

The conventional aggregates used in Florida as base or subbase material are limerock, sand-clay, shell, and rock material. These materials have to meet the specifications outlined in sections 911, 912, 913 and 913A respectively of the *Florida Department of Transportation Standard Specifications for Road and Bridge Construction, 1999*. The specifications include requirements on liquid and plastic limits, gradation and size, and Limerock Bearing Ratio (FDOT, 1999). These specifications require that the base materials have a Limerock Bearing Ratio (LBR) greater than 100, and that the subbase materials have an LBR greater than 40.

Two of the most commonly used aggregates in Florida roadway base construction are cemented coquina and limerock. These materials have good strength-deformation characteristics, but poor drainage capabilities for highways. Ho (2000) reported permeability values of 3.05×10^{-7} ft/sec (1×10^{-5} cm/sec). The slowest hydraulic conductivity that a material may have and still provide good drainage is in the range of 3.05×10^{-6} ft/sec (1×10^{-4}cm/sec). In highway design,

the asphalt serves as an impermeable surface for the limerock and keeps the water out of the limerock to prevent weakening of the base due to the presence of water (Ho, personal communication, 2000).

1.2.3 Re-using RAP as a Base

The primary use for RAP, because of its desirable gradation, is as a percentage in the HMA mix. However, not all the RAP is being recycled into HMA mixtures. In 1996, the Strategic Highway Research Program implemented the Superior Performing Asphalt Pavements (SUPERPAVE) design system. It was implemented to increase the quality of paved roadways. Marshall mix design used previously allowed for up to 40% use of RAP in HMA. The constraints implemented by SUPERPAVE were more rigorous reducing the amount of RAP used in new mixes to 10 – 15% (Jester, 1997).

In the pavement industry, especially in Florida, there is a current need to use RAP in higher quantities. Florida is the fourth largest state by population and is growing at a rate that strongly fuels the construction market in the residential, commercial, and industrial sectors. Hectic expansion in infrastructure to support this development causes a backlog in transportation construction. There are insufficient practical uses of RAP and situations are needed where the volume of RAP used is high, such as in highway base and subbase applications (McCaulley, et al, 1990). Many of the advantages mentioned previously (economics, disposal capacity, availability for construction and environmental concerns) are also applicable to the reuse of RAP for other construction uses.

RAP is not widely accepted for base or subbase usage because there is limited laboratory and field performance data. The load-deformation characteristics of the material are almost unknown. Many DOT offices around the nation believe there is potential for using RAP as a pavement base material (Garg & Thompson, 1996). However, results of previous studies performed on RAP indicate it does not meet FDOT Limerock Bearing Ratio (LBR) base course requirements of 100. This material does not experience a typical moisture-density

relationship (Montemayor, 1998). With normal ASTM specified energy levels for compaction, RAP may not reach the specified LBR value of 100 for a base course (Sayed, 1993).

1.2.4 Engineering Characteristics

Research on the conventional soil properties of RAP, specifically shear and deformation characteristics, has not been reported (Garg and Thompson, 1996). The basic understanding of soil properties is essential before beginning to find the solution to other engineering problems (Bishop and Henkel, 1964). Cohesion (c), angle of friction (ϕ) and elastic properties need to be determined. The frictional forces developed during slip conditions at the contacts between soil particles, are essentially responsible for the shear strength of soils and granular materials. Triaxial testing is still among the most reliable tests in existence for testing the shear strength parameters (Holtz and Kovacks, 1981).

Practical experience has shown that RAP stored in stockpiles in Florida at ambient temperatures hardens over time. A 12-inch (30.5 cm) crust forms over the outside of the stockpile. Speculation from asphalt plant operators is that the crust forms due to a solar or thermal effect that causes RAP to gain enough heat to "melt" back together (Roads and Bridges, 1999). This author has observed a front-end loader having difficulty trying to excavate material from a RAP stockpile. Its blades left marks on the stockpile due to the scraping of the very hard RAP. Also, RAP that hardened was observed on an unpaved parking lot in an application similar to that of a base course. The RAP appeared to gain stability with time, attributed to high temperature exposure over time. This behavior has not been documented in the literature, however it appears to affect the field performance of RAP. Variables that may affect the engineering characteristics are the grain size distribution, temperature, storage time, and compaction method.

1.3 Objective

1.3.1 Laboratory Objectives

By determining the engineering properties of RAP and the effect that storage time at elevated temperatures has on these properties; the potential for use of RAP as structural fill or as highway construction material may increase.
The objectives of the laboratory study were:

- to determine the strength and deformation properties of RAP,
- to evaluate the effects of post milling on these properties,
- to evaluate the effect of storage time at elevated temperatures on these properties.

1.3.2 Field Objectives

The objectives of the field study were accomplished by the construction and observation of a field site comprised partially of RAP and partially of cemented coquina (to be used as a control section). A litany of tests was performed at two-month intervals for a total of 12 months. The test results for RAP were compared to the test results obtained for the cemented coquina and also with time and air temperatures. The objectives of the field study were:

- to analyze the performance of RAP in the field over a period of 12 months,
- to recommend which tests most accurately reflect the feasibility of RAP as a subgrade, subbase and base course based on ease of performance and reliability of results and
- to develop a set of developmental specifications for using RAP as a base, subbase or subgrade.

2. Literature Search and Theory

The primary use of RAP is in recycling it as aggregate into hot-mix asphalt (HMA) pavement. In Florida, before SUPERPAVE was implemented in 1996, 40% of the RAP could be used in the mixtures. Since SUPERPAVE was implemented these levels have dropped significantly to between 10 and 15% creating a surplus of RAP material available for other road construction applications (Jones, personal communication, 1999).

2.1 Recycled Asphalt Pavement (RAP) in Hot Mix Asphalt (HMA)

Four types of recycling methods are discussed: hot recycling, hot in-place recycling, cold in-place recycling, and full depth reclamation. The first three are used to replace the paving materials while full depth reclamation is used to construct an improved base course.

2.1.1 Hot Mix Recycling

In this process, RAP is mixed with new materials and with a recycling agent to produce HMA mixtures. Recycling additives improve the mechanical properties of the recycled mixture. They include emulsified asphalts and emulsified versions of commercial recycling agents. In some cases small

percentages of Portland cement concrete are added to help stabilize the recycled mix (National Center for Asphalt Technology, 1998).

The RAP is obtained from milling and crushing operations. The placement and compaction of the mix follow the same procedures used for regular HMA. The advantages of hot mix recycling as compared to other recycling methods include equal or better performance than conventional HMA and the correction of surface defects such as deformation or cracking (National Center for Asphalt Technology, 1998).

2.1.2 Hot In-Place Recycling (HIR)

In this process the existing pavement is heated and softened and then milled to a specified depth. The millings are then mixed with new HMA mixtures and a recycling agent. Lastly, the mix is compacted. The depth of this method varies from ¾ to 2 inches (1.9 to 5 cm). The advantage of this method is that it eliminates surface cracks and ruts, corrects shoves and bumps, revitalizes old asphalt, and reduces traffic interruption and hauling costs (National Center for Asphalt Technology, 1998).

2.1.3 Cold In-Place Recycling (CIR)

The pavement in this process is milled without the use of heat. The procedure starts with pulverizing the existing road, and then continues by sizing the RAP, applying the recycling agent, placing and finally compacting. It is common to use a recycling train in this procedure. The recycling train includes pulverizing, screening, crushing, and the mixing units. The depth of this treatment

is typically between 3 to 4 inches (7.6 to 10.2 cm). Advantages of this method are significant structural treatment of most pavement distresses, improved ride quality, minimum hauling, reduced air pollution, and the capability of widening the pavement (National Center for Asphalt Technology, 1998).

2.1.4 Full Depth Reclamation (FDR)

Full depth reclamation is when the entire asphalt pavement layer and a predetermined amount of the underlying base is treated to produce a stabilized base course. In order to obtain an improved base, different types of additives are added such as: asphalt emulsions, and chemical agents like calcium chloride, Portland cement, fly ash, or lime. The steps in this procedure are pulverization, introduction of additive, compaction and application of a new surface course. In the case where the milled material might not be enough to provide the required depth of the new base, new material will be imported and included in the mix. This method of recycling is usually performed on a range of depths varying from 4 to 12 inches (10.2 to 30.5 cm) (National Center for Asphalt Technology, 1998).

Full depth reclamation is used primarily for solving base course problems such as the lack of structural capacity. The procedure requires curing and will result in a new base. Construction specifications for this procedure are lacking and care must be taken to avoid unwanted material such as vegetation and large clumps of RAP from appearing in the mix The advantages of full depth reclamation are most pavement distresses are treated, hauling costs and disposal of materials are minimized, and structural improvements to the pavements are made, resulting in improved ride quality (National Center for Asphalt Technology, 1998).

2.2 Processing and Storing RAP

In the United States, there are various different milling processes used. The hammermill crusher and the tubgrinder crusher are used in Florida. The hammermill RAP is most commonly used in Hot Mix Asphalt (HMA) mixtures while tubgrinder RAP is not as common and is typically used as soil fill (P. Jones, personal communication, 1999).

2.2.1 Processing RAP

Some pavement engineers have put strict specifications on the use of RAP. They believe that the material is highly variable and thus cannot be adequately controlled during processing (Roads and Bridges, 1999). However, the Federal Highway Administration (FHWA) reports that properly crushed and sized RAP may not have any more variability than hot-mix asphalt (HMA) production. As with any other material, the final product is only as good as the sampling and property analysis procedures (Roads and Bridges, 1999).

RAP must be crushed before being used in pavements. Several types of crushers and configurations are available for use. The first two sections describe the methods most commonly used in Florida, followed by other methods used in the United States.

2.2.1.1 Hammermill Impact Crushers

A hammermill impact crusher is a type of horizontal impact crusher. Horizontal impact crushers are composed of a solid rotor and solid breaking bars. A high-speed impact force is applied to the rock. The initial hit causes particles to rebound with the sides of the chamber and with other particles (Barksdale, 1991). The RAP is crushed when it impacts with the solid breaking bars and the striker plate. Smaller material is produced when higher speeds that increase the impact force are used; and when the distance between the striker plate and the breaking bar is decreased (Roads and Bridges, 1999).

Unlike typical horizontal impact crushers, the hammermill crusher's breaking bar pivots on a rotor creating a swing-hammer type action. Horizontal impact crushers have solid bar impactors. While operating, the hammermill's crusher hammers are extended due to the centrifugal force applied by the rotor (Roads and Bridges, 1999). Screens control the particle size. If a desired size is not achieved after crushing, it is re-cycled through the hammermill crusher again for secondary crushing (P. Jones, personal communication, 2000).

2.2.1.2 Tubgrinder Units

Although the tubgrinder process is not used in the entire country, it is used at the APAC-Florida, Inc. asphalt plant at 6210 North US 1 in Melbourne, Florida (Jones, Personal Communication, 1999). The tubgrinder process works by having a wall push the material to a rotating drum that contains milling spokes. This squeezes the RAP material between two solid plates. This process is very similar to the milling reduction units that are used to excavate the RAP from the road. Tubgrinder machines are not primarily used for aggregate processing. Their

primary use is for clearing land with woods and brush. The tubgrinder process causes more material of a coarse sand size to appear when grinding aggregate materials. Coarse sand is defined, by ASTM D3282 (1983), as particles of rock or soil that will pass the No. 10 – 0.079 inches (2 mm) sieve and are retained on a No. 40 – 0.017 inches (0.425 mm) sieve. Operators that have been experimenting with asphalt recycling believe that the RAP causes less wear and tear to the machine than when it is used for land clearing. This causes the maintenance costs of the machine to be lower and more economical when the machine is used to crush RAP instead of land clearing. Operators of tubgrinders are searching for alternative uses and have reported that roof shingles have been crushed effectively (Smith, 2000).

2.2.1.3 Jaw/Roll Combination Crushers

The jaw/roll combination crushers are compression-type machines that apply a compressive force to rock trapped between their crushing surfaces. The different size of the machines, crushing and chamber configurations, and speed and action make the crushers suitable for different applications. An important characteristic of these types of crushers is that the particles must pass through a fixed but adjustable opening before being discharged (Barksdale, 1991). They use re-circulating conveyors to recycle the oversized material back into the roll crusher until it is properly sized. The greatest advantage of this crusher is that it can be used for downsizing large slabs of RAP. It reduces the slabs to more manageable sizes that can be easily handled by a secondary crusher. (Roads and Bridges, 1999).

A disadvantage of both the jaw and roll crushers that does not occur in horizontal or hammermill crushers is a phenomenon known as “pancaking.” “Pancaking” occurs when RAP sticks together and agglomerates in the crusher,

forming a flat, dense mass between the crusher surfaces. This slows production because the crusher has to be stopped and the "pancaked" RAP removed to continue crushing. This phenomenon is costly, but does not affect the quality of the processed RAP (Roads and Bridges, 1999).

Field experience has shown that consistent RAP can be produced through careful crushing operations. Essentially, the asphalt-aggregate bond must be broken and large particles must be removed. Smaller crushers allow smaller quantities of RAP to be crushed, increasing consistency. Also, crushing smaller quantities of RAP allows for the material to be used more quickly and does not allow as much moisture gain (Roads and Bridges, 1999).

2.2.1.4 Milling/Grinding Reduction Units

Milling/grinding reduction units are similar to the tubgrinder machine described earlier; however, these machines' primary use is crushing RAP. These machines have milling machine-type heads installed in the discharge area of the bin so that large slabs of RAP can be deposited into the bin for size reduction. These units are not crushers and do not reduce the stone size of the RAP. Instead, the asphalt-aggregate bond is broken in a machine similar to that of a milling machine. This method is the least commonly used of all the methods described (Roads and Bridges, 1999).

2.2.2 Storing and Handling RAP

Depending on the quantity, RAP millings can be segregated into different stockpiles. RAP is typically stockpiled so that it will have the same stone

gradation, asphalt content and asphalt characteristics for the crushing and sizing procedures. Many times large quantities of RAP need stockpiling but suitable space is not available. RAP may arrive in small quantities from various sites, where it may be combined with other sources into one stockpile. The RAP is then processed by crushing it to a specified largest aggregate size termed "top size." This is done to create a consistent product from several sources. A consistent stone gradation can be achieved through blending and crushing (Roads and Bridges, 1999).

In the past, RAP was stored in low horizontal stockpiles to prevent the RAP from rearranging and compacting under its own weight in the large conical piles. Experience has revealed that this does not happen and the large conical piles are acceptable.

An aggregate stockpile usually allows water to drain. RAP has been observed to retain moisture and not drain like a conventional stockpile (Roads and Bridges, 1999). Increased moisture in the RAP raises costs by increasing fuel consumption and limiting overall production rates in HMA applications (Roads and Bridges, 1999). Covering RAP can be economical. However, in humid climates it is preferable to leave RAP uncovered because condensation will form under the tarp or plastic and add moisture to the RAP pile. The recommended storage facility would be an open-sided building, with a roof. This allows air to pass over the stockpile but prevents precipitation from falling directly on the pile. If RAP utilization is high, then the cost of this building would be justified (Roads and Bridges, 1999).

Construction machinery is not driven directly on the stockpile because it compacts the RAP, making it more costly to handle. Additionally, when front-end loaders place RAP into bins it should be done by slowly dribbling the material into

the bin. RAP is not a free-flowing material, so if the whole load is dropped into the bin (especially on hot humid days) the material may pack and not flow smoothly. Also, RAP should not be left in the bin for extended periods of time because the material will re-compact under its own weight. When the material is stuck in the bin, vibrators should not be used to solve the feed problem. Vibrators will further compact the material (Roads and Bridges, 1999).

2.3 RAP Recycling for Base and Subbase Construction

Rap has been evaluated by several states for construction of road base and subbase. The following is a summary of the most important findings in each study.

2.3.1 Lincoln Avenue RAP Project

In 1996, Garg and Thompson conducted a study to evaluate the use of reclaimed asphalt pavement as a base course. The study, referred to as the Lincoln Avenue study, was performed with the cooperation of the Illinois Department of Transportation (IDOT), University of Illinois and the City of Urbana. The study included both laboratory and field work.

The RAP used in this site was obtained from the Mid America Recycling Center. Even though it is essential, the process used to crush or size the RAP and the rock mineral identification was not reported. This is unfortunate because the RAP gradation depends on the gradation of original aggregate and the processes used to size and crush the material. Engineering properties of RAP may also be a

function of the rock minerals of aggregate in RAP. The properties of aggregate and aggregate binder mixtures and their interaction with each other are important to the life span of the system where the aggregate is being used. Most of the mineral qualities are inherent in the mineral deposit the aggregate was originally mined from and cannot be altered significantly by processing (Barksdale, 1991).

2.3.1.1 Lincoln Avenue Laboratory Results

The RAP was classified as well-graded (GW) by the United Soil Classification System (USCS) and A-1-a by the American Association of State and Highway Officials (AASHTO). The gradation result for the control material used, CA-6 with a 1.5-inch (3.8 mm) top size crushed stone, classified the material as a poorly graded aggregate (GP) or A-1-a. The CA-6 gradation does not allow for more than 8% of the material to pass the number 200 sieve. No information is presented on the processing of the RAP.

The ASTM D 1557 modified Proctor test was performed on the RAP and the crushed stone material. The moisture density relationship is shown in Figure 2.1. The maximum dry density for RAP was 125.2 pcf (19.7 kN/m^3) at a moisture content of 7.2%. The maximum dry density of the CA-6 control material was 141.5 pcf (22.2 kN/m^3) at a moisture content of 5.8%. The tests on RAP were conducted for a very narrow range of moisture contents, and maximum dry density was very sensitive to moisture content. The RAP densities were considered low in comparison to the conventional dense graded aggregate materials. The authors stated that this was due to the presence of less fine sand, (between 0.425 and 0.075 mm) in the RAP material.

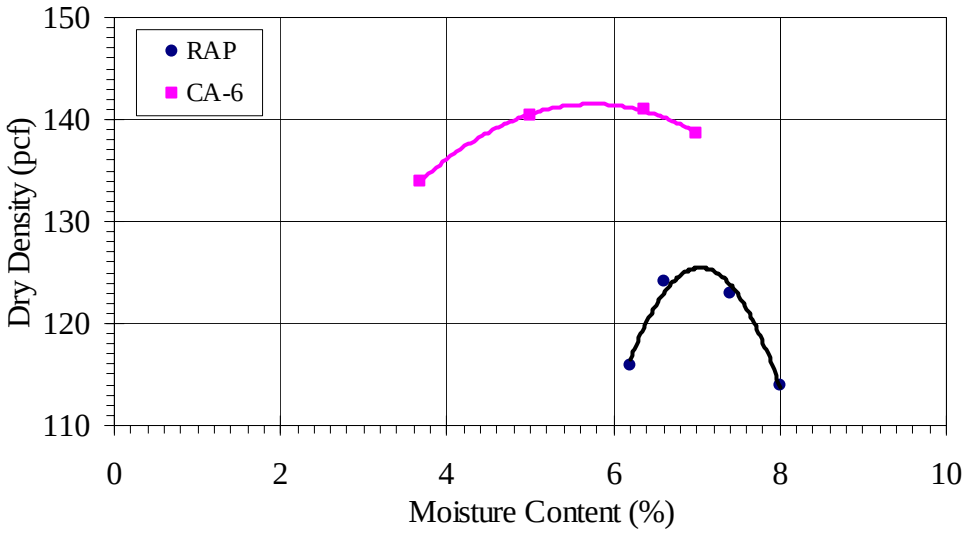

2.1 Lincoln Avenue moisture density curves for RAP and CA-6 aggregates using ASTM D1557 (Garg & Thompson, 1996). (1 pcf = 0.157 kN/m^3)

The laboratory program also included a triaxial testing program to determine the engineering properties of RAP and the crushed stone. Twelve-inch (30.5 cm) tall samples with a six inch (15.2 cm) diameter were tested triaxially in rapid shear tests. Three different gradations of RAP were tested to determine the gradation effects on friction angle (ϕ), cohesion (c), rutting potential, stress history effects, and moisture susceptibility. Deviator stress was applied axially at a constant rate of 1.5 in/min (3.81 cm/min). Four different confining pressures were used: 5, 10, 15 and 20 psi (35, 70, 105 and 140 kPa).

The results reported were angles of friction of 44° and 45° for crushed stone and RAP materials, respectively. The cohesion intercept values reported were 25 psi (175 kPa) for the crushed stone CA-6 materials and 19 psi (131 kPa) for the RAP. For the crushed stone, the maximum deviator stress achieved for a

confining pressure of 15 psi (105 kPa) was 229 psi at 5% strain. For the RAP, the maximum deviator stress achieved at the same confining pressure was 176 psi (1232 kPa) at 5% strain.

2.3.1.2 Lincoln Avenue Field Results

The field site was composed of an 8-inch (20.3 cm) RAP base laid over a 12-inch (30.5 cm) lime modified fine-grained subgrade. A control section was constructed with CA-6 crushed stone to allow for comparisons between both materials. Nuclear moisture and density tests were conducted on the RAP and crushed stone sections of the field site. The field density measurements for the RAP were all higher than those achieved in the lab. The mean field dry densities for the RAP and crushed stone were 132 pcf (20.7 kN/m^3) and 145 pcf (22.7 kN/m^3), respectively. The methods used for compaction in the field yielded a relative compaction of 105%; however, the field compaction techniques for this study were not reported.

Field CBR values were calculated using a correlation to the dynamic cone penetrometer (DCP) correlation equation. The relation Garg and Thompson (1996) reported was:

$$\text{Log CBR} = 0.84 - 1.26 * \log(\text{penetration rate})$$

The penetration rate is reported as inch per blow. The average CBR values reported were 150 and 65 for the crushed stone and RAP respectively. IDOT requires CBR values higher than 80 for a base of Type A aggregate.

Additional deformation tests were performed on the field site using the falling weight deflectometer. The testing was conducted four weeks after the

construction of the site and then at four-month intervals after that for a duration of two years. The crushed stone and the RAP experienced increased deflections during the warmer months. The deflection directly under the load varied from 13 to 23 mils (0.33 to 0.58 mm) for the RAP base pavement and 11 to 21 mils (0.28 to 0.53 mm) for the crushed stone base. Garg and Thompson (1996) did not observe any AC fatigue cracking or transverse cracking for the duration of the field testing. RAP did show an increased amount of rutting compared to the crushed stone aggregate. The RAP sections averaged 13% more deflection than the crushed stone sections. However, the author reported that the subgrade under the crushed stone was initially stronger than the subgrade under the RAP. This was attributed to the difference in deflection between the crushed stone and the RAP. Complete penetration data was not available and the strength difference between the subgrades was not available.

2.3.1.3 Lincoln Avenue Conclusions

Garg & Thompson (1996) concluded that RAP and crushed stone bases have similar stiffness and provide the same structural support and subgrade protection. Even though CBR values for the RAP are lower than for CA-6, the field performance of the RAP shows its potential for applicability as a base course material. Pavement evaluations performed by the IDOT showed only minor rutting distress after nineteen months of performance.

2.3.2 Performance of Shoulders Using Untreated Reclaimed Asphalt Pavement (UNRAP) Base (FDOT)

In 1993, Sayed, Pulsifier and Schmitt conducted a study in conjunction with the Florida Department of Transportation (FDOT), to establish guidelines for using untreated reclaimed asphalt pavement (UNRAP) to construct shoulder base courses. The location of this study was on US 192 southeast of St. Cloud, FL to SR 15 in Holopaw, FL. The project consisted of milling, resurfacing and constructing a paved shoulder using UNRAP for the base course material. The physical and mechanical properties of the material were determined using laboratory and field testing.

The term UNRAP is used in this study as opposed to RAP because the material used for construction was defined as untreated, moisture-modified, milled pavement containing asphalt and aggregate. The material used was not processed after milling and removal from the road. The shoulders were constructed with a 4-inch (10.2 cm) base of UNRAP under a 1.5-inch (3.8 cm) layer of S-1 asphalt concrete and friction course. The subgrade, a poorly graded sand, was consistent throughout the site.

2.3.2.1 US 192 UNRAP Laboratory Results

The gradation of the UNRAP ranged between well-graded gravel (GW) and well-graded sand (SW) in the USCS soil classification system. The UNRAP was classified as A-3 using the AASHTO classification system.

Standard Proctor (ASTM D698) and modified Proctor (ASTM D1557) compaction tests were conducted on UNRAP samples. The maximum dry density

achieved was 122.9 pcf (19.3 kN/m^3) at a moisture content of 6.2%, using ASTM D1557. No information on the shape of the moisture density curve was provided. The maximum dry density was comparable to typical granular materials. The authors concluded that due to decreased water absorption of particles coated with asphalt, the optimum moisture content was lower than that of other granular materials. Florida method (FM 5-515) was used to conduct LBR tests on the UNRAP samples. Sayed, Pulsifier and Schmitt reported LBR values for UNRAP of 25-30 and 29-38 for soaked and unsoaked samples, respectively. The average asphalt content reported for the UNRAP by Sayed, Pulsifier and Schmitt was 5.5%.

2.3.2.2 US 192 UNRAP Field Results

FM 1-T238 field density tests were performed at the field site. The average range for dry field densities was 118-123 pcf (18.5-19.3 kN/m^3), a relative compaction of 96% to 100%. The average moisture content range was 2.5-3.5%. The dry densities compare well to that of typical granular materials. However, the moisture content for RAP in the field was much lower than comparable moisture contents for other granular materials. Also it was much lower than the value reported for the lab investigation which was 6.2%. Sayed, Pulsifier and Schmitt (1993) report that a higher moisture content appears to yield higher dry densities.

Field CBR tests were conducted at several locations with both an UNRAP base and a limerock base. The average LBR values for the UNRAP and the limerock were 27 and 77, respectively. The investigators claim that the low LBR values in the UNRAP are due to low fine sand content, resulting in a less dense material. Fine sand material (between 425 mm and 0.075mm) tends to fill the

voids between larger grains, making the structure denser and increasing stiffness.

The UNRAP and limerock base sections were also tested using a Dynaflect, an electromechanical system that produces the dynamic deflections of a surface by applying an oscillatory load. These measurements indicated that the limerock base deflection was 70 to 85% of the deflection of the UNRAP. The pavement stiffness and strength of the UNRAP found with the Dynaflect method compared better with the stiffness and strength of the limerock. The authors believe that the Dynaflect measurements were more accurate than LBR measurements in determining the in-place stiffness and strength properties of UNRAP.

2.3.2.3 US 192 UNRAP Conclusions

Sayed, Pulsifier and Schmitt (1993) concluded that the potential of using UNRAP as a base is good, simply because it is mainly aggregate with binder. However, there is lack of information on how to implement its usage. Another issue of concern is the doubt about the applicability of the equipment and procedures used presently by the FDOT in determining the LBR according to FM 5-515. The deformation measurements obtained by the Dynaflect are positive and they suggest modifications to the current LBR test methods are needed to properly replicate the actual strength of the UNRAP.

2.3.3 Batinah Highway RAP Project

This study represents the first attempt to use recycled pavement materials in the Sultanate of Oman. Taha, Ali and Basma (1999) performed a laboratory

investigation on RAP and RAP-aggregate mixtures conventionally used in road bases and subbases. Physical, compaction and California Bearing Ratio (CBR) tests were performed on aggregate mixtures that contained 100, 80, 60, 40, 20, and 10% RAP. Virgin aggregate was collected from the Batinah highway project. The RAP was obtained from an old section of Batinah highway that was rehabilitated. A cold milling machine was used to remove the RAP. An extraction test following the specifications in AASHTO T164 (Method A) showed an asphalt content of 5.5% by weight.

2.3.3.1 Batinah Highway Laboratory Results

The gradation tests were performed in accordance to AASHTO T27. RAP was classified as a well-graded gravel (GW) by the USCS system. The virgin aggregate was a mixture of well-graded sands and gravels with little or no fines (material passing the No. 200 sieve). No further information was given regarding possible processes to size the RAP.

Liquid limit testing was performed in accordance to AASHTO T89. The RAP was essentially non-plastic with a liquid limit of eight. Specific gravity data was obtained as being 2.12 on the RAP.

Modified Proctor testing was conducted in accordance with AASHTO T180. All the mixes were tested with different percentages of RAP. As the RAP percentage increased the dry density decreased. The maximum dry density achieved with the 100% RAP was 117.4 (18.4 kN/m^3) pcf at a moisture content of about 7%. The densities increased with less percentage of RAP but the optimum moisture content for each different sample did not display any visible trend. The optimum moisture content varied from 6 to 8%.

The CBR testing was performed according to AASHTO T193 to determine the bearing value of the RAPs and RAP-aggregate mixtures compacted at optimum moisture. This test was conducted on un-soaked samples and CBR values were calculated for varying percentages of the virgin aggregate used in the testing program. The lowest CBR of 11 corresponded to the mix containing 100% RAP. Similar to the behavior of dry density, the CBR values increased, as the percentage of RAP in the aggregate mixture decreased. With only 20% RAP and 80% virgin aggregate, the CBR was 64. One hundred percent virgin aggregates produced the only mixture with a CBR greater than 100.

2.3.3.2 Batinah Highway Conclusions

Results indicate that RAP could be mixed in with virgin aggregate in a base if RAP material did not exceed 10% of the mixture. RAP may be used as a subbase if it did not exceed 80% of the mixture. Higher dry density and CBR values were obtained as the percentage of RAP in the mixture decreased.

2.3.4 NJDOT Project

Papp, Maher, and Gucunski (1998) conducted laboratory and field investigations to consider the use of RAP in roadway base and subbase applications. The RAP for this investigation was obtained from a stockpile on a New Jersey Department of Transportation (NJDOT) highway construction project. The dense graded aggregate (DGA) was obtained from a local quarry pit. No further information is presented on the material used and if the RAP was processed or not.

2.3.4.1 NJ DOT Laboratory Results

The gradation tests performed on the RAP were in accordance to AASHTO designation T 27-93. The material classified as well-graded gravel (GW) and A-1-a by the USCS and AASHTO, respectively.

Four standard Proctor (ASTM D698) compaction tests were performed on RAP samples. The maximum dry density achieved was 119 pcf (18.7 kN/m^3) at a moisture content of 6%. No additional information on the shape of the moisture density curve is given. The drying method used to determine moisture content after compaction was modified. The presence of asphalt binder in the material did not permit oven drying. The asphalt binder would soften causing the binder to stick to the aggregate and pan. The investigators air-dried the material for 24 hours and then applied short intervals of heating.

The resilient modulus testing was performed in accordance to ASSHTO TP46-94. Each sample was compacted to maximum dry density by using a vibratory compaction hammer. The test is set up in similar fashion to a triaxial test. The difference is that the loading frame has the capability of applying a 0.1 second haversine load cycle.

Papp's results are shown in Table 2.1. The 100% RAP sample produced the highest resilient modulus while the 100% DGA produced the lowest. The resilient modulus increased with an increase in RAP percentage.

Table 2.1 Comparison of Resilient Modulus Tests at Maximum Density.

(1 psi = 7 kPa)

Material	M(r) @ Bulk Stress of 20 psi (psi)	M(r) @ Bulk Stress of 50 psi (psi)	% Increase in Mr @ Bulk Stress of 20 psi compared to DGA	% Increase in Mr @ Bulk Stress of 50 psi compared to DGA
100% DGA	16100	22800	0	0
75% DGA, 25% RAP	22800	41870	41.4	83.4
50% DGA, 50% RAP	28100	40200	74.7	76.4
25% DGA, 75% RAP	26500	39700	64.8	74.5
100% RAP	36700	49600	127.9	117.8

Permanent deformation tests were also performed to determine the permanent deformations and strains of each material. In these tests the samples were also compacted to maximum dry density using a vibratory compaction hammer. The samples were subjected to constant confining stress of 15 psi (105 kPa). The samples were loaded under a cyclic load that applied a deviator stress of 45 psi (315 kPa) for 100,000 repetitions. The accumulation of strain was the highest for RAP. While 100,000 repetitions RAP accumulated a permanent strain of 0.055 mm/mm, DGA accumulated a permanent strain of less than 0.01 mm/mm after 100,000 repetitions.

2.3.4.2 NJDOT Conclusions

Papp, Maher, and Gucunski (1998) conclude that the resilient modulus for RAP in the laboratory testing was higher than that of the conventional materials. However, RAP also had the highest permanent strain. Although RAP seems to be a viable and cost-effective alternative for use in a base course, the authors suggest that investigations be conducted where the deformations are monitored on a field site for an extended period of time.

2.3.5 Structural Numbers for RAP (UMass)

This study was performed at the University of Massachusetts, Amherst by Highter, Clary, and DeGroot (1997). Their objective was to determine how the structural number of a pavement section is affected by installing base and subbase courses with different percentages of RAP. The structural number is an empirical number that is a function of the layer coefficient, layer thickness and the drainage characteristics of each layer. The structural number is required for the pavement design equation used by AASHTO and many state agencies (Highter, et al; 1997).

Crushed stone and gravel were the two different aggregates used in this investigation. Mixtures of aggregate containing 100, 50, 30, and 10% RAP were tested. Resilient modulus and hydraulic conductivity were determined from repeated loading tests and constant head tests, respectively.

2.3.5.1 UMass Laboratory Results

The RAP combined with the aggregate classified as A-1-a or A-1-b by AASHTO and as well-graded sand (SW) by USCS. The results of the gradation and classification tests indicate that RAP falls within the ranges established by the Massachusetts Highway Department (MHD). The results indicate that the aggregates are good materials for road support.

The specific gravity of the materials was determined in accordance with ASTM C128-88 and ASTM C127-88 for fine and coarse aggregate respectively. The specific gravity for RAP was 2.38, considerably lower than for the crushed stone (2.61) and the gravel (2.58). No trend was observed in specific gravity for the mixtures with increased percentages of RAP.

Standard Proctor tests in accordance with ASTM D 698-91 were performed on all the mixes. The optimum moisture content of the aggregate mixtures was between 5.5 and 7%. The dry density ranged from 123.5 to 133.5 pcf (19.4 to 21.0 kN/m^3) for the different RAP-aggregate mixtures. The density of the sample that contained only RAP was reported as 130.4 pcf (20.5 kN/m^3). As the percentage of RAP increased, the dry density of the material decreased. However, no trends for moisture content were observed.

The hydraulic conductivity of the mixes was determined using a procedure outlined in ASTM D2434-68. The hydraulic conductivity of the gravel and crushed stone did not vary with increasing percentages of RAP. The range of values achieved for hydraulic conductivity was between 0.98 x 10^{-3} and 3.0 x 10^{-3} ft/sec (0.03 – 0.1 cm/sec). The hydraulic conductivities were typical of clean sands (Holtz and Kovacs, 1981).

The resilient modulus was conducted at various combinations of pressure and deviator stress. The test specification used was AASHTO T294-92I. The researchers showed that the resilient modulus tends to increase for a given value of bulk stress with an increase in RAP percentage in the mixture. The results also show that the resilient modulus of the base material increases with the higher percentages of RAP in the aggregate mixture.

A slight increase in layer coefficient was observed with increasing RAP percentages. The layer coefficient is an empirical measure of the relative ability of the material to function as a structural component of the pavement. Each layer coefficient is a function of the resilient modulus. The structural number is also a function of the layer coefficient. The structural number did increase slightly with an increase in the percentage of RAP in the mixtures. The small increase in structural number does not have an effect on the layer thickness determined from

the AASHTO design equation.

2.3.5.2 UMass Conclusions

The grain size of RAP falls within gradation limits established by the MHD and the hydraulic conductivity is not affected by the addition of RAP. The resilient modulus increases with the addition of RAP to the aggregate mixtures. This increase in resilient modulus results in an increase in layer coefficient and therefore an increase in structural number. The researchers did not focus on the influence of water content and density on the RAP's structural number. They recommended that this be done and that long-term performance of RAP/aggregate mixtures in the field be studied.

2.3.6 Performance Evaluation of Reclaimed Asphalt Pavement as a Dense Graded Aggregate Base Course

In the fall of 1993, Rutgers University, in conjunction with the New Jersey Department of Transportation, constructed and tested a road section comprised of a RAP subbase. The location of this project was Cedar Lane, in the town of Edison, New Jersey. The purpose of this project was to compare various test results of the RAP with those of the commonly used dense graded aggregate base course (DGABC).

The field site on Cedar Lane consisted of a subbase, base and asphalt overlay on approximately 4500 feet of the two-lane road. Approximately 3900 feet was comprised of RAP subbase, with the remaining 600 feet comprised of DGABC subbase to be used as a control section. Thickness specifications called

for an 8-inch subbase (either RAP or DGABC) and an 11-inch asphalt layer comprising the surface, binder, and base (Palise, 1994).

2.3.6.1 Rutgers University Lab Results

Results of sieve analyses indicate that both the RAP and DGABC were classified as A-1-a type soils according to the AASHTO soil classification system (Holtz & Kovacs, 1981). The average percentage of fines passing the #200 sieve for the RAP and DGABC were reported to be 2.3% and 9.5%, respectively (Palise, 1994).

Results of the Proctor moisture-density relationship for the RAP reported that the maximum dry density was 117 pcf (18.4 kN/m^3), attained at an optimum moisture content of 7.0%. It should be noted that the +¾ inch material was not removed from the sample prior to compaction.

Laboratory CBR's were conducted on the DGABC, the RAP at the field site, and the RAP at the quarry. CBR's taken prior to saturation yielded results of 98, 177, and 178 for the DGABC, field site RAP, and quarry RAP, respectively. CBR's performed after a 4 day saturation yielded results of 144 for the DGABC, 199 for the field site RAP, and 180 for the quarry RAP (Palise, 1994).

The values obtained for both RAP samples are larger than any of the CBR and LBR values reviewed in any of the other studies. A possible reason could be the use of trap rock as the aggregate in the RAP. Trap rock is a very hard material derived from crushed stone. Trap rock constitutes only 8.3% of the aggregate mined in the United States (Barksdale, 1991).

2.3.6.2 Rutgers University Field Results

Nuclear densities of the RAP were taken after subbase installation at the surface, 2-inch depth, and 4-inch depth. Recorded average dry densities from the RAP testing were 114 pcf (17.9 kN/m^3) at the surface, 115 pcf (18.1 kN/m^3) at 2 inches deep, and 119 pcf (18.7 kN/m^3) at a 4-inch depth. The average field dry density of the DGABC was 135 pcf (21.2 kN/m^3) (Palise, 1994).

SWK Pavement Engineering performed FWD testing once in 1994, 1995, and 1996 on both the RAP and the DGABC. Results of these tests indicated an increase in stiffness from 1994 to 1996 for both the RAP and DGABC. The results also indicated that the RAP was stiffer than the DGABC, and that the stiffness of the RAP increased more than the stiffness of the DGABC over the testing cycle. Overall, the RAP section was 1.5 to 1.8 times stiffer than the DGABC (Rowe & Chang, 1997).

2.3.6.3 Rutgers University Conclusions

Placement of the RAP occurred during the cool air temperatures of fall. The author acknowledged that it is not known what effects high temperatures would have on the gradation, placement and compaction of the RAP. Also, Palise (1994) mentioned the positive remarks made by the equipment operators who installed the RAP. The operators said that they liked working with the RAP because “It did not get dusty, did not need priming and could be placed in inclement weather”.

Palise (1994) concluded from this experiment that RAP can be successfully used as a replacement for DGABC based on the results of the FWD, CBR and

density tests. Palise (1994) also concluded that the controlling factors in the performance of the RAP is dependent on where the RAP is obtained and its gradation.

2.3.7 UNRAP – Are We Ready for It?

In July 1992, a temporary 600-foot roadway was constructed to provide maintenance of traffic for a construction site located on SR 600 (US 92) near the intersection of Interstate 95 in Volusia County, Florida. The roadway was designed to have three 200-foot sections (Sections A, B, and C). Section A and B were designed to have 9-inch Untreated Recycled Asphalt Pavement (UNRAP) base courses. Section C was designed to have a 7-inch limerock base section. The difference between Sections A and B was to have been that Section A was designed to have an unstabilized subgrade as compared to a stabilized subgrade of Section B. Unfortunately, the subgrade material used for Section A behaved in similar manner as that of Section B. Therefore, the authors of this paper concluded that there was no significant difference between Sections A and B, and that they both should be considered to have stabilized subgrades (Sayed, et al., 1996). A table of the material used and construction thickness is presented in Table 2.2.

Table 2.2. – Material and Thickness Designations used for SR 600 UNRAP Project

Test Section	A	B	C
Wearing Surface Type	S-1	S-1	S-1
Wearing Surface Thickness	2"	2"	2"
Base Type	UNRAP	UNRAP	Limerock
Design Base Thickness	9"	9"	7"
Subgrade Type	Compacted & Unstabilized	Compacted & Stabilized	Compacted & Stabilized
Subgrade Thickness	12"	12"	12"

2.3.7.1 SR 600 UNRAP Laboratory Results

Results from the sieve analysis (FM 1-T 027) performed on the UNRAP indicated that it is classified as a GP (poorly graded gravel) according to the USCS system and A-1-a according to the AASHTO classification system (Holtz & Kovacs, 1981). The asphalt content (FM 5-563) of the UNRAP ranged between 6.9% and 7.2% (Sayed, et al., 1996).

2.3.7.2 SR 600 UNRAP Field Results

Field nuclear densities and moisture contents were performed after construction and prior to the asphalt overlay. Results of these tests showed that the UNRAP attained an average dry density of 101.5 pcf (15.9 kN/m^3) at a moisture content of 11.3%. The average dry density of the limerock was recorded at 115 pcf (18.1 kN/m^3) at a moisture content of 15.8% (Sayed, et al., 1996).

Field LBR's, Dynaflect, and FWD testing was also performed on this site immediately after construction and after four months, prior to demolition. Results of the LBR tests indicate that the UNRAP had an initial average value of 13 that increased to 39 prior to demolition. The initial LBR value of the limerock was

recorded at 68 and increased to a value of 103 prior to demolition (Sayed, et al., 1996).

Comparison of the Dynaflect and FWD results indicated that the UNRAP produced lower deflections than the limerock for both the initial testing phase and prior to demolition. Also, the deflections produced by the UNRAP decreased 8% to 10% from the initial testing to demolition (Sayed, et al., 1996).

2.3.7.3 SR 600 UNRAP Conclusions

Sayed concluded that there was "a substantial improvement of the properties of UNRAP with time". He also concluded that the construction of UNRAP base courses can be achieved through normal construction practices and that, based on the Dynaflect and FWD test results, "UNRAP is at least equivalent to limerock".

2.3.8 Compaction Characteristics of RAP (Florida Tech)

In 1998, Tomas Montemayor conducted a study to determine moisture-density behavior and the bearing strength of dynamically compacted RAP as a function of compaction energy and temperature. A typically used limestone aggregate extracted from the Miami Oolite/Ft. Thompson limestone formations was used as a control material. The study was performed at the Florida Institute of Technology and included only laboratory testing.

The RAP was obtained from the APAC-Florida, Inc. asphalt plant located in Melbourne, Florida. The process used to crush and size the RAP or the mineral

identification was not specified.

2.3.8.1 Florida Tech Laboratory Results

The RAP classified as a well-graded sand (SW) or gravel (GW) by the USCS classification system and A-1-a by the AASHTO system. The material had a top size of 0.60 inches (1.5 cm).

Montemayor (1998) found that RAP moisture density characteristics did not follow traditional Proctor behavior. The densification of RAP is not dependent on moisture content. The dry densities of RAP ranged from 97.2 to 118.5 pcf (15.2 – 18.5 kN/m^3). The compaction energies used to achieve these densities were standard Proctor (ASTM D698), modified Proctor (ASTM D1557) and an energy level of double modified Proctor. The author also compacted samples at three temperatures, 35°F, 75°F, and 120°F (1.7, 23.9 and 48.9°C). RAP compacted at 120°F (48.9°C) increased dry density values by approximately 3.5% over samples compacted at 70°F (23.9°C). Montemayor (1998) attributes this density gain to the viscosity of asphalt cement increasing at the higher temperature to produce tackiness and binding between particles.

The laboratory program also included LBR testing to determine the bearing strength. LBR values for modified Proctor compaction efforts ranged between 25 and 50. The LBR also increased for RAP that were compacted at 120°F (48.9°C), yielding range for LBR values between 42 to 125.

2.3.8.2 Florida Tech Conclusions

Montemayor (1998) concluded that RAP does not meet minimum LBR requirements for a construction of a base in highways. RAP does not behave in accordance with traditional Proctor moisture-density behavior. Montemayor (1998) suggests that Mohr-Coulomb shear strength theory be investigated while considering the effects of temperature and dry density.

2.3.9 Summary

A summary table of the results of all the investigations reported is shown in Table 2.3. The moisture contents of every investigation are within a similar range, from 4 to 7%. Only the Lincoln Ave. study reports a distinctive optimum moisture content. The other studies do not present moisture density curves. The dry densities range from 109 pcf to 130 pcf (17.1 to 20.4 kN/m^3). The University of Massachusetts investigation achieved a density of 130.4 pcf (20.5 kN/m^3) using standard Proctor compaction energy. This value seems unusually high compared to the other studies. Initial investigations at Florida Tech yielded dry densities considerably lower than the other investigations. The material used was not processed and contains larger amounts of coarse particles. This may be the reason for the slightly lower densities.

The source of the RAP and the aggregate included in the RAP are very important to the strength parameters and even though they have the same soil classification, these investigations are all based on different sources of RAP. Different gradations and contents of fine sand may be the reasons for some discrepancies between studies.

Table 2.3 Summary of Laboratory and Field Data Found in Reported Investigations. (1 pcf = 0.157 KN/m^3)

	Water Content (%)	Maximum Dry Density/Modified (pcf)	Maximum Dry Density/Standard (pcf)	Maximum LBR	Soil Classification	
					USCS	AASHTO
Lincoln Avenue	7.2	125.2	--	78	GW	A-1-a
US 192 UNRAP	6.2	122.9	--	38	GW-SW	A-1-a
Batinah	7.0	117.4	--	11	GW	A-1-a
NJDOT	6.0	--	119.0	--	GW	A-1-a
UMASS	5.5-7.0	--	130.4	--	GW	A-1-a
Rutgers Univ.	7.0	--	117.0	239*	--	A-1-a
SR 600 UNRAP (initial)	11.3	101.5	--	13	GP	A-1-a
SR 600 UNRAP (final)	--	--	--	40	--	A-1-a
Florida Tech	4.0-5.0	114.0	105.0	50	GW-SW	A-1-a

*Converted from CBR value (x1.2)

2.4 Conventional Base/Subbase Materials

Cemented coquina and limerock are two of the most commonly used materials in highway base and subbase applications in Florida. They have desirable strength and deformation characteristics and they occur naturally in sufficient quantities throughout Florida, making them less expensive than other materials.

2.4.1 Limerock

Limerock is defined by the mineral industry as rock from which lime is produced. Its formations range in age from 0.5 to 42 million years. Three

important areas in Florida supply limerock: Ocala, Ft. Myers, and Miami. Ocala limerock generates the highest densities while limerock from the other two sources have similar densities. The rock is drilled and fractured with explosives to a size suitable for primary crushing. It is then hauled to secondary crushing units for a screening process that sizes the material into size groups conforming to the sizes specified for the particular applications (McCaulley, et al; 1990).

The properties used to evaluate these aggregates in Florida are specific gravity, absorption, gradation and Los Angeles abrasion loss. For FDOT use, limerock has to meet the specifications in Section 911 of the FDOT's *Standard and Specifications for Road and Bridge Construction 1999.* Its gradation should allow a minimum of 97% by weight to pass the 3.5-inch (8.9 cm) sieve and the entire material should be graded uniformly.

2.4.2 Cemented Coquina

Cemented coquina is derived from the calcarnite stone consisting of broken mollusk deposits, corals and other marine invertebrates. The presence of silica sands should be avoided to permit bonding (Schmidt, et al; 1979).

Cemented coquina's gradation should have a minimum of 97% by weight passing the 3.5-inch (8.9 cm) sieve and no more than 7.5% passing the number 200 sieve. The Limerock Bearing Ratio value for any material to be used as a base should not be less than 100 (Standard Specifications for Road and Bridge Construction,1999).

2.4.3 Gradation Specification for Aggregate Material

The gradation of base and subbase materials require a distribution that resists deformation. This resistance is called mass stability and is greatest when the particles are densely graded. Densely graded materials demonstrate good performance and placement characteristics because they contain a large range for all particle sizes, including dust. The voids are minimized when the void spaces between large particles are filled with smaller ones (Barksdale, 1991).

In order to determine an ideal dense aggregate grading and achieve a good representation of all particle sizes, the Talbot equation is frequently used in selecting suitable gradation (Barksdale, 1991).

The Talbot equation states:

$$P = (d/D)^n * 100$$

where:

P = percent passing sieve size "d" expressed in inches,

d = sieve size opening expressed in inches for which the percent passing (P) is applicable,

D = maximum aggregate size (inches),

n = an empirical gradation exponent (ranges from 0.3 to 0.5).

Another specification that is used is ASTM D 2940-92, "Standard Specification for Graded Aggregate Material for Bases and Subbases for Highways and Airports." It specifies quality control for graded aggregates that may be expected to provide stability and load support for highway bases and subbases. The Talbot and the ASTM design ranges are discussed further in Chapter 4.

3. Laboratory Testing Program

In developing a data base of RAP engineering properties, three testing programs were conducted. These programs included grain size distribution tests, moisture density tests, limerock bearing ratio tests, and triaxial compression tests.

The first of the three laboratory studies was developed to determine the relationship between Proctor moisture-density relationships and LBR on unsoaked samples of an unprocessed RAP. Standard, modified and what was termed double modified Proctor tests were performed on samples compacted at room temperature using water as the wetting agent. For the double modified Proctor tests the number of blows/lift were doubled to compact the samples. Tests were also conducted on RAP samples by applying modified Proctor energy at compaction temperatures of 35^{o}F and 120^{o}F, and room temperature. Limerock Bearing Ratio (LBR) tests were performed on all compacted samples. An aggregate sample equivalent to RAP in gradation, and composed of typical Florida pavement aggregates (Miami limestone) was produced and used as a comparison basis. Moisture density and LBR tests were performed on these formulated limestone samples, compacted at room temperature using standard and modified Proctor energies with water as the wetting agent. This portion of the study was conducted to assess the effects that the presence of asphalt binder has on the bearing strength behavior of RAP.

The second of the three laboratory studies was developed to evaluate the relationship between a broader variety of compaction techniques and LBR on RAP processed using either a tubgrinder or hammermill crusher. Samples were characterized by their gradation and then tested for their bearing strengths using four laboratory compaction methods, modified Proctor (56,250 ft-lb/ft^3), modified Marshall (56,250 ft-lb/ft^3), vibratory (0.013 inches @ 60 Hz, 2 psi surcharge load) and static (212, 400, 700, 1000 psi pressure).

The third of three laboratory studies was developed to evaluate the effects that storage time at elevated temperatures had on the strength and deformation characteristics of RAP from tubgrinder and hammermill post-milling processes. The engineering properties determined through triaxial compression testing were angle of internal friction (ϕ), cohesion (c) and elastic (Young's) modulus (E).

3.1 Material Sampling

3.1.1 Recycled Asphalt Pavement (RAP)

RAP samples were obtained from two sources in Florida, the FDOT stockpile in Madison and the APAC-Florida MacAsphalt Plant in Melbourne. Three visually distinct RAP stockpiles at the APAC plant were sampled. They included RAP directly from pavement milling operations unprocessed and RAP processed using either a tubgrinder or hammermill crusher. In addition, a site visit was conducted at Ranger Construction Asphalt Plant located in Grant, Florida. Samples were not collected however; available material was found to be visually similar to the APAC plant RA

3.1.1.1 Limestone Aggregate

Limestone aggregate was obtained from the Rinker City Point plant located in Cocoa, Florida. It originated from pit 87-090, terminal 447 in Miami, Florida. The aggregate was mined from the Miami Oolite/Ft. Thompson limestone formations.

3.1.1.2 Sampling Protocol

The samples were obtained in accordance with the procedures outlined in ASTM D 75-87, "Standard Practice for Sampling Aggregates." Approximately 1000 pounds were obtained for sampling throughout the project. The samples obtained were quartered in size to smaller sizes following ASTM C702 –93, Method B, "Standard Practice for Reducing Samples of Aggregate to Testing Size."

3.2 Grain Size Distribution

3.2.1 Methodology

In order to classify the aggregate, sieve analyses were performed on the unprocessed and processed RAP, following ASTM C136-96a "Standard Test Method for Sieve Analysis of Fine and Coarse Aggregates." The samples were air-dried instead of oven-dried due to the presence of the asphalt binder. The U.S. standard sieve sizes used were 1.5-inch, 0.75-inch, 0.375-inch, #4, #8, #16, #30, #60, #100, and #200. Approximately 3.3 pounds (1500 g) of material was sieved per sample. The test was performed three times on samples from each RAP process. For each sample the grain size distribution was plotted and the D_{10}, D_{30}, and D_{60} coefficients were determined. The coefficients of uniformity (C_u) and gradation (C_d) were also calculated to classify the material. The material was classified using the United Soil Classification System (USCS), the American Association for State Highway and Transportation Officials (AASHTO), and ASTM's (D448) Standard Classification for Sizes of Aggregate for Road and Bridge Construction.

3.2.2 Results

A visual classification of the RAP would be to describe the material as a coarse sand. The material is dark gray in color. The original aggregate can occasionally be seen through the asphalt material. The material is clean (no coatings of clay or silt), hard, strong, durable, rough, sound and well shaped.

The gradation curves for the sieve analysis performed using the average of three tests per sample on the RAP are shown in Figure 3.1. Unprocessed RAP classified as a well-graded sand to gravel (GW/SW) based on the Unified Soil Classification Systems (USCS) and an A-1-a in the Association for State Highway and Transportation Officials (AASHTO) system (Montemayor 1998). Hammermill RAP classified as a well-graded sand (SW) and tubgrinder RAP classified as a poorly graded sand (SP) using USCS. Both materials classified as A-1-a in the AASHTO. Table 3.1 shows a summary of the various gradation parameters, D_{10}, D_{30}, and $D_{60,}$ the coefficients of curvature and uniformity, C_c and $C_{u,}$ and the two classification systems (Doig, 2000).

Hammermill RAP had a larger D_{30} value, 0.07 inches (1.9 mm) than tubgrinder RAP 0.04 inches (0.9 mm). This means more coarse sand sizes (between 2 mm and 0.425 mm) were created with the tubgrinder process than the hammermill process.

In Figure 3.2 the grain size distributions of the hammermill and tubgrinder materials were compared to ranges recommended by the Talbot equation for use as roadway construction materials (Barksdale, 1991). About 40 percent of the materials are within the range recommended by the Talbot equation. This includes the coarse sand sizes from 4 mm to 0.3 mm. The percentage of aggregate sizes from 1.5 inches to 4 mm needs to be increased in order to allow the RAP gradation curves to fall within the Talbot range. The percentage of fine sand size material, between 0.3 mm 0.075 mm, would also have to be increased to achieve the range suggested by the Talbot equation for maximum mass stability.

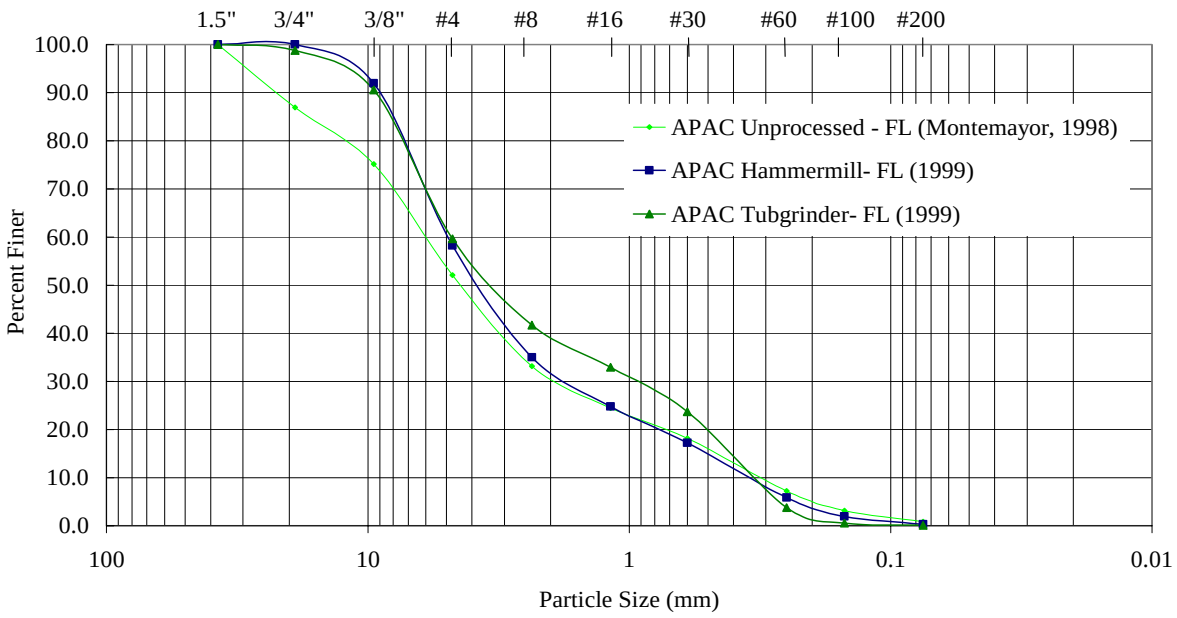

Figure 3.1 Particle Size Distributions for RAP Samples (From Doig, 2000)

Table 3.1 Gradation Parameters and Classifications for RAP.

(1 mm = 0.04 inches)

Description	Unprocessed RAP	Hammermill RAP	Tubgrinder RAP
D(10) mm	0.28 to 0.32	0.35	0.35
D(30) mm	1.30 to 2.00	1.9	0.9
D(60) mm	5.10 to 6.00	3.7 to 5.0	5.0
Cu	17.1	10 to 14.3	14 to 14.3
Cc	1.2 to 2.2	1.5 to 2.1	0.5
AASHTO	A-1-a	A-1-a	A-1-a
USCS	GW/SW	SW	SP

From the grain size curves it can be seen that more hammermill material passes the number 16 sieve (1.18 mm) than tubgrinder material. This resulted in a smaller value of C_c for tubgrinder RAP and the material classified as poorly graded in the USCS classification system. In general, the material displays good physical properties.

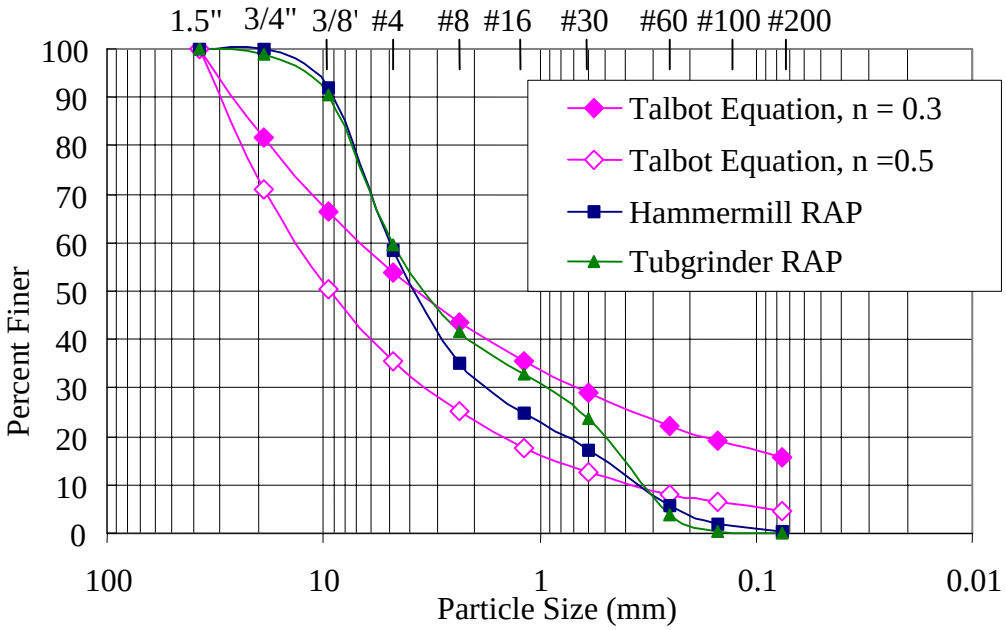

Figure 3.2 Comparison of Hammermill and Tubgrinder RAP to the Talbot Range (From Doig, 2000)

The materials used in this investigation were also compared to the ASTM design range for base and subbase materials in Figure 3.3 and 3.4 respectively. The Talbot range and the ASTM specification D 2940–92 are similar. Again, it can be seen from the Figures 3.3 and 3.4 that about 40 to 50 percent of the materials tested in this investigation are within the ASTM range. The only sizes that are in the appropriate ASTM range for both bases and subbases are the coarse sand sized material, between 4 mm and 0.3 mm. As with the Talbot range, the percentage of aggregate sizes from 1.5 inches to 4 mm needs to be increased and the fine sand size material between 0.3 mm and 0.075 mm needs to be increased to achieve the range recommended by ASTM specification D 2940-92 (Doig, 2000).

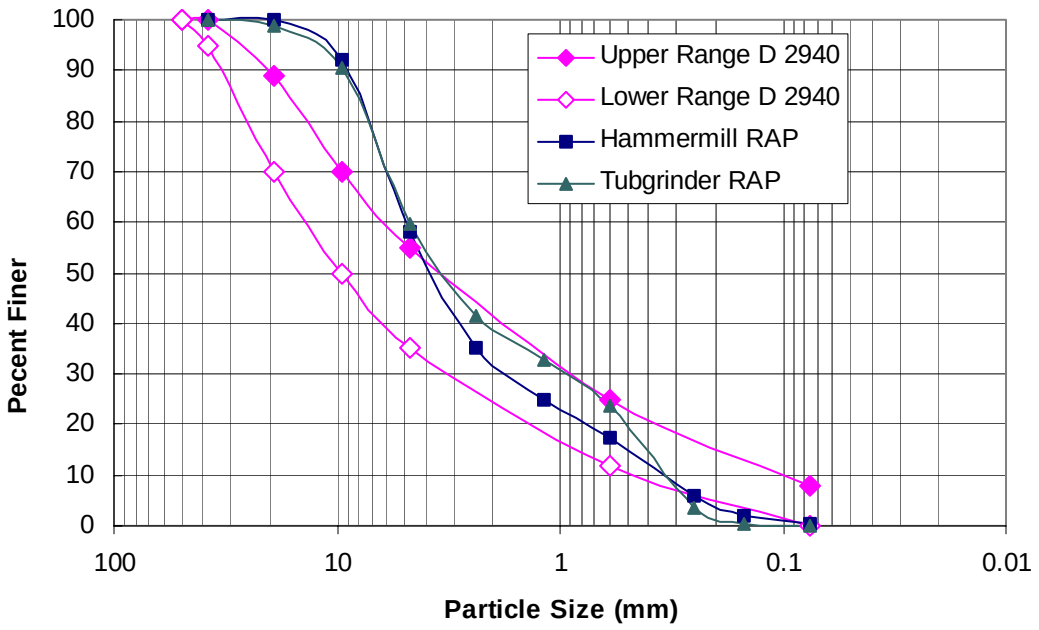

Figure 3.3 Comparison of Hammermill and Tubgrinder RAP to the ASTM Standard Specification Range for Base Material (From Doig, 2000)

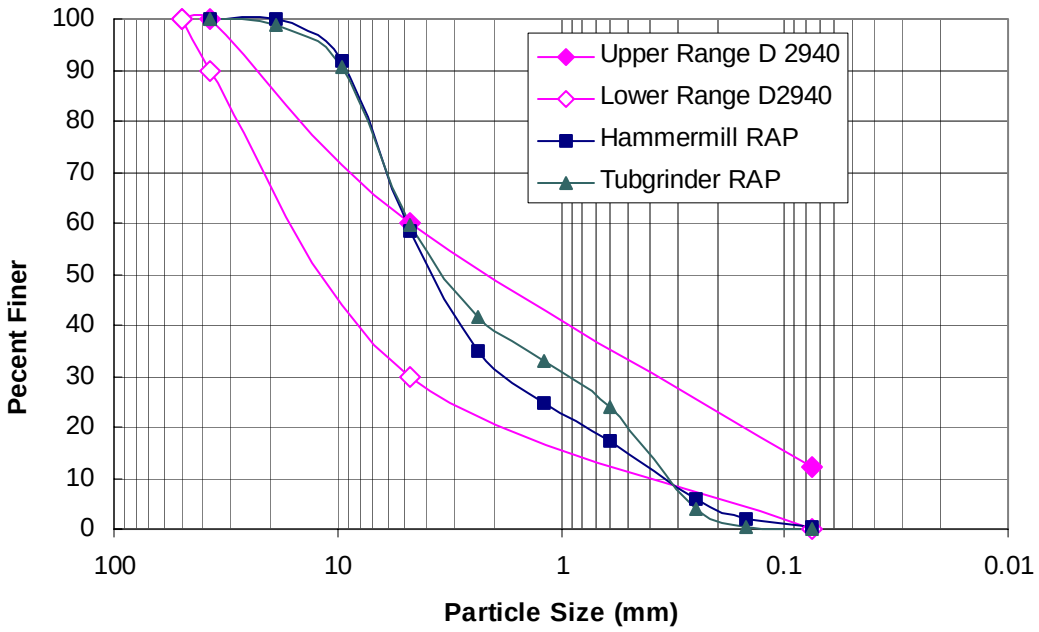

Figure 3.4 Comparison of Hammermill and Tubgrinder RAP to the ASTM Standard Specification Range for Subbase Material (From Doig, 2000)

3.3 Asphalt Content and Specific Gravity

3.3.1 Methodology

The FDOT District 5 Materials and Research Division in Deland, Florida performed asphalt content tests on representative RAP samples. The procedures followed were Mechanical Analysis of Extracted Aggregate Florida Method (FM) 1-T-0303 and Quantitative Determination of Asphalt Content from Asphalt Paving Mixtures by Ignition Method, FM-5-563. Three samples of approximately 3.3 pounds (1500 g) each were tested for both the hammermill processed RAP and the tubgrinder processed RAP. A Thermolyne National Center for Asphalt Technology asphalt content tester was used to determine the average asphalt content value. Specific gravity testing was performed in accordance with Florida Method (FM) 1-T 100-September, 1994 "Specific Gravity of

Soils." Asphalt content testing was performed in accordance with FM 1-T 164-September, 1994 "Quantitative Extraction of Bitumen from Bituminous Paving Mixtures."

3.3.2 Results

The average asphalt content was 5.80±0.13% for the hammermill RAP and 5.47±0.04% for the tubgrinder RAP. The average asphalt content for the unprocessed RAP was 6.73±0.14%. Asphalt content test results were within expected values of 4 to 8 percent by weight for structural asphalt concrete mixtures used in Florida (Montemayor, 1998). The bulk specific gravity (G_{mb}) was 2.30 and the theoretical maximum specific gravity was 2.42. The range of G_{mb} for limestone is 1.88 – 2.81. Asphalt's specific gravity is approximately 1. The laboratory determined G_{mb} and theoretical maximum specific gravity were within acceptable limits.

3.4 Compaction Methods

3.4.1 Methodology

The samples were tested for their bearing strengths using six laboratory compaction methods, 1) standard Proctor (AASHTO-T99), 2) modified Proctor (AASHTO-T180), 3) double modified Proctor, two times the energy of modified, 4) modified Marshall, Marshall hammer with an enlarged striking plate, 5) vibratory (0.013 in @ 60 Hz, 2 psi surcharge) and 6) static compaction compression @ 212, 400, 700, 1000 psi. The specifications of each test method are summarized in Tables 3.2 and 3.3.

3.4.2 Compaction Processes

RAP was compacted using the processes described below to determine the moisture density characteristics of the material. The compacted moisture density samples were used for the LBR test.

3.4.2.1 Standard Proctor

Standard Proctor tests followed AASHTO-T99. To investigate RAP material as close as possible to its original state, the particle size correction specified in ASTM D698 (method D) applies to samples with content of ¾ inch particles greater than 10 percent. The only particle size adjustment made during compaction tests was the removal of material larger than 1.5-inch (3.8-cm). The content of RAP and limestone particles coarser than ¾-inch sieve was approximately 13 percent by weight. Based on the small percentage, the specified particle size adjustment was considered non-critical in obtaining appropriate testing results.

3.4.2.2 Modified Proctor

Modified Proctor tests were performed according to section four of FM 5-515, September, 1993, "Florida Method of Test for Limerock Bearing Ratio" and AASHTO-T180, using a 10-lb (4.54-kg) hammer and 18-in. (457-mm) drop height. To accommodate for material that did not pass the 3/4-in sieve, material that passed the 3/4-inch sieve but was retained on the 3/16-inch was substituted for the material greater than 3/4-inch (Department of Road Research, 1952).

3.4.2.3 Double Modified Proctor

In an effort to increase the dry density of RAP, a test method termed double modified Proctor followed the same procedure as AASHTO-T180 except the number of blows per layer for the 6-inch mold was increased from 56 to 112. This effectively doubled the compaction energy to 111,972 ft-lb/ft^3 (5,386 m-kN/m^3).

3.4.2.4 Modified Marshall Compaction

When HMA is compacted using a Marshall hammer in the 3-inch high, 4-inch diameter mold, the material is compacted in one layer using 25, 50, or 75 blows. A modified Marshall Compaction method was developed on the RAP at different moisture contents to create a moisture density curve. This method followed closely with the compaction procedure outlined in section 3.4 of Florida Method of Test, FM 5-511, September 1994, "Florida Method Test for Resistance to Plastic Flow of Field Produced Plant Mixed Asphalt Concrete Mixtures Using Marshall Apparatus." The Marshall hammer was modified by enlarging the striking plate from 4-inches to 6-inches in diameter. This plate remained in contact with the sample throughout testing (Figure 3.5). The Marshall hammer has the same 10 lb mass and 18-inch drop height as a Modified Proctor hammer. RAP was compacted in an LBR mold using 5 layers with 56 blows per layer. This is equal to the compaction energy achieved in the Modified Proctor test (56,250 ft- lb/ft^3).

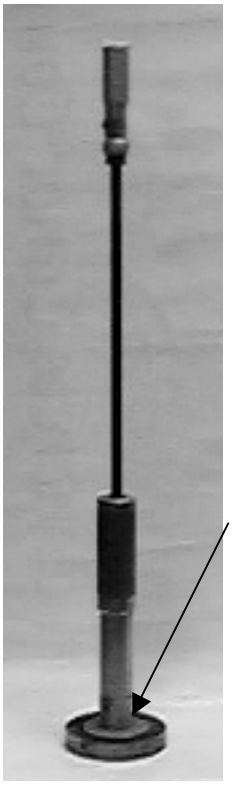

Figure 3.5 Modification fitted to Marshall hammer to accommodate six-inch diameter mold.

3.4.2.5 Vibratory Compaction

RAP samples were compacted to the minimum and maximum densities using vibratory compaction. Maximum densities were achieved in accordance with ASTM D 4253-93 “Standard Test Method for Maximum Index Density and Unit Weight of Soils Using a Vibratory Table.” The standard specification calls for the test to be run on both dry and wet samples. The wet samples were assumed to be saturated at the minimum and maximum densities. Additional tests were performed at different moisture contents to determine the effect of moisture on the achieved density. Testing for the minimum

density was performed in accordance with ASTM D 4254-91 “Standard Test Method for Minimum Index Density and Unit Weight of Soils and Calculation of Relative Density.”

3.4.2.6 Static Compaction

The static compaction procedure generally followed those outlined in *Soil Mechanics for Road Engineers* (1952). The compaction on the RAP was performed using three layers. Each layer was compacted to the desired test pressure using a universal testing machine. The load was increased to the specified compaction pressure, held for 15 seconds, then released slowly over a 15 second period. Pressures of 212, 400, 700 and 1000 psi were used for this study.

3.4.3 Compaction Methods Summary

Tables 3.2 and 3.3 are a summary of the specifications for the compaction tests performed to prepare the LBR samples. All molds had the same diameter. The vibratory compaction mold has a height of 5.08 inches (12.90 cm).

Table 3.2 Summary of Specifications Used for Proctor and Impact Test Methods

Description	Test Method			
	Standard	Modified	Double Modified	Modified Marshall
Specification	AASHTO T99	AASHTO T180	N/A	N/A
Mold Volume, ft^3 (m^3)	1/13.33 (1/470)	1/13.33 (1/470)	1/13.33 (1/470)	1/13.33 (1/470)
Hammer Weight, lbs (kg)	5.5 (2.5)	10 (4.5)	10 (4.5)	10 (4.5)
No. Layers	3	5	5	5
No. Blows Per Layer	56	56	112	56
Compaction Energy, ft-lb/ft^3 (m-kN/m^3)	12,314 (592)	56,250 (2,693)	111,972 (5,386)	56,250 (2,693)
Mold Diameter, inch (cm)	6 (15.3)	6 (15.3)	6 (15.3)	6 (15.3)
Mold Height, inch (cm)	4.58 (11.6)	4.58 (11.6)	4.58 (11.6)	4.58 (11.6)

Table 3.3 Summary of Specifications Used for Vibratory and Static Test Methods

	Test Method	
Description	Vibratory	Static
Compaction Energy	0.013 inch amplitude @ 60 Hz w/ 2 psi surcharge	212, 400, 700, 1000 psi
No. of Layers	1	3
Mold Volume, ft^3 (m^3)	1/9.78 (1/345)	1/13.33 (1/470)
Mold Diameter, inch (cm)	6 (15.93)	6 (15.3)
Mold Height, inch (cm)	5.08 (12.90)	4.58 (11.6)

3.5 Moisture-density characteristics of RAP

3.5.1 Standard, Modified and Double Proctor

A moisture-density relationship, for both of the post milled processed RAP's, compacted using AASHTO-T180 modified Proctor energy, is presented in Figure 3.6. RAP compacted using Proctor methods display an undefined moisture-density peak similar to that displayed by the sand. Both hammermill and tubgrinder processed materials achieved a relatively constant density at moisture contents greater than 5

percent, however, sands tend to have a greater reduction in density at the higher moisture contents. RAP samples prepared with moisture contents greater than 10% before compaction had water drain out on the base of the mold during compaction. The resulting compacted moisture content was less than the targeted water content.

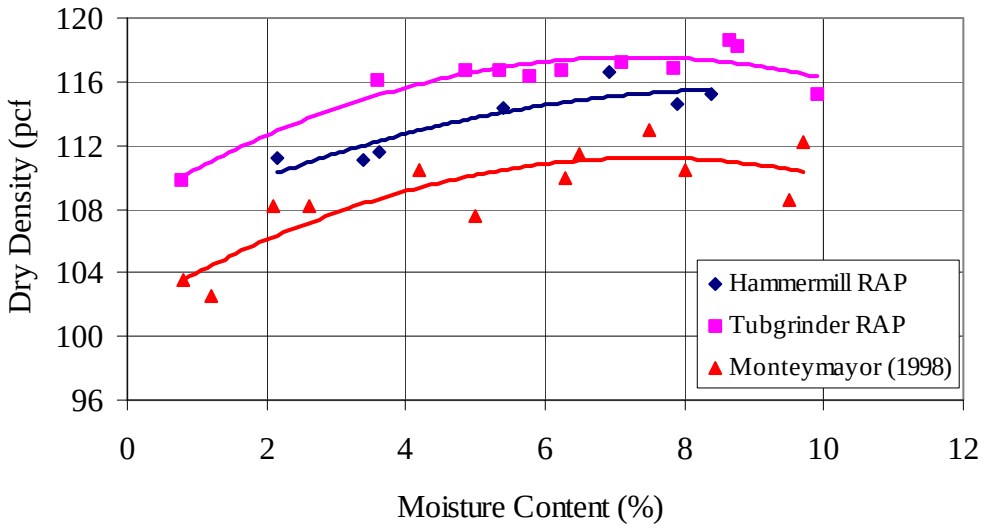

Figure 3.6 Moisture density curve for RAP. (1 pcf = 0.157 kN/m^3) using modified Proctor (AASHTO- T180) method.

RAP compacted at moisture contents less than 5% yielded a lower dry density than RAP compacted at moisture contents from 4% to 8%. The tubgrinder material, which classified as poorly graded, had greater dry densities than the well graded hammermill material. In general well-graded sands achieve greater compacted densities than poorly graded sands (Barksdale, 1991). The slight gap grading of hammermill RAP may have caused the lower densities. The unprocessed RAP used by Montemayor (1998) displayed compacted dry densities approximately 3 to 6 pcf less than the postmilled

processed RAP, however, the shape of the moisture-density curves were very similar. Processing of the RAP increased dry density. Compaction moisture contents in excess of 5% would be recommended.

3.5.2 Modified Marshall Compaction

The RAP material was compacted using a Marshall hammer with an enlarged striking plate. Figure 3.7 illustrates the results obtained. The RAP showed very slight increases in density with a change in dry density of 2 to 4 pcf as a function of moisture content. At moisture contents of 4 to 8% the dry density remained relatively constant, varying by about 2 pcf. Samples prepared at moisture contents greater than 10 percent were observed to have water forced out of the sample during compaction. The moisture density relationship of RAP compacted using this method were similar to relationships obtained from the modified Proctor compaction. Unlike the RAP compacted using Proctor and vibratory methods, the hammermill RAP compacted using the Marshall method had greater compacted dry densities than the tubgrinder RAP. The compacted dry densities compared reasonably well, within 2 pcf, with the RAP compacted using the Proctor methods. The higher compacted dry densities were obtained between 3 and 9% moisture contents.

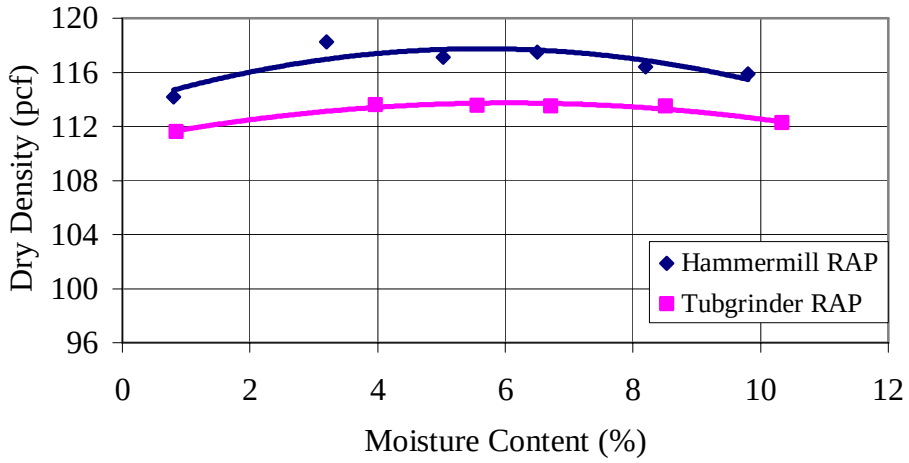

Figure 3.7 Moisture density relationships for RAP using the modified Marshall compaction method. (1 pcf = 0.157 kN/m^3)

3.5.3 Vibratory Compaction

Mechanical relative density equipment was used to evaluate the influence of vibratory compaction on the postmilled RAP. The moisture density relationships from the testing of the RAP samples are shown in Figure 3.8. RAP at very low moisture contents (dry) and at very high moisture contents wet had the greatest compacted dry density. Sand soils usually exhibit highest dry density at a moisture content of zero, followed by decreases and then increases in dry density as the moisture content increases (Mitchell, 1977). The RAP material showed similar behavior as seen in Figure 3.8 with density variations of 10% as a function of moisture content.

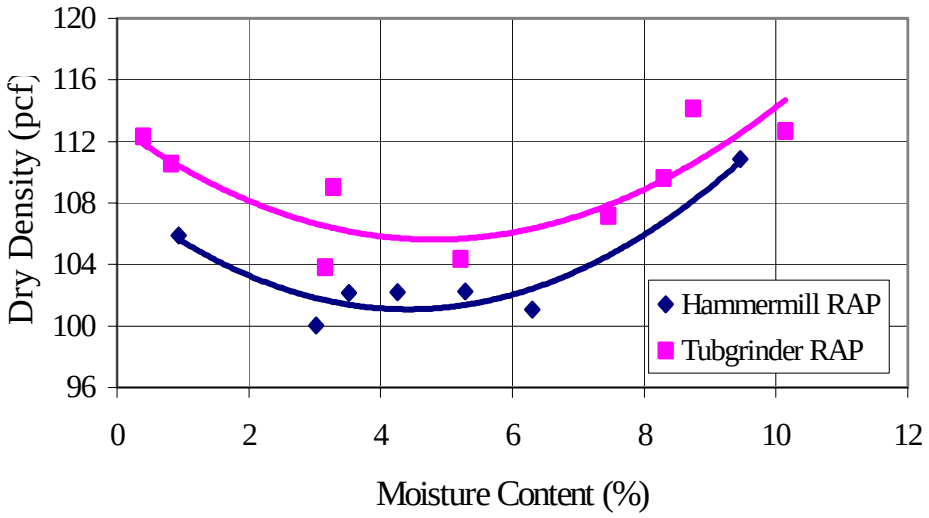

Figure 3.8 Moisture density curve for RAP compacted using vibratory method. (1 pcf = 0.157 kN/m^3)

With the exception of Marshall compaction, tubgrinder RAP consistently had a dry density slightly greater than the hammermill RAP. This behavior was observed in the same manner as the Proctor test data and believed to be due to the gap graded characteristics of the hammermill RAP.

3.5.4 Static Compaction

Static compaction moisture density relationships were developed using 212, 400, 700, and 1000 psi pressures. RAP samples compacted at water contents above 9% had a final compacted moisture content below 9% and water was pushed out of the mold during

compaction. Figures 3.9 and 3.10 displays the results achieved for the hammermill RAP and the tubgrinder RAP respectively. A trend line was fitted to the data in Figures 3.9 and 3.10. The compacted samples displayed no definable optimum moisture content. Higher static compaction pressures yielded variations in dry density with changes in moisture content. The compacted dry densities varied at each compaction pressure by approximately 4 pcf. As static compaction pressure increased the compacted dry densities increased. The static compaction testing indicates that the RAP can be compacted at field moisture contents ranging from 2 to 6 percent.

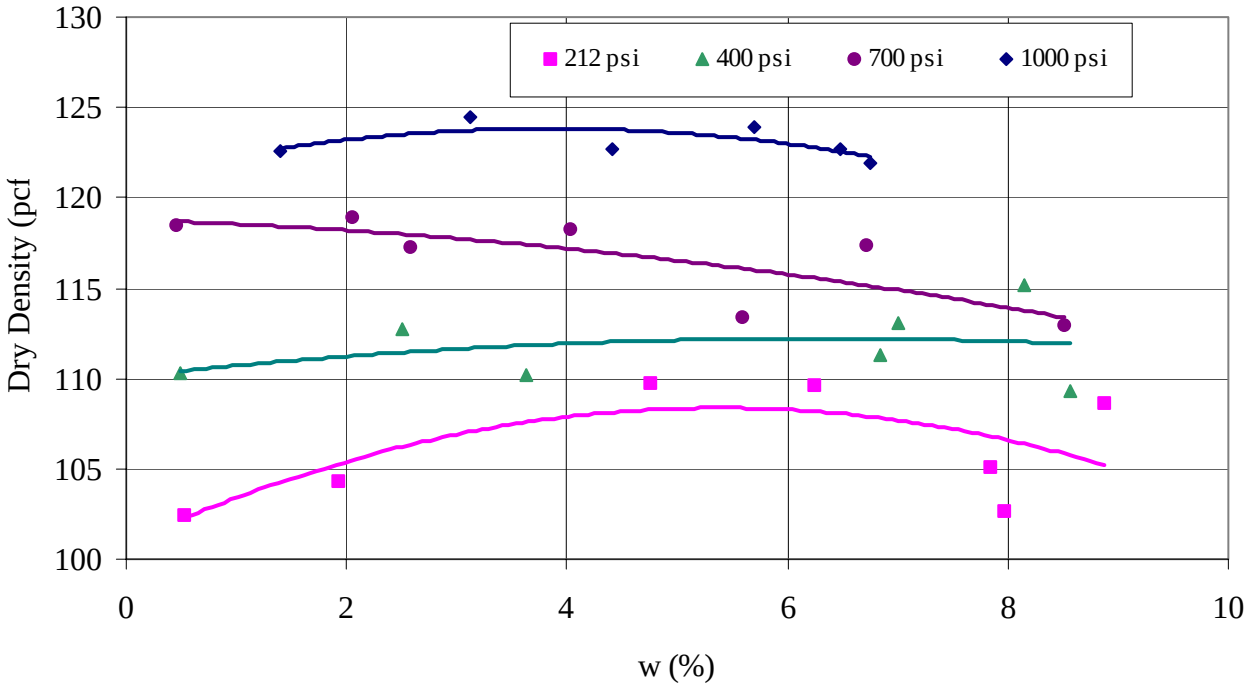

Figure 3.9 Moisture density relationships for hammermill RAP using static compaction method. (1 pcf = 0.157 kN/m^3)

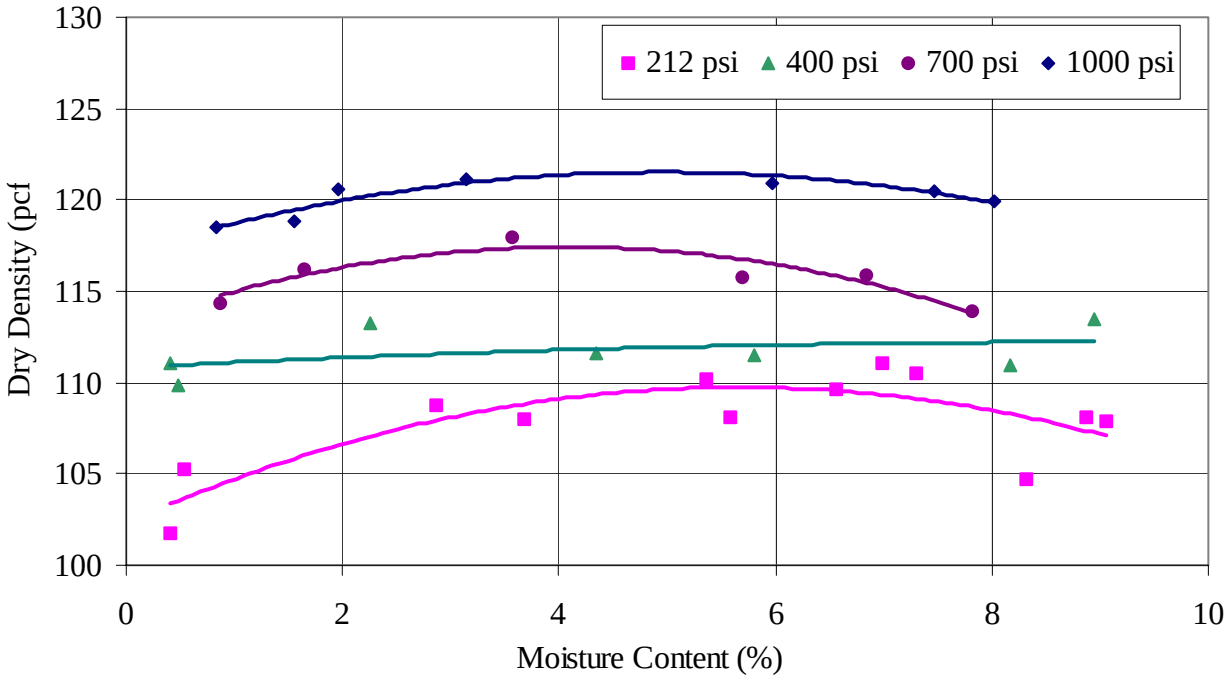

Figure 3.10 Moisture density relationships for tubgrinder RAP using static compaction method. (1 pcf = 0.157 kN/m^3)

Figure 3.11 presents a plot of maximum dry density of both RAP's as function of static compaction pressure. The dry density of the RAP linearly increased with static compaction pressure. Hammermill and tubgrinder RAP compacted at 212, 400, and 700 psi had similar dry densities to each other. The hammermill RAP had slightly higher (2 pcf greater) dry density than the tubgrinder RAP for samples compacted at 1000 psi.

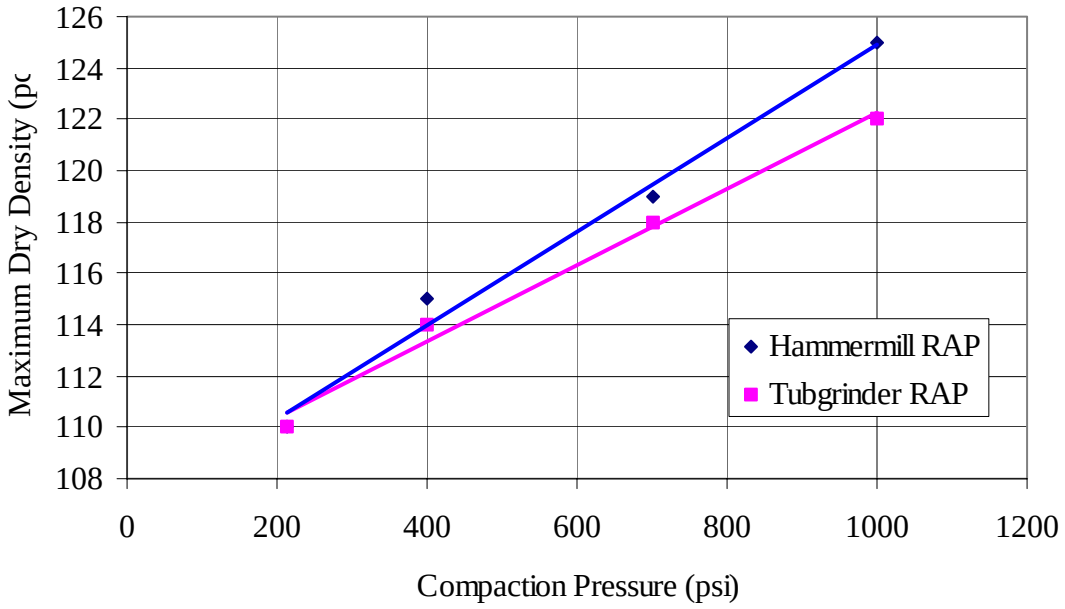

Figure 3.11 Compaction pressure versus maximum dry density of RAP (1 pcf = 0.157 kN/m^3)

3.5.5 Compaction Summary

RAP compacted using Proctor, Marshall, vibratory and static methods did not exhibit a classic moisture density relationship. The dry density was relatively constant at moisture contents greater than 4 percent with all methods. All compaction methods caused water to drain from the RAP during compaction at moisture contents greater than 10 percent. There were very slight differences in dry density due to processing that could be attributed to sampling variation.

3.6 Limerock Bearing Ratio

3.6.1 Methodology

For each compacted sample prepared during the moisture-density testing portion of the study, unsoaked Limerock Bearing Ratio tests were conducted following FM 5-515 September, 1993 standards. LBR testing served to quantify the effects of dry density and moisture content on bearing strength. A surcharge load of 15 lbs. (6.8 kg) was applied for all tests. The FDOT "Standard Specifications for Road and Bridge Construction" (1996) specifies that base materials have a minimum LBR value of 100. Stabilized subgrade and subbase typically have a specified LBR value of 40 and according to FDOT, the minimum LBR is specified by the engineer's pavement design. FDOT further specifies the nominal undervalue of the LBR tests. The LBR testing was conducted on samples prepared in the moisture-density phase of the research. This portion of the research focused on studying the bearing strength effects of amount of compaction energy, temperature during compaction, and the addition of a lubricating substance as the wetting agent. Two complete sets of LBR experiments were conducted to validate the accuracy of results obtained.

3.6.2 Influence Of Compaction Methods On Bearing Strength

The results of the LBR tests on the RAP compacted using modified Proctor, vibratory and modified Marshall are presented in Figures 3.12 and 3.13. The RAP compacted using the vibratory methods had a LBR value slightly greater than the RAP compacted using Modified Proctor method over the range of moisture contents. The RAP compacted by these methods displayed a slight parabolic relationship between the LBR value and moisture content. The exception to this behavior was the tubgrinder RAP compacted using vibration shown in Figure 3.13, which displayed an increase in strength with increasing moisture content.

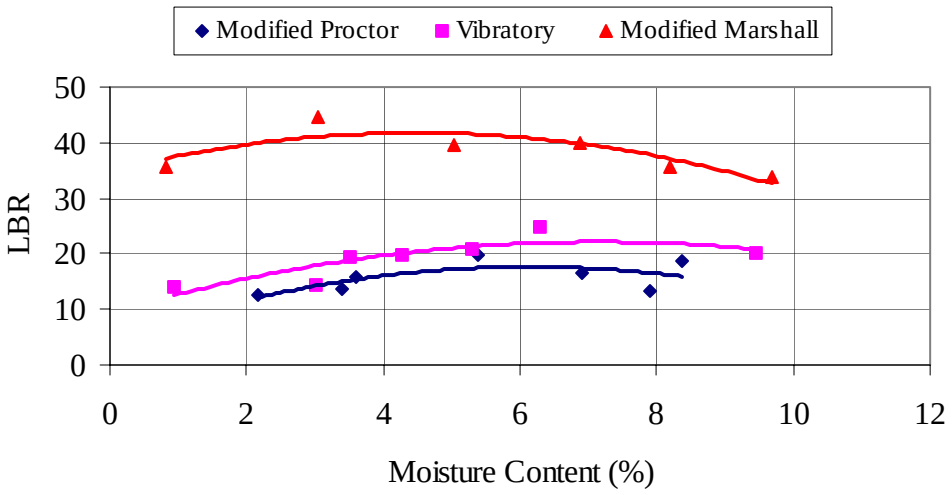

Figure 3.12 Moisture content LBR relationship for hammermill RAP.

RAP samples compacted using the modified Marshall hammer had the greatest bearing strength with a maximum LBR value greater than 40, at optimum moisture contents between 3 – 6 %. The modified Marshall compacted method confines the sample during compaction as compared to the other methods.

Material with LBR values less than 100 can be used for subgrade and subbases if specified by the pavement design. A specified LBR of 40 is typical for compacted subbase material. RAP compacted in the laboratory using the modified Marshall compaction at optimum moisture content does give an LBR greater than 40, for both the hammermill and tubgrinder RAP.

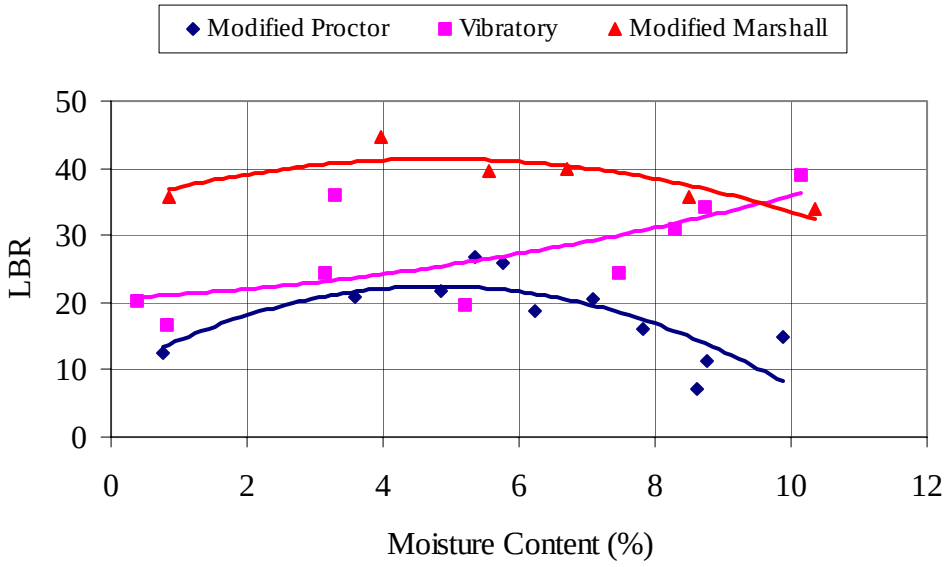

Figure 3.13 Moisture content LBR relationship for tubgrinder RAP.

The LBR values of RAP compacted using static compaction are presented in Figures 3.14 and 3.15

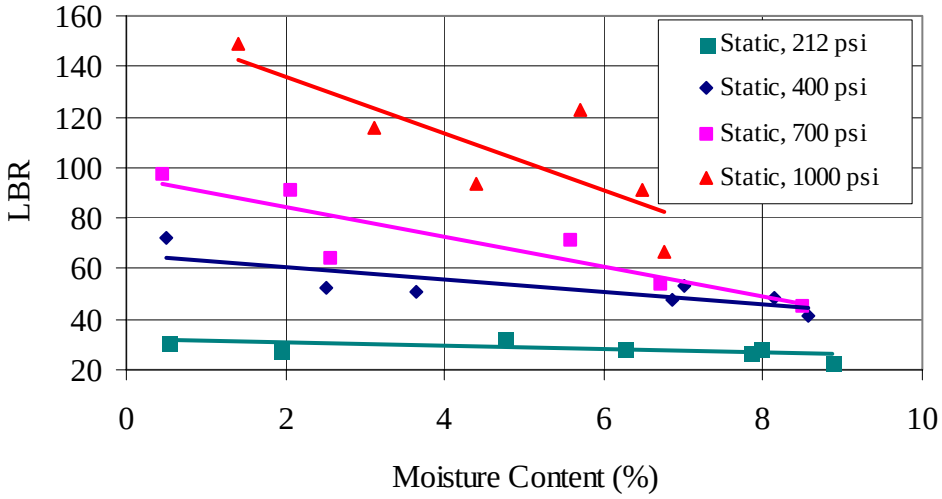

Figure 3.14 Bearing strengths of statically compacted hammermill RAP samples.

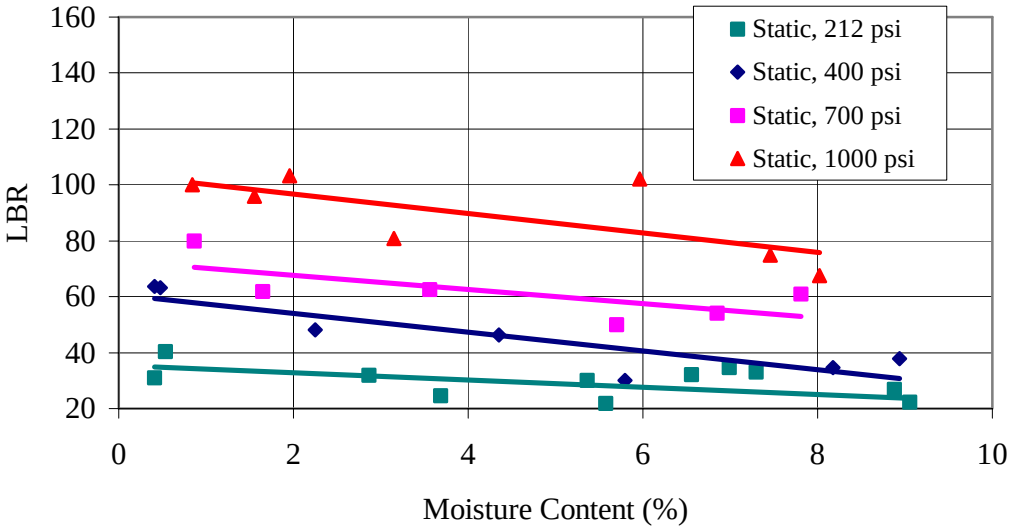

Figure 3.15 Bearing strengths of statically compacted tubgrinder RAP samples

Samples of RAP compacted statically at 212, 400, 700 and 1000-psi pressures displayed decreasing bearing strengths with increasing moisture contents. The trends were slightly more pronounced with the hammermill RAP. The tubgrinder RAP strengths at 1000 psi static compaction were lower than the hammermill strengths. The bearing strengths of the two RAP materials are similar at the lower compaction pressures. The friction energy developed at 1000 psi allowed the hammermill RAP to have a significant increase in strength at the dry condition. Static compaction forces the material together by pressing the material into a mold. The dynamic methods were observed to separate and push the material's grains. The RAP samples compacted dry displayed a structure change, exhibited by the increase in bearing values. It was theorized that the static method allowed for increased binding contact between the RAP grains to cause the sample to re-agglomerate. This is also displayed at the lower moisture contents, as the increase in strength, under increasing compaction pressure, is greater than at the higher moisture contents. Static compaction generated consistent densities over a range of moisture contents, however the bearing strengths of the samples decreased with increasing moisture content. Figure 3.16 displays the decreasing strength trend for the hammermill RAP samples. The decrease in strength with increased moisture content becomes less pronounced at the lower compaction pressures.

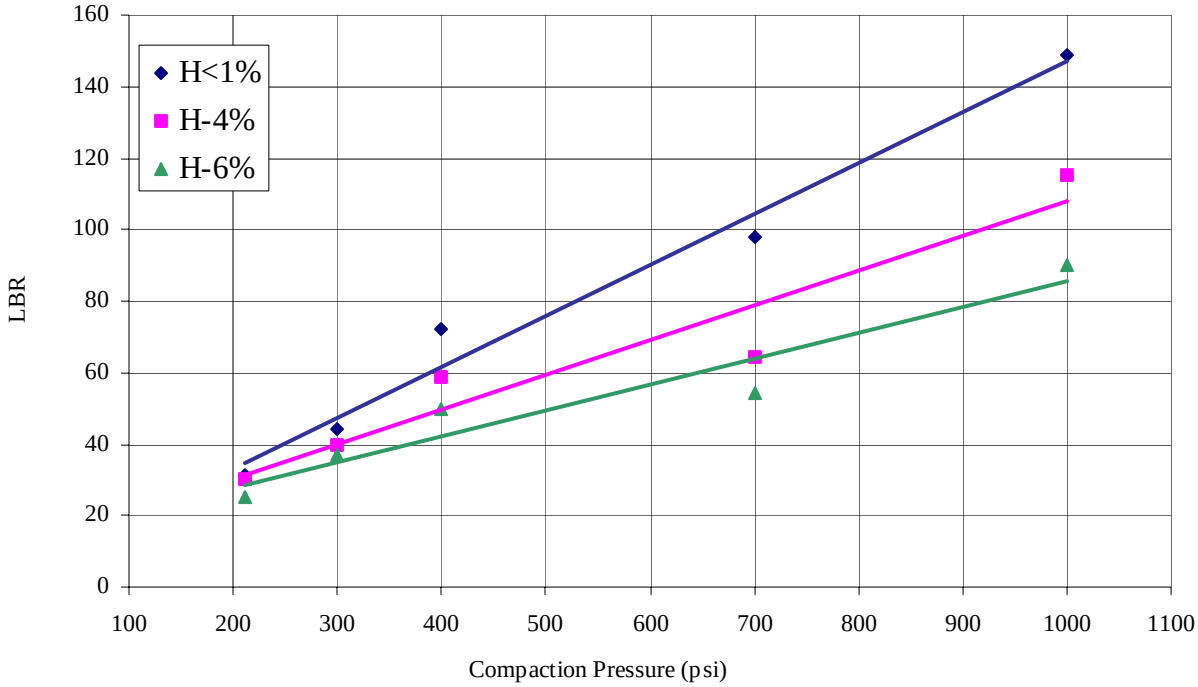

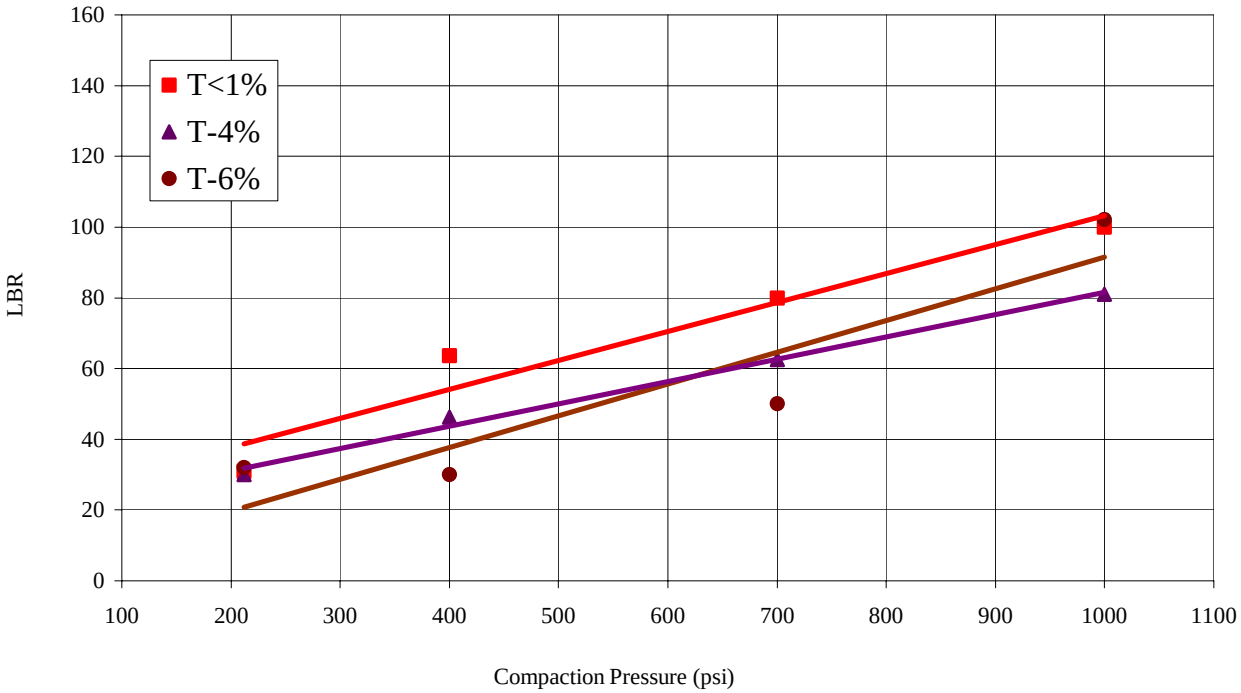

Figure 3.16 Compaction pressure versus LBR value of RAP at different moisture contents. (1 psi = 6894.8 Pa)

The range of bearing strength of the RAP compacted at 1000 psi was between 150 and 80. The LBR value range for samples compacted at 212 psi was between 40 and 20. An increase in compacted moisture content reduced the bearing strength of the RAP. RAP compacted statically at 400 psi had dry densities (range of 110 to 112 pcf) that were similar to the RAP compacted using the modified Proctor (112 to 115) and modified Marshall (116 to 118) methods. Figure 3.17 shows the difference in bearing strength as illustrated by LBR values between the compaction methods with similar dry density.

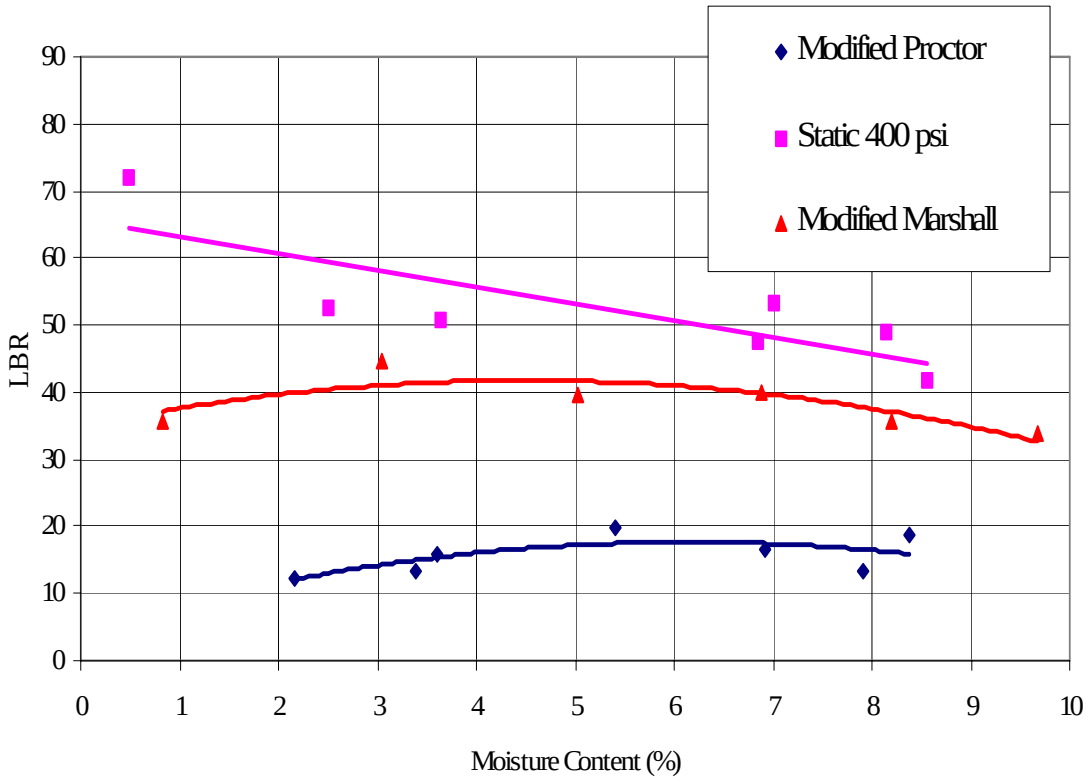

Figure 3.17 RAP compacted with static and modified Proctor and modified Marshall methods with similar densities.

The LBR values of the RAP compacted using either the static or modified Marshall method were greater than 40 for most moisture contents. Since the densities of the three materials are similar, the differences in LBR are attributed to the structure or the binding of the asphalt occurring during confined compaction. Decreasing the moisture content of the RAP that was compacted statically increased the bearing strength.

The moisture content of the samples compacted using modified Proctor or modified Marshall methods had little or no effect on the strength. RAP samples compacted dry using the Proctor compaction methods could not be tested for strength, as they would "fall" out of the mold. The samples statically compacted dry had the largest strengths and were observed to adhere to the mold.

3.6.3 Effects Of Compaction Method On Bearing Strengths

The effects of compaction method were compared to the bearing strength as measured by the LBR test for the RAP. Figure 3.18 displays the range of bearing strengths, as measured by the LBR value, for the hammermill and tubgrinder RAP.

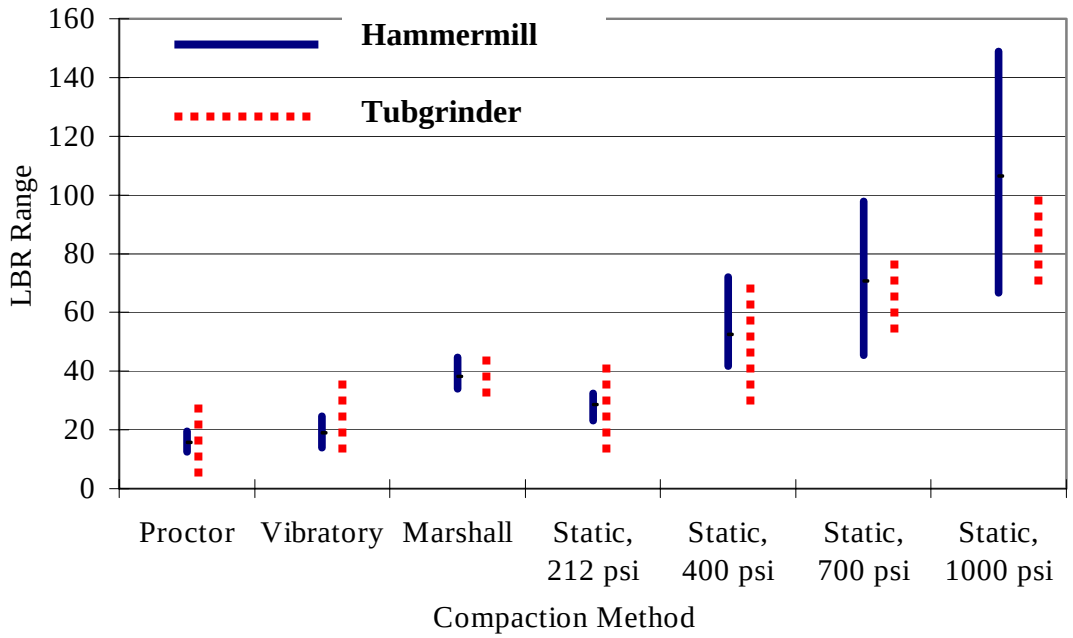

Figure 3.18 Range of bearing strengths for hammermill RAP compared to compaction method.

The post milling processes of the RAP had little effect on the final LBR value as can be seen by the overlap of the values. For both materials, the bearing strength of RAP compacted using Proctor, vibratory, modified Marshall and 212 psi static were less than 45. The modified Marshall compaction method yielded the highest LBR values for a dynamic compaction method. This is attributed to the confinement provided by the plate during compaction. Both the hammermill

and tubgrinder RAP samples displayed an increase in strength, as measured by the LBR value, when compacted statically. The minimum LBR value for soil used as a base in the state of Florida is 100. This was only reached by compacting the RAP statically at an applied pressure of 1000 psi. An apparent change in the structure of the RAP occurred as the samples were statically compacted at greater pressures.

3.6.4 Effects Of Dry Density On Bearing Strength

The methods used to compact the RAP samples yielded a range of compacted dry densities between 100 and 125 pcf. As the dry density increases an increase in the bearing strength occurs, shown in Figure 3.19. To yield the required LBR strength of 100 for base courses, a density greater than 118 pcf had to be reached. These densities were only reached using the static method with a compaction pressure of 1000 psi.

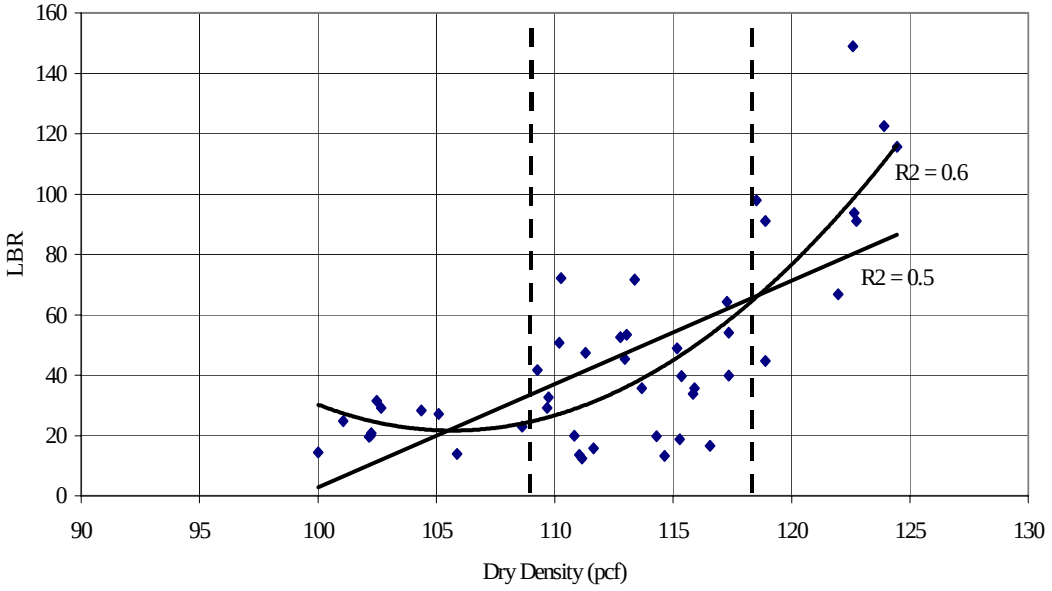

Figure 3.19 LBR versus dry density of RAP. (1 pcf = 0.157 KN/m^3)

Three distinct zones are shown in Figure 3.19. RAP samples with a compacted dry density below 109 pcf had LBR values below 30. RAP compacted to a dry density between 109 and 118 pcf had an LBR's from 10 to 75. The samples compacted statically typically had the larger LBR values. All samples with compacted dry density above 118 pcf had LBR values greater than 40, and as high as 149. Again, the higher LBR values occurred due to static compaction rather than the dynamic, vibratory or Proctor compaction methods. This trend seemed to indicate that a change in structure or binding with asphalt, increasing the bearing strength of the RAP, occurs by compacting statically at greater pressures.

3.7 Strength Deformation Testing

3.7.1 Methodology

Triaxial tests were performed on compacted RAP samples stored for four different durations of time (0,10, 20, and 30 days) and for three different temperatures: 75°F, 100°F, and 125°F (23.9, 37.8 and 51.7°C). Room temperature was 75°F (23.9°C). The samples at 100°F (37.8°C) and 125°F (51.7°C) were stored in an oven for the required amount of time. Table 3.4 shows the tests that were performed. A total of 63 samples were prepared of which three samples were duplicates. After removal from the oven, samples were cooled to room temperature, prior to testing under triaxial conditions. The testing program was developed and performed according to appropriate ASTM standards.

Table 3.4 Variables used in Testing Program. (1 psi = 7 kPa)

Variable	Test Condition		
RAP Type	Hammermill and Tubgrinder		
Temperature (degrees F.)	75	100	125
Storage Time (days)	10	20	30
Confining Pressure (psi)	5	10	15

3.7.2 Sample Preparation

Mechanical energy has been used to densify and increase the soil bearing strength of the soils (Holtz and Kovacks, 1981). All samples in the testing procedure were compacted to a target moisture content of 6%. Moisture content samples were found to be dry and no further loss of moisture content was observed after drying for 24 hours at 100°F. Montemayor (1998) reported that Proctor methods of compaction have minimal effects on the moisture content and dry density relationship of RAP. Garg and Thompson (1996) suggest that the optimum moisture content for RAP is seven percent. Palise (1994) reports an optimum moisture content of 5.5%.

Triaxial samples should have a height to diameter ratio of 2 to 1 or greater in order to reduce error (Bishop and Henkel, 1964). This minimizes the interference of potential shear cones and end-friction against the testing caps (Fwa, et al; 1994). Each compacted sample for triaxial testing was 8.5 inches (21.6 cm) high and 4 inches (10.2cm) in diameter. The compaction mold for fabricating triaxial samples has different dimensions than that of the modified Proctor compaction mold. Even though the mold dimensions are different, similar compaction energies were used. Every other aspect of the procedure was performed in accordance with ASTM D1577 “Moisture Density Relations of Soils

and Soil-Aggregate Mixtures Using a 10-lb (4.5 kg) Manual Rammer and an 18 inch (45.7 cm) Drop."

In order to achieve a similar energy level the number of layers used during compaction was adjusted. The compaction energy (E) for the modified Proctor test was determined.

Particles larger than 3/4-inch (1.9 cm) were removed to allow for proper compaction. This limit is recommended by Bishop and Henkel (1964) to prevent gaps from forming along the edges of the sample. To assist in creating the smooth contact areas at the top and bottom layers of the sample that are critical in the triaxial test, these layers were prepared using material that would pass the 3/8-inch (0.96cm) sieve.

To determine densities the samples were weighed and removed from the mold by using a hydraulic jack. Major density changes were not expected from this procedure because the samples were jacked out slowly and because the material was stiff. The dimensions of the sample were measured when it was removed from the mold. A typical test specimen of RAP is shown in Figure 3.20

Figure 3.20 Typical Test RAP Specimen on the Triaxial Base.

3.1.1 Triaxial Testing

Three triaxial tests were performed for each time and temperature variable. The confining pressures (σ_3) used were the traditional values of 5, 10, and 15 psi (35, 70, and 105 kPa). Water was used as the chamber fluid for applying the confining pressure. The samples were not saturated and were sheared rapidly.

The sample was placed on the triaxial base plate on top of the bottom and covered with a rubber membrane that seals the sample from water. O-rings in tension were used to seal the membrane on the top and bottom of the sample. A thin, 1/8 inch (0.3 cm) rubber spacer with a 4-inch (10.2 cm) diameter was used between the base and the sample and between the sample and the top cap. This was done to improve the contact areas at the top and bottom of the sample. Figure

3.20 shows the sample on top of the base prior to testing. Figure 3.21 shows a schematic diagram of the triaxial apparatus.

The triaxial chamber was placed around the sample and the loading piston was checked for good contact with the top cap. Then the triaxial set-up was transferred to the loading machine to begin the test. The “Brainard-Kilman S-610” triaxial apparatus was used with the “Brainard-Kilman S-500” triaxial/permeability panel and the “Brainard-Kilman E-214” load cell to conduct the test. Figure 3.22 shows the entire assembled triaxial apparatus on the loading machine.

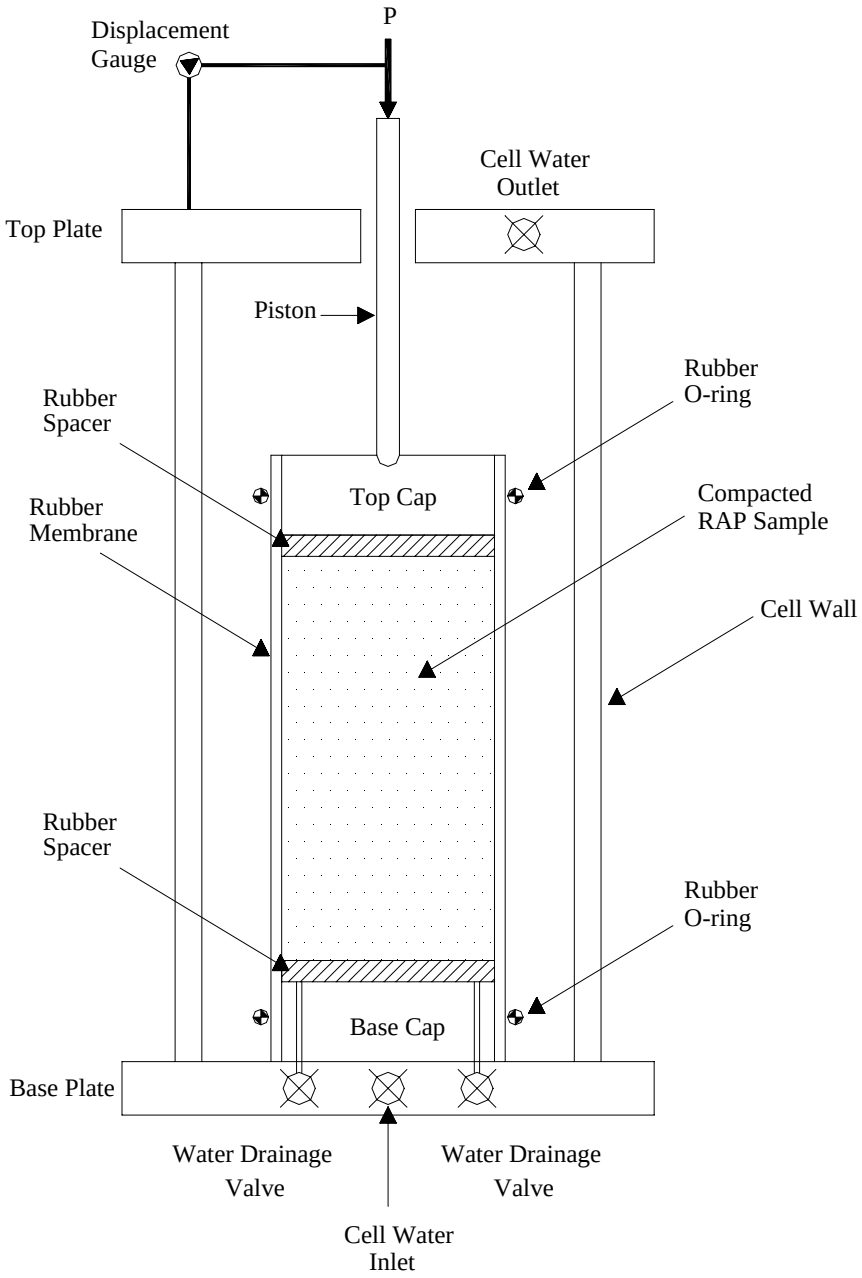

Figure 3.21 Schematic Diagram of the Triaxial Chamber.

Figure 3.22 Assembled Triaxial Apparatus on Loading Machine

The axial deviator stress was applied through the ram acting on the top cap, at a constant rate of 0.01 inches/minute (0.06 cm/min). Load and vertical displacement readings were taken at predetermined strain intervals. Data was input to MS-Excel and reduced to provide stress-strain curves. Secant elastic moduli were determined using the stress-strain charts. Failure envelopes were found to determine the angle of friction (ϕ) and the cohesion (c).

3.8 Triaxial Characteristics

All RAP samples for testing were compacted, using modified dynamic compaction equivalent energy. Triaxial samples were prepared at a moisture content of 6% with the objective of achieving a specified dry density. Table 3.5 shows the variability in results for moisture and density for both hammermill and tubgrinder RAP.

Table 3.5 Standard Deviation, Average and Median for Moisture Density Data for Hammermill and Tubgrinder RAP. (1 pcf = 0.157 kN/m^3)

	Moisture Content (%)		Dry Density (pcf)	
	Hammermill	**Tubgrinder**	**Hammermill**	**Tubgrinder**
Average	5.5	6.6	117.7	121.1
Standard Deviation	0.5	1.1	2.0	0.8
Median	5.5	6.3	117.3	121.2

Tubgrinder RAP's moisture content was 1% higher than hammermill's. The average dry density for hammermill RAP was almost 118 pcf (18.4 kN/m^3) while the average density of tubgrinder RAP was 3% higher. This resulted from the presence of approximately 10% higher content of the coarse sand size (between 2 mm and 0.425 mm) in the tubgrinder material.

As seen in Table 3.5, the hammermill and tubgrinder RAP had very little variance in moisture content or dry density values. The material can be compacted to a desired density with minimal concern for moisture content. Hammermill's standard deviation is greater for the dry density values while the tubgrinder's moisture content has a higher standard deviation than hammermill's. The data is consistent because the median and the average values are all very similar.

3.8.1 Stress versus Strain

A stress versus strain curve was developed for each RAP triaxial sample. Figure 3.23 shows an example of the stress versus strain curves for three samples at increasing confining pressures and with the same time and temperature characteristics. On each plot the maximum dry density and the moisture content were recorded. The total principal stress at failure and the secant modulus of elasticity were determined. The example used in Figure 3.23 was hammermill RAP stored for 10 days in the oven at 100°F (37.8°C). The stress strain curves for the other tests are shown in Appendix A and were used to determine the triaxial characterization of RAP.

The modulus of elasticity was calculated using two different methods. The first value reported ($E_{initial}$) is for the modulus of elasticity found by using the initial tangent method. It was found by drawing a line tangent to the initial portion of the stress-strain curve and calculating the slope of this line. The second value of modulus of elasticity, secant modulus, is the slope of a line drawn from the point on the curve where the stress is half of the maximum stress to the origin. The results of secant modulus will be discussed later in this chapter.

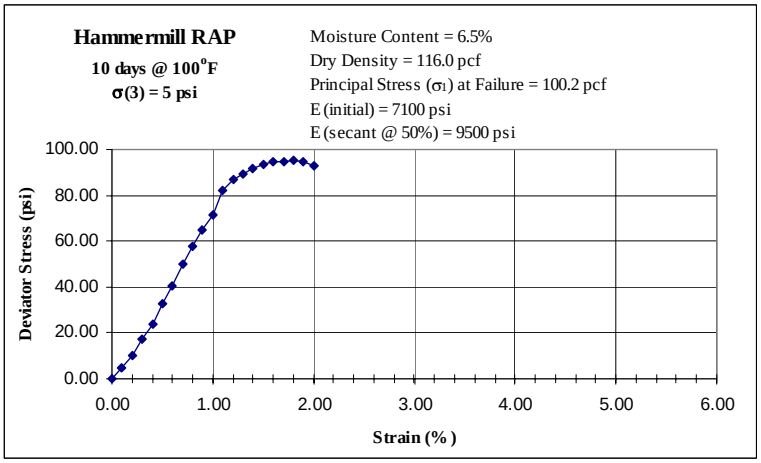

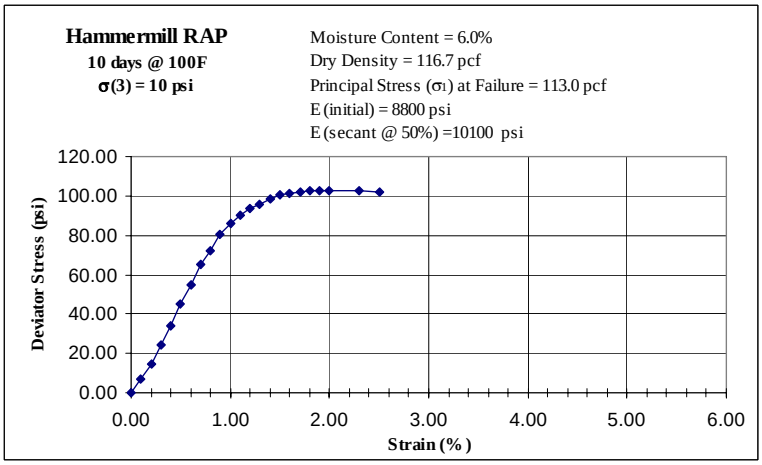

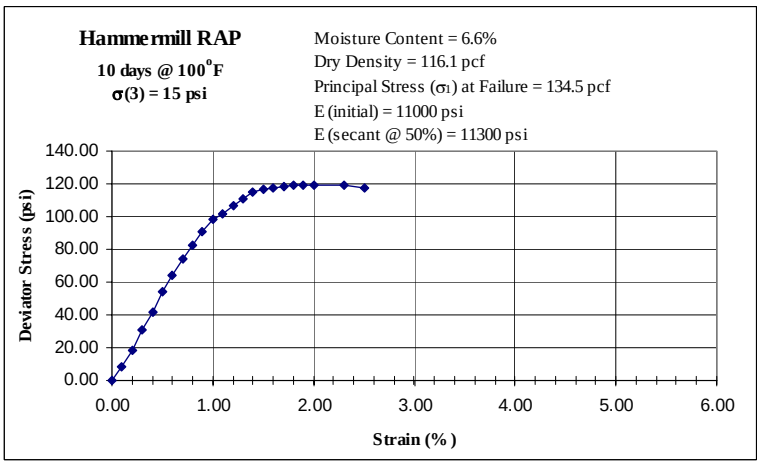

Figure 3.23 Triaxial Test Results for Hammermill RAP Stored at 100°F (37.8°C) for 10 Days. (1 psi = 7 kPa and 1 pcf = 0.157 kN/m^3)

3.8.2 Maximum Stress at Failure

Figures 3.24 through 3.26 present the maximum principal stress at failure for hammermill RAP and tubgrinder RAP at 10, 20 and 30 days of storage as a function of storage temperature. These figures also show the influence of confining stress.

The maximum principal stress at failure is higher for tubgrinder RAP than it is for hammermill at all storage times and temperatures. Tubgrinder RAP is consistently 10-30 psi (70 – 210 KPa) stronger than hammermill RAP. At every equivalent point in Figures 3.24 to 3.26, where the major difference between tests is the post milling processing of the material, tubgrinder RAP withstands higher maximum stress levels. Tubgrinder samples had a higher coarse sand content and slightly higher density than hammermill samples. This is believed to be the reason the tubgrinder samples exhibit greater strength than hammermill samples.

Examination of individual figures indicates the maximum principal stress at failure for the RAP increases with confining pressure. The increase in confining pressure created a very uniform increase in maximum principal stress at failure.

For both the hammermill and tubgrinder processes the maximum principal stress at failure was achieved at a temperature of 100°F (37.8°C). Samples tested at 100°F (37.8°C) were 30 to 60 psi (210- 420 kPa) higher than samples tested at 75°F (23.9°C). When RAP samples were tested at 125°F (51.7°C), the maximum principal stress at failure decreased by 2 to 12 %. Hammermill RAP at 30 days was the only test condition that caused continual increase in maximum principal stress at failure, with an increase in temperature from 100°F to 125°F (37.8°C to 51.7°C) for all three confining pressures.

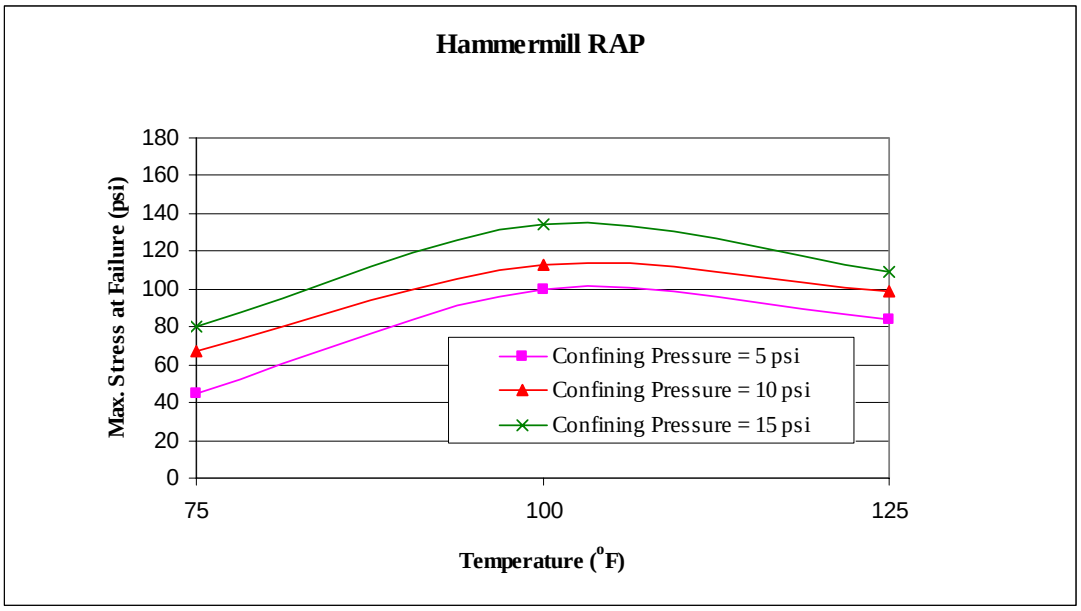

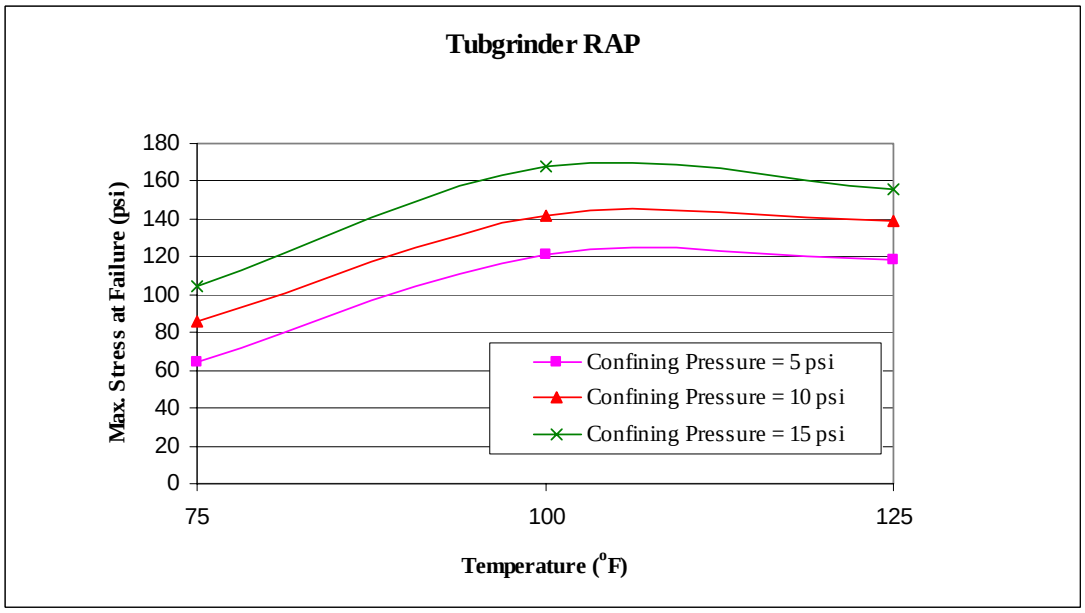

Figure 3.24 Maximum Stress (σ_1) vs. Temperature for Three Confining Stresses for Hammermill and Tubgrinder RAP Stored for 10 Days. (1 psi = 7 kPa)

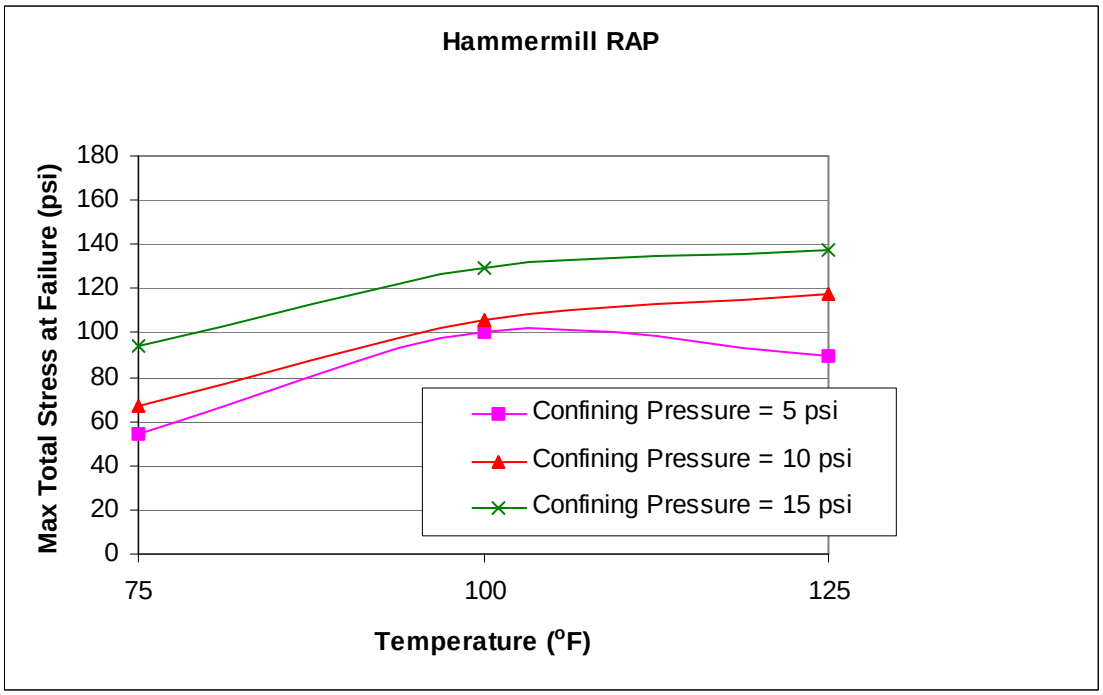

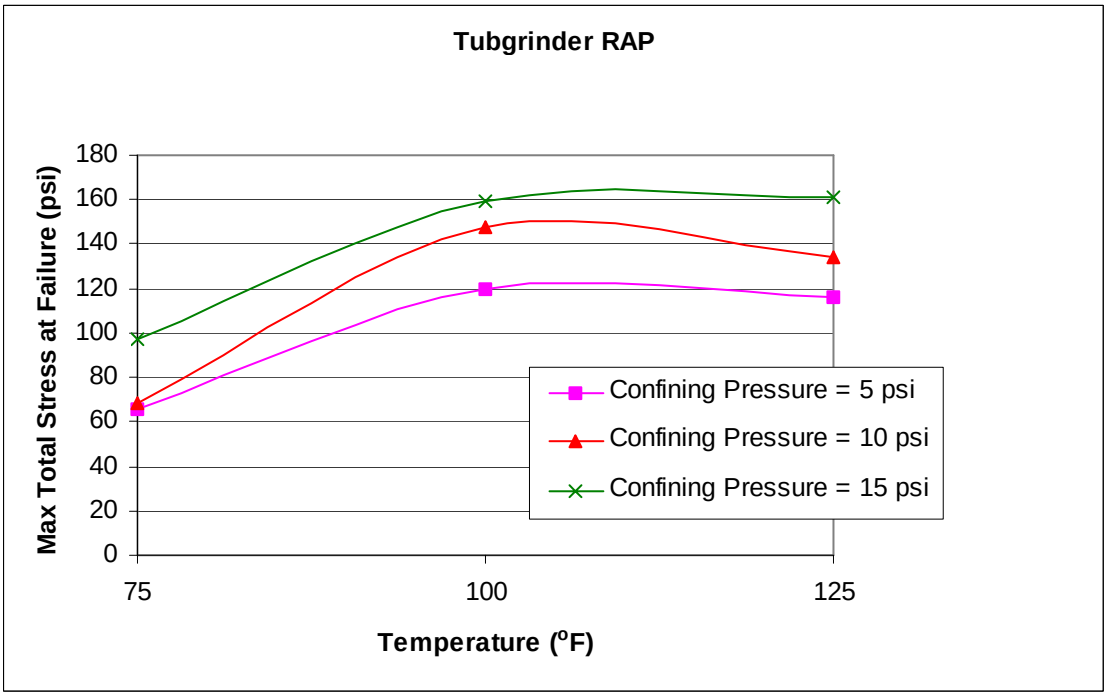

Figure 3.25 Maximum Stress (σ_1) vs. Temperature for Three Confining Stresses for Hammermill and Tubgrinder RAP Stored for 20 Days. (1 psi = 7 kPa)

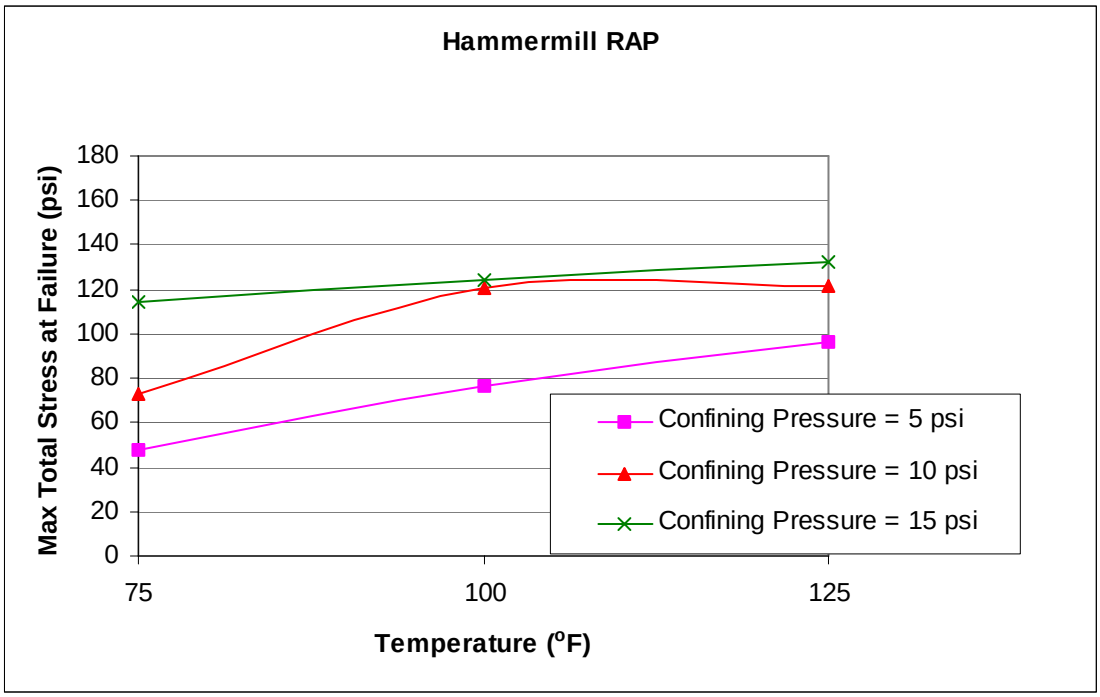

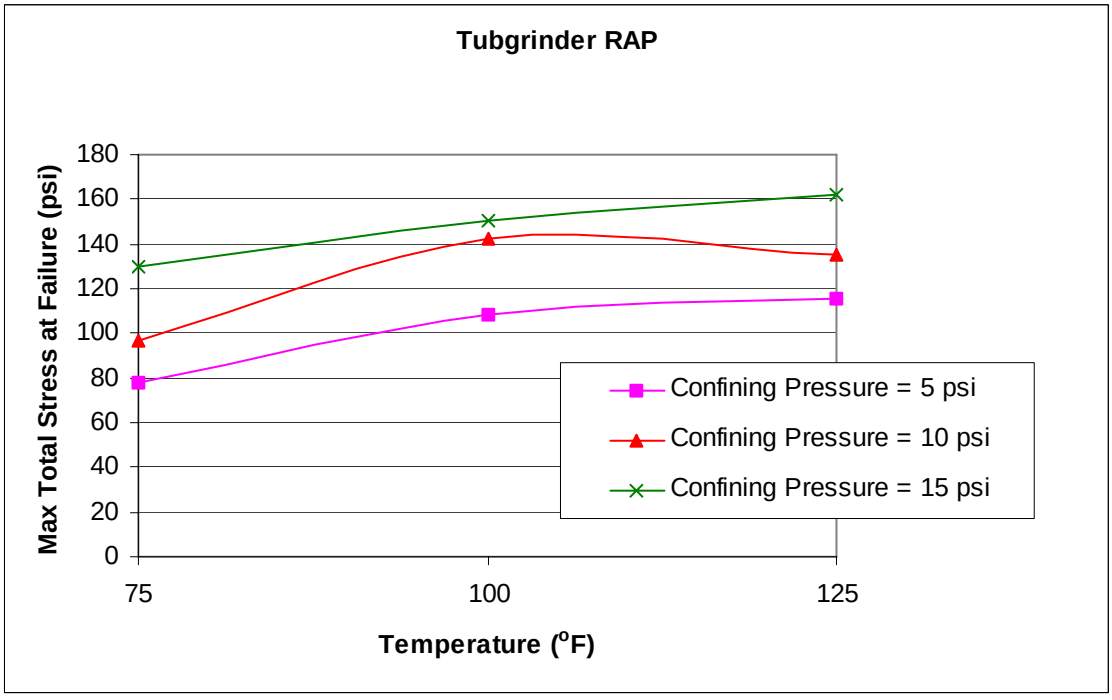

Figure 3.26 Maximum Stress (σ_1) vs. Temperature for Three Confining Stresses for Hammermill and Tubgrinder RAP Stored for 30 Days. (1 psi = 7 kPa)

Figures 3.27 through 3.29 present the relationship of maximum principal stress at failure for hammermill and tubgrinder RAP at confining pressures of 5 psi, 10, psi and 15 psi (35, 70, and 105 KPa) as a function of storage time. The figures also show the influence of storage temperatures. Since the curves are parallel to the time x- axis, the length of storage time does not greatly affect the maximum stress of RAP at any temperature.

To summarize, the maximum principal stress at failure is higher for tubgrinder RAP than it is for hammermill RAP, and for both materials the stress increases with increasing confining pressure and with increased temperature. The duration of storage time does not affect the maximum stress of the RAP.

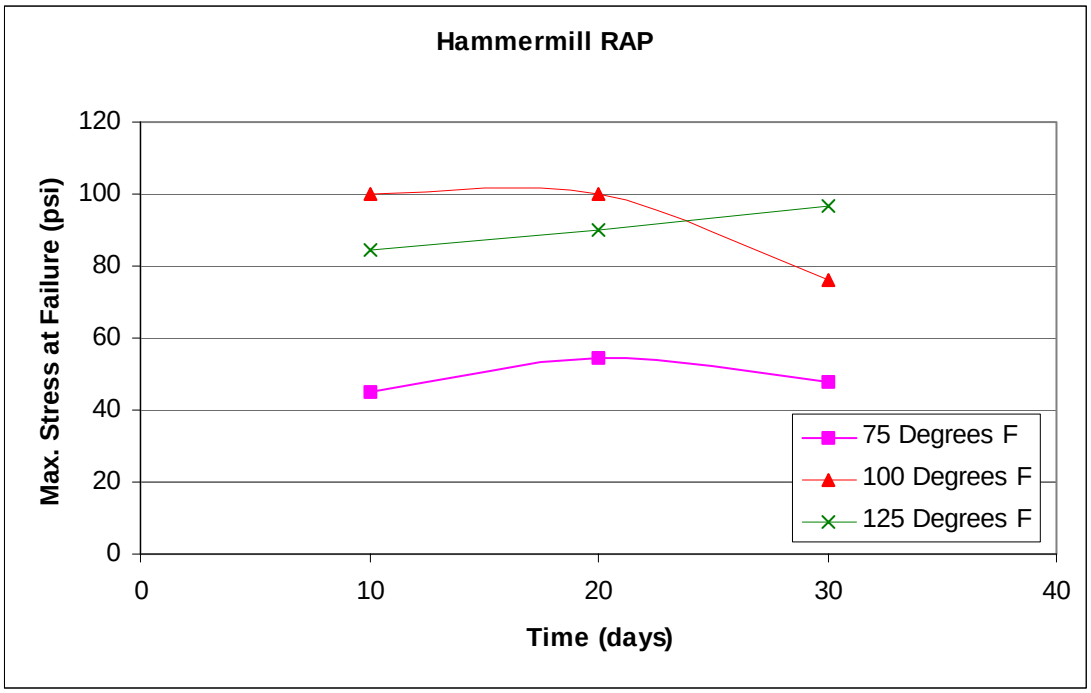

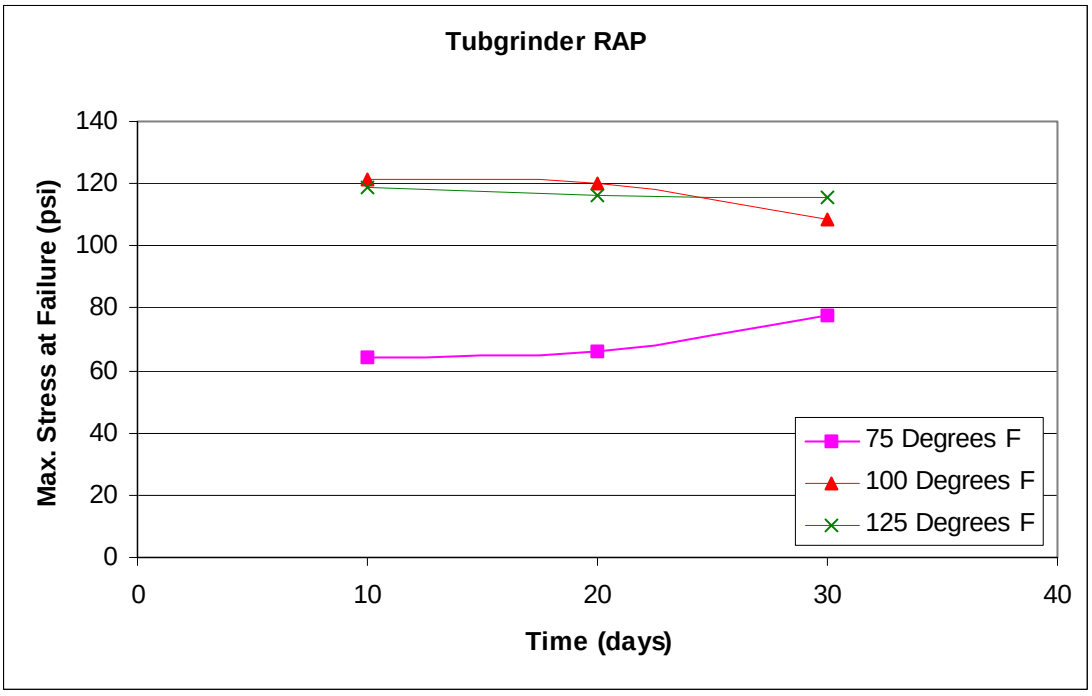

Figure 3.27 Maximum Stress (σ_1) vs. Storage Time for Three Temperatures for Hammermill and Tubgrinder RAP at Confining Pressure of 5 psi. (1 psi = 7 kPa)

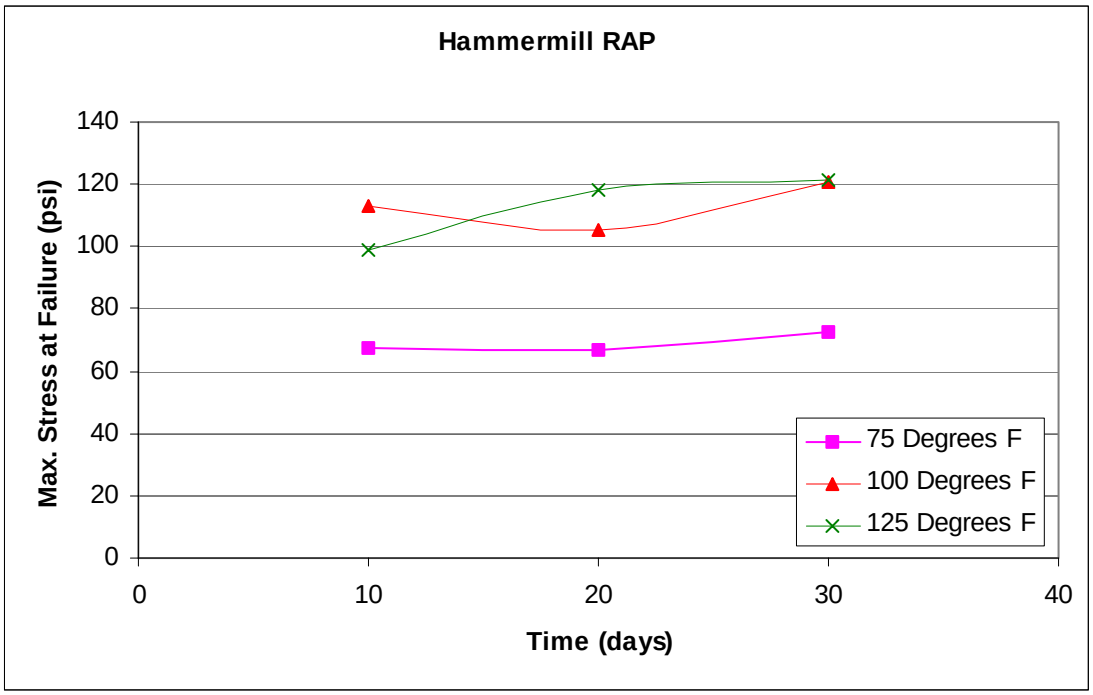

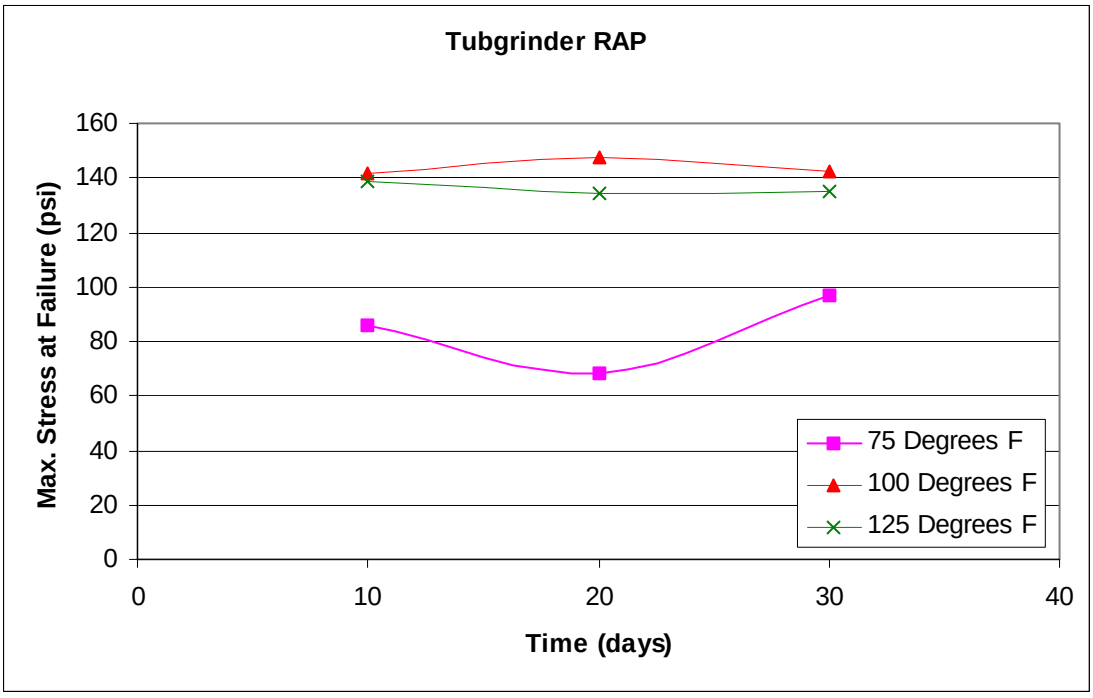

Figure 3.28 Maximum Stress (σ1) vs. Storage Time for Three Temperatures for Hammermill and Tubgrinder RAP at Confining Pressure of 10 psi. (1 psi = 7 kPa)

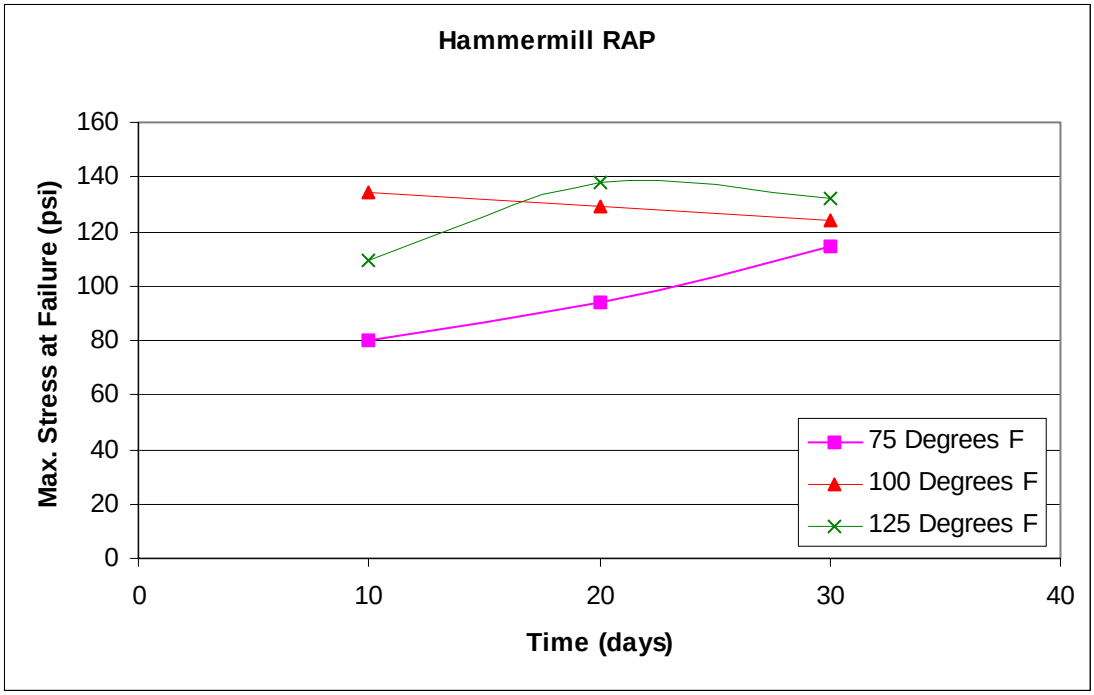

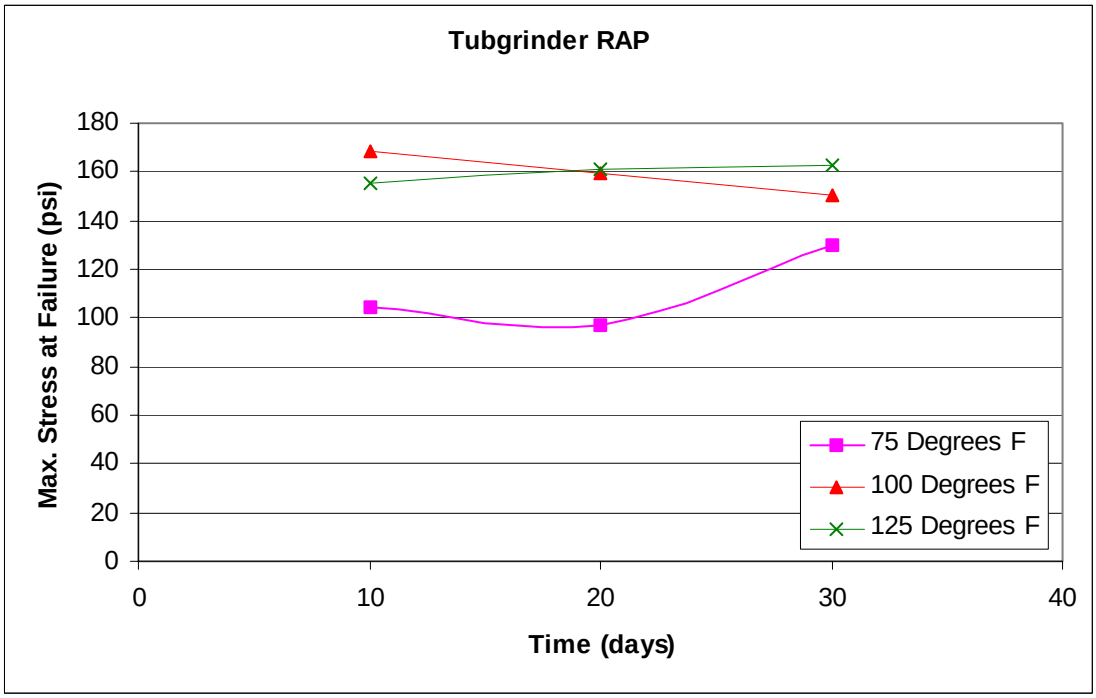

Figure 3.29 Maximum Stress (σ_1) vs. Storage Time for Three Temperatures for Hammermill and Tubgrinder RAP at Confining Pressure of 15 psi. (1 psi = 7 kPa)

3.8.3 Modulus of Elasticity – Secant Method

Figures 3.30 through 3.32 present the modulus of elasticity values determined using secant method for hammermill and tubgrinder RAP. The secant modulus at 10, 20 and 30 days of storage as a function of storage temperature is shown.

Tubgrinder RAP is 2000 to 6000 psi (14,000 to 42,000 kPa) stiffer than hammermill RAP. As stated earlier, tubgrinder samples had more coarse sand content and higher dry density than hammermill samples, suggesting the increase in stiffness which was observed.

For both hammermill and tubgrinder processes, the maximum secant modulus was achieved when testing at a confining pressure of 15 psi (105 kPa). The secant modulus tends to increase as confining pressure increases. However, the increases in the secant modulus are not as predictable.

For both the hammermill and tubgrinder processes, the maximum secant modulus was achieved for samples stored at a temperature of 100°F (37.8°C). When RAP samples were tested at 125°F (51.7°C) the secant modulus exhibited a tendency to not deviate much from the value achieved for the tests at 100°F (37.8°C). Tubgrinder RAP tested at a confining pressure of 15 psi (105 KPa) were the only tests that exhibited a large decrease in secant modulus with an increase in temperature to 125°F (51.7°). For all the storage times, the modulus decreased an average of 4,000 psi (28000 KPa) from storage at 100°F (37.8°C) to storage at 125°F (51.7°C).

The RAP exhibits similar ranges in elastic modulus as a dense sand, 5,000-10,000 psi (35,00 to 70,000 kPa) (Das, 1994). The RAP samples that were stored at elevated temperatures display moduli slightly above this range.

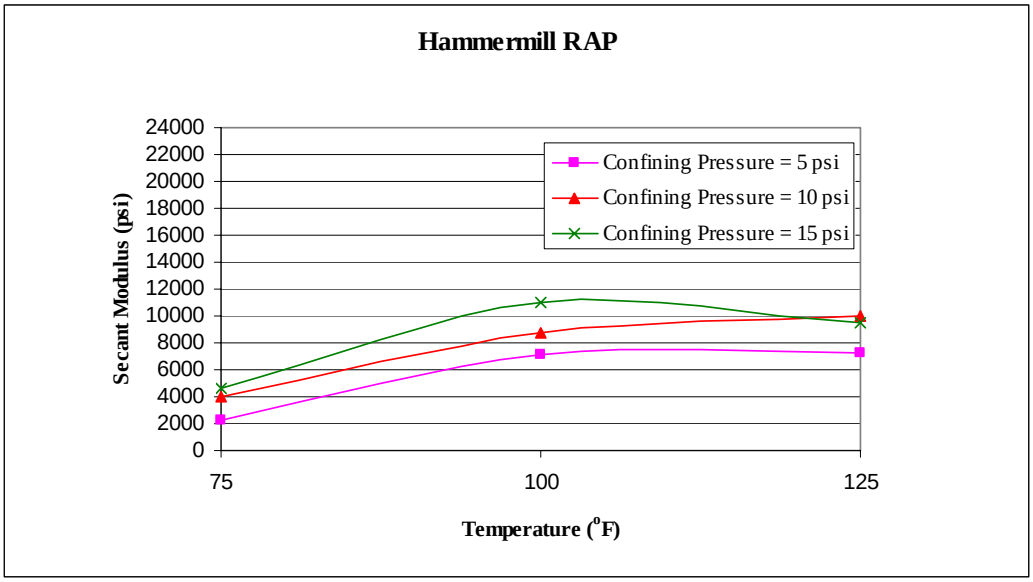

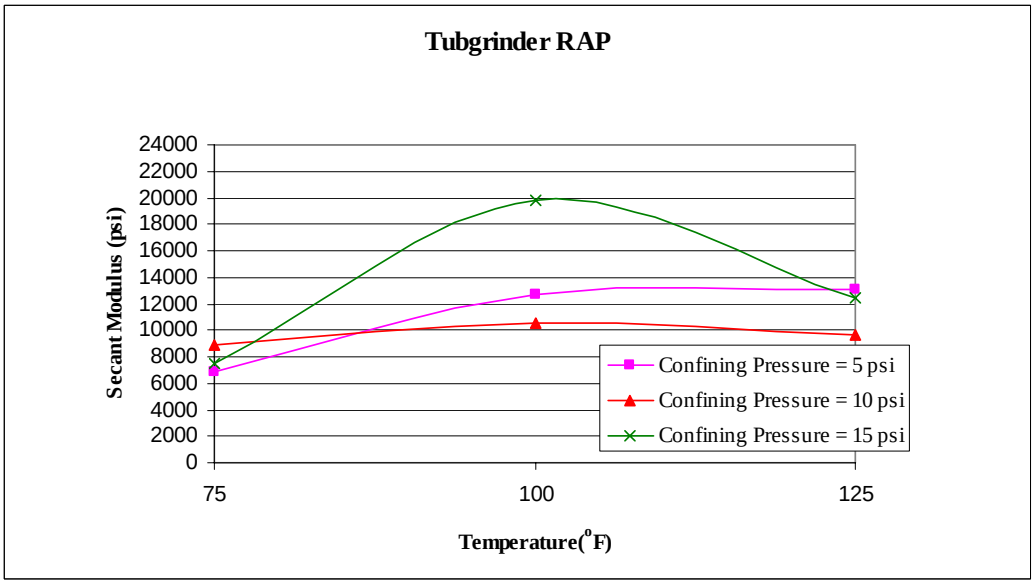

Figure 3.30 Secant Modulus vs. Temperature for Three Confining Stresses for Hammermill and Tubgrinder RAP Stored for 10 Days. (1 psi = 7 kPa)

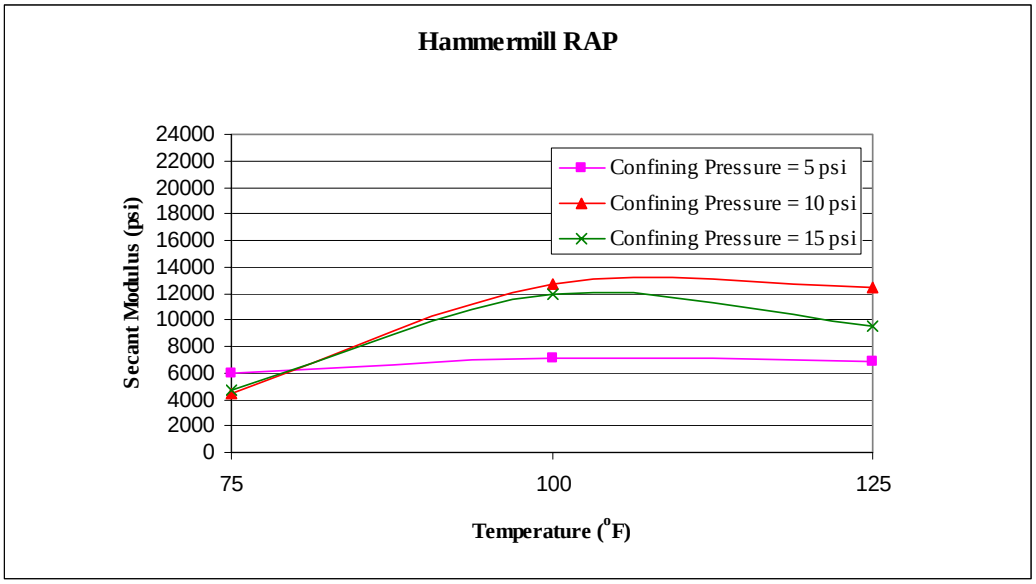

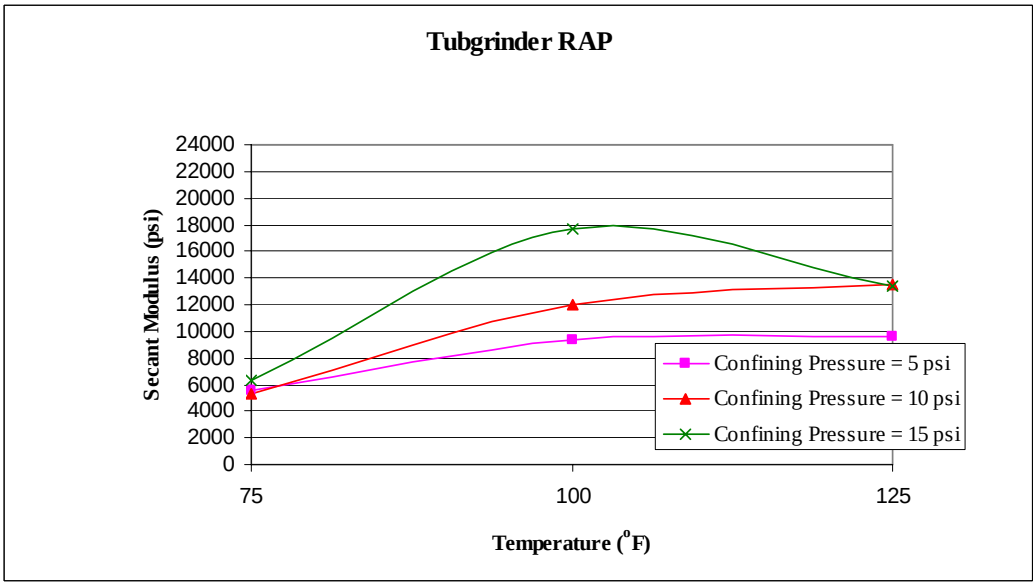

Figure 3.31 Secant Modulus vs. Temperature for Three Confining Stresses for Hammermill and Tubgrinder RAP Stored for 20 Days. (1 psi = 7 kPa)

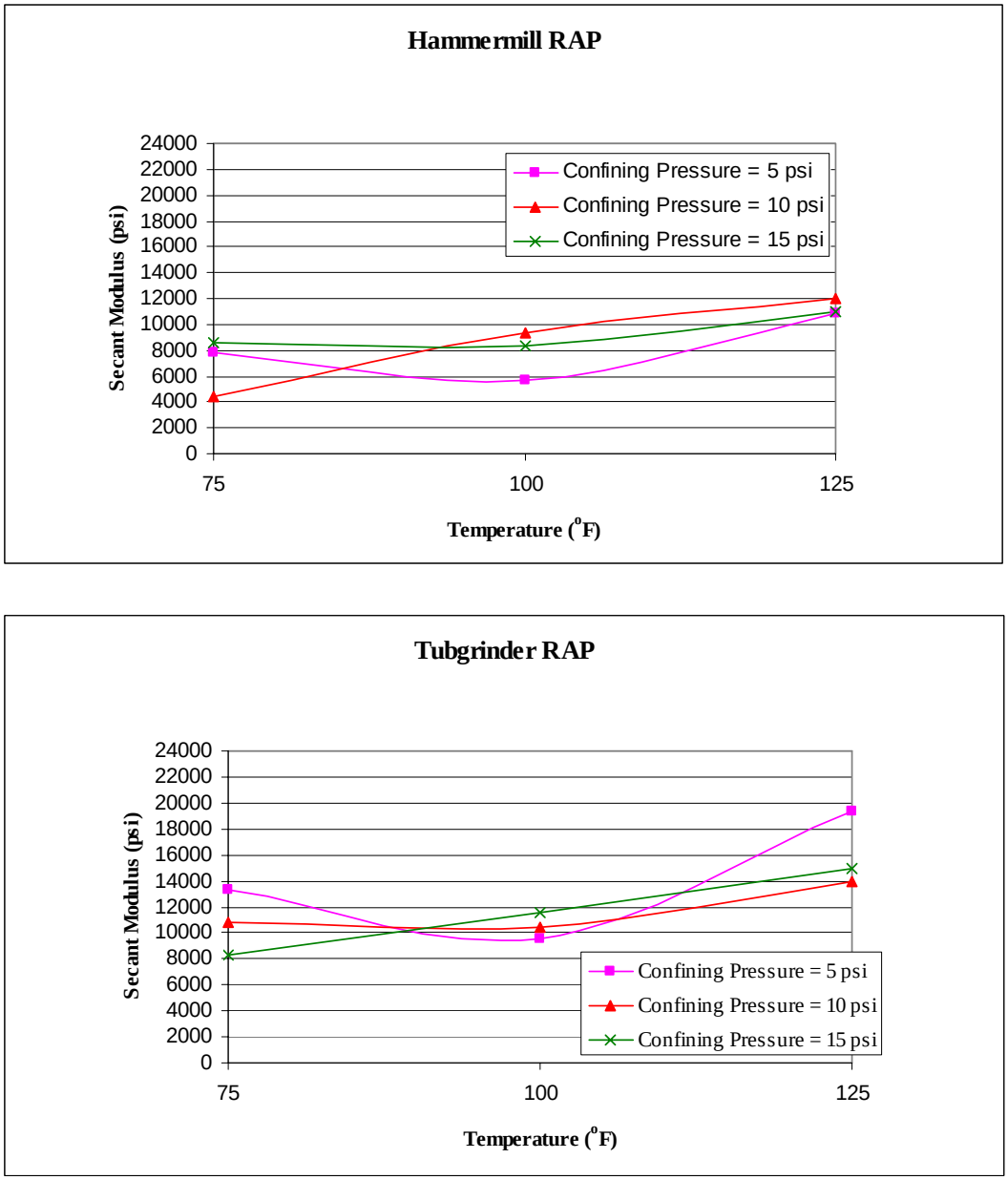

Figure 3.32 Secant Modulus vs. Temperature for Three Confining Stresses for Hammermill and Tubgrinder RAP Stored for 30 Days. (1 psi = 7 kPa)

Figures 3.33 through 3.35 present the secant modulus for hammermill and tubgrinder RAP at confining pressures of 5 psi, 10, psi and 15 psi (35, 70, and 105 KPa) as a function of storage time. The figures also show the influence of storage temperatures. No definite trend is observed with increasing storage time. The

length of storage time does not increase or decrease the secant modulus of the RAP consistently, regardless of the temperature.

To summarize, the secant modulus of elasticity at failure is larger for tubgrinder RAP than it is for hammermill RAP and for both materials the modulus increases with increasing confining pressure and with increased temperature. The duration of storage time does not have an impact on the secant modulus of the RAP.

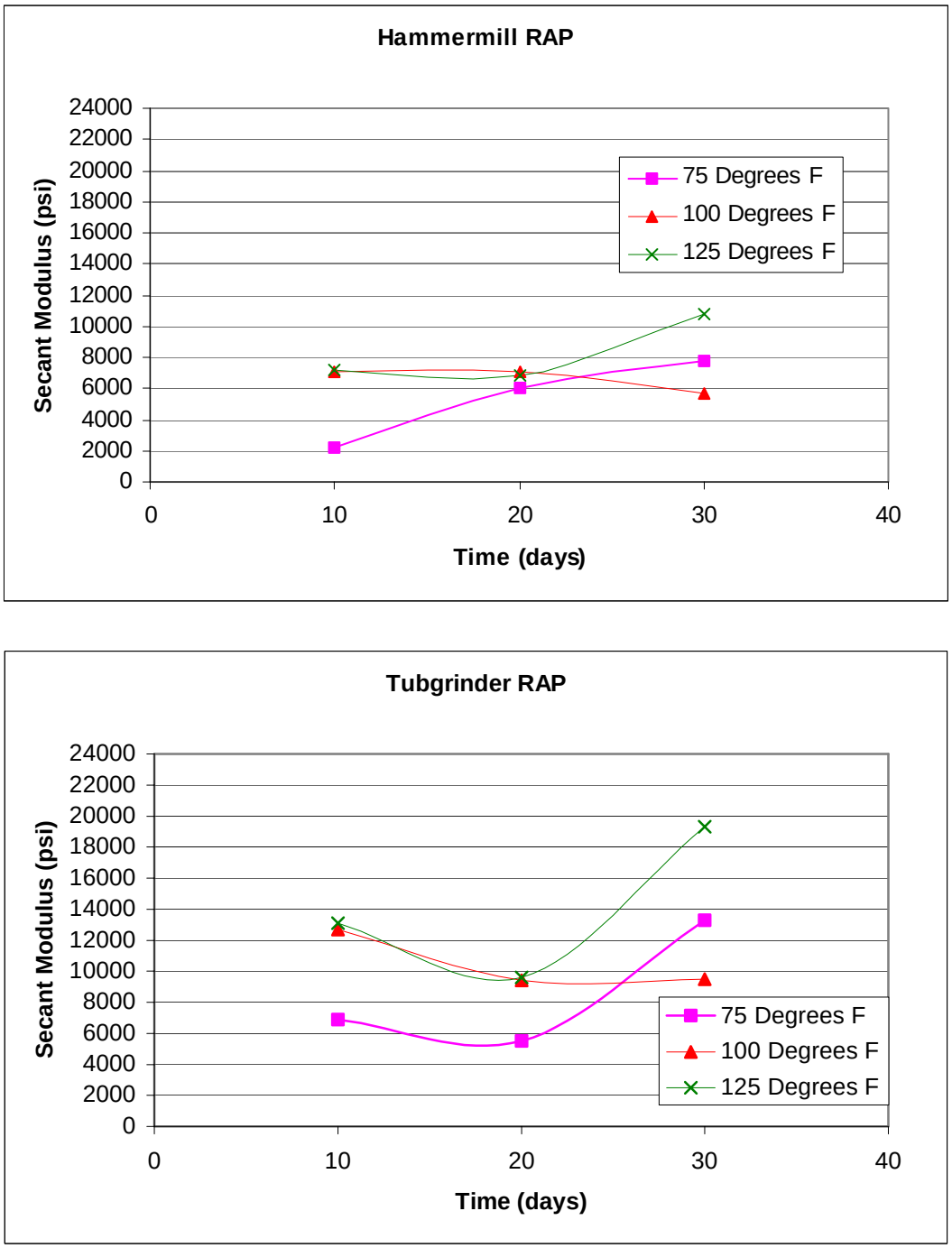

Figure 3.33 Secant Modulus vs. Storage Time for Three Temperatures for Hammermill and Tubgrinder RAP at Confining Pressure of 5 psi. (1 psi = 7 kPa)

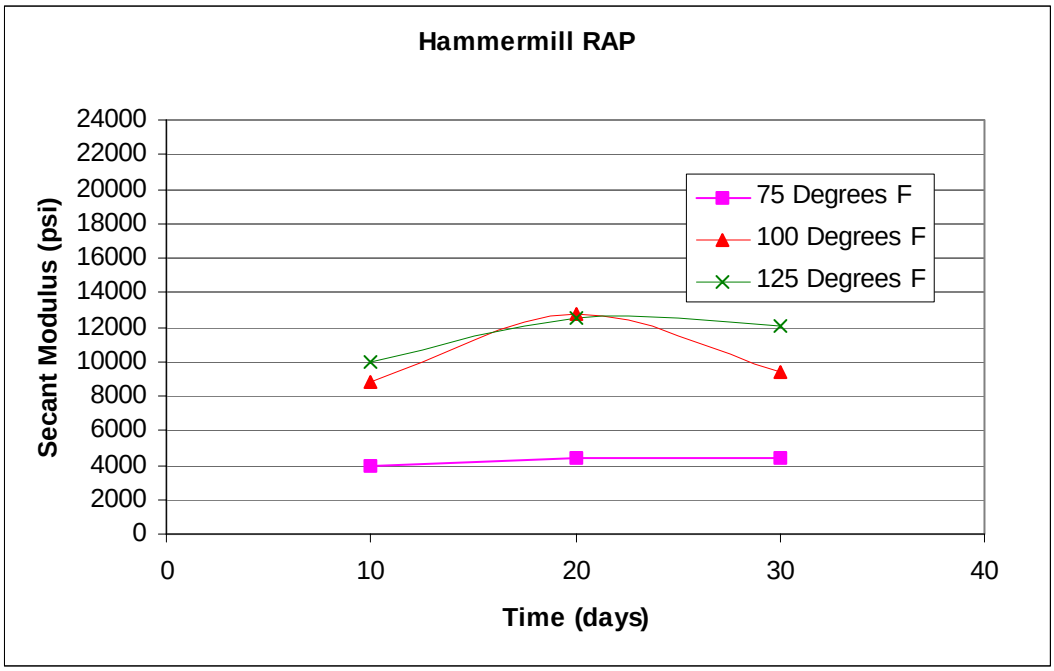

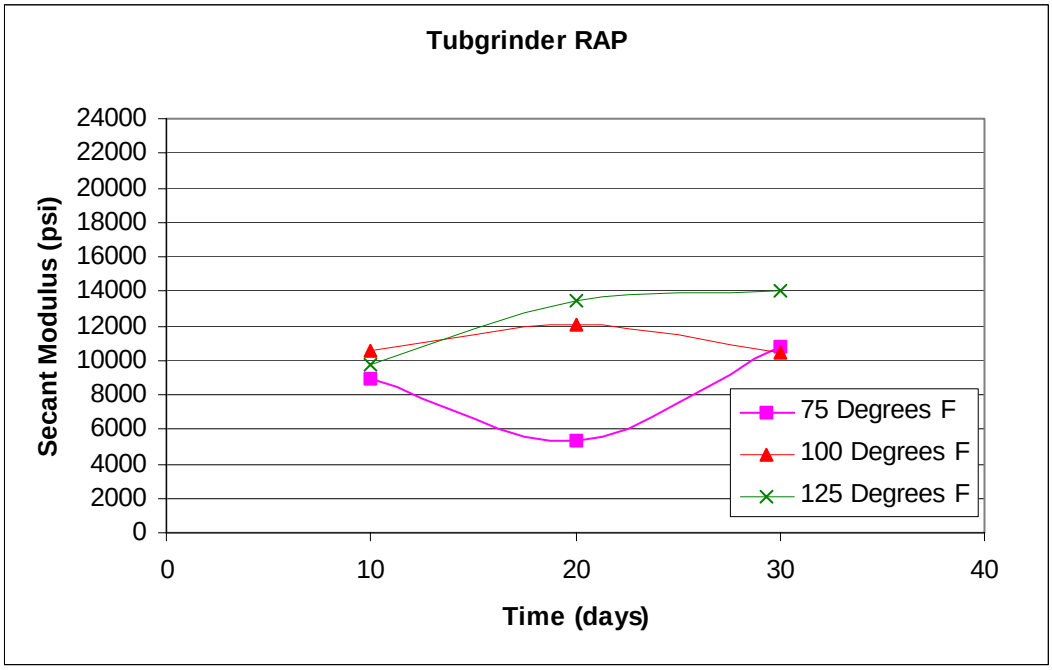

Figure 3.34 Secant Modulus vs. Storage Time for Three Temperatures for Hammermill and Tubgrinder RAP at Confining Pressure of 10 psi. (1 psi = 7 kPa)

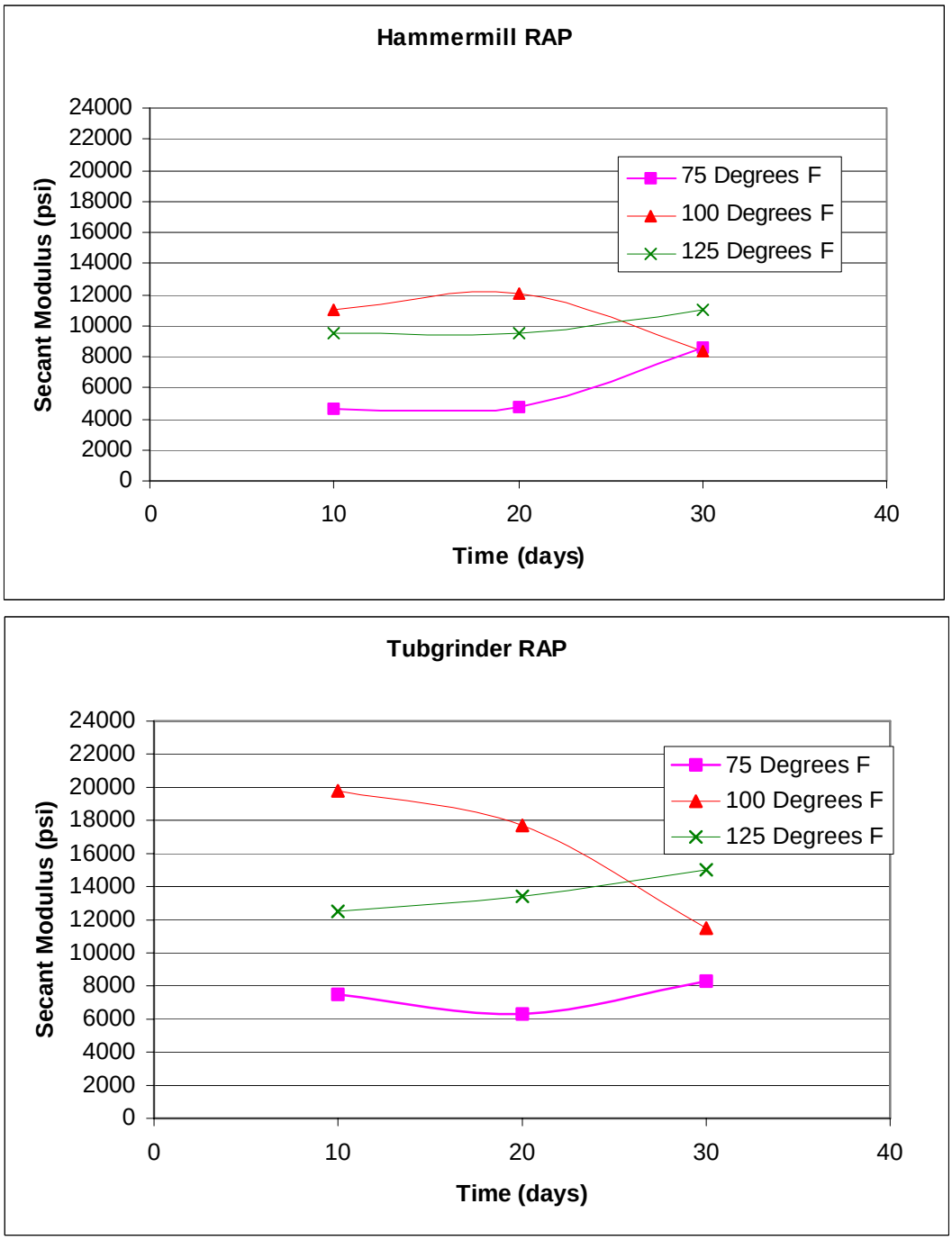

Figure 3.35 Secant Modulus vs. Storage Time for Three Temperatures for Hammermill and Tubgrinder RAP at Confining Pressure of 15 psi. (1 psi = 7 kPa)

3.8.4 Mohr – Coulomb Strength Criteria

To plot the Mohr circle and the failure envelope a minimum of three samples at different confining pressures were used. A typical set of results from hammermill tests stored at 100°F (37.8°C) for 10 days is shown in Figure 3.36 This plot was developed using the data from the stress strain curves in Figure 3.23 to fabricate the Mohr circles. The remaining Mohr-Coulomb failure envelopes are presented in Appendix B.

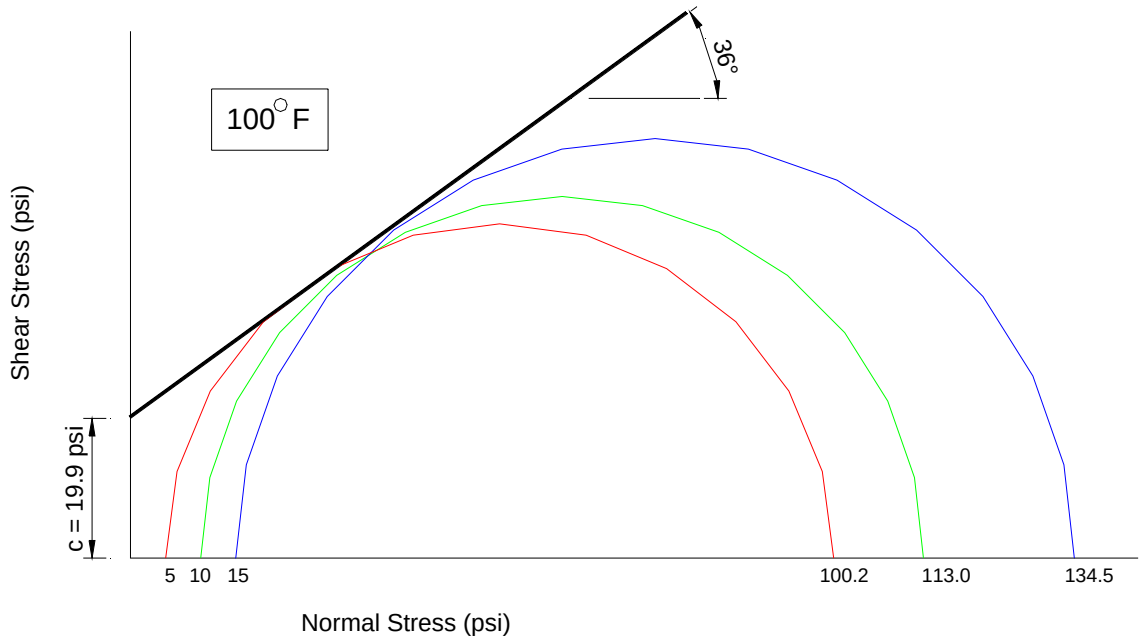

Figure 3.36 Mohr-Coulomb Failure Criteria for Hammermill RAP stored for 10 Days at 100°F. (1 psi = 7 KPa)

3.8.5 Angle of Internal Friction

The effects of storage time and temperature on the angles of friction for both hammermill and tubgrinder RAP are shown in Figure 3.37. The frictional angles ranged from 35 to 44 degrees for both materials. The angles of friction for both materials do not vary greatly with time or temperature. The typical range for angles of friction for medium-dense sand with angular grains is 35-40 degrees (Das, 1994). Garg and Thompson (1994) found an angle of friction of 45° for RAP. The angles of friction of limerock and cemented coquina (two of the most widely used aggregates for base applications) were reported by Bosso (1995) to be 44° and 41°, respectively.

For the hammermill RAP at no storage time an angle of friction of 44° was achieved, an angle much higher than other values determined for this material. The three tests used to achieve this angle were the first three tests prepared in the testing program so the samples had a density of 3% higher than the rest of the hammermill samples, which averaged 117 pcf (18.3 kN/m^3). This density increase was assumed to cause the angle of friction to be outside of the range found for all the other tests and was considered a statistical outlier for this study.

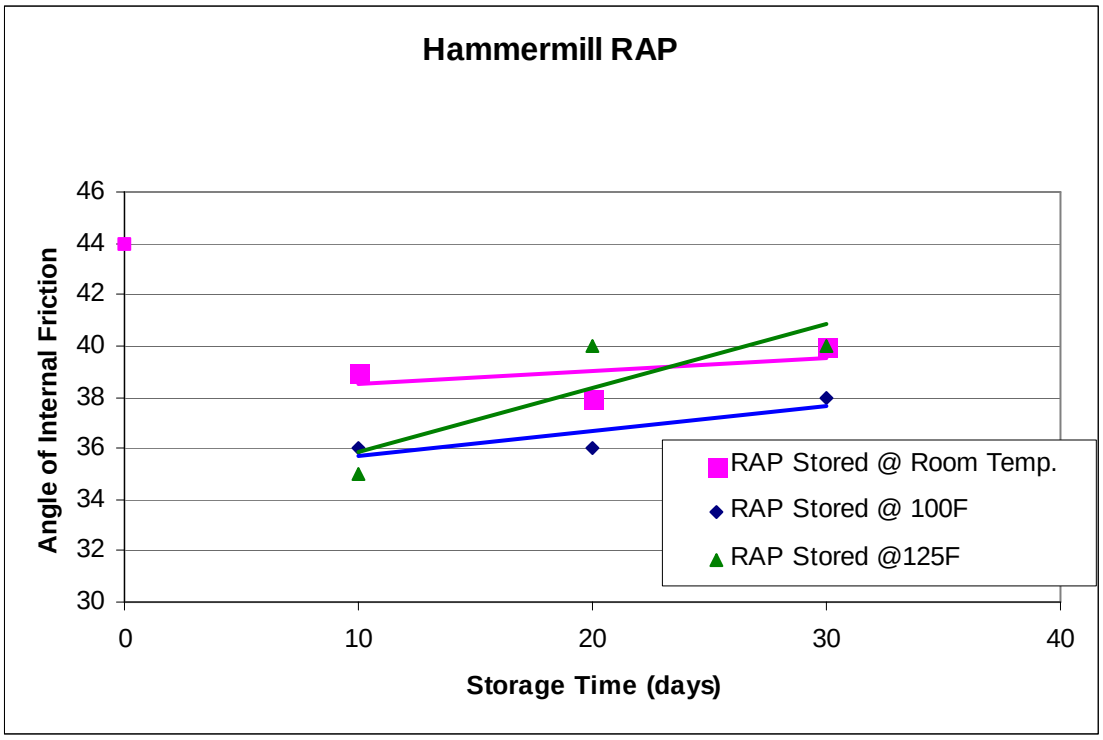

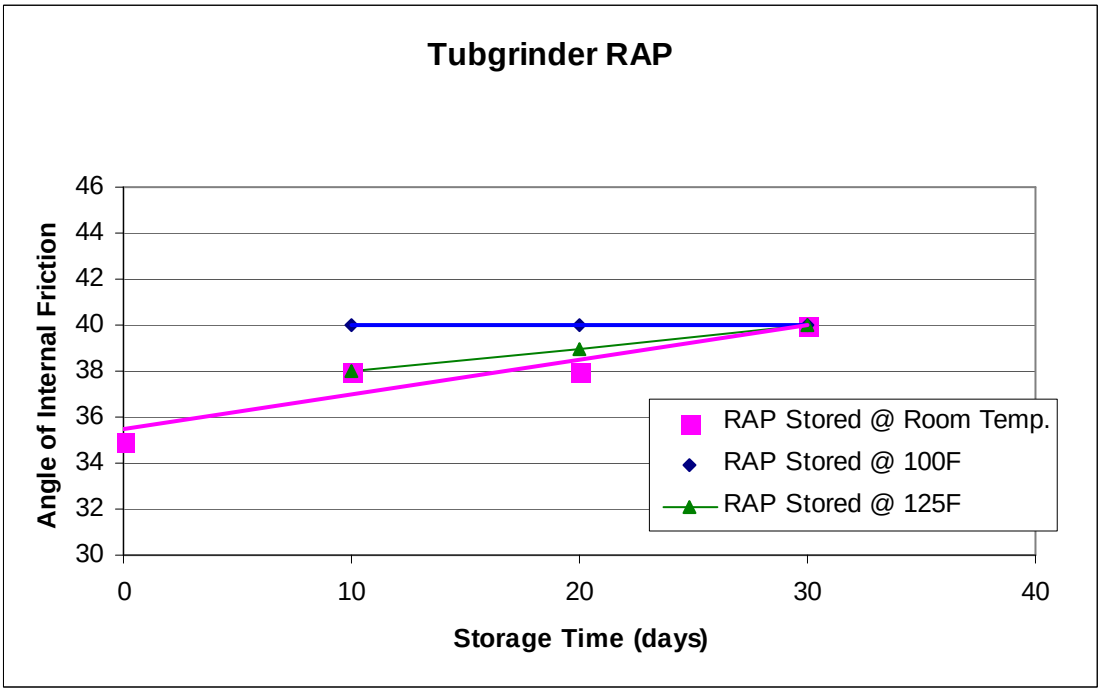

Figure 3.37 Effects of Storage Time on Angle of Friction of Hammermill and Tubgrinder RAP at Three Different Temperatures.

3.8.6 Cohesion Intercept

The effects of storage time and temperature on the cohesion intercept for hammermill and tubgrinder RAP are shown in Figure 3.38. The cohesion for tubgrinder tests stored at room and elevated temperature is approximately 20% higher than the hammermill tests.

The cohesion of both hammermill and tubgrinder RAP increases when the samples are stored at higher temperatures. In both materials the cohesion more than doubles after the samples have been stored at elevated temperatures. However, the difference between the cohesion of samples stored at 100°F (37.8°C) and 125°F (51.7°C) for an extended period of time is relatively small.

The increase in storage time does not cause a noticeable increase or decrease in cohesion for the samples stored at elevated temperatures. When RAP was stored at room temperature its cohesion doubled after 30 days had elapsed. This means that the effect of the elevation of temperature is much greater on the RAP than the effect of the length of storage. It is assumed that the asphalt binder in the RAP affects the cohesion. It causes the compacted particles stored at elevated temperatures to adhere in a stronger bond than particles that have just been stored at room temperature.

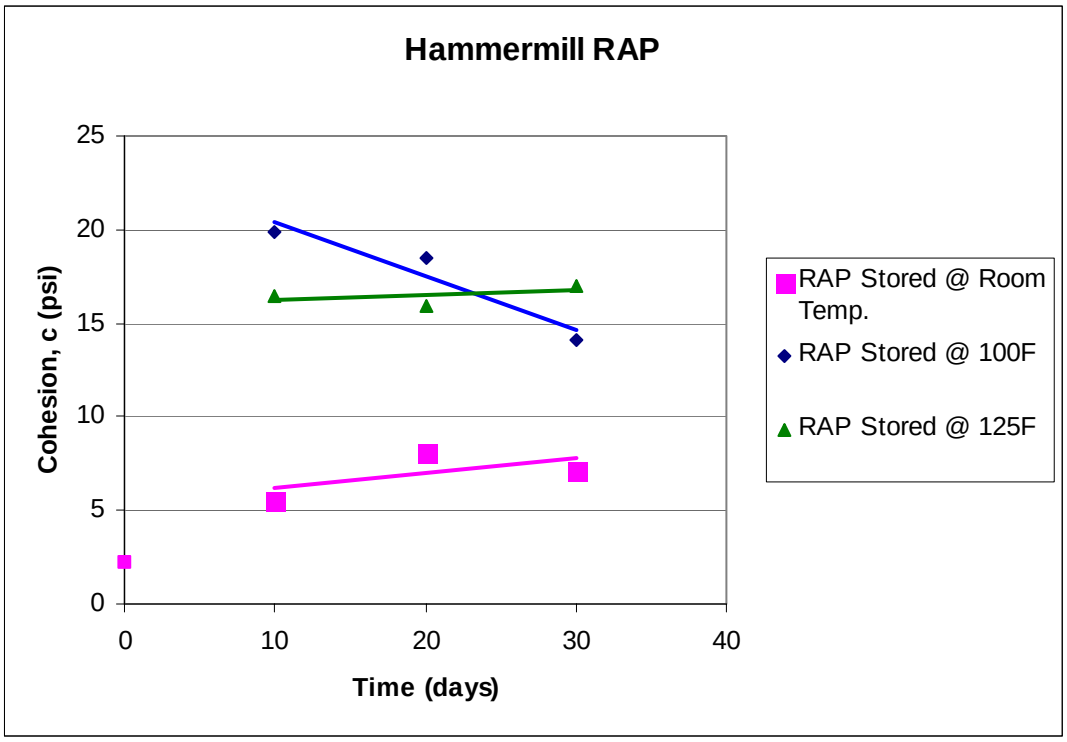

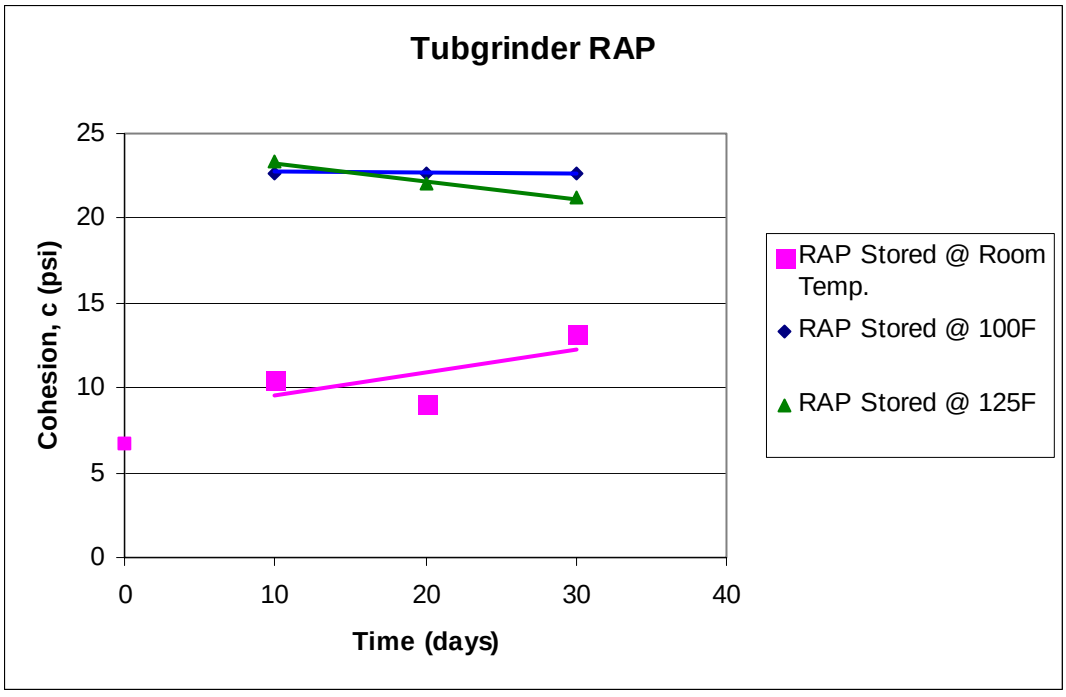

Figure 3.38 Effects of Storage Time on the Cohesion of Hammermill and Tubgrinder RAP at Three Different Temperatures. (1 psi = 7 kPa)

3.8.7 Summary of Triaxial Results

The triaxial test results are summarized in Tables 3.6 and 3.7 for hammermill and tubgrinder RAP respectively. The angle of friction and cohesion are reported for each test condition of time and temperature.

Table 3.6 Summary of Triaxial Test Results for Hammermill RAP. (1 psi = 7 kPa)

	Temperature = 75 degrees		Temperature = 100 degrees		Temperature = 125 degrees	
Storage Time (days)	**Angle of Friction (degrees)**	**Cohesion (psi)**	**Angle of Friction (degrees)**	**Cohesion (psi)**	**Angle of Friction (degrees)**	**Cohesion (psi)**
0	44	2.3	No Test	No Test	No Test	No Test
10	39	5.6	36	19.9	35	16.5
20	38	8.1	36	18.5	40	15.9
30	40	7.2	38	14.1	40	17.02
Average	40	6	37	18	38	16
Standard Dev.	2.6	2.6	1.2	3.0	2.9	0.6

Table 3.7 Summary of Triaxial Test Results for Tubgrinder RAP (1 psi = 7 kPa)

	Temperature = 75 degrees		Temperature = 100 degrees		Temperature = 125 degrees	
Storage Time (days)	**Angle of Friction (degrees)**	**Cohesion (psi)**	**Angle of Friction (degrees)**	**Cohesion (psi)**	**Angle of Friction (degrees)**	**Cohesion (psi)**
0	35	6.7	No Test	No Test	No Test	No Test
10	38	10.5	40	22.7	38	23.3
20	38	9.1	40	22.7	39	22.1
30	40	13.2	40	22.6	40	21.2
Average	38	10	40	23	39	22
Standard Dev.	2.1	2.7	0.0	0.1	1.0	1.1

4. Field Testing Methodology and Results

4.1 Material Sampling

4.1.1 Hammermill Impact Crusher

When the asphalt is milled from the road surface, the gradation is limited in that there is a high percentage of large diameter particles and very little, if any fines. For this reason, RAP is commonly processed again, most often by crushing or grinding. This additional processing reduces the large aggregates to the required gradation size for use in roadway construction as well as increasing the fines content (Road & Bridges 1999).

The type of equipment used to process the RAP for this project was a hammermill impact crusher. This type of crusher reduces the aggregate size of the material as it passes through individual breaker bars mounted to a rotor. As the rotor spins, the breaker bars are extended by centrifugal force. When the RAP is fed into the machine, it will pass within striking distance of the breaker bars (Road & Bridge 1999). The breaker bars will impact the RAP and crush it in between the bars and the striking plate. As the distance between the breaker bars and the striking plate narrows, the resulting aggregate size decreases. The materials rebounding against each other and internal machine surfaces also aids reduction (Barksdale 1991). Particle size can be controlled further by the aid of screens or sieves positioned at the exit of the machine. Material retained on these sieves is simply processed through the machine again (Jones, Personal Communication 2000).

4.1.2 Grain Size Distribution

Classification of the RAP was achieved through a sieve analysis process performed by Bruce Doig in the laboratory portion of this project. The sieve analysis implemented was ASTM C136-93 (FM 1-T 027), *Standard Test Method for Sieve Analysis of Fine and Coarse Aggregates*. Because the material contained an asphalt binder, the samples were allowed to air dry. U.S. standard sieve sizes used during the sieve analysis were 1.5", 0.75", 0.375", #4, #8, #16, #30, #60, #100, and #200 (Doig 2000). The gradation curve for the sieve analysis performed on the RAP is shown in Figure 4.1.

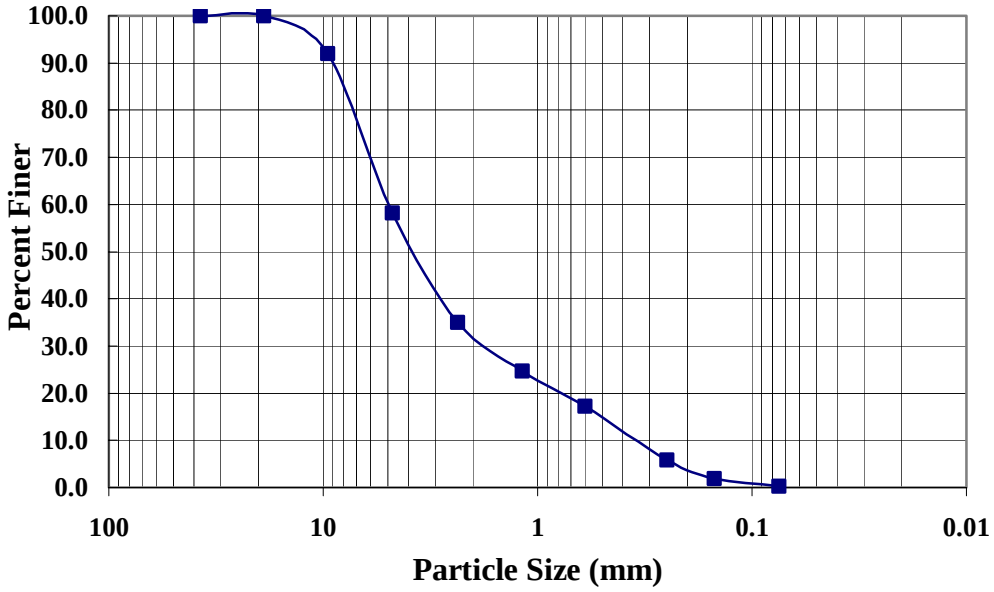

Figure 4.1 Particle Size Distribution of RAP (after Doig, 2000)

Three samples of approximately 3.3 lb (1500 kN) each were tested. The grain size distribution curve for each sample was plotted. The D_{10}, D_{30}, and D_{60} gradation parameters were calculated, as well as the coefficient of uniformity (C_u) and gradation (C_d). Both the United Soil Classification System (USCS) and the American Association for State Highway and Transportation Officials were used to

classify the material (AASHTO) (Doig, 2000). Table 4.1 shows the gradation parameters presented by Doing (2000).

Table 4.1 Gradation Parameters and Classification of RAP (after Doig, 2000)

Gradation Parameters	
D_{10}	0.35 mm
D_{30}	1.90 mm
D_{60}	5.00 mm

Classification	
AASHTO	A-1-a
USCS	SW

4.1.3 Asphalt Content

Asphalt contents derived for this project were obtained using test method FM 5-563 (*Quantitative Determination of Asphalt Content from Asphalt paving Mixtures by the Ignition Method)* of the 2000 Florida Sampling and Testing Methods Manual. The proceeding is a summary of the procedure as designated by FM 5-563.

First, the ignition oven is preheated to 1000º F (538º C) and the two sample baskets, including catch pan are weighed. Next, a sample ranging from 35 oz. to 70 oz. (1000g to 2000g) is prepared. The size of the sample is dependent on the asphalt mixture to be tested. A 1527 g size sample was used during this research. Minimum size of samples can be viewed in Table 4.2.

Table 4.2 Minimum Sample Size Per Asphalt Mixture

Mixture	Minimum Grain Size ounces	(grams)
ABC-3, S-II, SP-19.0, SP-12.5	70	(2000)
S-I, SP-9.5, FC-5, FC-6	53	(1500)
S-III, FC-2, FC-3, Type III	42	(1200)
Type II, ABC-1, ABC-2, SAHM	35	(1000)

The samples are then evenly divided and placed into two sample baskets and then weighed. The weight of the empty assembly is subtracted from the weight of the assembly plus sample material (AC_{actual}). The baskets are then placed in the ignition furnace.

The samples remained in the oven until all of the asphaltic material was burned off. The oven electronics interprets that this has happened using an internal scale. When the oven's scale ceases to record a loss in weight, it sounds an alarm to indicate the test is complete. Once the test is completed, the sample baskets and catch pan are removed from the oven, allowed to cool to room temperature (approximately 30 minutes), and weighed. Again, the weight of the empty assembly is subtracted out ($AC_{measured}$). The assembly is then cleaned out and the procedure is repeated again.

The asphalt content ($AC_{calibrated}$) is determined by using the following equations:

$$W_{Lx} = ((AC_{actual} - AC_{measured})/ AC_{actual})*100 \quad (4.1)$$

where W_{Lx} = aggregate weight loss of the calibration sample as a percent of the total mix and *x* refers to either the 1st or 2nd calibration sample.

$$CF = (W_{L1} + W_{L2})/2 \quad (4.2)$$

where CF represents the calibration factor or average percentage weight loss of the samples.

$$AC_{calibrated} = AC_{measured} + CF \quad (4.3)$$

4.2 Field Site Development and Layout

The criteria examined in developing the field site included size and configuration, loading conditions, and construction parameters. The main emphasis in determining the size and configuration was to provide adequate spacing for three destructive tests throughout the five testing cycles. It was assumed that each destructive test had an "influence zone" of 5 feet. Also, it was determined that two differently-installed RAP's and cemented coquina would be tested at three different thickness. Therefore, nine different areas were mandated and each area required a minimum size of 15 feet by 45 feet.

It was determined that the field site would not be subjected to vehicular loading. Vehicular loading was presumed to add a variable to the test results that could not be readily defined or quantified.

The project field site is located at APAC-Florida, Inc.'s asphalt plant located in Melbourne, Florida. In plan it covers a 51-foot by 99-foot area. It is divided into three sections measuring approximately 33 feet by 50 feet each. One section consisted of cemented coquina and the other two sections were comprised of RAP. Of the two major RAP sections, one was installed by comparable industry standards equal to that of cemented coquina (i.e. equal number of passes with a vibratory roller). The other RAP section was installed using elevated compaction energy (i.e. increased number of passes with the vibratory roller in conjunction with density readings).

Each of these sections was subdivided into minor sections measuring 17 feet by 33 feet. The first minor section was 36” thick (12” layers for each of the subgrade, subbase, and base). The second minor section was 24” thick (12” layers each for the subgrade and subbase). The third minor section was 12” thick and comprised only of the subgrade.

For the purpose of simplicity, the field site has been divided into columns A, B, and C (RAP installed at elevated compaction energy, RAP installed at normal compaction energy, and cemented coquina, respectively) and rows 1, 2, and 3 (36” layer, 24” layer, and 12” layer, respectively). A schematic of the field site layout is presented in Figure 4.2.

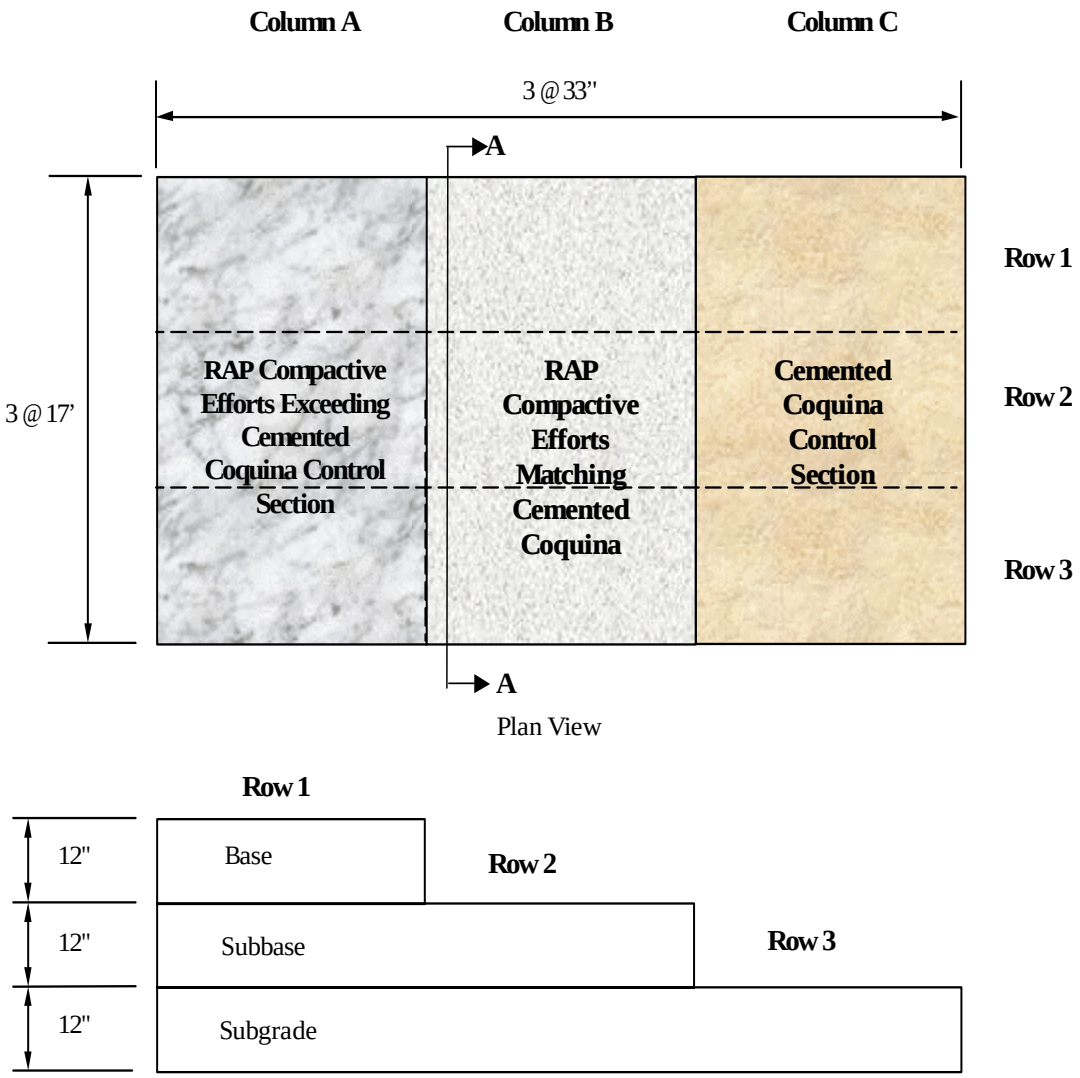

Figure 4.2 Field Site Layout (Not to Scale)

4.3 Field Site Installation

Construction of the field test site began on Monday, September 27, 1999. During the weekend prior to construction, over 8 inches of rainfall occurred in the area, causing the water table to rise to within 10 inches below the ground surface (www.accuweather.com, 1999). The densities taken at various locations are listed in Appendix AA. The conditions encountered at the site during construction can be viewed in Figure 4.3.

Figure 4.3 Subsurface Conditions

The large quantity of rainfall forced some modifications to the planned construction process to complete installation within the time frame allocated. Due

to the high subsurface moisture conditions, a 6-inch lift of cemented coquina was placed in the control section only and allowed to dry. This was based on discussions between the researchers and field personnel. It was assumed that if the subsurface were sealed with the cemented coquina, the high water table would minimally affect the additional lifts. Placement of the 6-inch lift of cemented coquina can be viewed in Figure 4.4.

Figure 4.4 Installation of 6-inch Lift of Cemented Coquina Used to Hold Down Water Table

One of the RAP sections (Column B) was to be constructed using the same compaction energy as the cemented coquina. The wet site conditions prohibited the

installation of the cemented coquina, but not the RAP. Therefore, Column B was installed using compaction energies normally associated with cemented coquina placed under normal, average site conditions. After 4 days the cemented coquina had sufficiently dried, and was subsequently compacted using the equivalent compaction energy of the RAP in Column B. The RAP in Column A was installed by increasing compaction energies and taking nuclear density readings at every two passes. A summary of the final compaction energies for each minor section is presented in Appendix BB

The equipment operators noted the ease in which the RAP was installed in the adverse subsurface conditions. They likened it to installing cemented coquina under average, normal dry conditions.

Thermocouple probes were installed to study the relationship between the seasonal thermal fluctuations in the RAP and changes in the strength of RAP. These probes are capable of providing temperature data but are not capable of recording and storing the data. Five thermocouple probes were installed in each RAP section (Columns A & B). One probe was installed at a depth of 30 inches, two probes were installed at depths of 18 inches, and two probes were installed 6 inches below the top surface. A photo of the completed field site can be viewed in Figure 4.5.

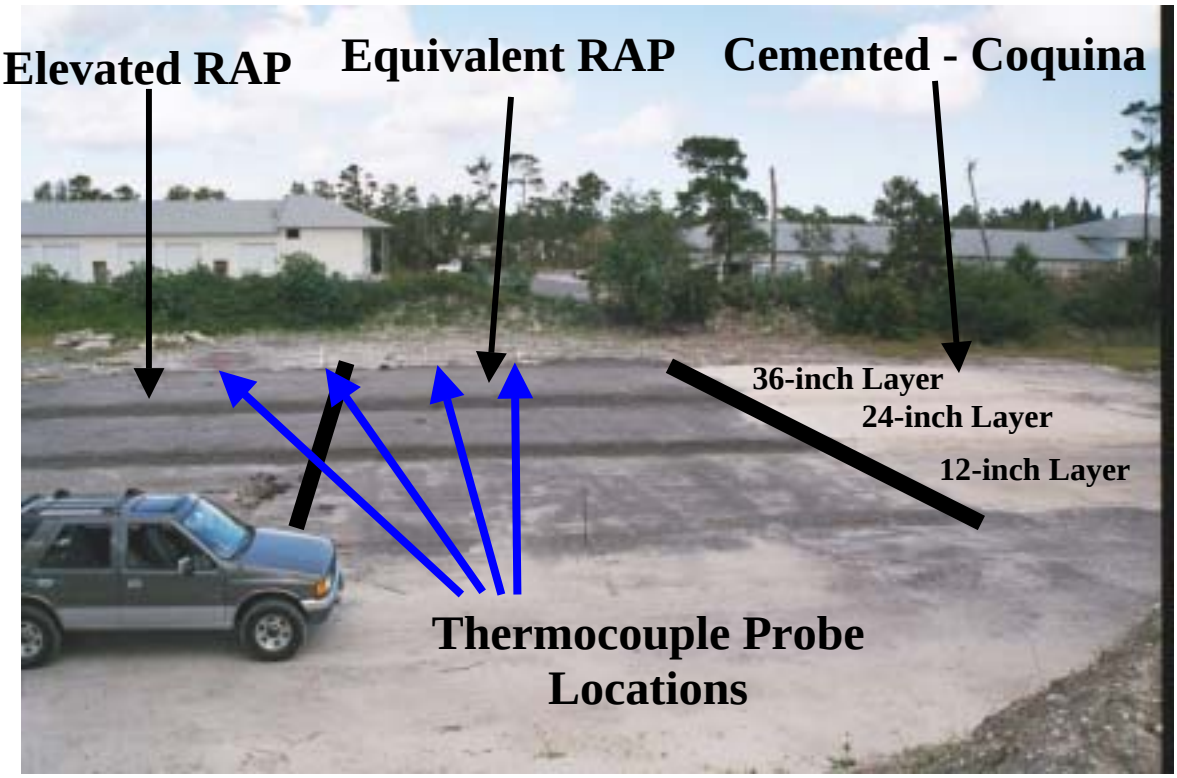

Figure 4.5 Completed RAP Field Site

4.4 Testing Protocol

4.4.1 Cone Penetrometer Test (CPT)

In basic terms the CPT is a cone on the end of a series of rods that are pushed, either manually or mechanically, into the ground at a constant rate. Measurements of the cone point resistance and skin friction of the rod sleeves are recorded and empirically correlated to determine subsurface soil characteristics.

The practice of probing or sounding with rods to determine the subsurface soil conditions has been practiced since the early 20th century. It was used by the Swedish State Railways as early as 1917 and then by the Danish Railways around 1927. In 1934 the CPT developed into the recognizable form that is used today. The first electronic CPT was introduced in 1948 but didn't come into general use until the 1960's. The electronic CPT measures cone resistance and skin friction by means of transducers mounted directly above the cone tip (Meigh, 1987). A schematic of the electronic penetrometer tip can be viewed in Figure 4.6.

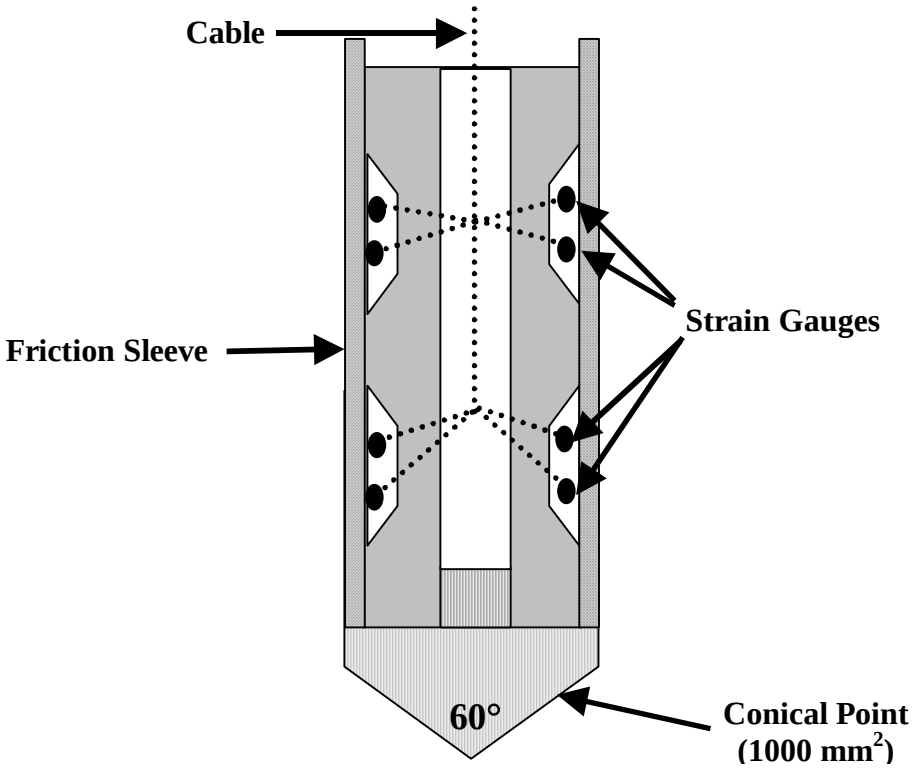

Figure 4.6 Schematic of the Electronic Penetrometer Tip

The CPT has three main applications: 1) to determine soil profiles and identify the soils present; 2) as an aid in interpolating soil profiles between boreholes, and 3) as an aid in determining the bearing capacity and settlement of foundations placed in the soil.

There are three main types of CPT rigs in use today. The first is the light rig. The light rig is a mobile rig that can be manually set up in areas inaccessible by vehicles. The light rig is capable of imparting a thrust load of 4500 lb to 5600 lb (20 kN to 25 kN) and is used mainly for exploration of weak upper layers of soil. The load is normally imparted manually through a chain drive mechanism and is indicated by a pressure gauge or proving ring (Meigh, 1987).

The second type is the medium rig. This rig is capable of imparting a 11,200 lb (50 kN) thrust. It is commonly a trailer-mounted assembly and the load is applied by means of a hydraulic jacking system. The medium rig is used mainly for stiff clays and medium-dense sands. A penetration depth of approximately 65 ft (20 m) can be obtained with this rig (Meigh, 1987).

The third type of CPT rigs is the heavy rig. These rigs are capable of attaining thrust of up to 45,000 lb (200 kN). The heavy rig is usually fitted with an electronic cone and friction sleeve. The CPT assembly is commonly mounted on a all-terrain or all-wheel drive vehicle that is ballasted to provide the reaction required for penetration. Also, the vehicle is raised by hydraulic jacks to provide stability during testing. The power required for penetration is supplied by a power take-off, geared through the vehicle's engine (Meigh, 1987).

As stated previously, the main application of the CPT is to develop a soil profile and identify the soils present. Many empirical relationships between cone resistance and friction ratio (skin friction divided by cone resistance) have been developed to classify soils with the CPT. The relationship used by FDOT's CPT for this project was developed by Robertson and Campanella (1983). This empirical relationship is based on the ratio of tip resistance, q_c to friction ratio, f_r. When the

ratio is high (400 bars to 1%) the soil encountered is most likely sand. As the ratios drop, the soil characterization moves from sand to silty sands to sandy silts to clayey silts to clays. When the ratio is low (4 bars to 6%) the soil in question is most likely peat.

The CPT is a more time efficient method than conventional borings, but borings provide the opportunity to visually inspect the soil. Another drawback of the CPT is the imprecision of identifying thin soil layers within the stratum. The cone resistance only responds to soil changes within 5 to 10 tip diameters; the stiffer the soil the increase in this distance. Hypothetically, if a thin layer of sand is located within a clay stratum, the CPT will not detect the sand layer if it is less than 4 in. (100mm) thick. Greater accuracy and understanding of the tested soil can be obtained if the CPT is used in conjunction with other testing procedures such as the pore-pressure probe and core borings (Meigh, 1987).

4.4.2 Falling Weight Deflectometer (FWD)

The Falling Weight Deflectometer (FWD) is a trailer mounted testing apparatus used to evaluate the structural integrity of a pavement system over time by simulating vehicular traffic. A photo of the FWD can be seen in Figure 4.7.

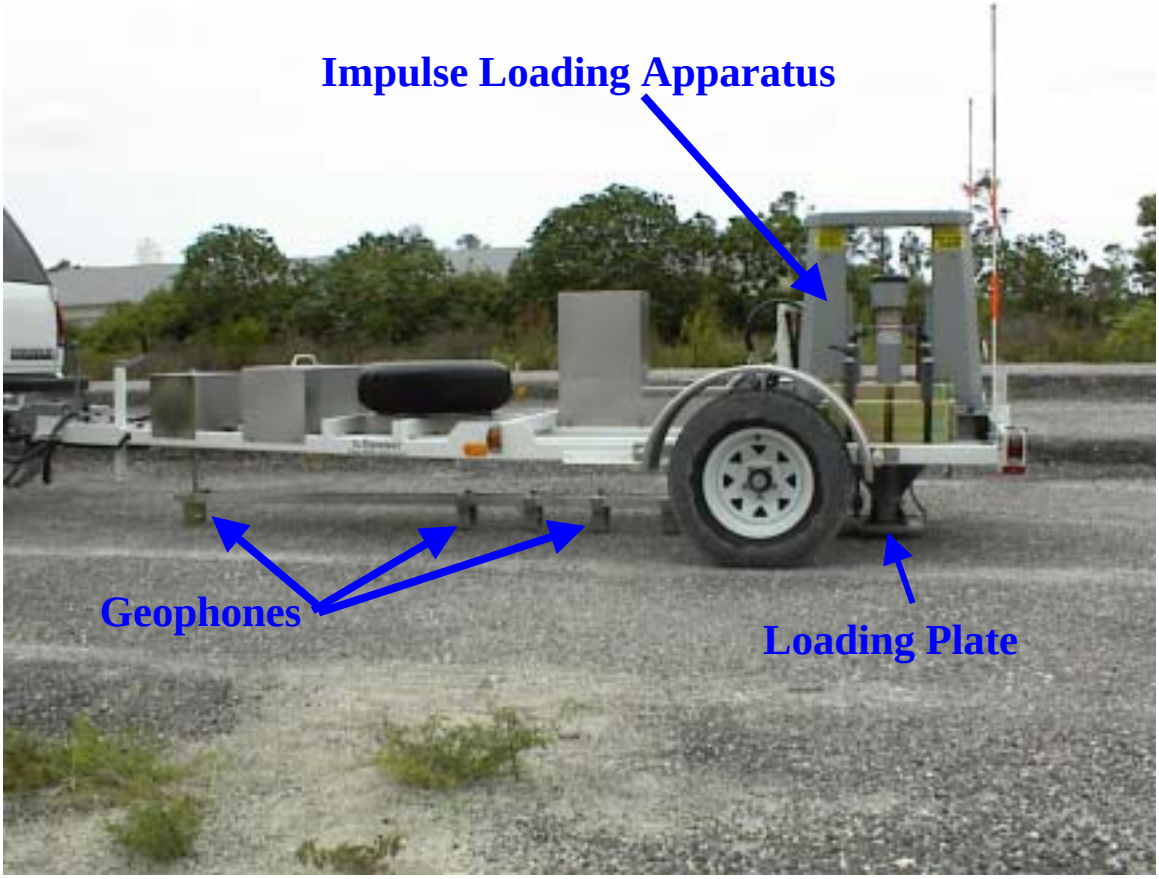

Figure 4.7 Falling Weight Deflectometer Used by the Florida Department of Transportation.

The FWD uses a hydraulically operated loading system to impart a known load onto the testing surface. This dynamic impulse load produces a half-sine,

seismic velocity wave, lasting 25 to 30 msec. This loading condition, in both size (1,500 lbs to 27,000 lbs, 7 kN to 120 kN) and frequency, mimics various vehicular loading patterns (Dynatest®, 2000).

The load-induced wave is recorded by a series of seven geophones. The first geophone is located directly underneath the loading plate. The remaining eight can be positioned up to 8 feet (2.45 m) from the load source. The geophones record the vertical displacement from their initial station to the peak of the half-sine wave (Holt, personal communication, 2000). This displacement is recorded in mils (10^{-3} in) or microns (10^{-6} m).

Conceptually, when the FWD load is imparted to the surface, a zone of influence of the impulse stress is created within the underlying layers (Federal Highway Administration, 1987). The basic geometry of this zone of influence varies with the composition of the materials making up the layers. However, a zone of influence of 2 to 1 (horizontal to vertical) is often assumed.

Data from the FWD can be used for a variety of purposes. Among others, the elastic modulus of individual layers can be determined through back calculation. Also, overall pavement response can be determined by either the Dynamic Stiffness Modulus (DSM) or the Impulse Stiffness Modulus (ISM). In both cases the modulus is calculated by dividing the load by the deflection directly under the loading plate. The formulas for the DSM (Green and Hall, 1975) and ISM (Bush, 1990), respectively, are:

$$DSM = \frac{\text{Max Load} - \text{Min Load (in lbs)}}{D_0 \text{ at Max Load} - D_0 \text{ at Min Load (in mils)}} \qquad (4.4)$$

$$ISM = \frac{\text{Load (in kips)}}{\text{Center Plate Deflection (in mils)}} \qquad (4.5)$$

Data from the geophones indicates a deflection basin, where the deflection is greatest directly underneath the load and decreases radially. It is assumed that the outer most geophones record deflections caused only by the soil layers still affected by the stress zone (Federal Highway Administration, 1987).

In Figure 4.8, the outer most geophone, in theory, is only recording the deflection caused by the load affecting Influence Zone 1 in Layer 4, L_4 (L_4 is assumed to be of infinite thickness). Influence Zone 1 is defined as the soil beneath the intersection of the Zone of Influence and vertical line from the outward geophone.

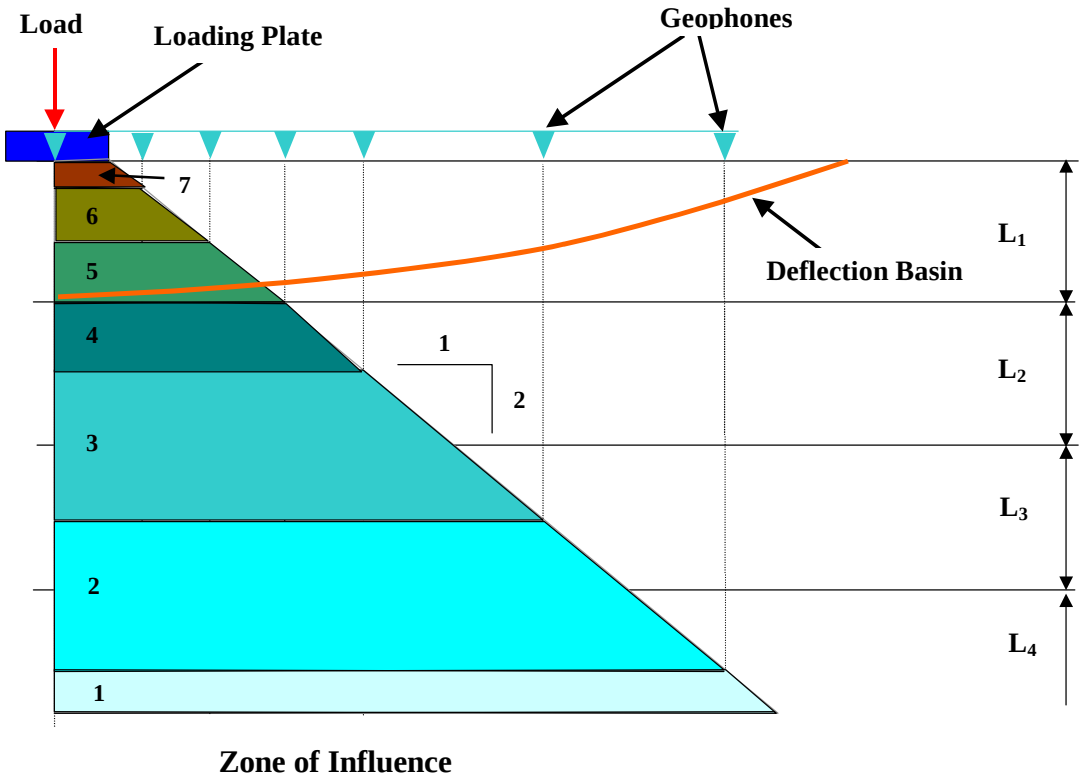

Figure 4.8 Zone of Influence and Typical Shape of Deflection Basin Due To FWD Loading (Not to Scale)

In the case of a recorded deflection being influenced by two or more layers, the total deflection is the sum of the deflection of each influencing layer. For

example, the geophone under the loading plate is reading the total deflection of Influence Zones 1 thru 7 because all seven layers are encompassed within the stress zone at that location. The deflection attributed to each influencing layer is a ratio of their respective elastic moduli (E) and layer thickness (Huang, 1993).

If the deflection's location, magnitude and layer thickness are known, then by back calculation (i.e. from the bottom layer up), the elastic modulus of each layer can be determined. Once the elastic modulus is determined, the structural integrity of each soil layer can be determined and appropriate rehabilitation, if necessary, can be recommended.

Due to the complexity of back calculation, a computer program is typically employed. The program recommended by the manufactures of the equipment used in this particular testing program was ELMOD4 (Dynatest®, 2000). However, there are other programs that can be used for this type of application, such as ILLISLAB (Federal Highway Administration, 1987) and KENLAYER (Huang, 1993).

4.4.3 Nuclear Density Testing

Field wet densities for this project were performed using test method FM 1-T 238 (*Density of Soils and Bituminous Concrete Mixtures In Place by the Nuclear Method*) of the 1994 Florida Sampling and Testing Methods Manual. The proceeding is a summary of the procedure as designated by FM 1-T 238.

After selection of a test site free of surface irregularities, all loose and disturbed material is removed, exposing the top of the material to be tested. The drill rod is then placed on the material and hammered to a depth approximately 2 in. (5 cm) deeper than the desired testing depth, vertical to the surface to be tested. The drill rod is then removed by rotating and pulling straight up.

The testing unit is then placed on the soil and the source probe is extended to the desired depth. It is then seated firmly by rotating it about the source rod.

The gauge should have firm contact with side of the hole nearest the scaler. A schematic of the nuclear densometer can be viewed in Figure 4.9.

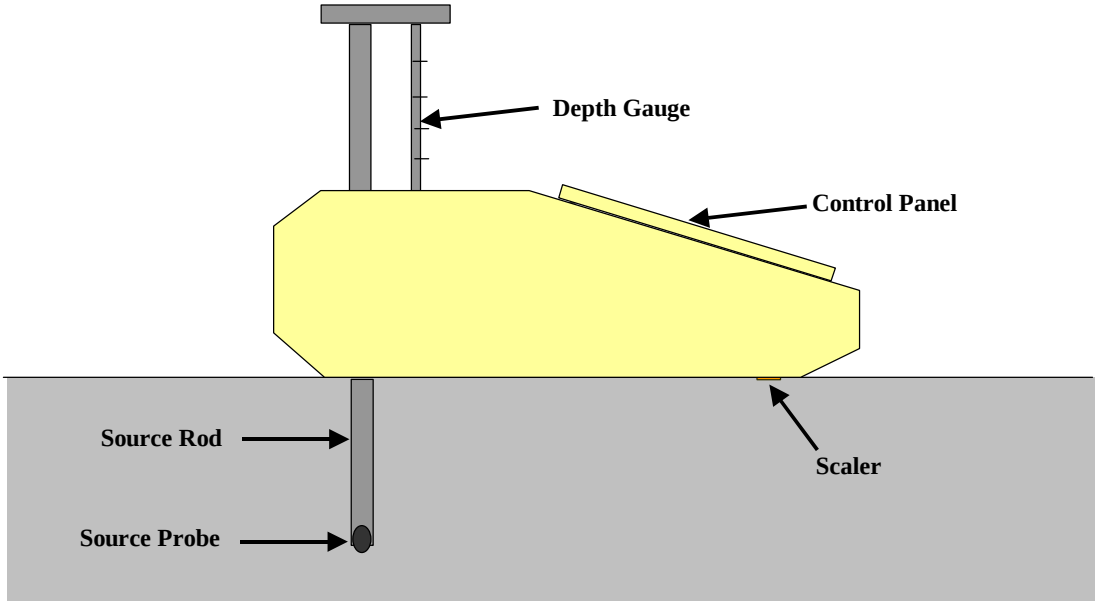

Figure 4.9 Schematic of the Nuclear Densometer

When the densometer is activated, radiation is emitted from the tip of the source rod. As the radiation is transmitted through the soil, it is filtered out by soil particles. The denser the soil, the more radiation is filtered out. A gauge on the underside of the testing unit records the unfiltered radiation. The densometer will then correlate a wet density based on the ratio of recorded radiation to the initial amount emitted.

The nuclear densometer also has the capability to record moisture contents for certain approved soils such as cemented coquina and limerock. RAP is not an approved material. Therefore, moisture contents were obtained by using a Carbide Gas Pressure Moisture Tester (FM 5-507).

4.4.4 Carbide Gas Pressure Moisture Tester

Field moisture contents for this project were performed using test method FM 5-507 (*Determination of Moisture Content by Means of a Calcium Carbide Gas Pressure Moisture Tester*) of the 1994 Florida Sampling and Testing Methods Manual. The proceeding is a summary of the procedure as designated by FM 5-507.

A representative sample of the material to be tested is collected from the site. From this sample, a 0.71 oz. (20 g) specimen is placed into the Calcium Carbide Pressure Moisture Tester with two 1¼ -inch (31.755 mm) diameter steel balls. The steel balls are used to breakdown lumps in the soil specimen.

In the cap of the moisture tester, 2 scoops (2 tsp) of the calcium carbide reagent are placed. Holding the moisture tester horizontally, the cap is inserted and tightened by a stirrup. The tester is held in this manner to prevent the reagent from reacting with the soil specimen until the tester is sealed.

Once the moisture tester is sealed, it is turned slightly vertical to allow the reagent and soil specimen to mix. The moisture tester is then shaken for 1 minute in a manner consistent with allowing the steel balls to rotate radially inside. After 1 minute, holding the tester horizontal, the moisture content is read from the dial gauge located on the opposite end of the cap.

The concept behind the Carbide Gas Pressure Moisture Tester, also known as the Speedy Moisture Tester, is that as the reagent reacts with the moisture of the soil specimen to produce acetylene gas, the gas, in turn, creates pressure inside the tester which is displayed on a dial gauge. By correlation, the pressure is converted to moisture content (Ron Lewis, FDOT, personal communication, 2000).

4.4.5 Limerock Bearing Ratio (LBR)

The LBR, in simplified terms, is the load (in lbs) required to plunge a 3 in^2 circular piston into a test specimen 0.1 inches divided by the load required to plunge the same size piston, the same depth into a limerock specimen. Florida has adopted a standard pressure for limerock as 800 psi at 0.1 inches. The ratio, multiplied by 100 and omitting the percent symbol, is known as the LBR (Ping, 1994).

In Florida, the LBR test was adopted for use in construction for subgrade strength in the early 1960's. It wasn't until the mid 1970's that it was adopted for use in determining base course strength. The origin of the LBR test traces its origins back to the California Bearing Ratio (CBR) test (Ping, 1994).

In 1929, the California Division of Highways (now known as CALTRAN) devised a laboratory bearing ratio test in order to compare available subgrade and subbase materials. To facilitate this, numerous samples of typical crusher-run material were compacted in 6-inch diameter, 6-inch high molds to an approximate density obtained under normal construction procedure. The method of compaction adopted consisted of twenty blows with a 10-lb hammer on each 1-inch layer. The compacted specimens were then soaked for 4 days under a surcharge representing the weight of the soil layers that normally would be above it in the field. The soaking process was used to simulate the worst-case field moisture conditions. After 4 days, the specimens were drained and a penetration test was performed. The penetration test consisted of vertically loading into a soil specimen to a depth of 0.1 inches. The load required to reach 0.1 in. was then recorded. After all the trials were performed, the recorded loads were averaged and the resulting value was deemed a CBR value of 100%. All individual load values were then expressed as a percentage of the 100% (Porter, 1949).

In 1955, the FDOT wanted to develop a standardized design criteria for flexible pavement. The first step in this process was to identify a testing procedure that could be correlated with the known performance of the existing pavements. Throughout the course of the investigation, it was discovered that the CBR test was the most widely used. Each state and federal agency that employed the CBR, had modified it to best suit the specific climate conditions, materials, and construction procedures of that particular region (Ping, 1994).

FDOT, like the other agencies that had adopted it, modified certain aspects of the testing procedure. The 4-day soaking period was deemed too long and that a 2-day soaking period would result in an approximation of the worst field conditions present in the state. Also, the compaction effort required in the standard CBR would not result in densities comparable to the densities found in Florida's pavements. A third finding was that Florida soils used in roadways do not exhibit the swell characteristics of those used in California. Therefore the "swell" criteria was excluded. The fourth modification made by FDOT was to establish a strength standard for Florida materials. Since the CBR was based on the average load of crusher-run California materials, such as stone, gravel, and granite, the strengths were considerably higher than those associated with Florida limerock. Because of this, FDOT conducted a series of tests to determine the strength of limerock suitable for base material. It was found that the average pressure required to penetrate 0.1 in. into limerock was 800 psi. The ratio would then be the pressure required to achieve a 0.1 in. penetration of a test specimen, by a 3 in^2 piston, divided by 800 psi (Ping, 1994). A picture of the testing apparatus can be seen in Figure 4.10.

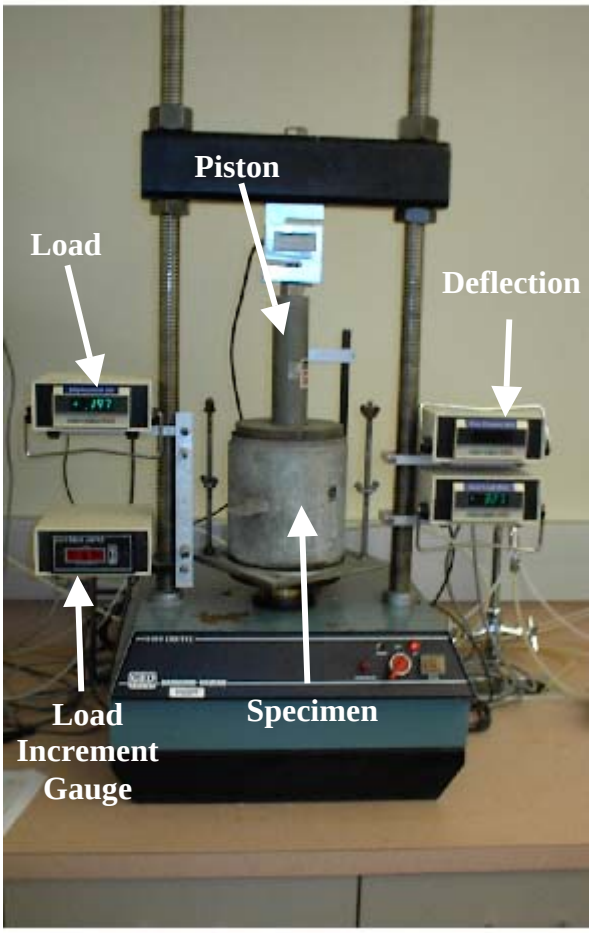

Figure 4.10 Limerock Bearing Ratio Testing Apparatus

With all of the modifications, the FDOT could no longer call their test version the CBR. It was renamed the Limerock Bearing Ratio (LBR) (Ping, 1994).

The field CBR is based on the same theory as the laboratory version. Instead of plunging the piston into a prepared lab sample, the piston is plunged into a constructed field site. The main variation between the laboratory LBR and the field CBR is soaking. The field CBR specimen is not saturated and is tested at its natural moisture content. The test is performed by manually rotating the hand crank and recording deflections from the penetration dial gauge at various load

increments read from the dial gauge in the proving ring. A picture of the field LBR testing apparatus can be seen in Figure 4.11.

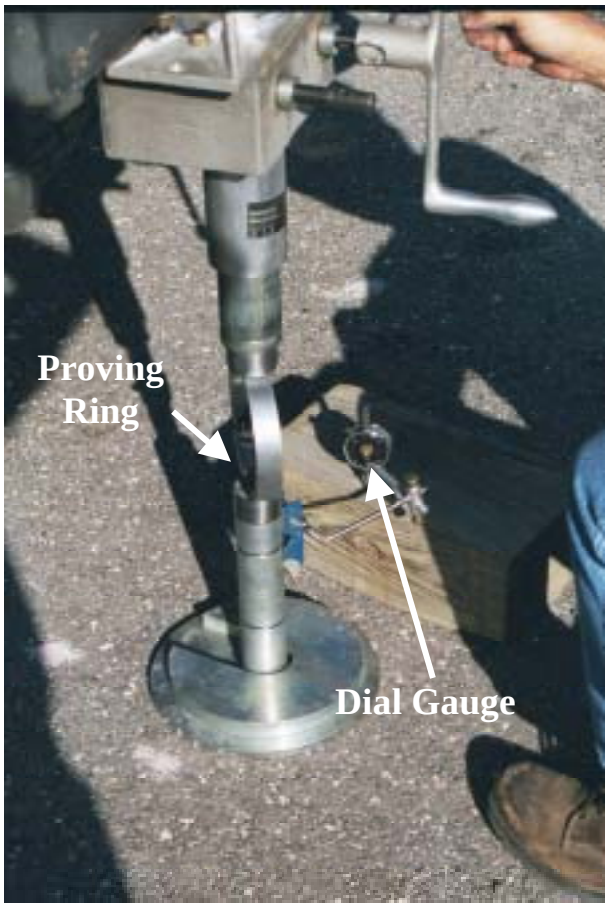

Figure 4.11 Field California Bearing Ratio Testing Apparatus

4.4.6 Automated Dynamic Cone Penetrometer (ADCP)

Research has shown that there is a direct correlation between the soil strength and its resistance to penetration by solid objects. The basic premise of the Dynamic Cone Penetrometer (DCP) is to push a steel rod into a soil by manually

striking the rod with a hammer. The penetration of the rod is recorded (usually in millimeters) along with the number of blows needed to attain penetration. The penetration depth is then divided by the number of blows to produce the Dynamic Cone Penetration Index (DCPI). The DCPI, empirically, is used to determine soil parameters such as LBR/CBR (Parker, 1998). The correlation used by FDOT equipment in this project was derived by Webster, Grau and Williams (1992) and is as follows:

$$LBR = 365/(DCPI)^{1.12} \qquad (4.6)$$

Parker (1998) proposed this correlation based on his findings in an FDOT-sponsored study of the ADCP.

The drawbacks of the manual DCP include variation due to the operator, difficulty in removing the probe from the soil upon completion, and time consumption needed to record data. Use of the Automated DCP (ADCP) reduces the effects of these drawbacks. The ADCP is a trailer mounted testing apparatus. Setup can be completed within minutes with the aid of hydraulic jacks. A program downloaded onto a portable laptop computer controls the testing procedure, collection and interpretation of data. Other than the setup, the ADCP is completely automated (Parker, 1998). Figure 4.12 pictorially shows a typical ADCP assembly.

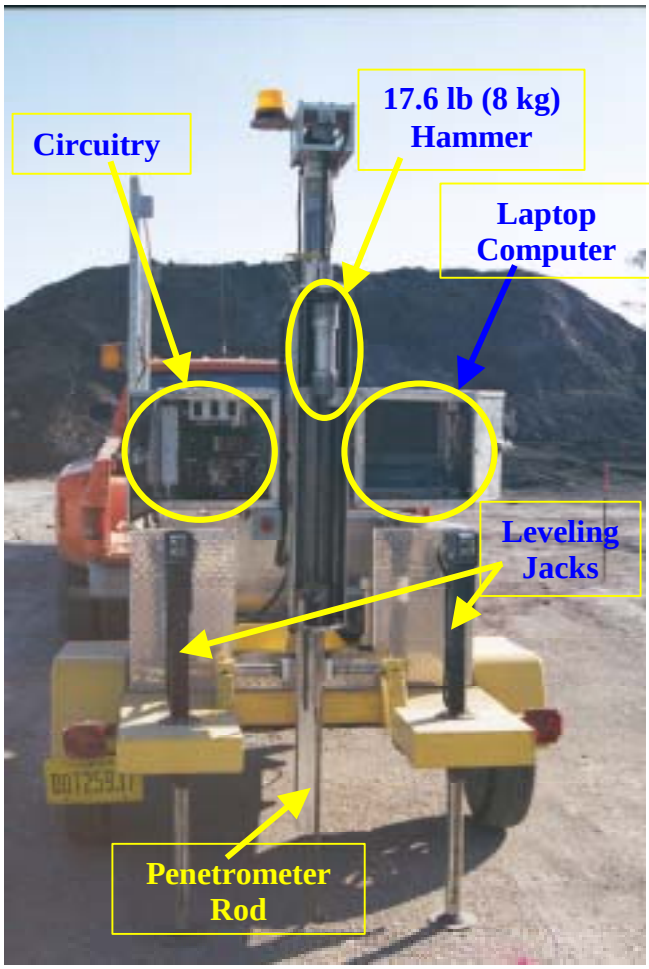

Figure 4.12 Automated Dynamic Cone Penetrometer Assembly

An advantage of the DCP/ADCP is that, unlike the conventional LBR test, which only produces a value at the ground surface, the DCP/ADCP produces values throughout the depth of the test. Unfortunately, there has not been a consensus as to the practical interpretations of the recorded data.

4.4.7 Testing Cycles

The following tests were performed on each minor section of the field site. Tests were performed immediately following construction in October, 1999 and at bi-monthly intervals thereafter.

Test	Tests Per Minor Section
Nuclear Densometer	1
Limerock Bearing Ratio	1
Falling Weight Deflectometer	3
Cone Penetrometer	1
Automated Dynamic Cone Penetrometer	1

4.5 Field Testing Results

4.5.1 Constructability

The RAP was able to be installed on high moisture content subsurface soils without any hindrance or need for dewatering. The procedure for placing the RAP under these soil conditions was identical to that of cemented coquina under favorable conditions.

Similar relative compactions between RAP and cemented coquina were met at identical compaction energies (i.e. same number of passes with a vibratory roller). The compaction procedure of both RAP and cemented coquina were identical.

4.5.2 Asphalt Content

FDOT personnel in accordance with FM 5-563 performed asphalt content of the RAP. The asphalt content of the RAP used in the field site was 5.67%. Montemayor (1998) reported asphalt contents ranging from 4% to 8% with an average of 6.73%.

4.5.3 Climatic Conditions

During the course of this study, daily high and low air temperatures as well as rainfall data were recorded. Figures 4.13 and 4.14 present this data.

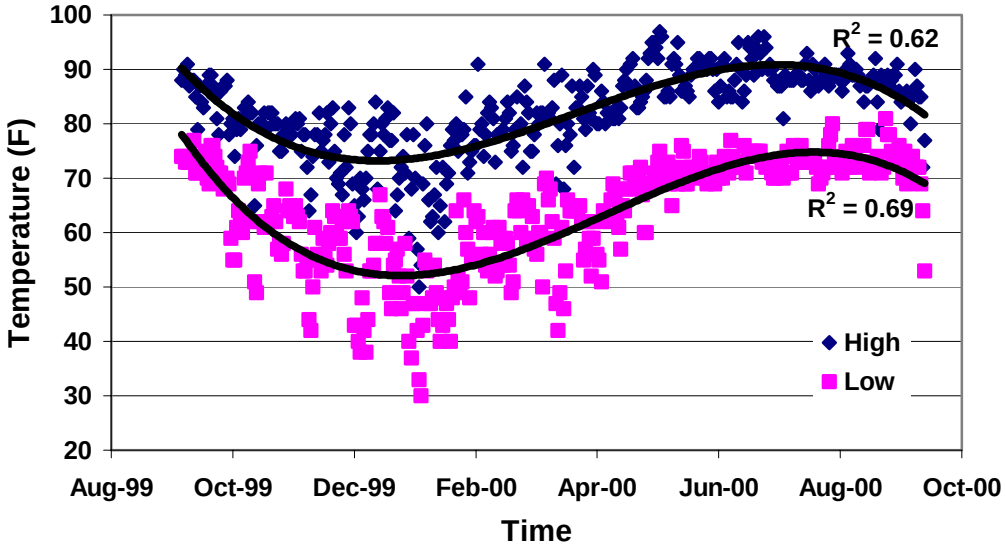

$$*\text{High} \quad y = -4*10^{-6}x^3 + 0.46x^2 - 16298x + 2*10^8 \qquad (4.1)$$

$$*\text{Low} \quad y = -5*10^{-6}x^3 + 0.53x^2 - 19541x + 2*10^8 \qquad (4.2)$$

where y = temperature in °F and x = number of days since January 1, 1900 (i.e. October 10, 2000 = 36809).

Figure 4.13 Daily High and Low Air Temperatures for Melbourne, Florida (www.accuweather.com)

According to Figure 4.13, testing began during a relatively warm period with a high of 85°F and a low of 71°F. From October 1999 to February 2000, the field site was subjected to cooler temperatures with daily high and low temperatures reaching 54°F and 30°F, respectively. From February to August 2000, a warming trend occurred with daily high and low temperatures reaching 97°F and 75°F, respectively. From August 2000 to the end of testing in October 2000, the field site was subjected to a cooling trend with daily high and low temperatures reaching 72°F and 64°F, respectively. A polynomial curve was used because it provided a better regression coefficient than either binomial or linear trend lines.

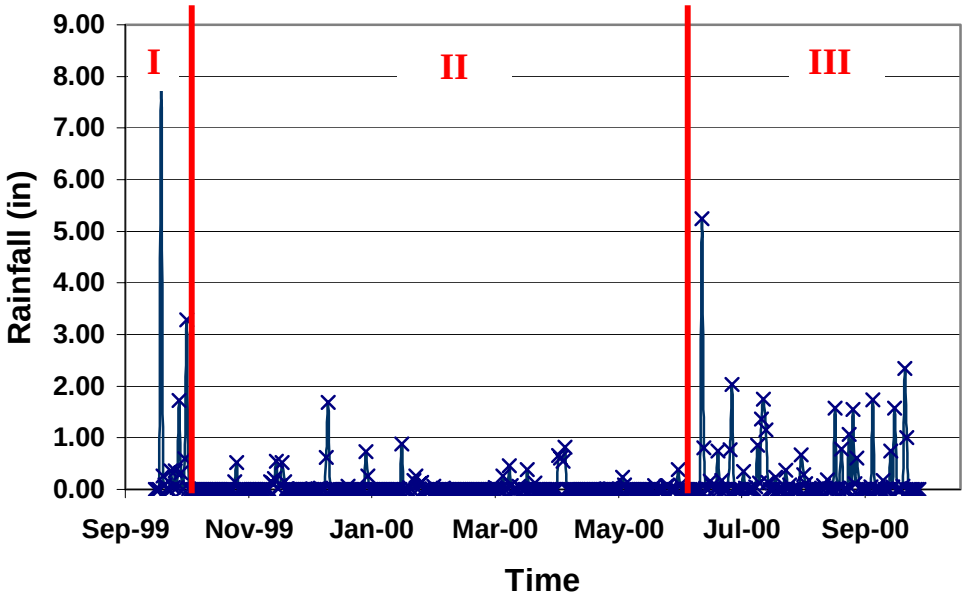

Figure 4.14 Daily Rainfall Data for Melbourne, Florida (www.accuweather.com)

Zones I, II, and III presented in Figure 4.14 represent the trends in rainfall as associated with testing. The high rainfall amount in zone I is a result of the rainfall events associated with of Hurricanes Floyd and Irene, respectively. This was also the time in which the field site was constructed and tested initially. In zone II, the field site experienced relatively low rainfall amounts. The beginning of zone III coincided with the end of spring/beginning of summer. Zone III presents the increased rainfall amount that is typical of this time period in Florida.

4.5.4 Temperature Data

Past research by Montemayor (1998) and Doig (2000) suggested temperature played a key factor in evaluating the behavior of RAP. Two methods for collecting temperature data from the field site were utilized.

4.5.4.1 Thermocouple Probes

A total of ten thermocouple probes were installed into the RAP section at depths of 6 inches (4 each), 18 inches (4 each) and 30 inches (2 each). Data was recorded using a digital hand-held Omega® HH507 thermometer at periodic intervals throughout testing dates. The thermocouple gave data on how rapidly thermal energy would be absorbed and dissipated in the RAP sections. In one instance during a December 2000 test cycle, a reading of 118° F was taken at noon on a sunny day at the 6-inch depth. Within two minutes of a cloud passing in front of the sun, the temperature dropped to 98° F.

Because the digital thermometer used only had the capacity to display, but not record, instantaneous data, it became impractical to constantly monitor the thermocouple probes in order to compile continuous temperature versus depth data. Therefore, another of method of evaluating temperature was chosen.

4.5.4.2 Temperature Probes

After investigating other possible alternatives, it was decided to use VEMCO mini-log temperature probes. The probes were ordered in March, 2000. Because they had to be custom built, they were not were received until May, 2000. In June, 2000, the probes were installed into a RAP test pit on the Florida Tech campus at the surface and depths of 6 inches, 12 inches, 18 inches, and 30 inches. The temperature probes had the capacity to constantly record temperature data at time intervals as small as five seconds for as long as five years. A photograph of a mini-log temperature probe can be viewed in Figure 4.15.

Figure 4.15 – VEMCO Mini-Log Temperature Probes

The probes were placed in the RAP for three days (June 8 - June 10) and temperature data was recorded at 2-hour intervals. During this three-day test period, the daily high air temperature remained constant at 87°F and the daily low temperature ranged from 69°F to 76°F, also, there was no reported rainfall. After the probes were removed and the data was downloaded to a computer, an average temperature profile was developed for each two-hour increment beginning at 12:00 pm through 8:00 am. Figures 4.16 and 4.17 graphically show these temperature profiles.

In Figure 4.16, the temperature profiles begin at 12:00 pm and conclude at 8:00 pm. As would be expected, the temperature at the surface increases throughout the afternoon, from 12:00 pm until 4:00 pm, and then decreases during the early evening from, 4:00 pm until 8:00 pm. However, temperatures obtained for the 6-inch and 12-inch depths increase continually from 12:00 pm to 8:00 pm. The maximum and minimum temperature gradients ($^{\Delta T}/_{\Delta z}$) from the surface to a depth of 18 inches were 0.72 and 0.06, respectively. The temperatures obtained at 18-inch and 30-inch depths remain constant over the 8-hour period. This suggests

that the RAP becomes insulated at 18 inches and that air temperature will have little effect at depths greater than this during summer months.

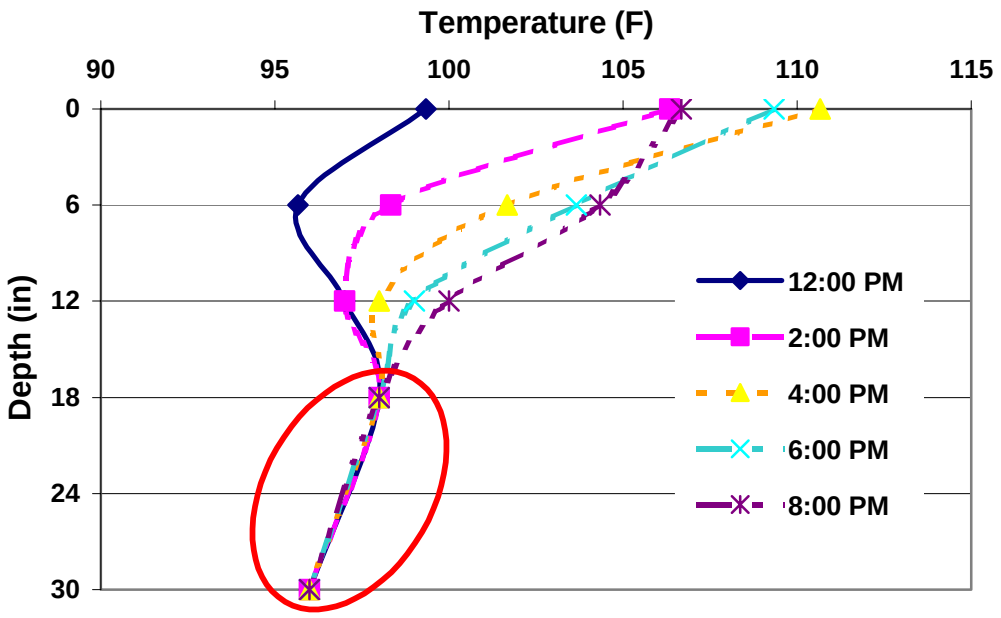

Figure 4.16 Average Temperature Profile of RAP From 12 pm to 8 pm (June 8-10, 2000)

Figure 4.17 represents the temperature profiles of the RAP during nighttime hours (10:00 pm to 8:00 am). The temperatures taken at 6-inch and 12-inch depths lag by 5 to 8 degrees with respect to the surface temperatures regarding heat dissipation as a function of time. The maximum and minimum temperature gradients ($^{\Delta T}/_{\Delta z}$) from the surface to a depth of 18 inches were 0.56 and 0.11, respectively. The 18-inch and 30-inch temperatures again remain constant not only for Figure 4.17 but are nearly identical with the values in Figure 4.16. This data, again, supports the conclusion that at 18 inches the RAP is insulated from the effects of air temperature during warm temperature cycles. It is also recommended that the probes be placed at depths greater than 30 inches to study the end of the temperature gradient.

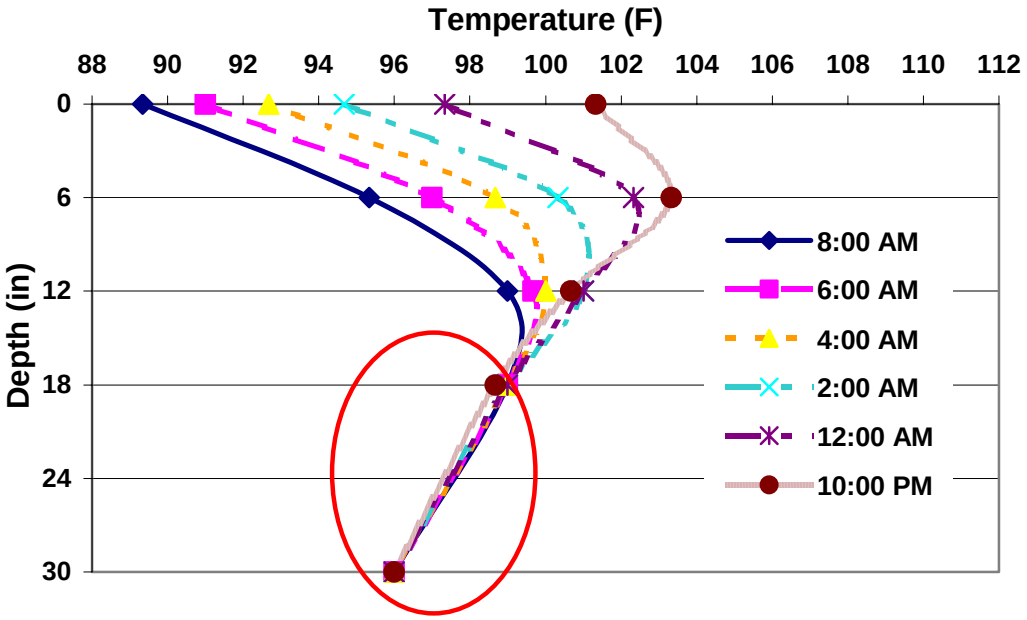

Figure 4.17 Average Temperature Profile of RAP From 10 pm to 8 am (June 8-10, 2000)

4.5.5 Density and Moisture Test Results

During the construction phase of the field site, the lifts were installed in 6-inch increments. Compaction was achieved using a single drum, Ingrasol SD-70 vibratory roller. The weight of the roller was 15,300 lbs (6940 kg). The drum was 7 feet (2.13 m) wide had a 1-inch (2.54 cm) contact surface width. Nuclear density tests were performed at a 6-inch depth every two passes beginning after the 4th pass and concluding after the 16th pass. In situ density results taken upon completion of the field site are presented in Table 4.3 along with the standard deviation of subsequent density tests. In situ densities for the cemented coquina are the average of two tests taken in each section. The moisture content of the RAP and cemented coquina were determined by test methods FM 5-507 and FM 1-T 238, respectively.

Table 4.3 Final Construction Field Densities

Material	Section	Section Thickness (in)	Moisture Content (%)	Initial In Situ Dry Density (pcf)	Standard Deviation Over Time (pcf)**
Elevated RAP	A1	36	5.4	121.2	+/- 1.3
	A2	24	5.4	118.2	+/- 3.0
	A3	12	4.8	116.2	+/- 2.0
Equivalent RAP	B1	36	5.7	117.4	+/- 1.5
	B2	24	5.4	115.0	+/- 3.2
	B3	12	3.6	114.5	+/- 2.0
Cemented Coquina	C1	36	10.1	126.4*	+/- 1.7
	C2	24	11.0	126.3*	+/- 1.9
	C3	12	11.7	125.0*	+/- 3.4

* Average of two tests
** Standard Deviation was determined from bi-monthly data
*** 1 lb/ft^3 = 0.157 kN/m^3

The cemented coquina achieved higher densities than both the elevated and equivalent RAP sections. Also, the densities for the three layers of the cemented coquina are very similar regardless of the layer thickness.

With regards to the RAP, the elevated sections achieved higher densities and lower standard deviations for each of the layer thicknesses as compared to the equivalent sections. Also, for both RAP sections, the densities increased and standard deviations decreased with increasing thickness of the layers. These two statements are supported by the fact that the elevated RAP layers were compacted more than the equivalent RAP layers and that the compaction of the layers of the thicker sections negated the effects of the subsurface.

Densities were then taken at two-month intervals for a period of one year. Data from these subsequent tests revealed little change in the density of either the RAP or the cemented coquina (Table 4.3). The average standard deviation over the twelve-month testing period of density for the RAP was less than 1.6 pcf with no individual sectional deviation exceeding 5.9 pcf. The average standard deviation in

density over the same time period for cemented coquina was less than 2.1 pcf with no individual sectional deviation exceeding 5.7 pcf.

4.5.6 Relative Compaction

Relative compaction was based on a maximum dry density determined from modified Proctor compaction, FM 5-521 (ASTM D1577). Maximum dry densities of 117 pcf (1.87 g/cm^3) for the RAP (Doig, 2000) and 128 pcf (2.05 g/cm^3) for the cemented coquina (Professional Engineering, Testing & Inspection, 1999) were reported. The relationship between relative compaction and number of passes for the RAP is presented graphically in Figure 4.18. With the exception of the results recorded at 6 passes, the relative compaction of the RAP increased from 4 passes to 14 passes and decreased after 14 passes. After 8 to 10 passes, 100% of modified Proctor maximum density for RAP is achieved.

Figure 4.19 presents the relative compaction achieved in the final 6-inch lift for each section of the field site. The cemented coquina section and the "equivalent" RAP were compacted with the same energy. From Figure 4.19, it can be concluded that by using the same compaction energy, the relative compaction of RAP will be nearly equal to the relative compaction of cemented coquina. Due to the increased compaction energy imparted on the "elevated" RAP, the relative compaction of this RAP section was found to be higher. This comparison can also be viewed in Figure 4.19.

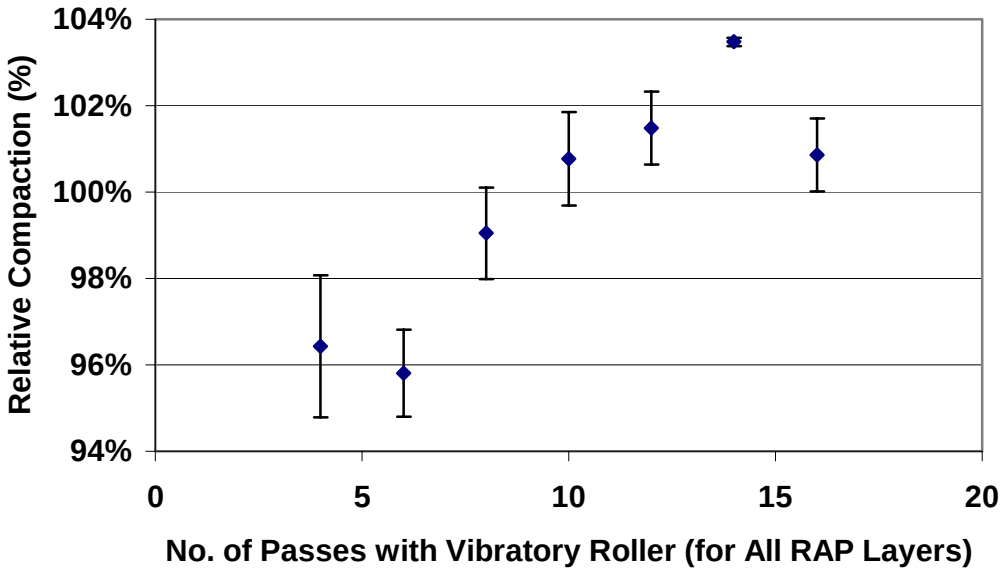

Figure 4.18 Relative Compaction (including Standard Deviation) of RAP based on Modified Proctor vs. Number of Passes with Vibratory Roller

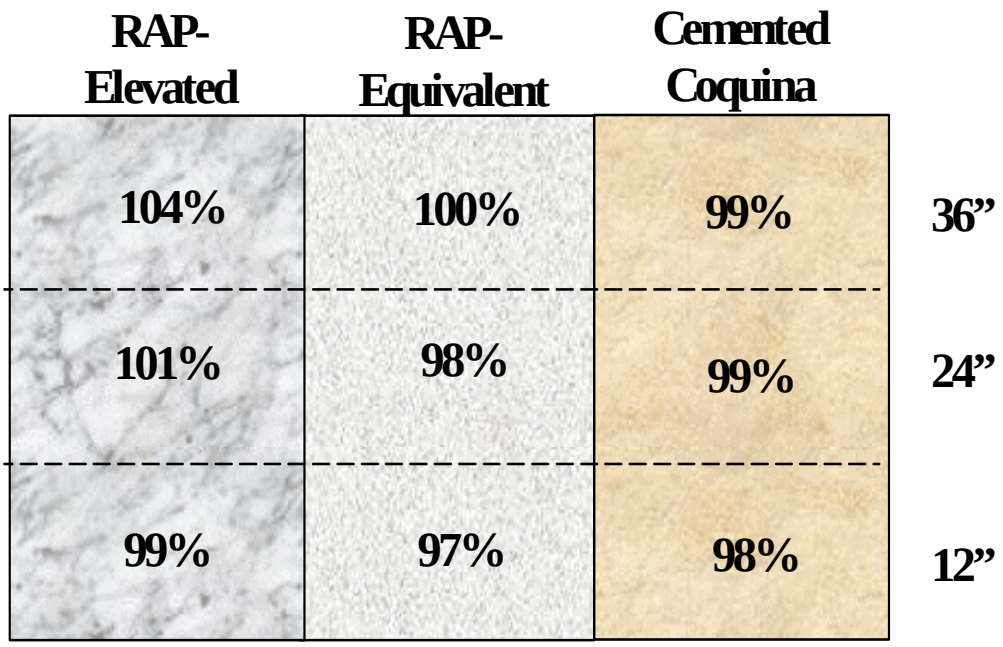

Figure 4.19 Relative Compaction of Each Field Site Section in Final 6-inch Lift

4.5.7 Cone Penetrometer (CPT)

Five sets of CPT's were performed bi-monthly beginning in October, 1999 and concluding in June, 2000. Testing was limited to five cycles due to the size of the field site and 'influence zones" developed for the destructive testing of the CPT. It was conservatively assumed that each CPT test disturbed a zone 5 feet in diameter around the hole (Janbu 1976). CPT readings were taken in both RAP sections and at all three depths. Raw CPT data is presented in Appendix CC.

Both the tip and frictional resistance (q_c and f_c, respectively) were obtained from the CPT. Schmertman (1970) proposed a correlation to estimate the equivalent elastic modulus of the soil, E_s. The correlation was developed by plotting field q_c of fine sands in Florida with their corresponding E_s value back-calculated from screw-plate tests performed at the same sites.

Schmertman proposed that E_s was 2 to 3.5 (Schmertman and Hartman, 1978) times the tip resistance, q_c, depending on the state of stress of the soil. For a soil experiencing volumetric expansion (i.e. such as during pile driving), a value of 2 was recommended. In a situation where the soil is experiencing a plane strain state of stress (i.e. continuous footing), the q_c should be multiplied by a factor of 3.5.

For this project, q_c was averaged for each 12-inch layer and then converted into an elastic modulus. Using a constant of 2, the range, average and standard deviation of E_s over the project duration for the RAP are summarized in Table 4.4.

Table 4.4 Modulus of Elasticity (E_s) for 36-inch RAP Based on Schmertman and Hartman's (1978) Correlation to CPT Data

	Range	Average	Std Dev
Layer	(ksi)	(ksi)	(ksi)
Top 12-inches	2.6 - 9.0	5.5	+/- 1.1
Middle 12-inches	4.6 - 9.1	6.9	+/- 0.7
Bottom 12-inches	4.9 - 9.6	6.9	+/- 1.4
Overall Average		6.2	+/- 1.0

Doig (2000) reported laboratory E_s values from triaxial testing of 7 ksi to 17 ksi for RAP stored at elevated temperatures of 100° F and 125° F, while values of 4 ksi to 12 ksi were recorded for samples stored at room temperature. As presented in Table 4.4, the field E_s values are lower than these laboratory E_s values that Doig (2000) reported. Doig (2000) reported using confining pressures of 5 psi, 10 psi, and 15 psi. Maximum confining pressure of the RAP in the field site was 2.5 psi. The difference between laboratory and field site confining pressures explains the reason why the field E_s values are lower than the laboratory E_s values.

The values for E_s varied greatly depending on when the tests were performed. In general, during the cooler times of the year, the E_s values increased during the warmer months, E_s decreased. Figure 4.20 graphically presents this trend for each of the three layers in the 36-inch RAP along with the daily high and low temperature of the day of testing. The moduli plotted in Figure 4.20 are the combined averages of the elevated and equivalent RAP for each layer at the time of testing. Average values were employed due to the similar test results obtained for each section. Note that only temperatures corresponding with CPT testing are presented.

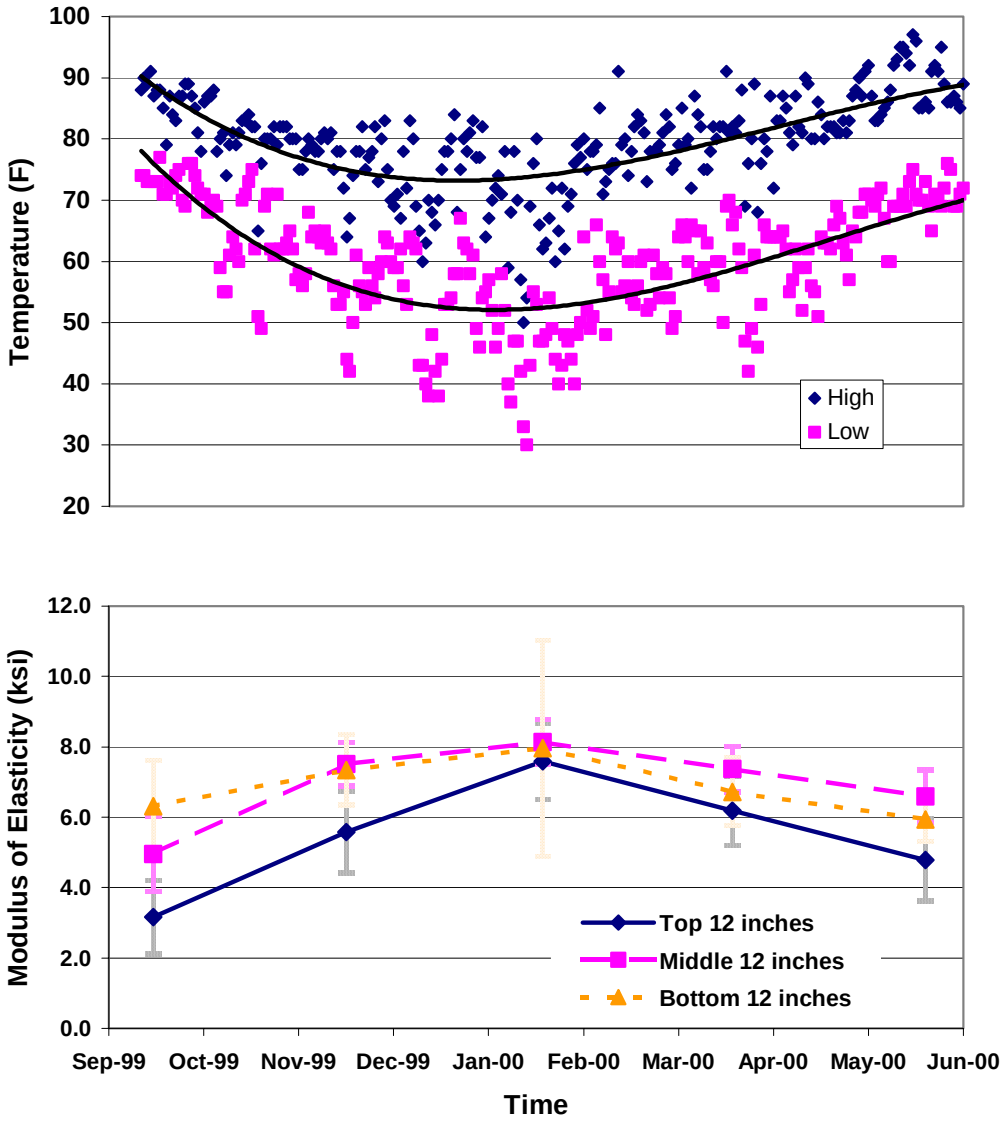

Figure 4.20 Variation in Elastic Moduli (with Standard Deviation) Based on Schmertman and Hartman's (1978) Correlation with the CPT vs. Time

With the exception of the December, 1999 test cycle, the data indicates that temperature controls the elastic modulus. From October, 1999 to February, 2000, the RAP experienced an increase in E_s of 140% for top 12 inches to 26% for the bottom 12 inches. During this period the daily high and low temperatures

decreased by 21% and 24%, respectively. From February, 2000 to June, 2000, the RAP experienced a decrease in E_s of 37% for the top 12 inches to 25% for the bottom 12 inches while the daily high and low temperatures increased by 36% and 30%, respectively. As is the case with any field study, all variables could not be controlled. The drier conditions prevalent during the period caused a drop in moisture content of the RAP from 5.7% to 4.8% from installation until December 1999 (Figure 4.14, Zone II).

As would be expected, the top layer of RAP is more susceptible to thermal changes and, therefore, exhibits the lowest and most varied E_s values. The bottom layer conversely exhibits the highest E_s initially. The higher moduli are most likely due to the higher confining pressure from the two layers above. The variations in E_s as time passed may be a result of interaction with the weaker subgrade than of thermal fluctuations due to the bottom layer being located within the "insulation zone". The middle layer avoids the major influencing factors of the top and yields moduli that are consistent and similar to the bottom 12-inch layer. As expected, its initial E_s is between the top and bottom layer values. This is a result of the middle layer being subjected to a both confinement and thermal insulation by the top layer. From February, 2000 to June, 2000 the middle layer exhibits a higher E_s than the bottom layer. This, again, was assumed to be a result of the bottom layer interacting with a weak subgrade, while the middle layer experienced both confining pressure and thermal changes

4.5.8 Limerock Bearing Ratio

Seven sets of field CBR's were performed bi-monthly on the field site beginning in October, 1999 and concluding in October, 2000. The field CBR's were converted to LBR's and will be referred to as LBR's from this point forward. Figures 4.21, 4.22, and 4.23 present the trends in LBR values throughout the

duration of testing for the 12-inch, 24-inch and 36-inch sections. At the completion of construction, the LBR values for the RAP ranged from 13 to 16. These values are well below the FDOT LBR thresholds for subbases and base courses, 40 and 100, respectively (FDOT, 1999). Throughout the duration of testing, the 12-inch layers consistently displayed results that did not fit the trends of the 24-inch and 36-inch layers. These variations are attributed to the influence of the weak subgrade affecting the 12-inch layers but not the thicker layers.

From October, 1999 to February, 2000 the LBR values of the 24-inch and 36-inch RAP increased an average of 524% as compared to 80% for the 12-inch layers. By December 1999, LBR values for the 24-inch and 36-inch layers surpassed the minimum FDOT requirement of 40 for a subbase.

Following the increase, the LBR values tended to decrease for the 24-inch and 36-inch layers until August 2000 and then increased dramatically from August to October, 2000. A complete set of LBR data collected during this project can be viewed in Appendix DD.

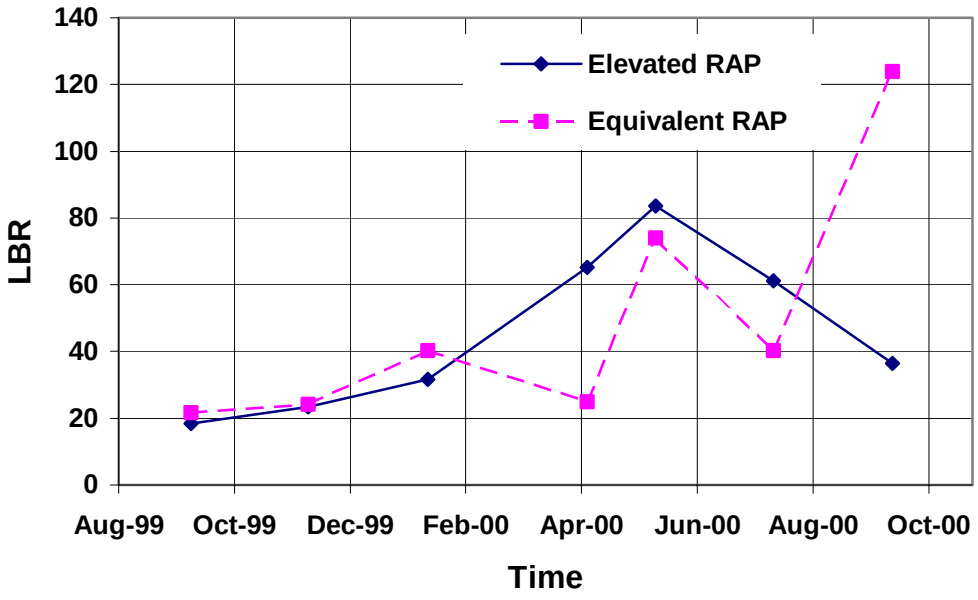

Figure 4.21 LBR Values Recorded for 12-inch Layers of RAP vs. Time

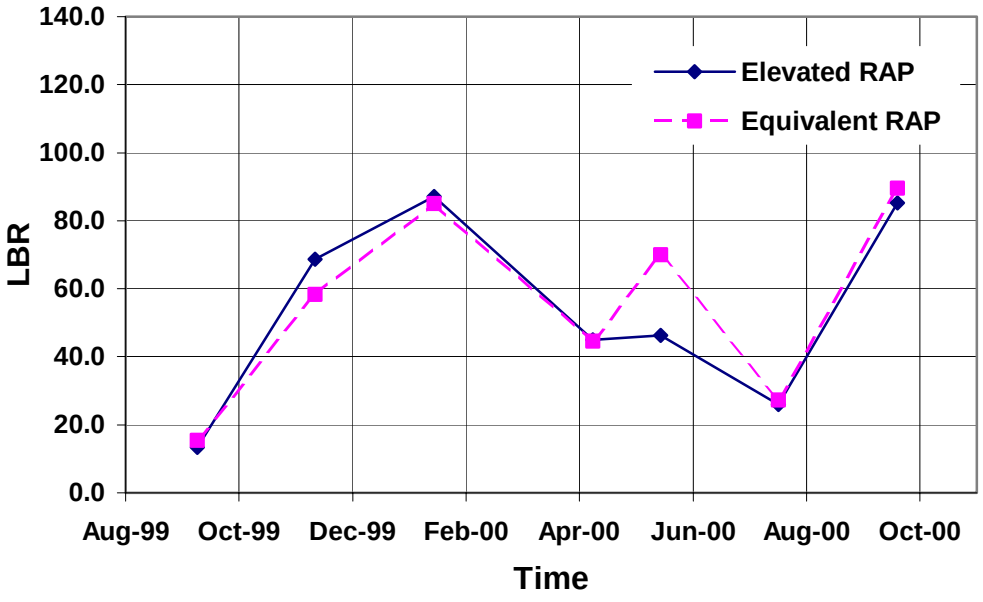

Figure 4.22 LBR Values Recorded for 24-inch Layers of RAP vs. Time

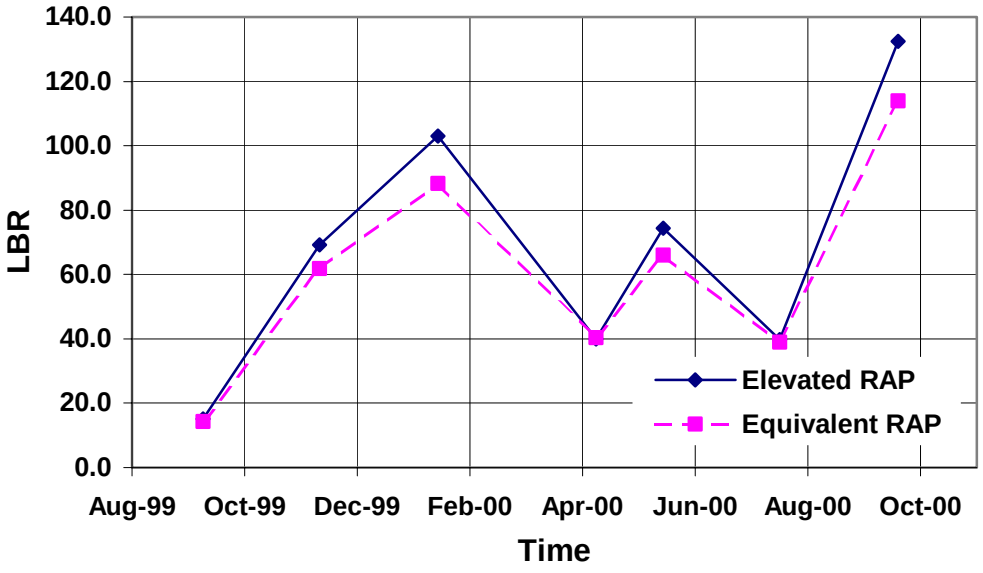

Figure 4.23 LBR Values Recorded for 36-inch Layers of RAP vs. Time

One of the possibilities as to why the RAP behaves in this manner may be attributed to the air temperature at the time of testing. By comparing the LBR value with the daily high and low temperature of the test date, an inverse relationship is observed. This relationship infers that as the temperature decreases the LBR value increases and vice versa. The variability of LBR values seen in the May, June, and August may be due to the increasing air temperature. Figure 4.24 demonstrates this relationship for the 36-inch RAP layer. It is recommended that during the spring and summer seasons, more than one LBR test should be performed in each section.

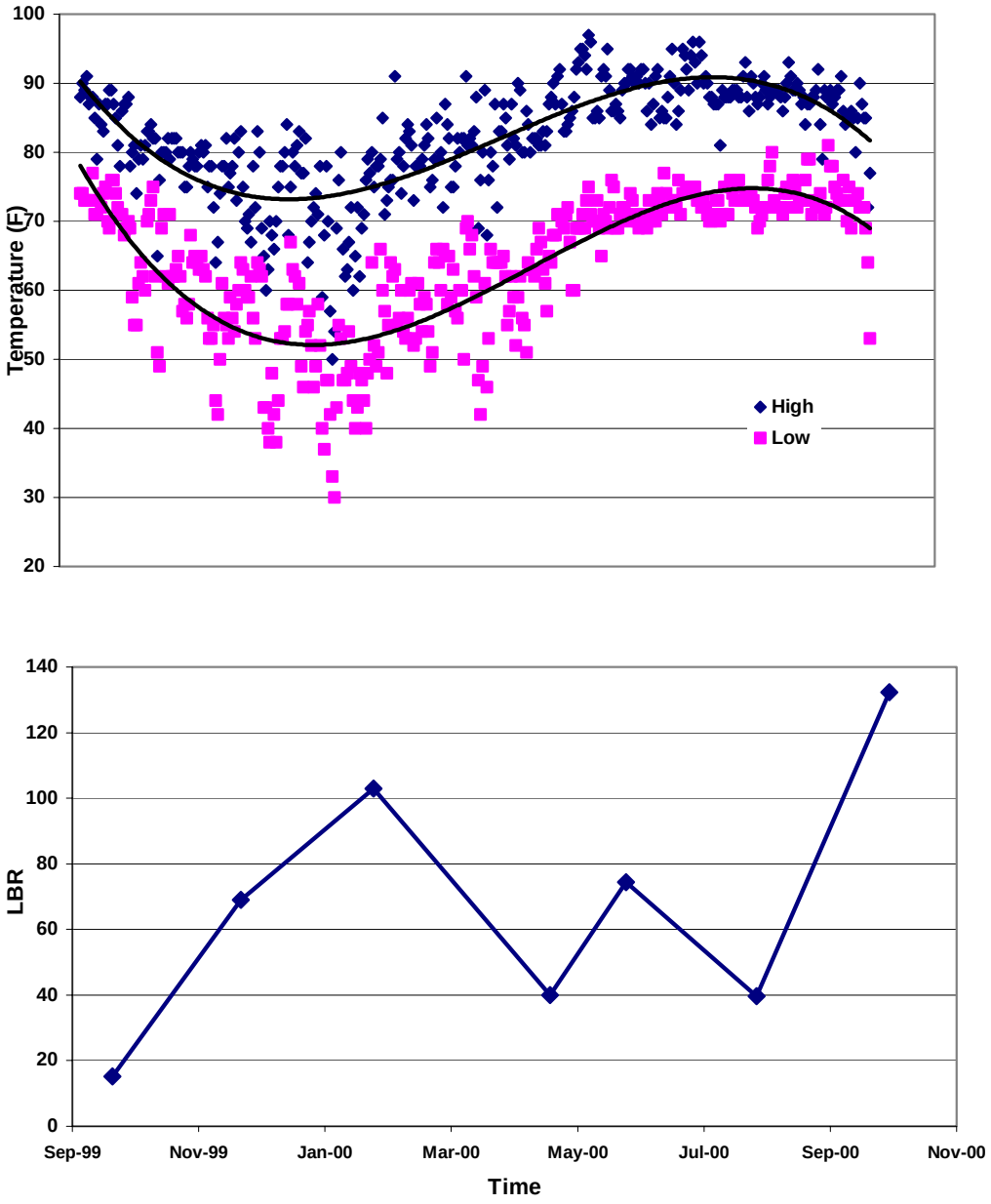

Figure 4.24 LBR and Temperature vs. Time for 36-inch Elevated RAP Layer

To further study this relationship, the LBR readings for the RAP were paired with the corresponding air temperature. The combined average LBR of the 24-inch and 36-inch layers for each temperature was calculated along with the

standard deviation. The relationship between LBR and air temperature is presented in Figure 4.25. This curve indicates that as the temperature increased from 72ºF to 89ºF the average LBR decreased by 55%. This supports the conclusion that temperature is a major factor in LBR strength of RAP and that at lower air temperatures, the RAP will be stronger.

Between 89ºF and 95ºF the average LBR begins to rise. This may have been a result of the combined effects of temperature and time and not primarily based on one or the other.

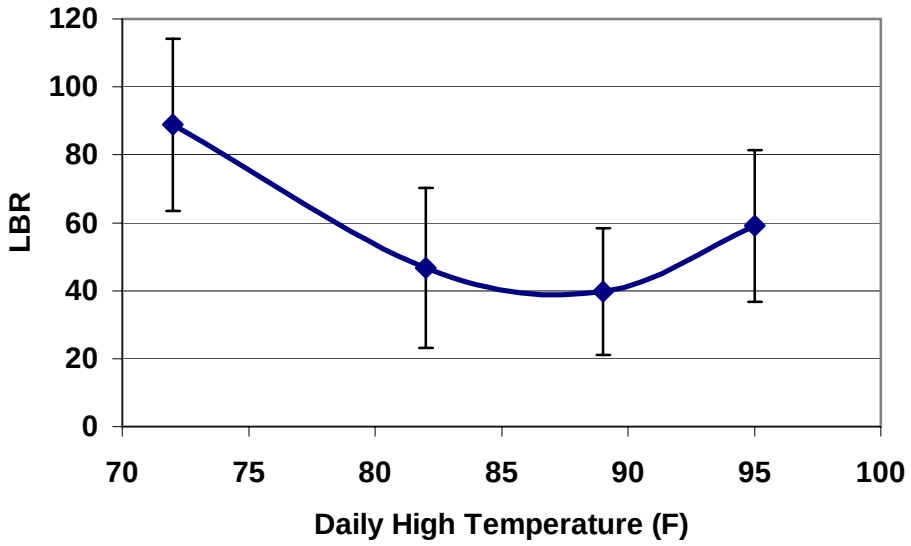

Figure 4.25 Combined Average LBR of 24-inch and 36-inch RAP Layers vs. Temperature

4.5.9 Automated Dynamic Cone Penetrometer (ADCP)

Three sets of ADCP tests were performed in October 1999, December 1999, and February 2000. Only three test cycles were performed due to continued mechanical failure of the testing equipment. Raw data collected by the ADCP is presented in Appendix EE.

According to Parker's (1998) studies of soil profiles produced by the ADCP, the top and bottom 10% to 20% of a layer should be ignored due to their weakness. He states the weakness of these portions is due to the "lack of confinement and or compaction". Parker (1998) recommends that only the middle 60% to 80% of the layer should be used in determining the acceptability of the material. For this study, the average DCPI values (in blows/mm of 17.6 lb (8kg) hammer) of the middle 70% of the top layer of each section were used to predict the correlated LBR values by means of the Webster's equation. As stated in Section 4.4.6, Webster's equation (1992) is:

$$LBR = 365/(DCPI)^{1.12} \qquad (4.6)$$

LBR values determined for the RAP using this methodology are presented in Table 4.5.

Table 4.5 Predicted LBR Values Correlated from ADCP

Layer thickness	Section Designation	Material	Predicted LBR Values		
			Oct-99	Dec-99	Feb-00
12"	A3	Elevated RAP	63	124	137
	B3	Equivalent RAP	52	92	106
24"	A2	Elevated RAP	49	114	176
	B2	Equivalent RAP	55	120	151
36"	A1	Elevated RAP	73	140	131
	B1	Equivalent RAP	80	139	146

As seen with the LBR's obtained from field CBR test, the predicted LBR's increased throughout the testing periods. Again, this overall increase may be attributed to the effects of air temperature at the time of testing. Also, as with the LBR findings, predicted LBR's of the elevated RAP sections tend to be higher than the predicted LBR's of the corresponding equivalent RAP sections.

4.5.10 ADCP vs. LBR

Data obtained from the field LBR testing was compared to Webster's predicted LBR's from the ADCP testing. In all cases, the LBR's predicted using the ADCP over estimated the recorded values from the field LBR tests by an average of 200%.

Webster's formula (1992) was derived by correlating the field CBR's of numerous soils with their corresponding DCPI's. The field CBR's ranged from 2 to 98 with approximately one-fourth of approximately 200 tests less than or equal to 10. Field LBR's of the RAP ranged from 13 to 132. Because Webster's correlation is based on a large number of values outside of the range of RAP, this correlation did not adequately provide realistic RAP LBR's.

In this study, two new comparisons were made between field LBR's and data obtained from the ADCP. The first involved plotting field LBR vs. the average LBR's as predicted by the ADCP. The predicted LBR's were derived at depths of 2-inches, 4-inches, 6-inches, 8-inches, and the middle 70% of the layer. The 2-inch depth is the shallowest increment in which data from this equipment can be processed. The results of this comparison were plotted using linear regressions and can be viewed in Figure 4.26.

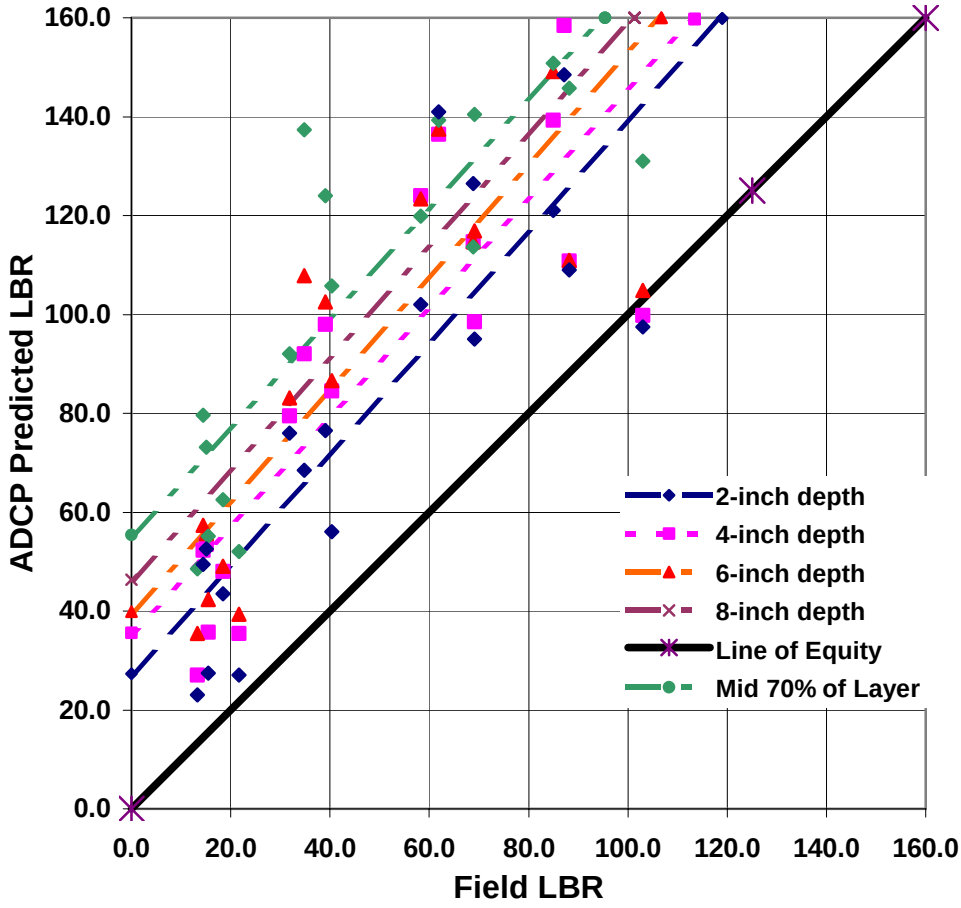

Figure 4.26 Linear Regressions of Field LBR vs. Average ADCP Predicted LBR Data at Various Depths

As can be seen in the preceding figure, the predicted LBR's from the shallow depths are closer to the line of equity than the deeper-depth correlations. However, all predicted LBR values exceed the measured values by 30 to 60. Also, the average of the middle 70% of the layer over predicts more severely than any of the comparisons made in this study. However, the 2-inch depth correlation over predicts by a value of 30 to 40. The linear regression coefficients (R^2) of the trend lines ranged from 0.69 for the 6-inch depth to 0.73 for the 2-inch and 8-inch lines.

The second comparison was based on Webster's correlation (1992). However, to further evaluate how DCPI values affected the equation, DCPI values

were averaged over depths of 2-inches, 4-inches, and 6-inches. These average DCPI's were then plotted versus their corresponding field LBR's and, by linear regression, the following formulas for each depth were calculated.

2-inch Depth	$LBR = 256/(DCPI)^{1.24}$	(4.7)
4-inch Depth	$LBR = 267/(DCPI)^{1.36}$	(4.8)
6-inch Depth	$LBR = 334/(DCPI)^{1.63}$	(4.9)

Graphical representations on a log-log scale of each formula along with Webster's equation can be seen in Figure 4.27.

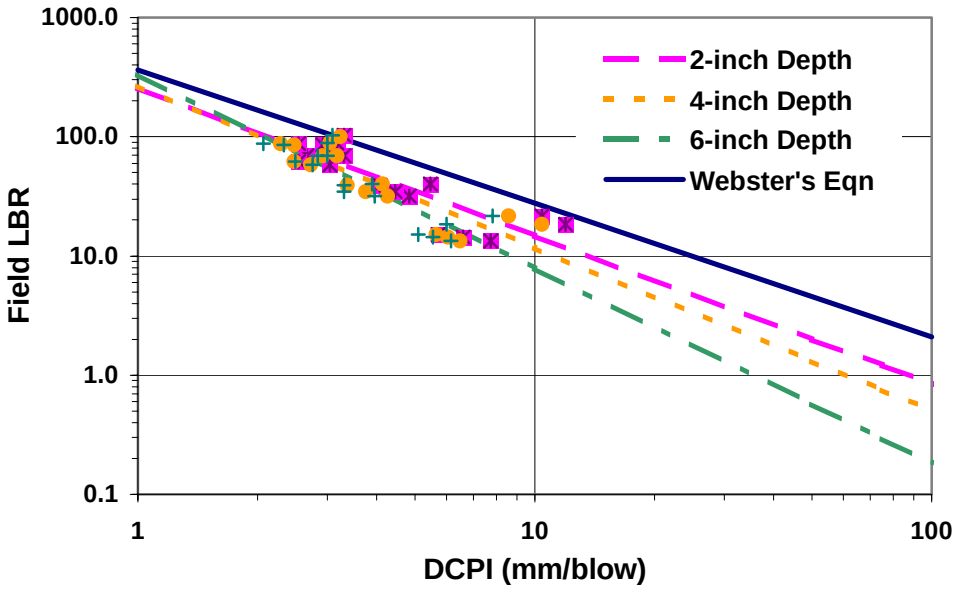

Figure 4.27 Field LBR vs. DCPI at Various Depths

From the preceding figure it can be shown that, with regards to RAP, Webster's equation over predicts the LBR value based on the DCPI. The 6-inch analysis yielded the most conservative predicted LBR. Also, based on this comparison, an equal DCPI will yield a higher LBR for the shallower depths than

for the deeper depths. This finding parallels Parker's (1998) recommendation that the upper 10% to 20% of the layer be negated. However, Parker made this recommendation based on weakness in the upper layer of soil due to lack of confining pressure. In this comparison, the upper 10% to 20% should be negated due to over prediction of LBR values caused by variations in the upper layer of soil and small size of the penetrating rod of the ADCP.

In summary, ADCP-predicted LBR's for RAP are over estimated using Webster's formula (1992). If Webster's formula is employed using ADCP-predicted LBR's to predict field LBR's, the average ADCP-predicted LBR's for the first 2 inches of the layer should be employed. However, this correlation will still over predict field LBR's by a value of 30 to 40.

If DCPI is employed to predict field LBR, it is recommended that the DCPI value used is an average DCPI of the top 6 inches of the layer to be used with Equation 4.9. This will predict a more conservative LBR than Webster's equation.

4.5.11 Falling Weight Deflectometer (FWD)

Seven sets of tests were performed bi-monthly beginning in October, 1999 and concluding in October, 2000. Three tests were performed at three locations in each of the nine sections during each testing cycle. Locations and test designation can be viewed in Figure 4.28. The test locations and designations are numbered from 1 through 9 for each section tested and subdivided within each section as 0.01, 0.02, and 0.03.

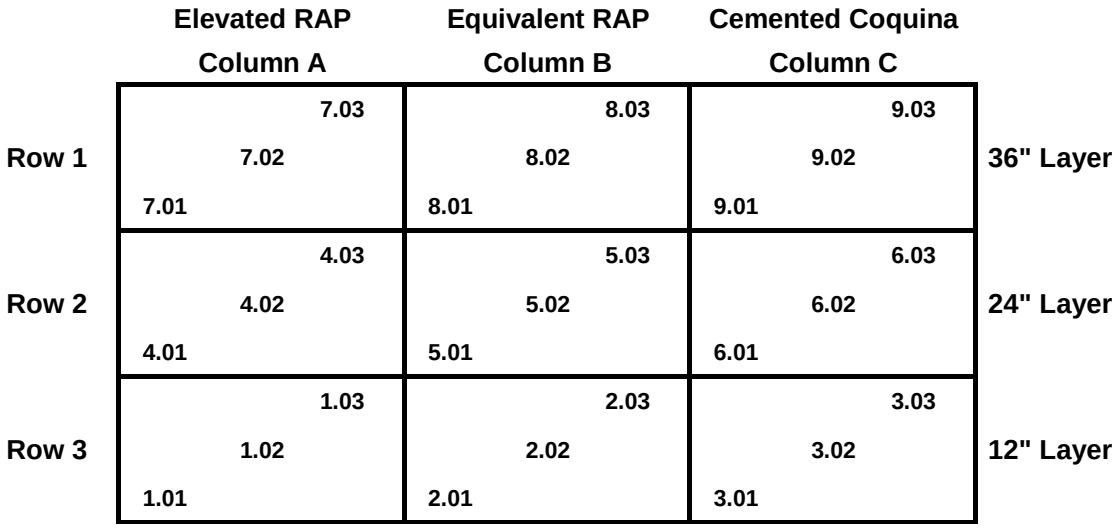

Figure 4.28 Test Designation and Location for FWD Testing

4.5.11.1 FWD Data Reduction

At each location, three tests were performed using three load levels. Although the individual loading conditions varied, the targeted values were 7,000 lbs, 9,000 lb, and 11,000 lbs (3,175 kg, 4,082 kg, and 4,989 kg). Raw data collected by FWD testing is presented in Appendix FF.

Each load produced a deflection basin with deflections recorded using the seven geophones. The data was the analyzed by evaluating the consistency of the deflection bowls. Geophone deflections were checked for outlier data that could have occurred from debris under the geophone recording pin. Following the data analysis, several techniques were used to reduce the data to meaningful results.

First, the overall pavement system stiffness was estimated by taking the average load of each test location and dividing it by the average deflection under geophone 1 (i.e. the maximum deflection). This overall pavement stiffness is termed the impulse stiffness modulus or ISM (Bush, 1990).

The second technique used for evaluation of the FWD data was the dynamic stiffness modulus (DSM). The DSM is also determined using the load and deflection of geophone 1. However, rather than using the average load and deflection, the DSM is defined as the difference between the maximum and minimum loads divided by the difference between their corresponding deflections. The equation for DSM (Green and Hall 1975) is as follows:

$$DSM = \frac{\text{Max Load} - \text{Min Load (in lbs)}}{D_0 \text{ at Max Load} - D_0 \text{ at Min Load (in mils)}} \qquad (4.10)$$

The final technique employed involved imputing the FWD loads and deflection basins into Modulus 5.0, a software package developed by Michelak and Scullion (1995) at the Texas Transportation Institute. This program is used to estimate the elastic modulus of the individual pavement layers. The tolerances required by this program for layer thickness were smaller than the variations in the field site. This caused difficulties in obtaining consistent back-calculated moduli. Therefore, results of this technique will not be discussed in this paper.

Although both the ISM and DSM reduced the data to workable parameters, the ISM consistently produced more uniform data, whereas, the DSM produced negative values in instances when the minimum load deflection exceeded the maximum load deflection. Therefore, the ISM was selected as the most efficient parameter to compare the data recorded from the FWD. As stated in Section 4.4.2, the ISM is defined as:

$$ISM = \frac{\text{Load (in kips)}}{\text{Center Plate Deflection (in mils)}} \qquad (4.11)$$

4.5.11.2 ISM vs. Time & Air Temperature

The ISM developed for this comparison was an average of the three different tests with their three loading conditions for each test cycle. For example, the ISM for section A1 is the average of three loading conditions at test locations 7.01, 7.02, and 7.03. The pattern developed when comparing the ISM of RAP with time and air temperature follows the same general trend as that of the LBR: as the temperature increases, the ISM decreases and vice versa. Figures 4.29 and 4.30 graphically represent this correlation.

In the 24-inch RAP sections, the elevated RAP's ISM's are noticeably higher for the elevated RAP in December, 1999 and February, 2000 (23% and 48%, respectively). From April to October 2000, both the elevated and equivalent RAP section ISM's are nearly identical. This comparison can be viewed in Figure 4.29.

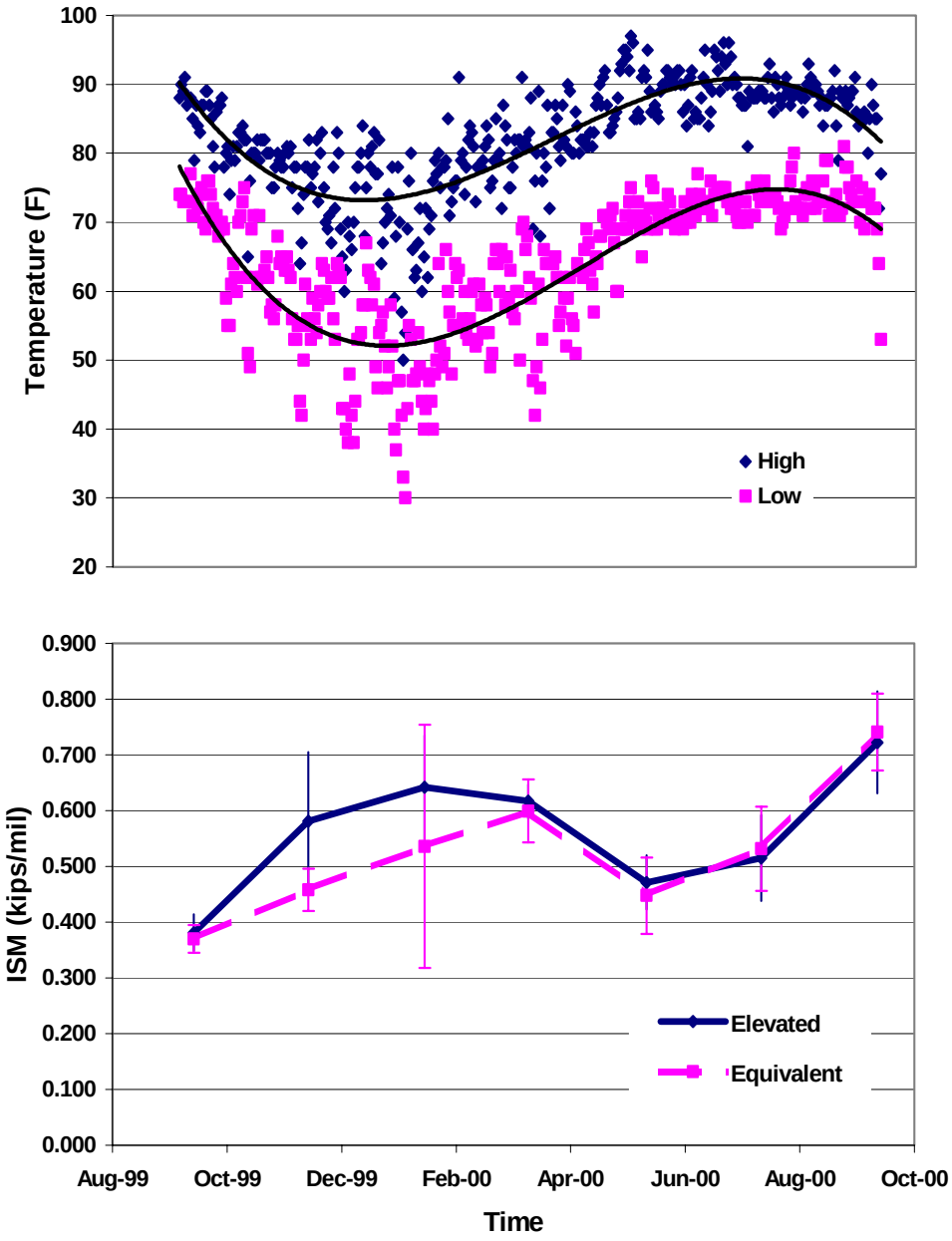

Figure 4.29 ISM and Air Temperature vs. Time for 24-inch RAP Layers

In the 36-inch layer, the elevated RAP produces slightly higher ISM values than the equivalent RAP as shown in Figure 4.30. From October to February, the percentage increases of the elevated and equivalent RAP sections are 79% and 99%

respectively. Between February and June 2000, the percentage increases from initial testing are 46% (elevated RAP) and 47% (equivalent RAP). From June to October 2000, the overall increases for the elevated and equivalent RAP section are 149% and 146%, respectively

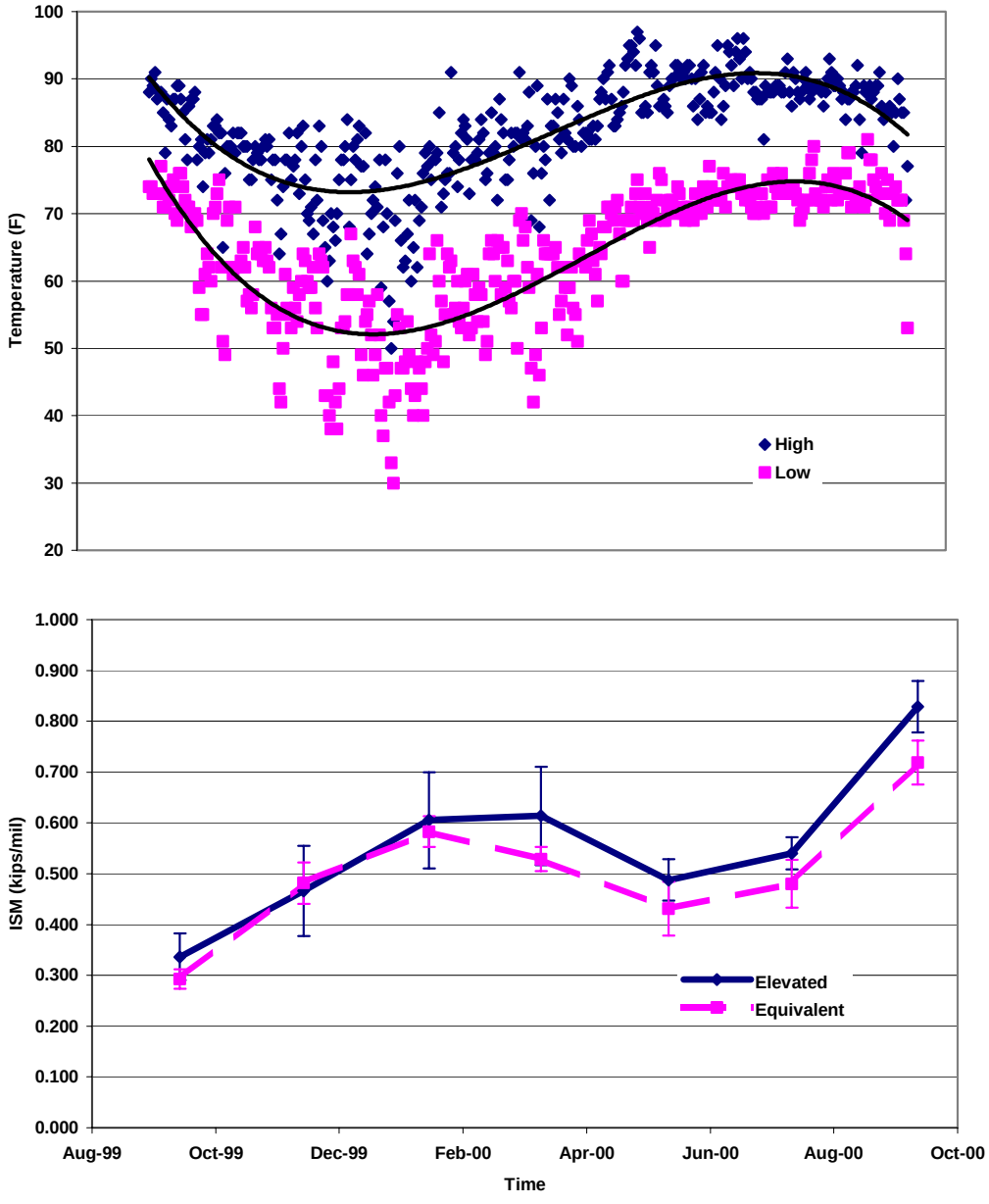

Figure 4.30 ISM and Air Temperature vs. Time for 36-inch RAP Layers

4.5.12 RAP Correlations

In the preceding sections, the results of each individual test were analyzed and compared to time and temperature. In this section comparisons between the data obtained from the LBR, FWD, and CPT tests will be discussed. In particular, relationships between the LBR, ISM, and equivalent modulus of elasticity, E_s, will be presented.

The methodology of this procedure was to plot one test value versus another test value of the same corresponding time, location, and compaction energy. From the scatter plot, a linear regression curve and its equation were determined.

Figures 4.31 and 4.32 represent the relationships between E_s vs. LBR and E_s vs. ISM, respectively, for the 36-inch thick RAP layer. The 12-inch and 24-inch layers displayed inconsistent results, yet showed the possibility of a correlation between the various parameters. This follows the same patterns from the previous analysis of LBR, CPT, and ISM data in this chapter; the 12-inch and 24-inch layers displayed general trends, whereas, analysis of the 36-inch layer produced the most uniform trends with the least amount of variations. A comparison of the relationships between E_s vs. LBR and E_s vs. ISM for the 12-inch, 24-inch, and 36-inch thick RAP layers is presented in Appendix GG.

In Figures 4.31 and 4.32, a limited number of LBR and ISM values were available for comparison with corresponding modulus of elasticity E_s. However the linear regression coefficients of these comparisons (0.76 and .069, respectively) indicates a correlation exists between E_s from CPT testing and LBR and E_s and ISM.

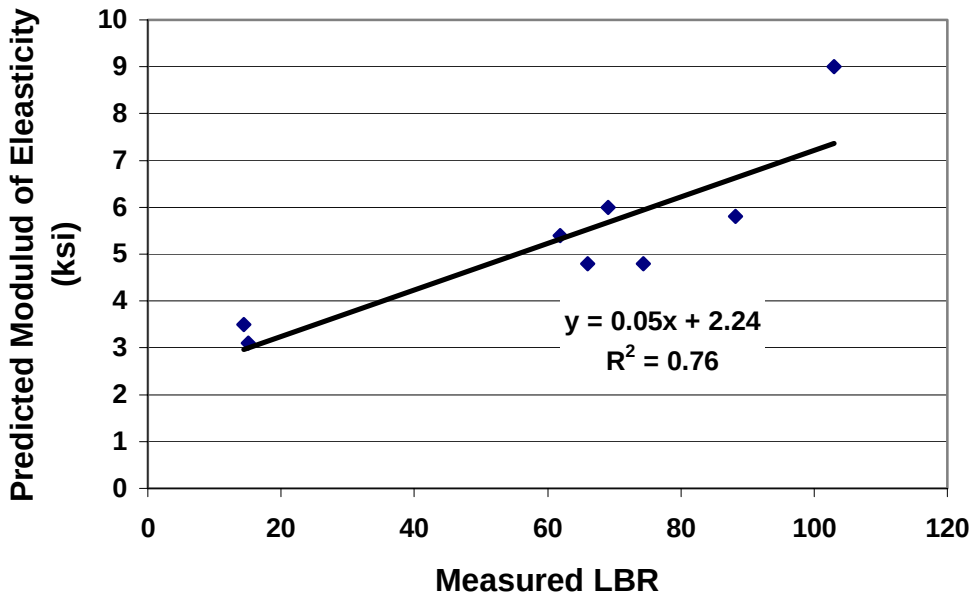

Figure 4.31 Predicted CPT Modulus of Elasticity, E_s vs. LBR for 36-inch RAP

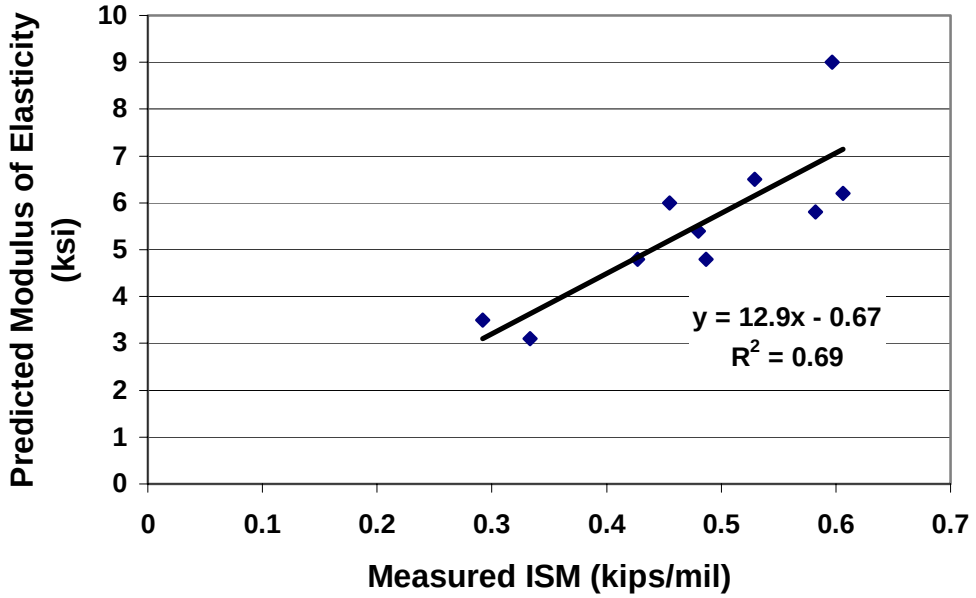

Figure 4.32 Predicted CPT Modulus of Elasticity, E_s vs. ISM for 36-inch RAP

The third comparison was between the ISM's of the middle FWD tests for RAP and their corresponding LBR. The middle FWD tests are those with the ".02" designation. These tests were chosen due to their central location within each section. It is assumed that these test values would be less influenced by the surrounding sections as compared to the tests located near section borders (".01" and ".03" tests).

Numerous graphical comparisons were made with the middle RAP ISM's, beginning with individual loadings for the 36-inch RAP and expanded to include the middle loading conditions of the 12-inch, and 24-inch layers. For each layer, a linear regression curve was calculated. In each case, the coefficient of determination increased with the thickness of the layer. Figure 4.33 graphically represents the plot of LBR vs. the RAP ISM's of the middle 36-inch FWD test. The linear regression curve was calculated using 36 data points and the regression coefficient of this curve (0.72) indicates a correlation exists between ISM from FWD testing and LBR. A graphical comparison of the 12-inch and 24-inch layers is presented in Appendix GG.

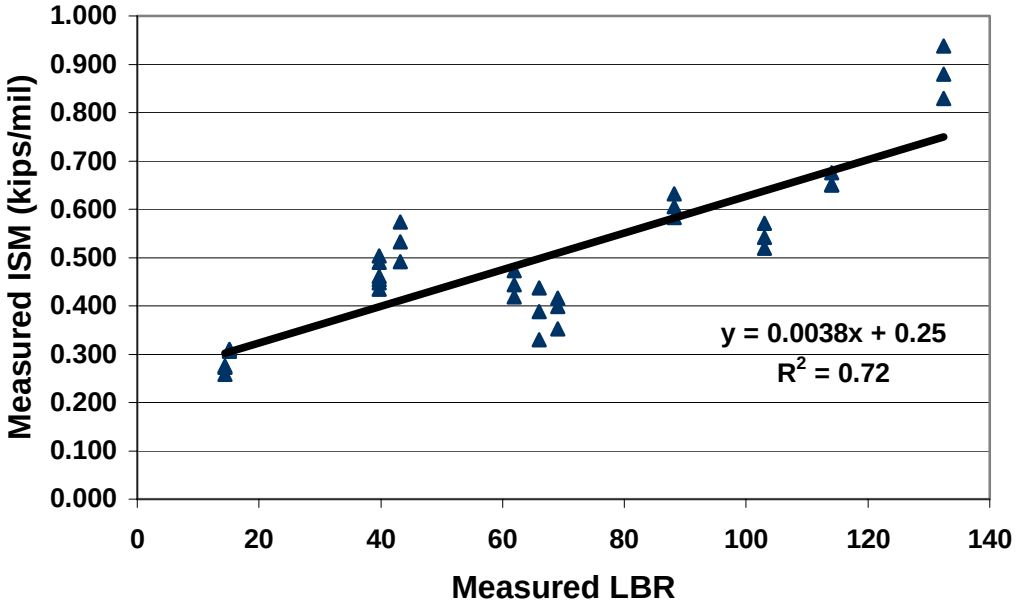

Figure 4.33 LBR vs. ISM of Middle FWD Tests for 36-inch RAP

Table 4.6 presents the percentage stiffness gains of RAP data obtained after the initial two months from the LBR, ADCP, FWD and CPT. The ADCP-LBR, ISM, and E_s all experienced similar stiffness gains in the range of 81% to 129%. The LBR experienced stiffness gains of approximately five times that of the other tests (548%). This infers that the field LBR test does not provide as uniform results as the other tests performed on this field site.

Table 4.6 Summary of Stiffness Gains After Initial Two Months

Test	Percentage Strength Gain
LBR	548%
ADCP-LBR	81%
ISM (from FWD)	89%
E_s (from CPT)	128%

In conclusion, based on the coefficient of determination values of these comparisons, it is possible to use the FWD and CPT, in lieu of the LBR, to evaluate the performance of RAP. Both of these test methods produced data with matching trends as those displayed by the LBR.

FWD tests can be performed very quickly and produce a larger amount of data than the LBR. In this study, there were nine complete sets of FWD data for each LBR value. Also, reducing the FWD data to an ISM format is fast, reliable, and can be performed in the field with simple software.

The correlation between ISM and LBR shows that it is possible to replace LBR specifications of 40 and 100 with approximate corresponding ISM values of 0.4 (kips/mil) and 0.63 (kips/mil), respectively.

It is also possible to predict elastic moduli from the CPT tip resistances. These values correlated well with the LBR. However, CPT testing is more tedious and time consuming than FWD testing and may limit its usefulness in this type of application.

4.5.13 Comparisons Between RAP and Cemented Coquina

LBR and ISM data collected from the RAP sections was compared to the data obtained from the cemented coquina control section. Cemented coquina is one of the most widely used and available materials. In Florida it is specified as a subbase and base course material (FDOT 1999).

Figures 4.34 and Figure 4.35 graphically depict the strength variations of both RAP and cemented coquina with respect to time and rainfall for the 36-inch layer. An initial field CBR test of cemented coquina could not be performed due to the high moisture content (9.6%) of the material, the high moisture content of the natural subgrade (21.5%) and the propensity of cemented coquina to absorb water.

These factors resulted in the cemented coquina being too weak to support the weight of the field CBR testing apparatus. The excessive moisture did not prevent the testing of the RAP. It showed no excess-moisture problems.

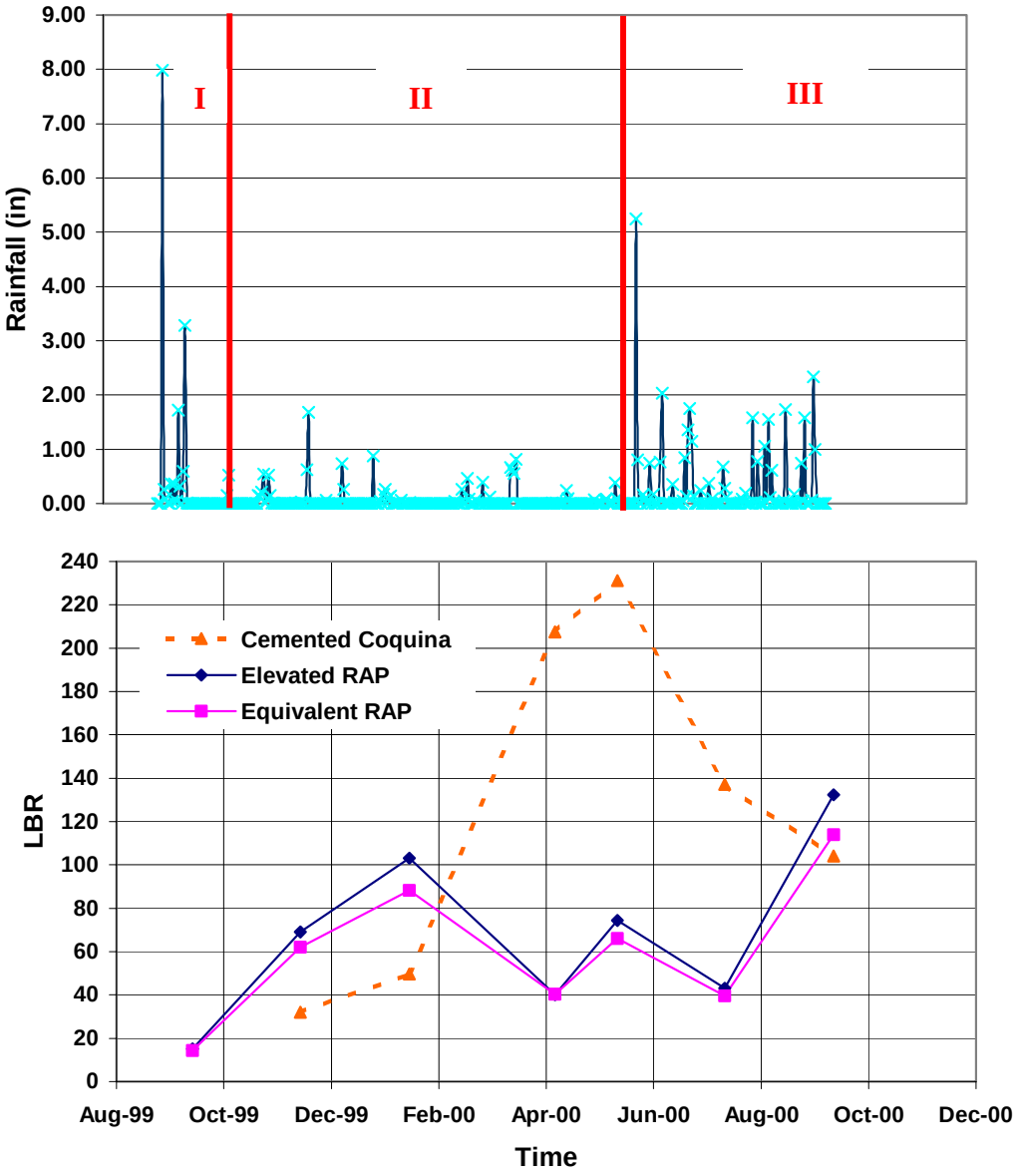

Figure 4.34 RAP and Cemented Coquina LBR's and Rainfall vs. Time for 36-inch Layer

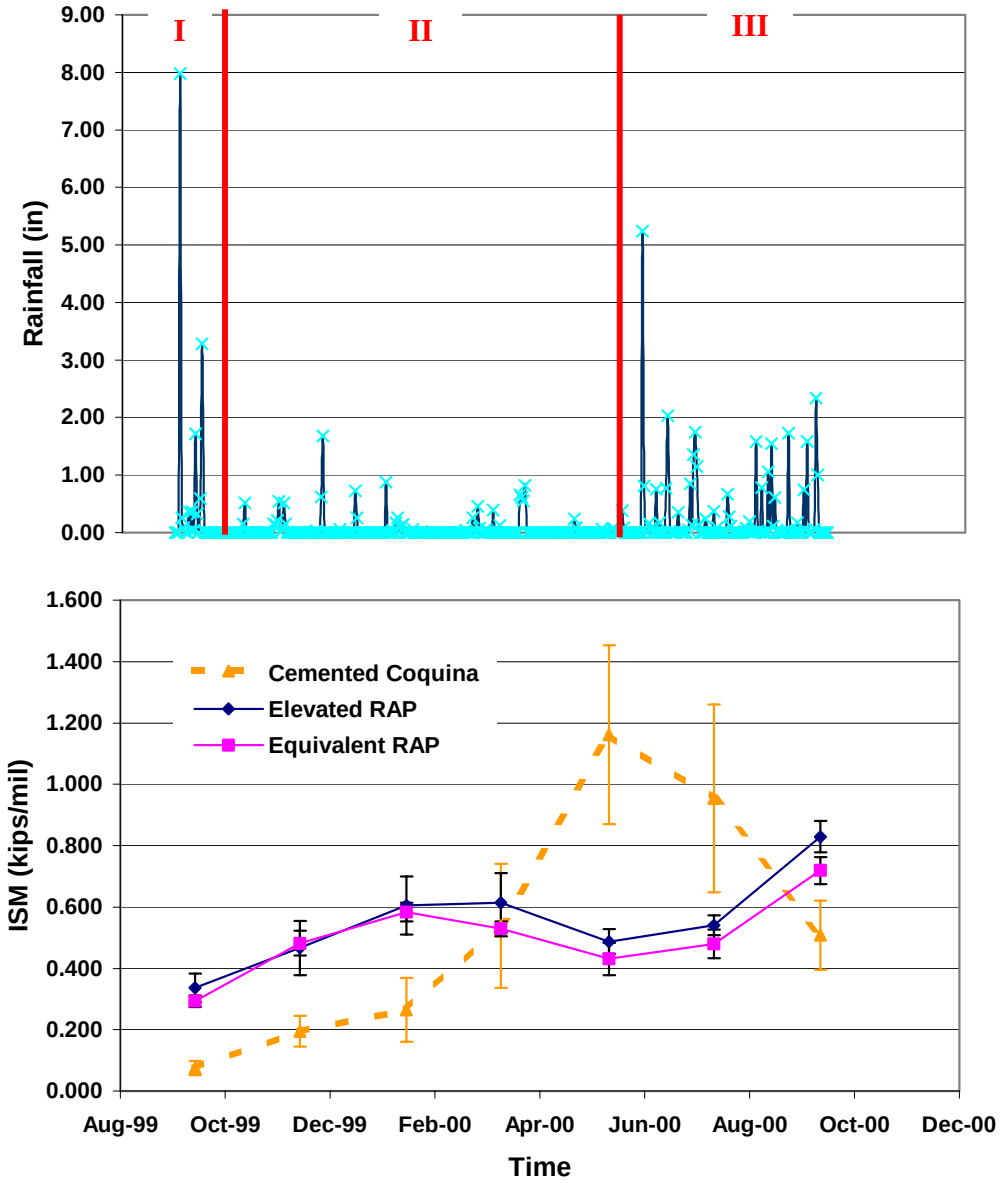

Figure 4.35 RAP and Cemented Coquina ISM's and Rainfall vs. Time for 36-inch Layer

The initially low values for the cemented coquina shown on these graphs for the December, 1999 and February, 2000 test cycles are most likely attributed to heavy rainfall in the preceding months. From the beginning of September, 1999 to the end of November, 1999 more than 33.5 inches of rain fell in the Melbourne area

(Zone I). (www.accuweather.com, 2000). This unusually heavy rainfall was due to the occurrence of two hurricanes and a series of intense rainstorms during this time.

From December, 1999 to June, 2000 the cemented coquina experienced strength gains of 622% for the LBR and 496% for the ISM. During this six-month period the field site was subjected to a total of 9.6 inches of rain (Zone II) (www.accuweather.com, 2000). From June, 2000 to October, 2000, the LBR and ISM values of the cemented coquina dropped 55% and 56%, respectively. During this four-month period, rainfall increased to 23.1 inches (Zone III) (www.accuweather.com, 2000). With the exception of April/May test cycles, the trends of the ISM and LBR for the cemented coquina were identical. This implies that the two tests are interchangeable.

As discussed previously, the LBR and ISM values of RAP are more likely to change with temperature whereas the cemented coquina's values are more likely to change with moisture content. Also, although the cemented coquina attains LBR and ISM values that noticeably exceed those of the RAP, in this particular study, the cemented coquina's values fluctuate more than those of the RAP.

5. Conclusions

5.1 Laboratory Testing Conclusions

These lab studies provided valuable information on the engineering properties of RAP. This information provides a basis to establish RAP as an accepted structural fill, or as a base or subbase course in roadway construction. The following conclusions were made from the results obtained.

5.1.1 Effects of Post-Milling Processing

The post-milling of RAP with the tubgrinder or hammermill process yields materials which fall outside the ranges specified by Talbot and ASTM D 2940-92 "Standard Specification for Graded Aggregate Materials for a Base or Subbase." The tubgrinder RAP used in this study averaged higher dry densities, higher strength, and higher stiffness than the corresponding hammermill RAP. This is attributed to a higher coarse sand content achieved during the particular grinding operation for the Tubgrinding operation. The dry density is not sensitive to small changes in moisture content.

The angle of friction did not vary between samples from the hammermill and tubgrinder RAP. The values obtained, 37 to 40 degrees, are within the angles suggested for materials to be used as base or subbase course materials. The cohesion of the

tubgrinder samples was 4-6 psi (28-36 kPa) higher than the hammermill samples. The secant moduli ranged from 7 to 17 ksi (49 to 199 kPa).

5.1.2 Compaction Effects

RAP compacted using modified Proctor, modified Marshall, vibratory and static methods did not display classical moisture-density behavior. The dry density was relatively constant at moisture contents greater than 4 percent. Samples from all compaction methods had free draining water at moisture contents greater than 10 percent. There were very slight differences in dry density due to processing. These differences most likely are due to grinding and sample variations. Field compaction of RAP should be conducted using moisture contents from 3 to 7 percent.

RAP compacted using modified Proctor, modified Marshall, vibratory and static pressures below 1000 psi, did not meet FDOT LBR specifications for use as a base course. RAP compacted using vibratory methods behaved similarly to sands.

The bearing strength of RAP compacted with confinement as used in the modified Marshall did achieve LBR values of 40 and may be used for subbase and subgrade construction.

5.1.3 Effects of Temperature

Increasing temperature has a significant effect on most of the triaxial properties of RAP. As the storage temperature increases from 75°F to 100°F (23.9°C to 37.8°C), the maximum principal stress at failure, secant modulus and cohesion intercept values of both post-milling processes increased. The RAP samples stored at 125°F (51.7°C) had similar behavior to RAP stored at 100°F (37.8°). The angle of friction for both materials does not vary with an increase in temperature.

5.1.4 Effects of Time

The triaxial properties of RAP are not affected by the duration of storage time. The maximum principal stress at failure, the secant modulus, the angle of friction and the cohesion intercept remain relatively constant with increased storage time.

5.1.5 Highway Construction Applications

The engineering properties of RAP found in this investigation show that RAP is a suitable material for use as structural fill and for roadway base and subbase applications. In general the material is clean (no coatings of clay or silt), hard, strong, durable, sound and well shaped. Appropriate crushing and sizing operations, can modify the gradation of RAP to meet specifications and increase mass stability. The densities achieved are stronger than typical dense uniform sands. The strength and stiffness of RAP is comparable to that of dense sand and provides appropriate resistance to deformation. The angle of friction (between 37 to 40 degrees) shows the material has high shear resistance and it provides strong aggregate interlocking and inter-particle friction. Lastly, most aggregates do not contain cohesion, but RAP has cohesion and it increases when exposed to typical temperatures found in pavements in Florida.

RAP could be used as backfill in roadways, construction materials for embankments around pipes and culverts. The RAP could potentially be used in roadway subbase and base applications if it meets appropriate highway construction specifications such as the Limerock Bearing Ratio.

5.2 Field Testing Conclusions

The study focused on analyzing the performance of RAP as a base, subbase or subgrade over 12-months in a field site. The data obtained from the testing provide valuable information in determining the variation in stiffness as a result of climatic changes. Several field tests were successfully used to evaluate this material. The following specific conclusions are presented.

5.2.1 Constructability

The RAP was successfully installed on high moisture content subsurface soils without any delays or dewatering. The installation procedure was identical to that for installing cemented coquina.

The variable subsurface conditions became evident during analysis of the 12, 24 and 36-inch layers. The data from the 12-inch layer displayed the highest variability, while the data from the 36-inch layer displayed the least variability. As a result the data from the 36-inch layer was used in the subsequent evaluations.

5.2.2 Applications

1) Base Course – The FDOT minimum requirements for a material to be used as a base (LBR = 100) were obtained during the cooler-temperature testing cycles, but could not be sustained during the warmer months nor were they attained during installation. Therefore, when using field LBR results, RAP is not a feasible base course material.

2) Subbase and Subgrade - RAP achieved field LBR values of 40 by the second testing cycle and maintained a minimum value of 40 for approximately 80% of the subsequent tests. Therefore, when using field LBR results, RAP is a potential subbase, subgrade material.

5.2.3 Testing

FWD testing proved to be the most viable alternative to field CBR testing. FWD tests can be performed very quickly and provide a larger volume of data for a specific area than field CBR's. Reducing FWD data into ISM format is quick and straightforward and can be accomplished easily in the field with simple software.

The field CBR tests provided the most readily acceptable LBR data. Individual tests took approximately 15 minutes to perform. Individual CPT tests required approximately 20 minutes to perform. Data from CPT testing varied more than the FWD and LBR test data.

5.2.4 Density and Relative Compaction

Density showed minimal correlation to any of the strength parameters measured in the field. Densities recorded throughout the project varied an average of 1.6 pcf from initial values, with no individual reading deviating more than 5.9 pcf. RAP moisture contents ranged from 2.6 to 5.7 %.

Equivalent compaction energy from smooth steel drum vibratory rollers, will result in equivalent relative compaction between cemented coquina and RAP.

5.2.5 Temperature

Temperature gradient is greater near the surface and decreases with increasing depth. Below 18 inches, air temperature variations showed limited effect on the temperature of the RAP during summer months.

5.2.6 Modulus of Elasticity, E_s

The predicted range of field E_s values for RAP (2.6 ksi to 9.6 ksi) were lower than the measured laboratory E_s values (7 ksi to 17 ksi). This predicted modulus was derived from the CPT point resistance correlation proposed by Schmertmann. Confining pressures from the lab testing were 5, 10 and 15 psi while the maximum estimated confining pressure in the field for RAP was 2.5 psi. This variation would indicate that lower values would be obtained in the field due to the lower confinement.

Over the course of testing, the E_s values for the top layer were consistently lower than the E_s values of the middle and bottom layers. This was assumed to be a result of both surface temperature effects and a lack confining pressure.

5.2.7 Limerock Bearing Ratio

Despite applying elevated compaction energies with a smooth steel drum roller during installation, initial LBR readings obtained from field CBR test for RAP averaged 16 ± 3 making it initially unsuitable for either a FDOT base or subbase.

LBR values for both RAP sections increased during Florida's cooler months and decreased during the warmer months. Despite differing compaction energies, both RAP sections exhibited nearly identical LBR values in each layer for each test cycle.

RAP achieved a minimum LBR of 40 in 50% of all tests performed on the 12-layer, 71% of the tests performed on the 24-inch layer and 79% of the tests performed on the 36-inch layer. Once the RAP achieved the FDOT minimum requirement for a subbase (LBR = 40), approximately 20 % of the subsequent tests dropped below 40.

5.2.8 Automated Dynamic Cone Penetrometer (ADCP)

LBR's predicted from ADCP index values for the RAP increased during the three test cycles the ADCP was employed. This followed the same trend as LBR and E_s during the same time frame.

Webster's correlation (1992) for the ADCP, using the average predicted LBR's over the full range of the layer, over predicted the RAP LBR values by an average of 200%. If the average predicted LBR's for the top 2-inches of the layer are used, a more realistic comparison between predicted LBR's and field LBR values results. However, the predicted values will still be 25 to 40 points higher than the field values.

The linear regression formula of:

$LBR = 334/(DCPI)^{1.63}$

using the average DCPI of the top 6 inches for the layer, provides a more conservative correlation to field LBR's than Webster's equation (1992) for RAP.

5.2.9 Impulse Stiffness Modulus, ISM

FWD testing of this field site provided the largest volume of data and was the quickest to obtain. During each testing cycle, twenty-seven (27) tests with three load increments each were performed in approximately 45 minutes.

The variation in the ISM's with time, is similar to the time variations of E_s and the LBR. During the cooler months the ISM increases and during the warmer months the ISM decreases.

Temperature appears to play a pivotal role in determining the ISM (kips/mil) of RAP. Values recorded during the cooler testing periods (February, 2000 and October, 2000) varied from 0.46 to 0.56 and 0.72 to 0.83, respectively. During the warmest testing period (June, 2000), ISM values ranged from 0.43 to 0.47.

5.2.10 Comparisons Between LBR, ISM, and E_s

There appears to be linear relationships between LBR, ISM, and E_s for RAP according to the following equations:

$LBR = 15.2 * E_s - 19.2$ $(R^2 = 0.76)$

$ISM = 0.053 * E_s + 0.12$ $(R^2 = 0.69)$

$ISM = 0.0038 * LBR + 0.25$ $(R^2 = 0.72)$

The strongest correlation appears to be between ISM and LBR. This may be due to the larger volume of FWD data used to determine ISM values and that both tests are derived from surface testing. The weakest correlation appears to be between E_s and LBR. This may be due to the inherent variability in the CPT data, which is taken at increasing depths.

5.2.11 RAP vs. Cemented Coquina

Overall, RAP did exhibit as high of strength as the cemented coquina; however, the cemented coquina exhibited very poor drainage characteristics making it unworkable during initial site construction.

LBR and ISM data showed that RAP strength did not fluctuate as much due to the effects moisture as the cemented coquina.

RAP performance varied more than cemented coquina when subjected to varying thermal conditions. The stiffness of RAP decreased when exposed to prolonged ambient air temperatures exceeding 80 ^{o}F.

6. Field Specifications

The following specifications are presented in the format currently used in the FDOT Specifications for Road and Bridge Construction. They are to be considered preliminary or developmental at this point and will be refined further during the second phase of this research which includes evaluating RAP mixtures and its environmental effects in the field.

SECTION 201
RECLAIMED ASPHALT PAVEMENT BASE

201-1 Description.

Construct a base course comprised of reclaimed asphalt pavement (RAP) material

201-2 Materials.

The contractor may use RAP material obtained by either milling or crushing an existing asphalt pavement, meeting the following gradation requirements:

Sieve Size	Percent By Weight Passing
1-inch	100
3/8 -inch	12 to 15
# 10	18 to 21
#200	Less than 5

Meet the gradation analyses of FM 1-T 027, with the following exceptions:

(1) Air dry samples to surface dry condition (2% or less moisture).

(2) If using mechanical shakers, use a sieving time of 15 minutes minimum.

When the RAP material is stockpiled from a previous Department project and the composition of existing pavement is known, the Engineer may approve the material on the basis of composition. When the composition of stockpiled RAP is not known, use the following procedure for approval:

(1) Conduct a minimum of six extraction gradation analyses of the RAP material. Take samples at random locations in the stockpile.

(2) Request the Engineer to make a visual inspection of the stockpile of the RAP material. Based on this visual inspection of the stockpiled material and the results of the gradation analyses, the Engineer will determine the suitability of the materials.

(3) The Engineer may require crushing of stockpiled material to meet gradation criterion.

201-3 Spreading Rap Material.

201-3.1 Method of Spreading: Spread the RAP with a blade or device which strikes off the material uniformly to laying thickness and produces an even distribution of the RAP.

201-3.2 Number of Courses: When the specified compacted thickness of the base is greater than 6", construct the base in multiple courses. Place the first course to a thickness of approximately one-half the total thickness of the finished base, or sufficient additional thickness to bear the weight of the construction equipment without disturbing the subbase or subgrade. The compacted thickness of any course shall not exceed 6".

201-4 Compacting and Finishing Base.

201-4.1 General.

201-4.1.1 Single-Course Base: Construct as specified in 200-6.1.1.

201-4.1.2 Multiple-Course Base: Construct as specified in 200-6.1.2.

201-4.2 Moisture Content: Meet the requirements of 200-6.2. Ensure that the moisture content at the time of compaction is within 3% of optimum.

201-4.3 Density Requirements: After attaining the proper moisture content, compact the material to a density of not less than 98% of maximum density as determined by FM 5-521. Perform base compaction using standard base compaction

equipment, vibratory compactors, trench rollers, or other special equipment that will provide the density requirements specified herein.

201-4.4 Density Tests: Meet the requirements of 200-6.4.

201-5 Testing Surface.

In the testing of the surface, do not take measurements in small holes caused by the grader pulling out individual pieces of aggregate.

SECTION 913B
RECLAIMED ASPHALT PAVEMENT
MATERIAL FOR BASE

913B-1 General.

This section governs materials to be used on construction on reclaimed asphalt pavement (RAP) material base and RAP stabilized base.

913B-2 Furnishing of Material.

Except as might be specifically shown otherwise, all RAP material and the sources thereof shall be furnished by the Contractor. Approval of RAP sources shall be in accordance with 6-3.3. Any RAP material occurring in State-furnished borrow areas shall not be used by the Contractor in constructing the base, unless permitted by the plans or other contract documents.

913B-3 Composition.

The material used shall be reclaimed asphalt pavement (RAP).

913B-4 Liquid Limit and Plasticity Requirements.

None required.

913B-5 Mechanical Requirements.

913B-5.1 Deleterious Material: RAP material shall not contain any lumps, balls or pockets of foreign material in sufficient quantity as to be detrimental to the proper bonding, finishing, or strength of the RAP base.

913B-5.2 Gradation and Size Requirements: Meet the requirements of 201-2. All crushing or breaking-up which might be necessary in order to meet such size requirements shall be done before the material is placed on the road.

913B-6 Limerock Bearing Ratio Requirements.

LBR values shall be obtained by one of the following test procedures:

913B-6.1 Field LBR: Field CBR (ASTM D4429) values shall be taken at the following time intervals and converted to LBR values. At each testing interval the corresponding minimum average LBR values should be met:

Testing Interval	*Minimum Average LBR Value*
Finished Construction	15
2 months	65
4 months	100

913B-6.2 Dynamic Cone Penetrometer: LBR values acquired using Dynamic Cone Penetrometer correlations shall be taken at the following intervals and shall have the corresponding average LBR values and standard deviations:

Testing Interval	*Minimum Average LBR Value from DCP Correlation*	*Minimum Individual Value*
Finished Construction	50	40
2 months	100	70
4 months	140	100

Recording of LBR values for use in determining minimum average LBR and minimum individual value shall begin with the first positive LBR value and shall conclude at a depth of 4” from the surface of the material.

7. Recomendations

7.1. Laboratory Testing Recommendations

It is recommended that future research conducted to evaluate the use of RAP as structural fill material or as a base or subbase material address the following topics:

- In order to achieve maximum mass stability in the material, additional gradations of RAP meeting recommended specifications should be examined. The investigation should also examine the drainage of the material.
- A field investigation should be conducted on the effects of climatic and temperature changes on the strength and stiffness of RAP.

7.2. Field Testing Recommendations

1) Continue research in the possible use of RAP as a subbase.
2) Research RAP mixtures for possible use in high moisture content soil conditions
3) Continue temperature profiling RAP
4) Research the visco-elastic properties of RAP with regard to temperature.
5) Develop a more rigid specification to be used statewide to ensure uniform material properties.
6) Continue research in the correlations between E_s, ISM, and LBR

7) Although LBR is the most widely accepted FDOT specification for acceptance of a material for base and subbase material, research should concentrate on developing an ISM specification due to the ease and quickness that FWD tests can be performed in the field.
8) It is recommended that future RAP field sites incorporate:
    a) A uniform subbase or subgrade that is carefully compacted and tested prior to construction
    b) A monitoring well to record the ground water table
    c) A leachate collection system to determine both surfacewater and groundwater environmental characteristics
    d) A field site with a 36-inch thick RAP and 36-inch thick cemented coquina control section
    e) Temperature probes capable of recording and storing continuous temperature data at varying depths
    f) Testing performed weekly during the first four to six weeks after installation
    g) Spacing for simultaneous testing of LBR and FWD for the express purpose of improving the ISM/LBR correlation

Appendix A:

Triaxial Test Results

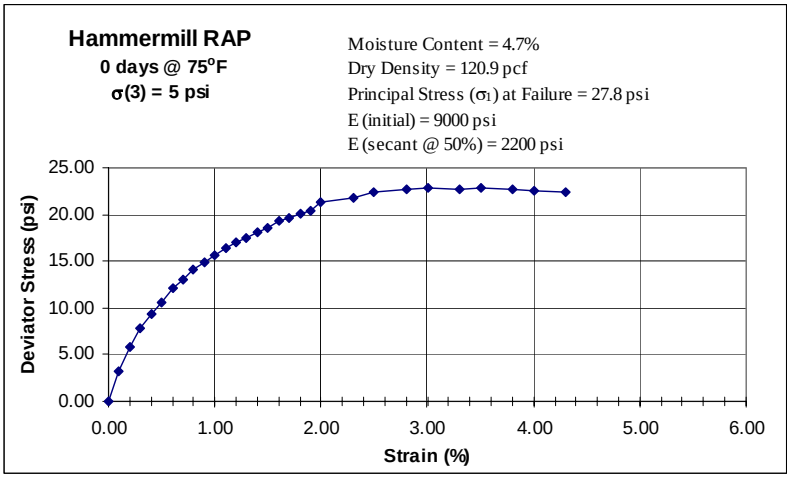

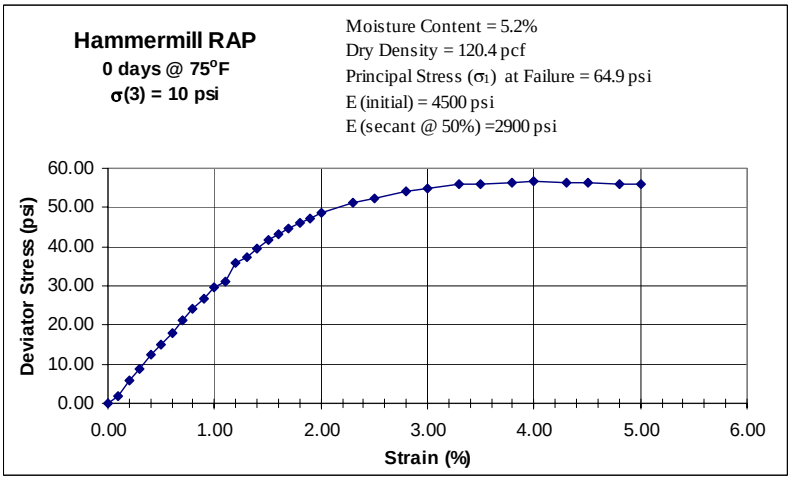

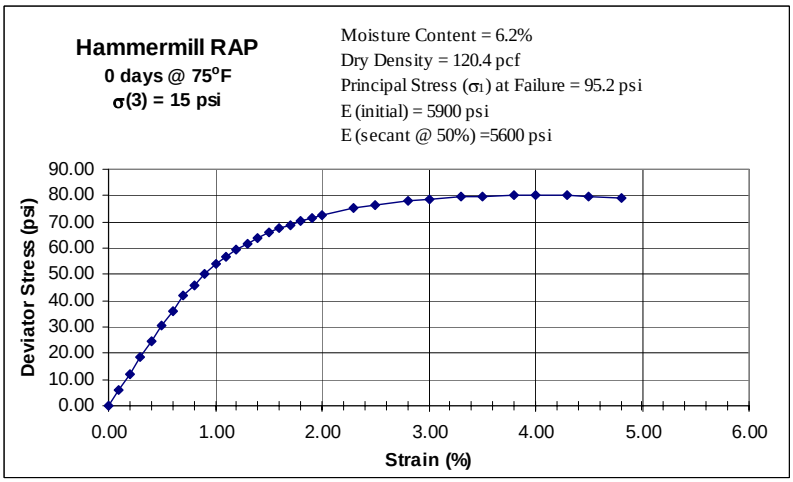

Figure A-1: Triaxial Test Results for Hammermill RAP with No Storage Time.

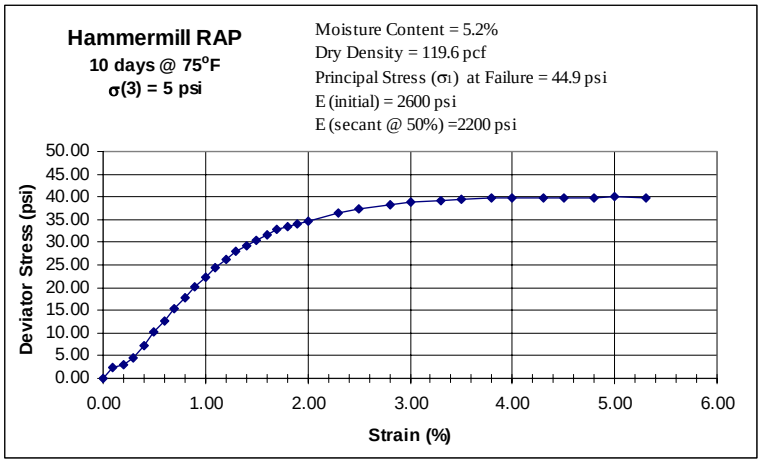

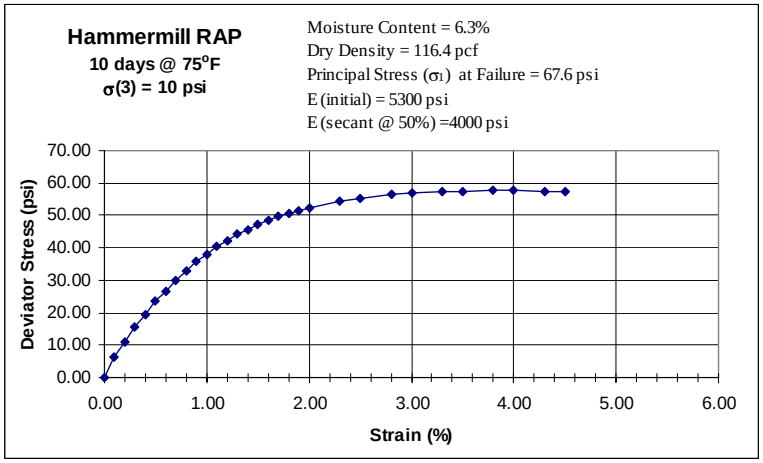

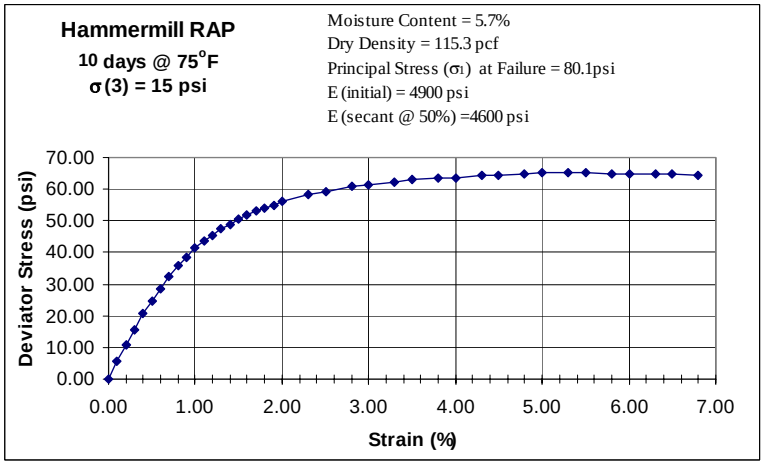

Figure A-2: Triaxial Test Results for Hammermill RAP Stored for 10 Days at 75ºF.

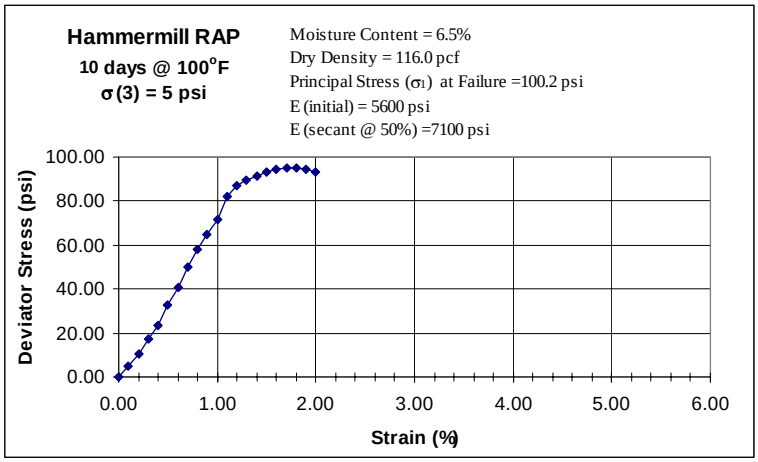

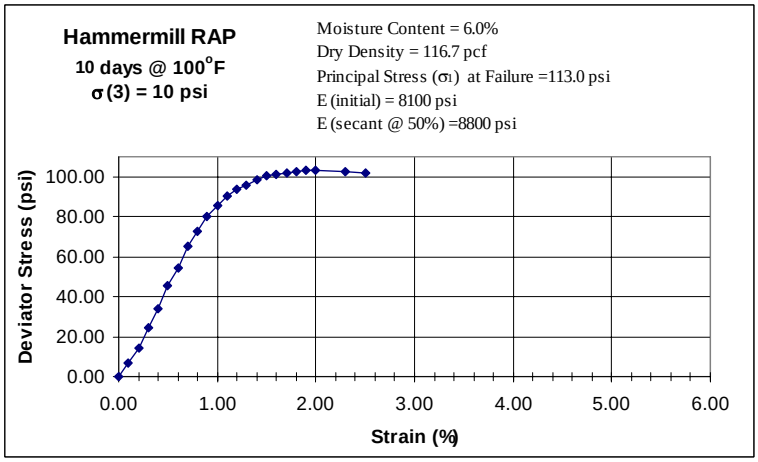

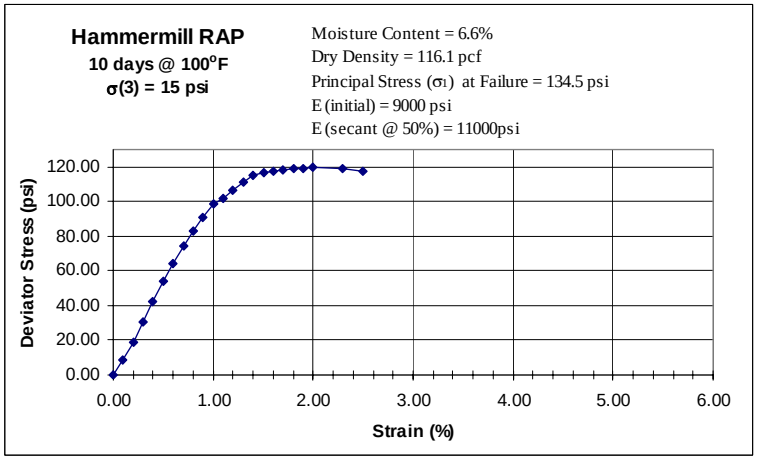

Figure A-3: Triaxial Test Results for Hammermill RAP Stored for 10 Days at 100ºF.

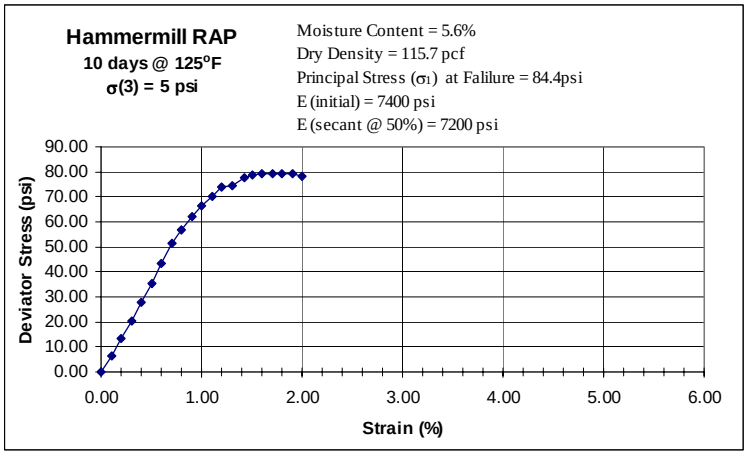

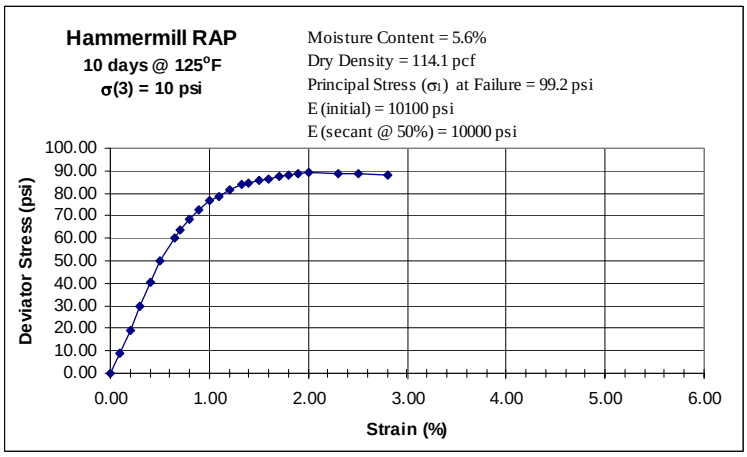

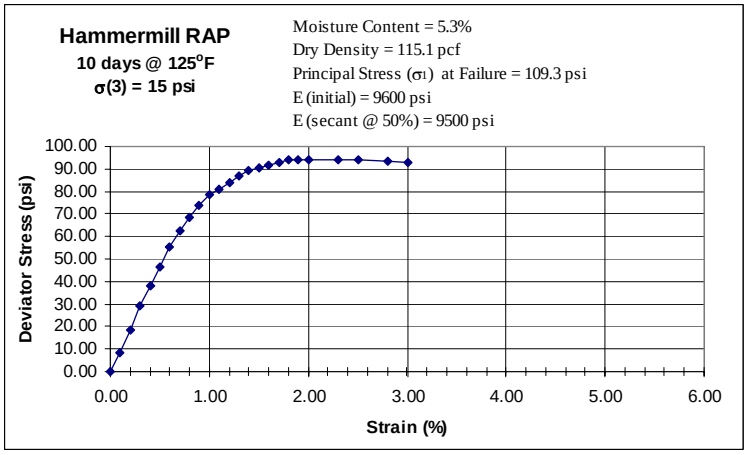

Figure A-4: Triaxial Test Results for Hammermill RAP Stored for 10 Days at 125ºF.

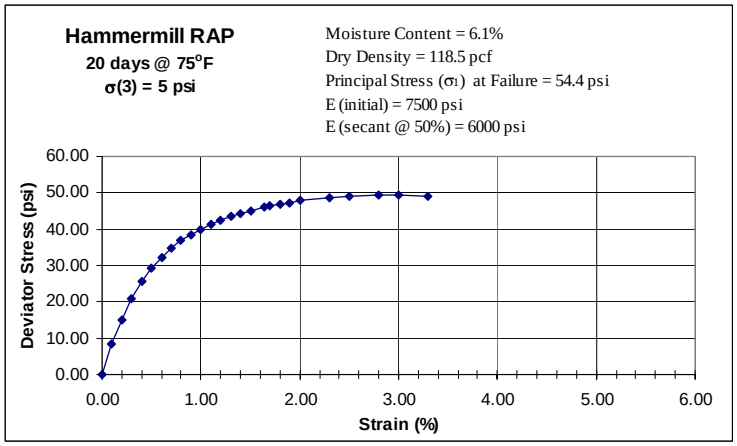

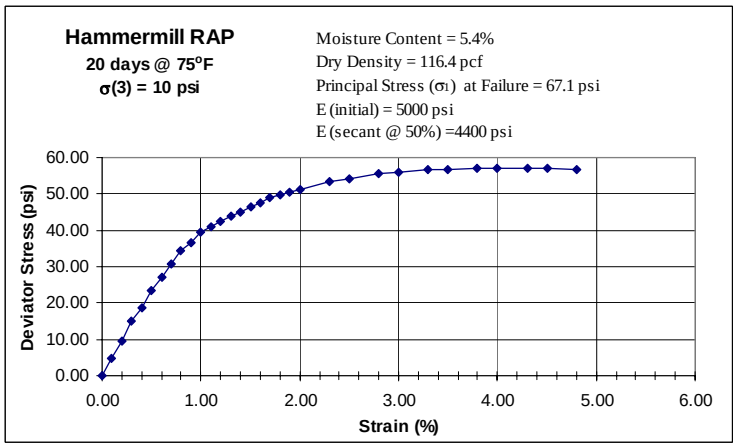

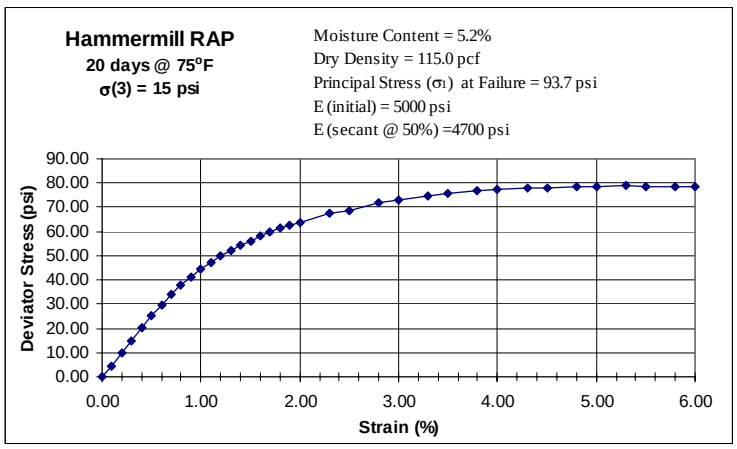

Figure A-5: Triaxial Test Results for Hammermill RAP Stored for 20 Days at 75ºF.

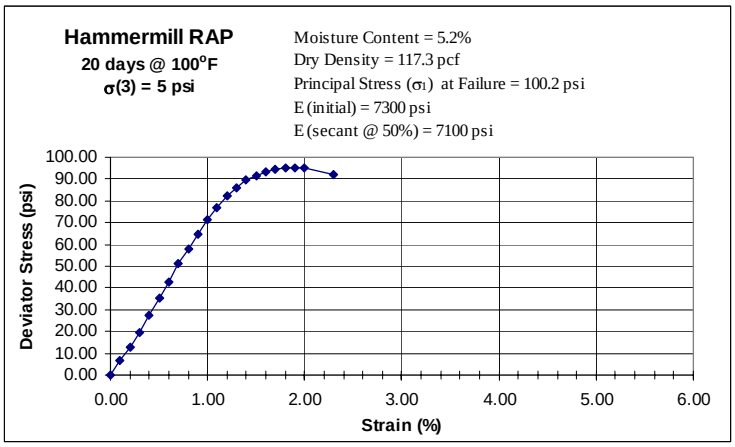

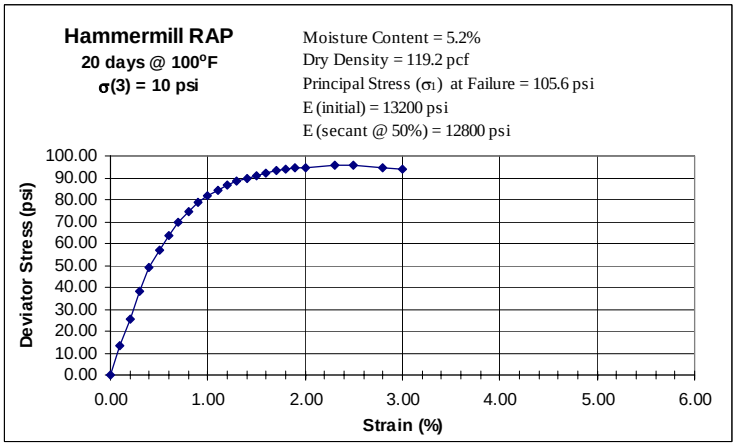

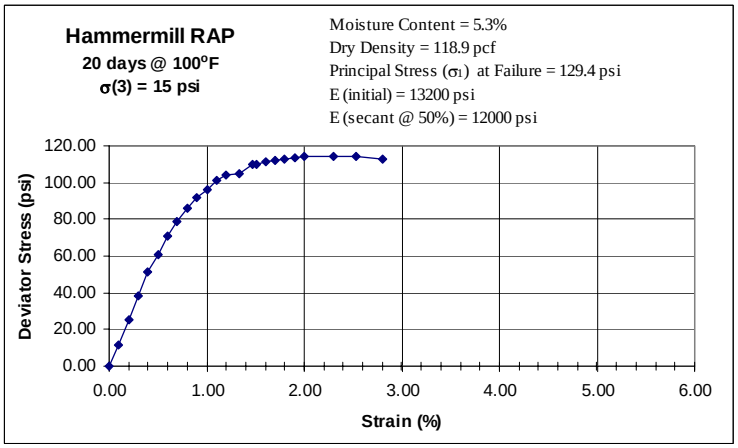

Figure A-6: Triaxial Test Results for Hammermill RAP Stored for 20 Days at 100ºF.

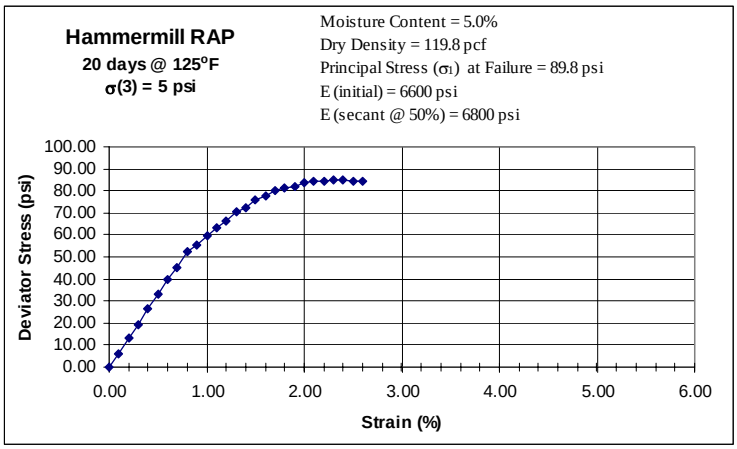

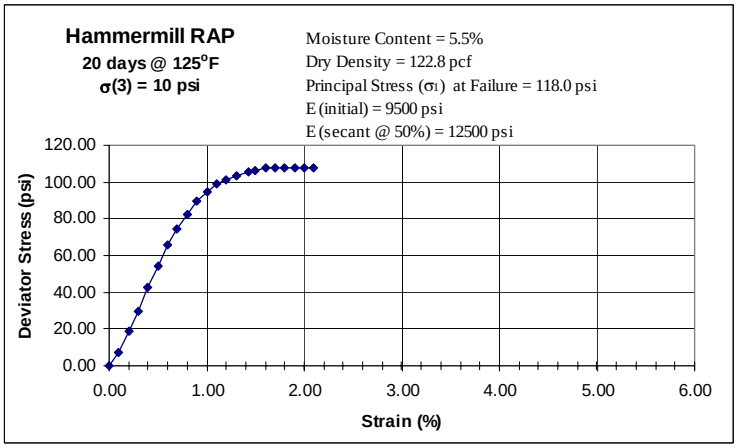

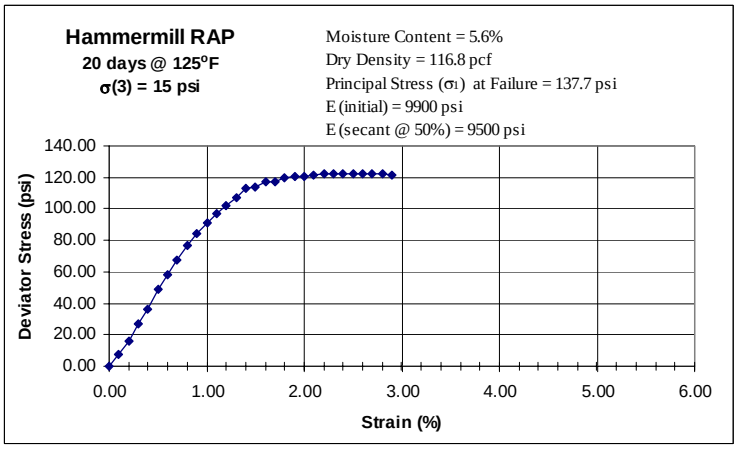

Figure A-7: Triaxial Test Results for Hammermill RAP Stored for 20 Days at 125ºF.

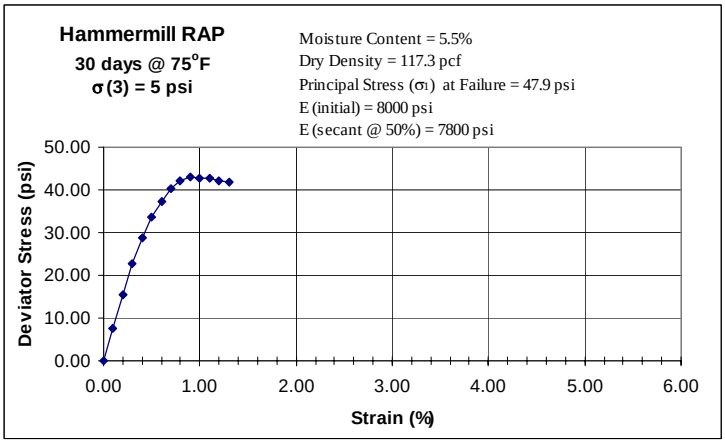

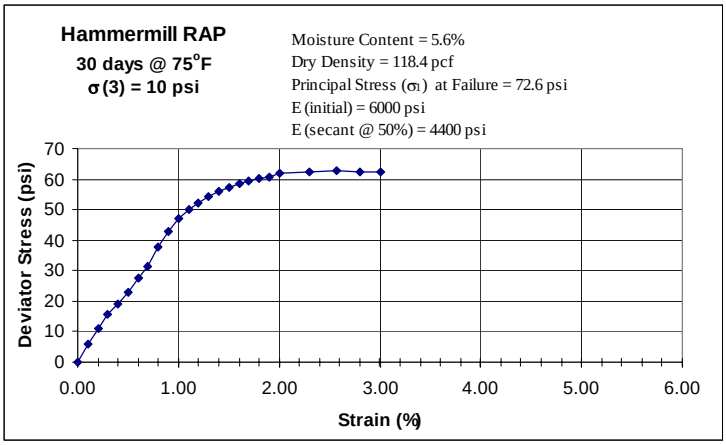

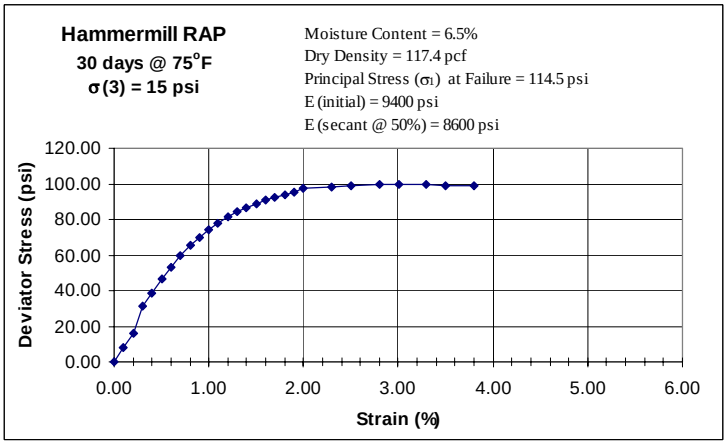

Figure A-8: Triaxial Test Results for Hammermill RAP Stored for 30 Days at 75ºF.

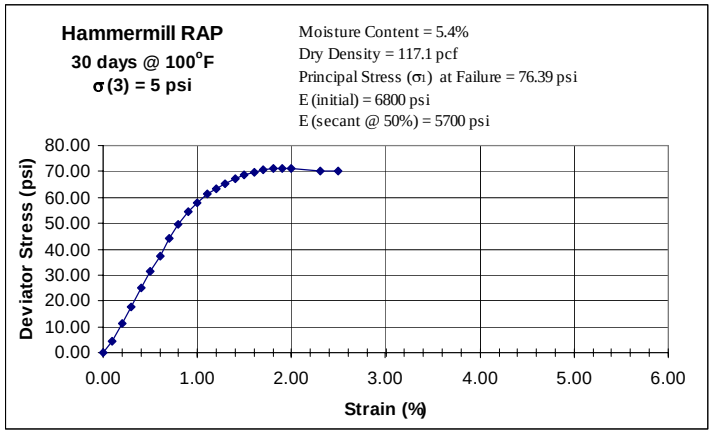

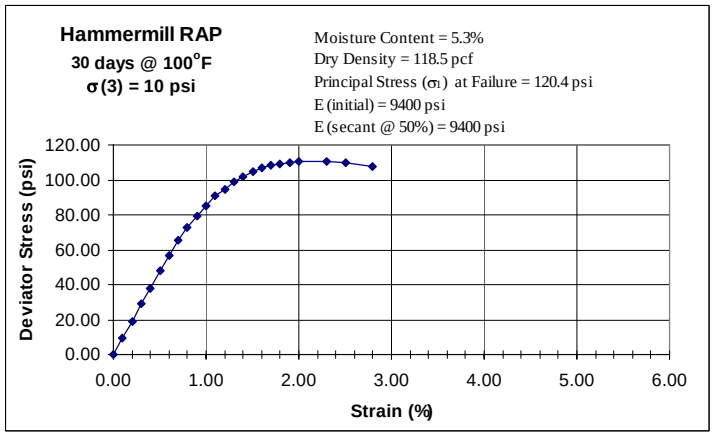

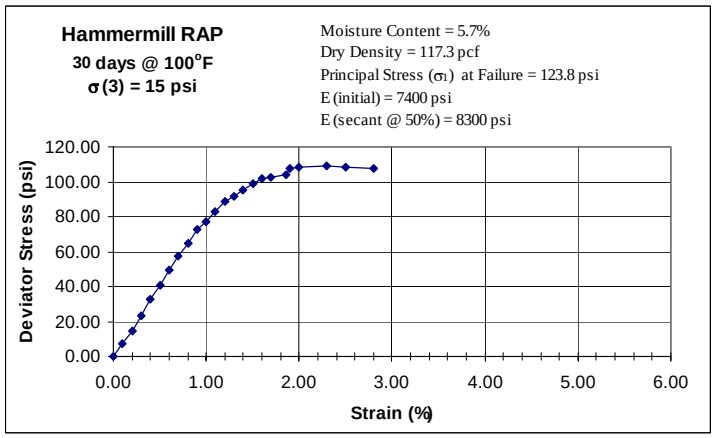

Figure A-9: Triaxial Test Results for Hammermill RAP Stored for 30 Days at 100ºF.

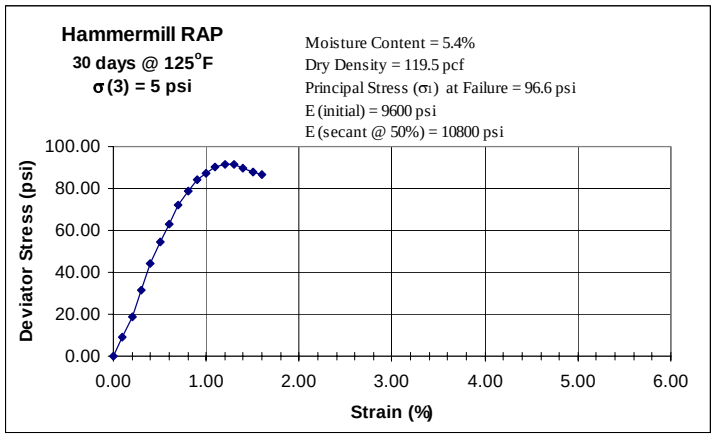

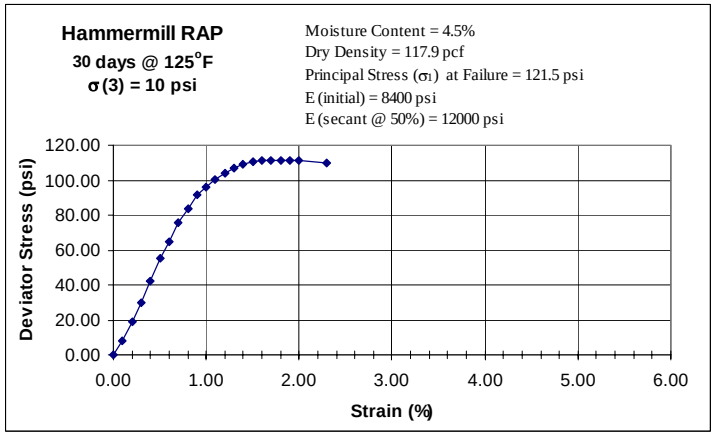

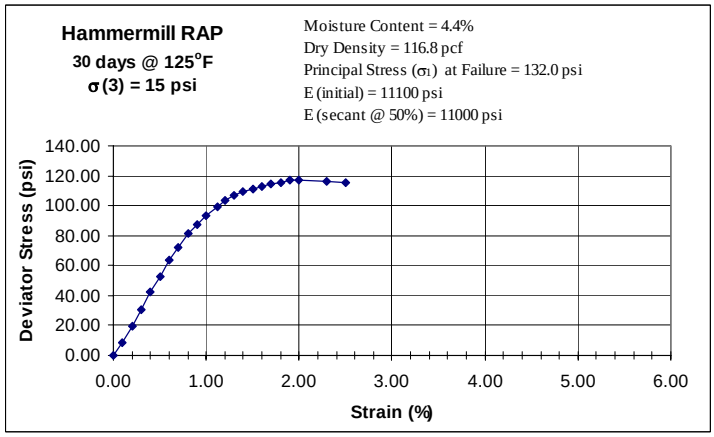

Figure A-10: Triaxial Test Results for Hammermill RAP Stored for 30 Days at 125ºF.

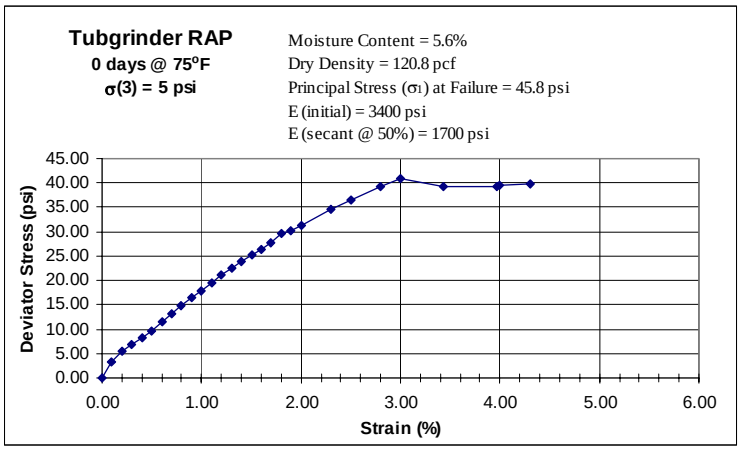

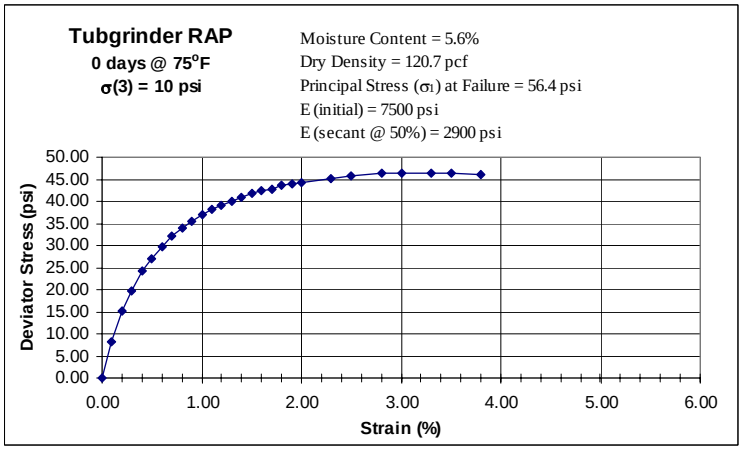

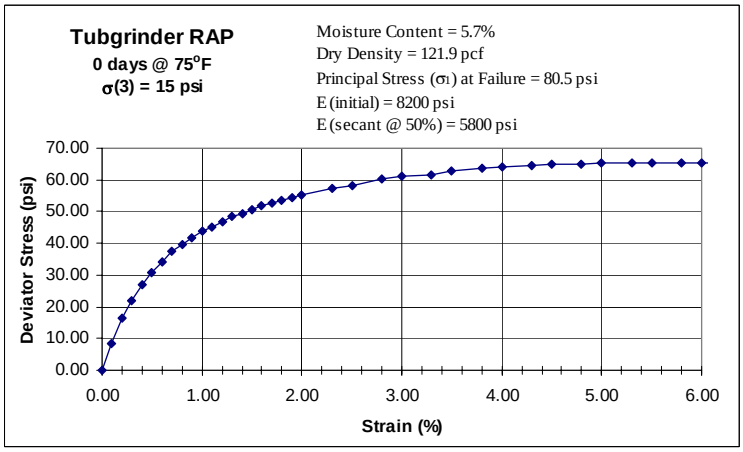

Figure A-11: Triaxial Test Results for Tubgrinder RAP with No Storage Time.

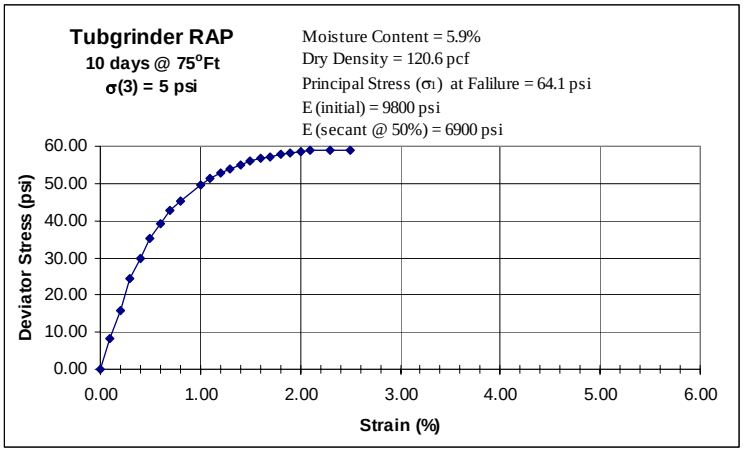

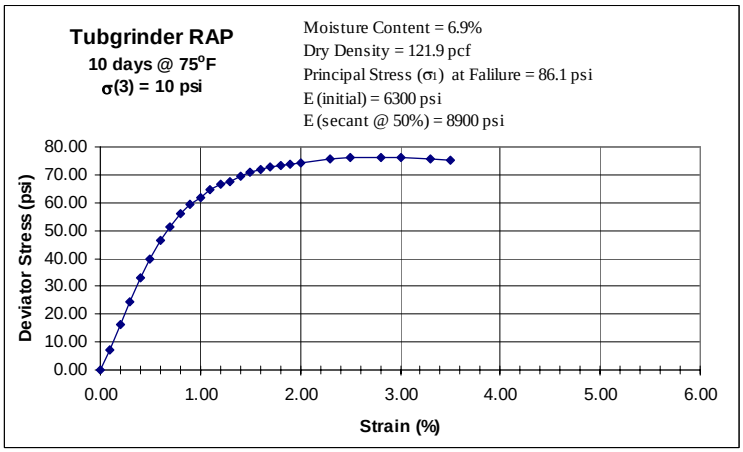

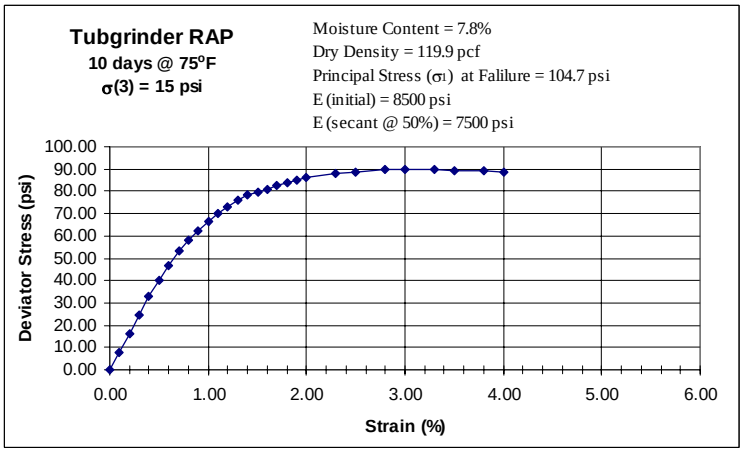

Figure A-12: Triaxial Test Results for Tubgrinder RAP Stored for 10 Days at 75°F.

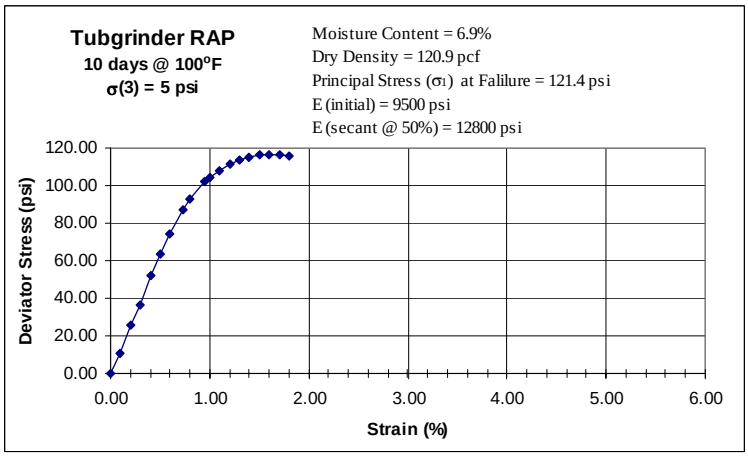

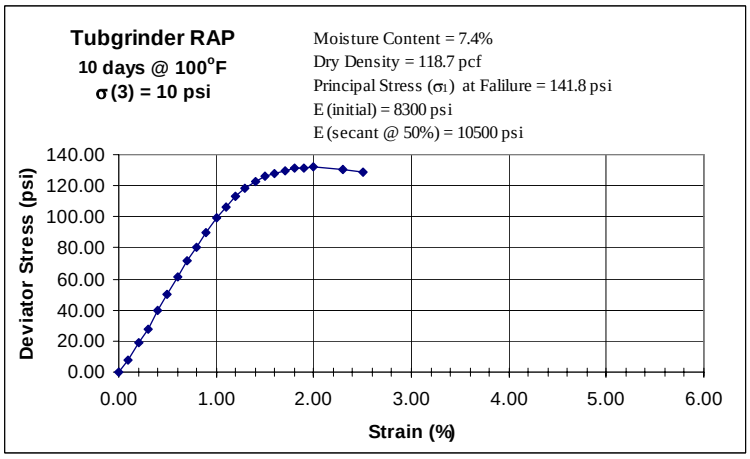

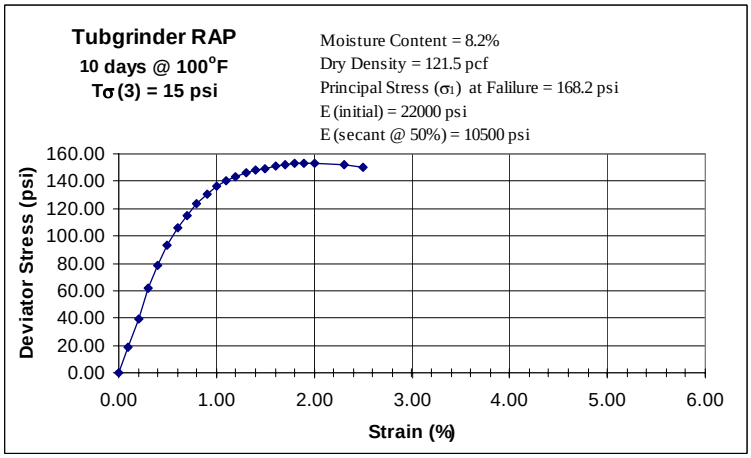

Figure A-13: Triaxial Test Results for Tubgrinder RAP Stored for 10 Days at 100°F.

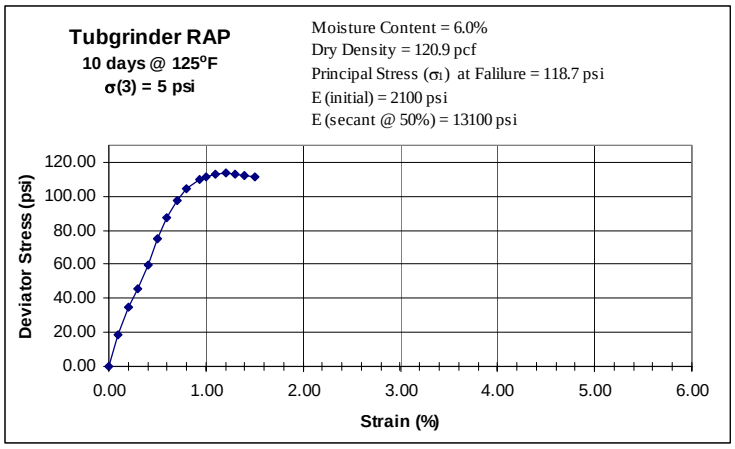

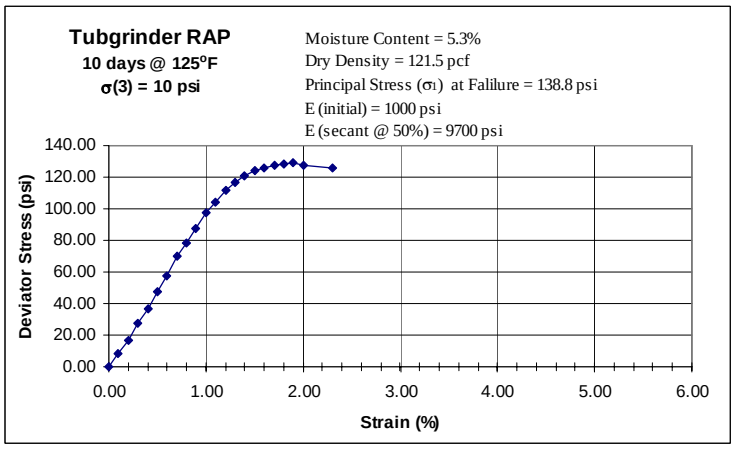

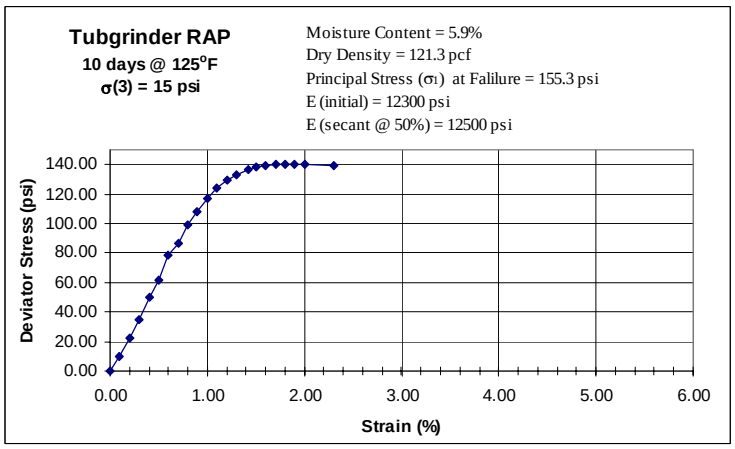

Figure A-14: Triaxial Test Results for Tubgrinder RAP Stored for 10 Days at 125°F.

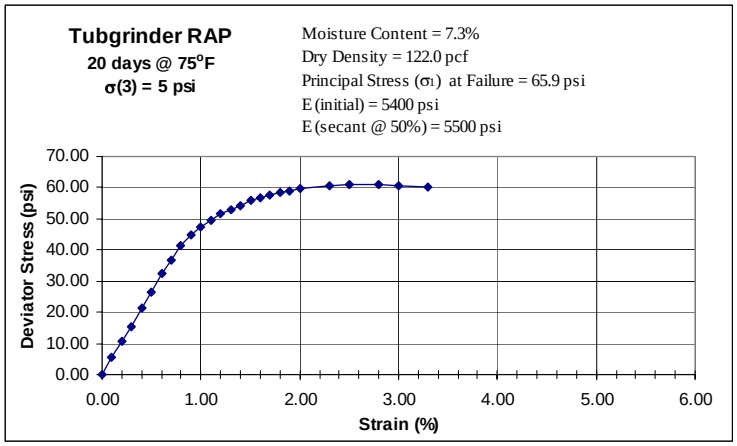

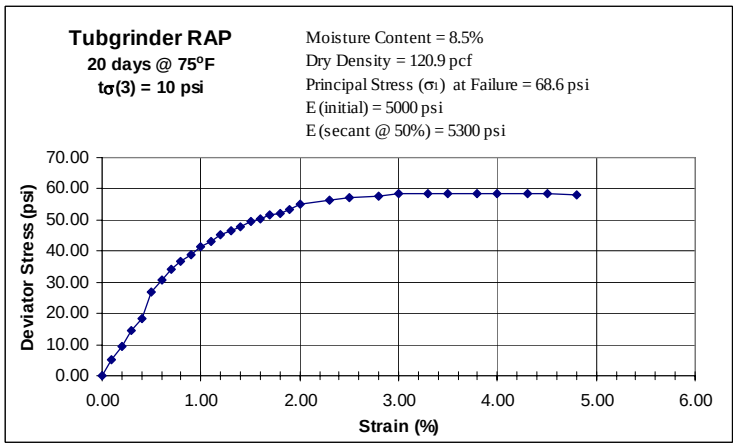

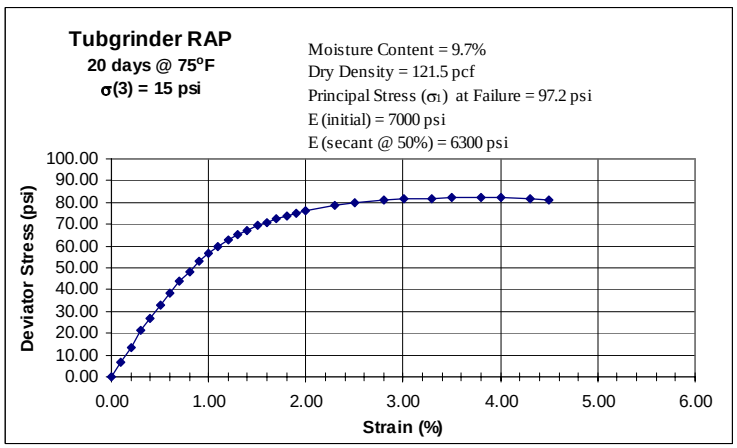

Figure A-15: Triaxial Test Results for Tubgrinder RAP Stored for 20 Days at 75°F.

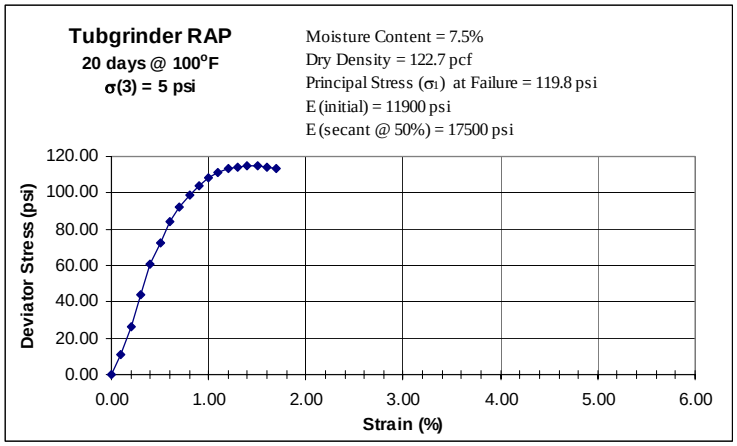

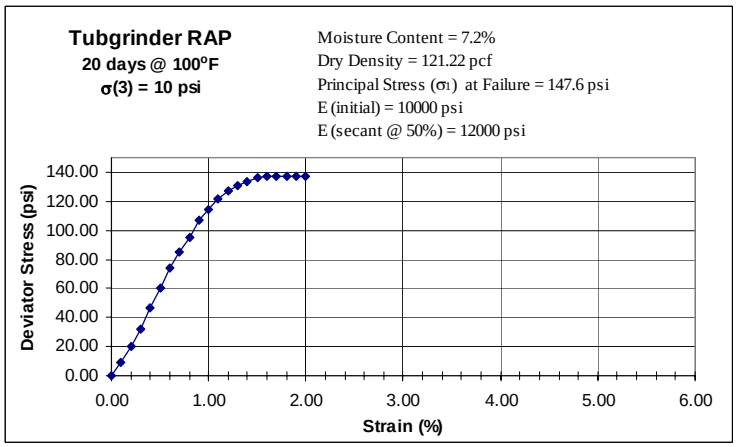

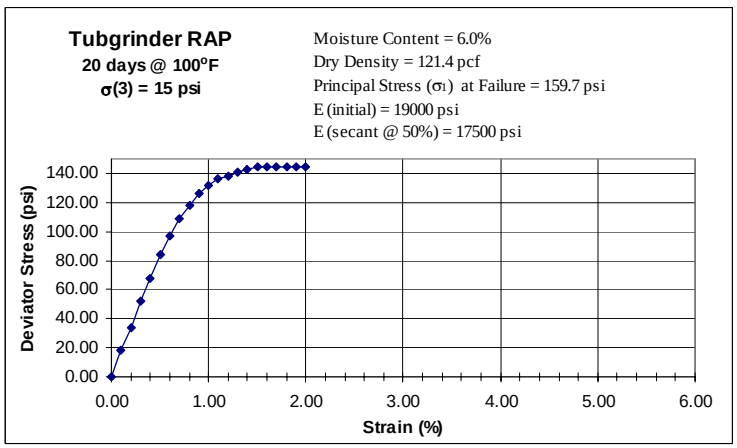

Figure A-16: Triaxial Test Results for Tubgrinder RAP Stored for 20 Days at 100°F.

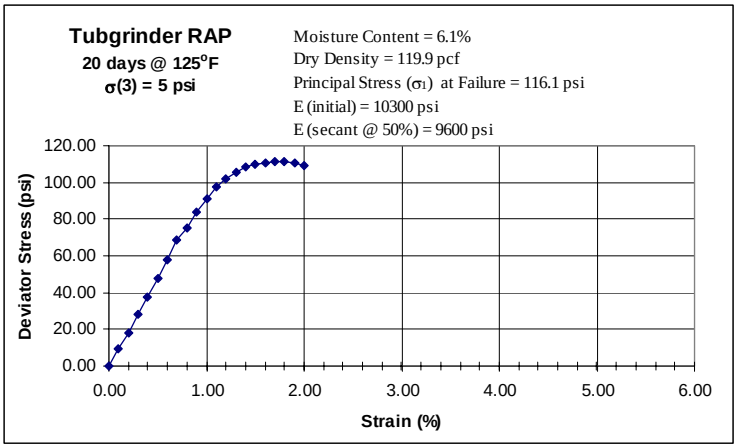

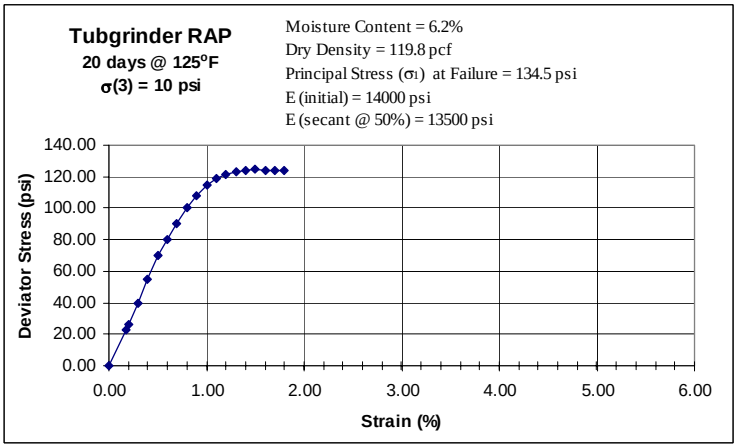

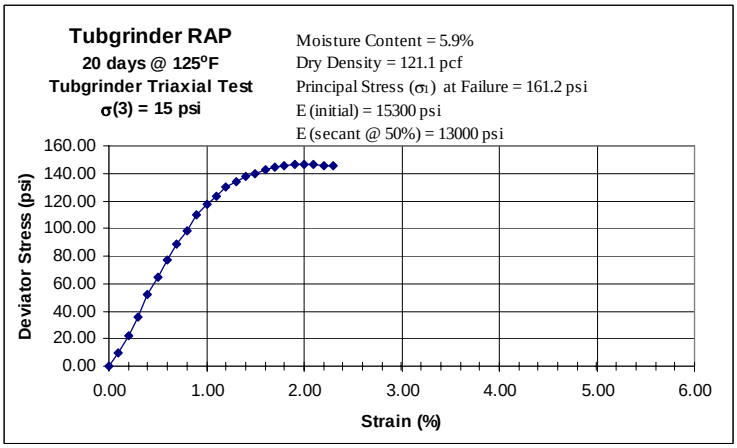

Figure A-17: Triaxial Test Results for Tubgrinder RAP Stored for 20 Days at 125°F.

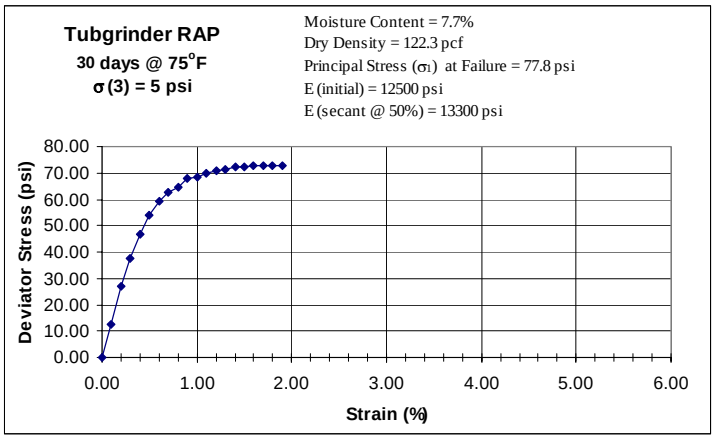

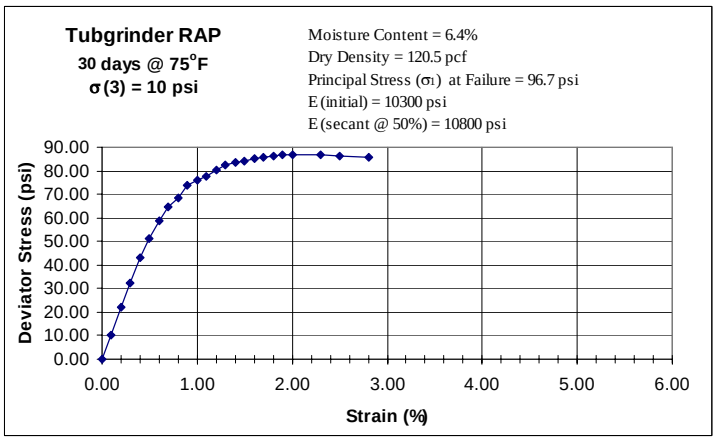

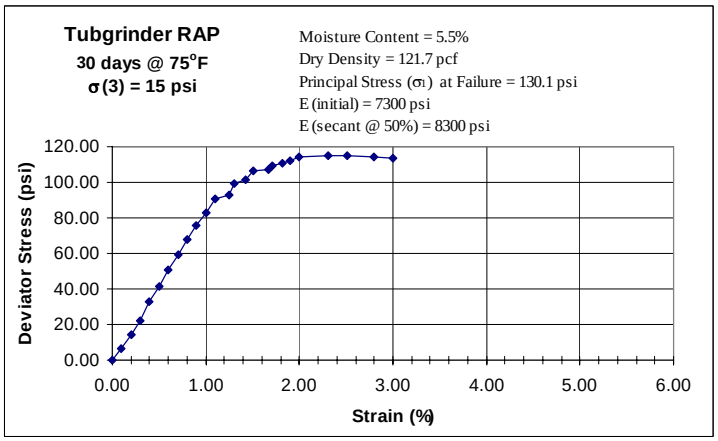

Figure A-18: Triaxial Test Results for Tubgrinder RAP Stored for 30 Days at 75°F.

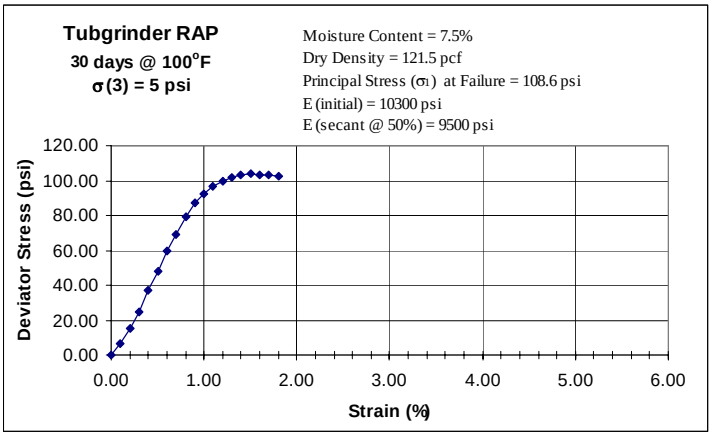

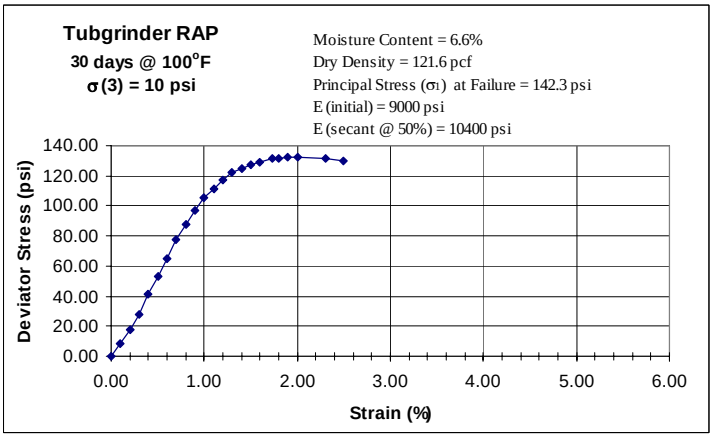

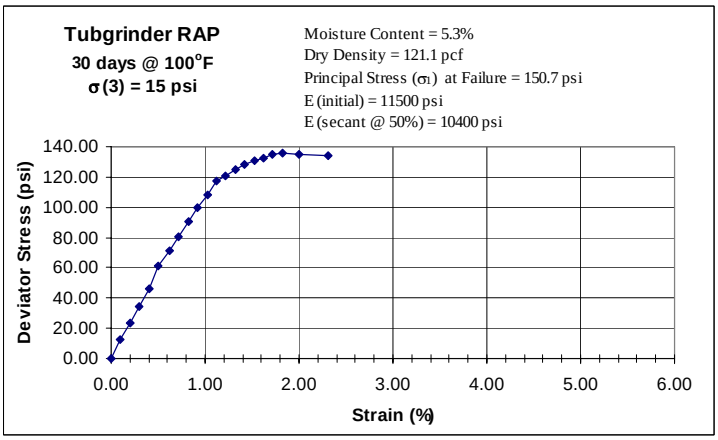

Figure A-19: Triaxial Test Results for Tubgrinder RAP Stored for 30 Days at 100°F.

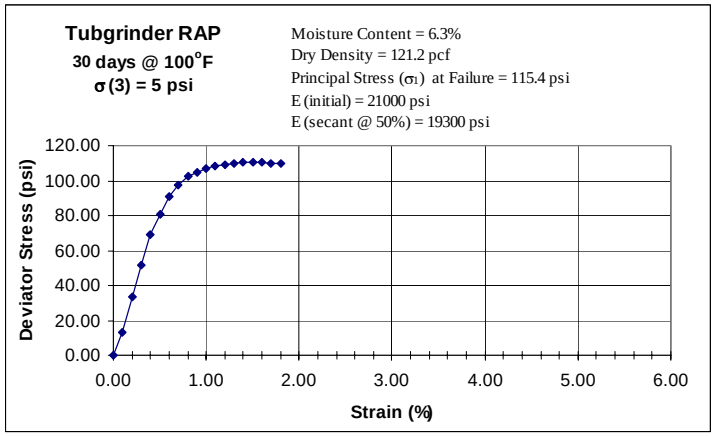

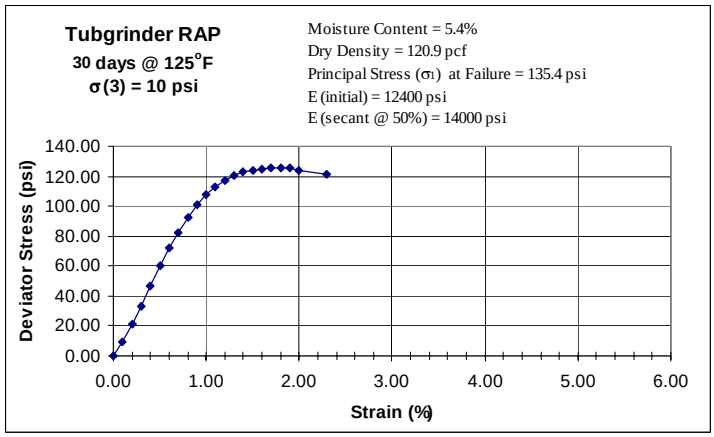

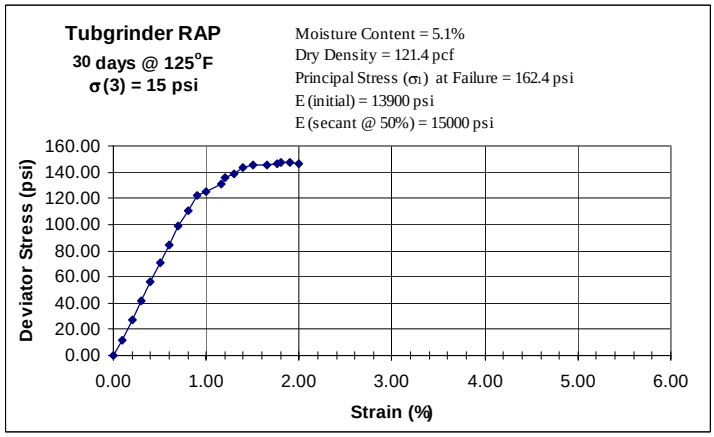

Figure A-20: Triaxial Test Results for Tubgrinder RAP Stored for 30 Days at 125°F.

Appendix B:

Mohr-Coulomb Failure Criteria Plots

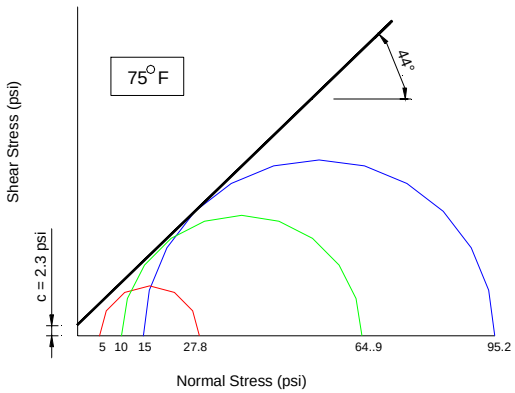

Figure B-1: Mohr-Coulomb Failure Criteria for Hammermill RAP with No Storage Time.

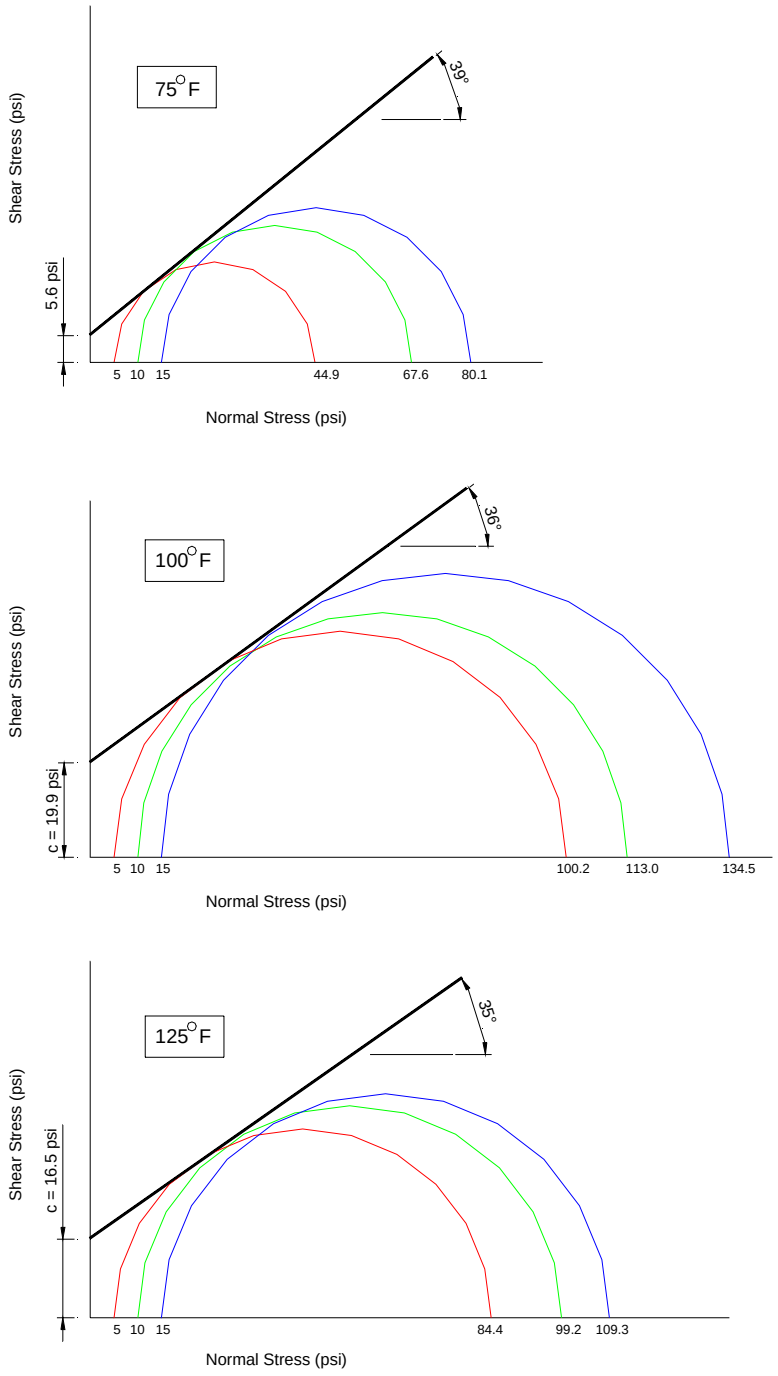

Figure B-2: Mohr-Coulomb Failure Criteria for Hammermill RAP Stored for 10 Days at 75°F, 100°F, and 125°F.

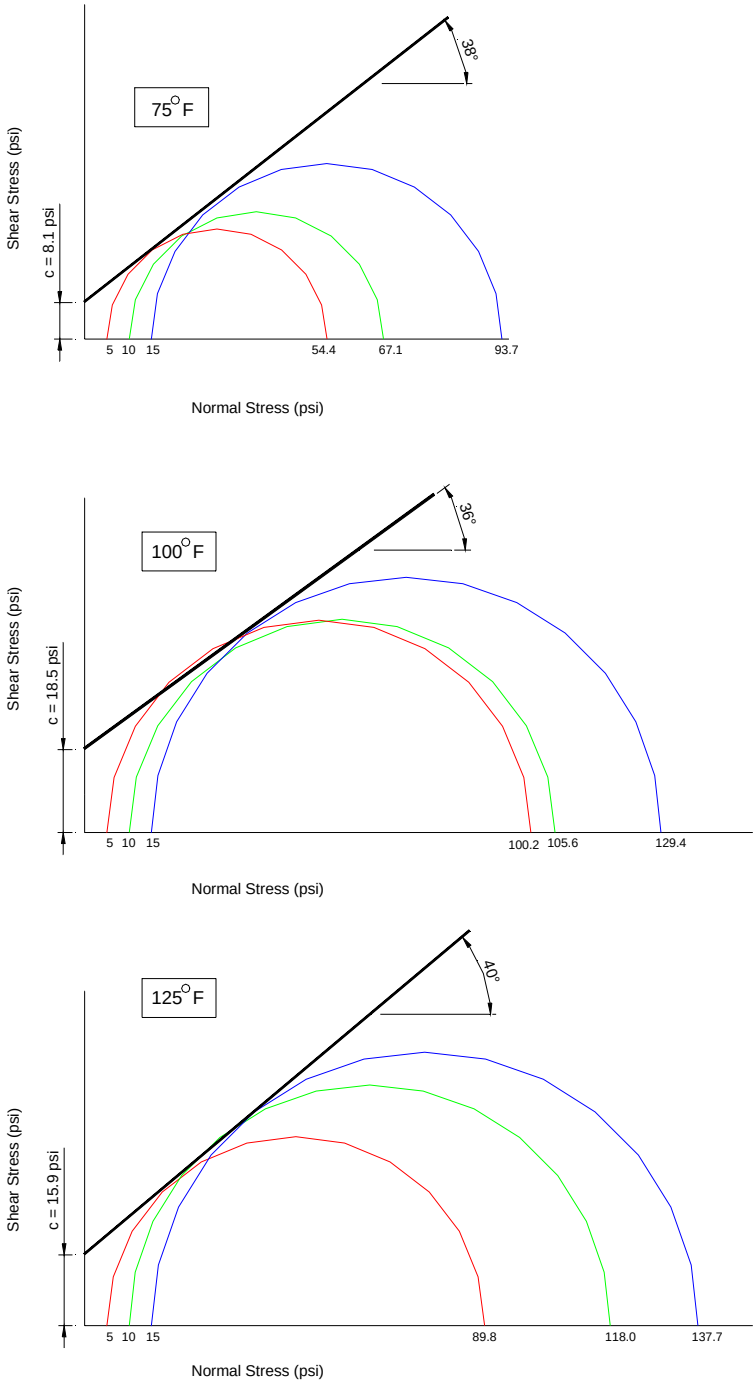

Figure B-3: Mohr-Coulomb Failure Criteria for Hammermill RAP Stored for 20 Days at 75°F, 100°F, and 125°F.

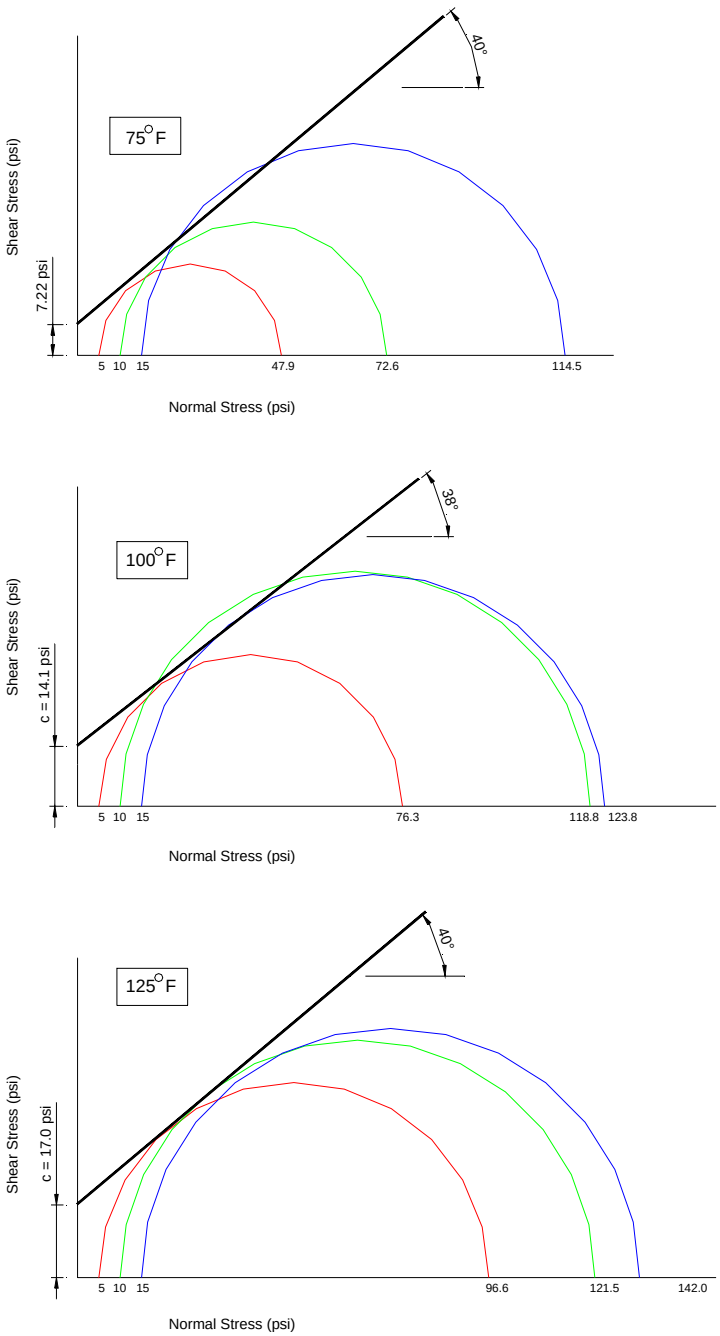

Figure B-4: Mohr-Coulomb Failure Criteria for Hammermill RAP Stored for 30 Days at 75°F, 100°F, and 125°F.

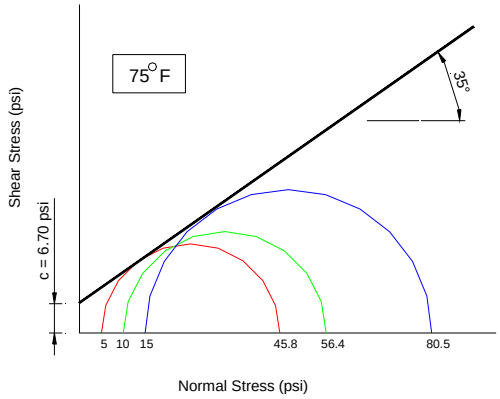

Figure B-5: Mohr-Coulomb Failure Criteria for Tubgrinder RAP with No Storage Time.

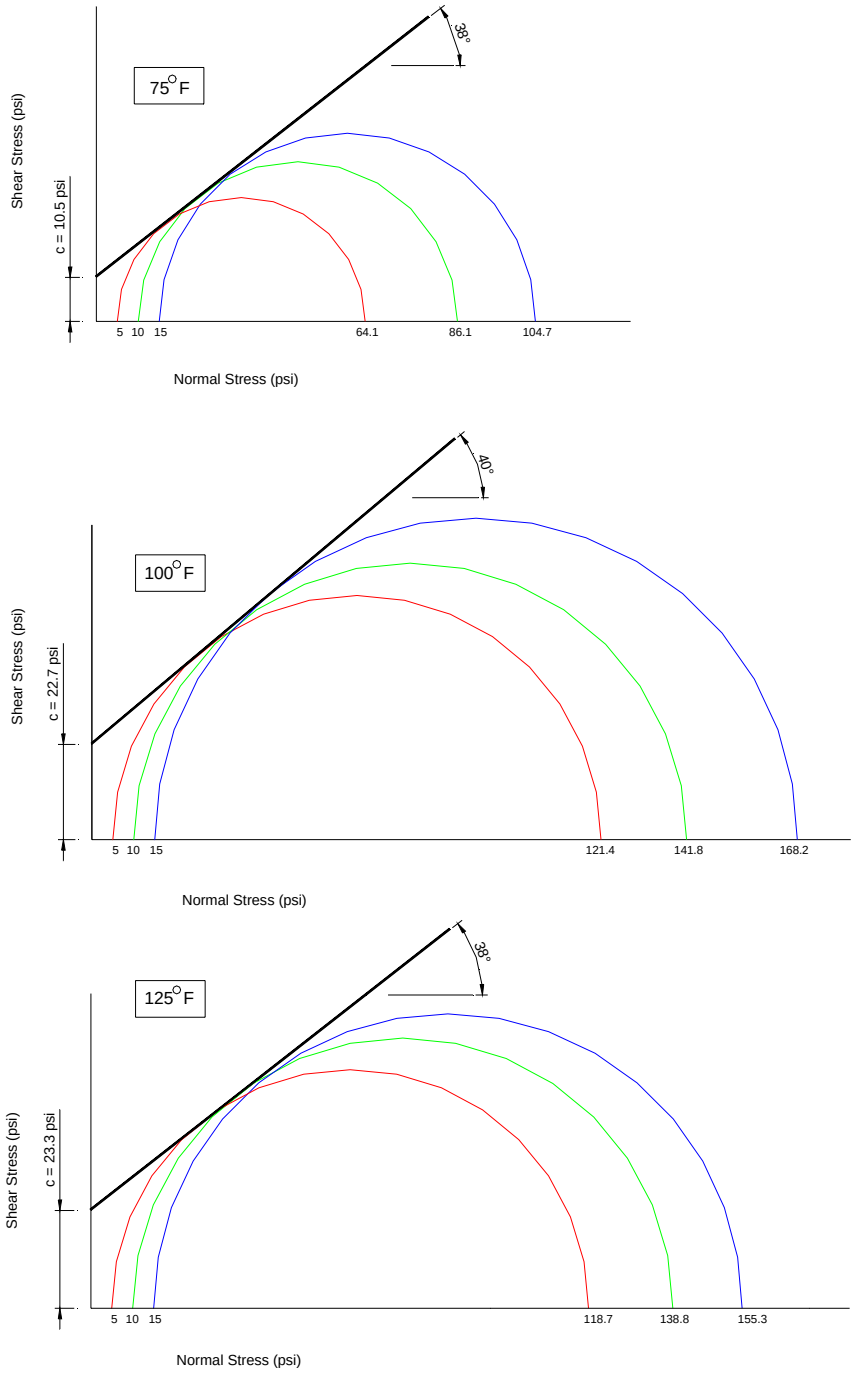

Figure B-6: Mohr-Coulomb Failure Criteria for Tubgrinder RAP Stored for 10 Days at 75°F, 100°F, and 125°F.

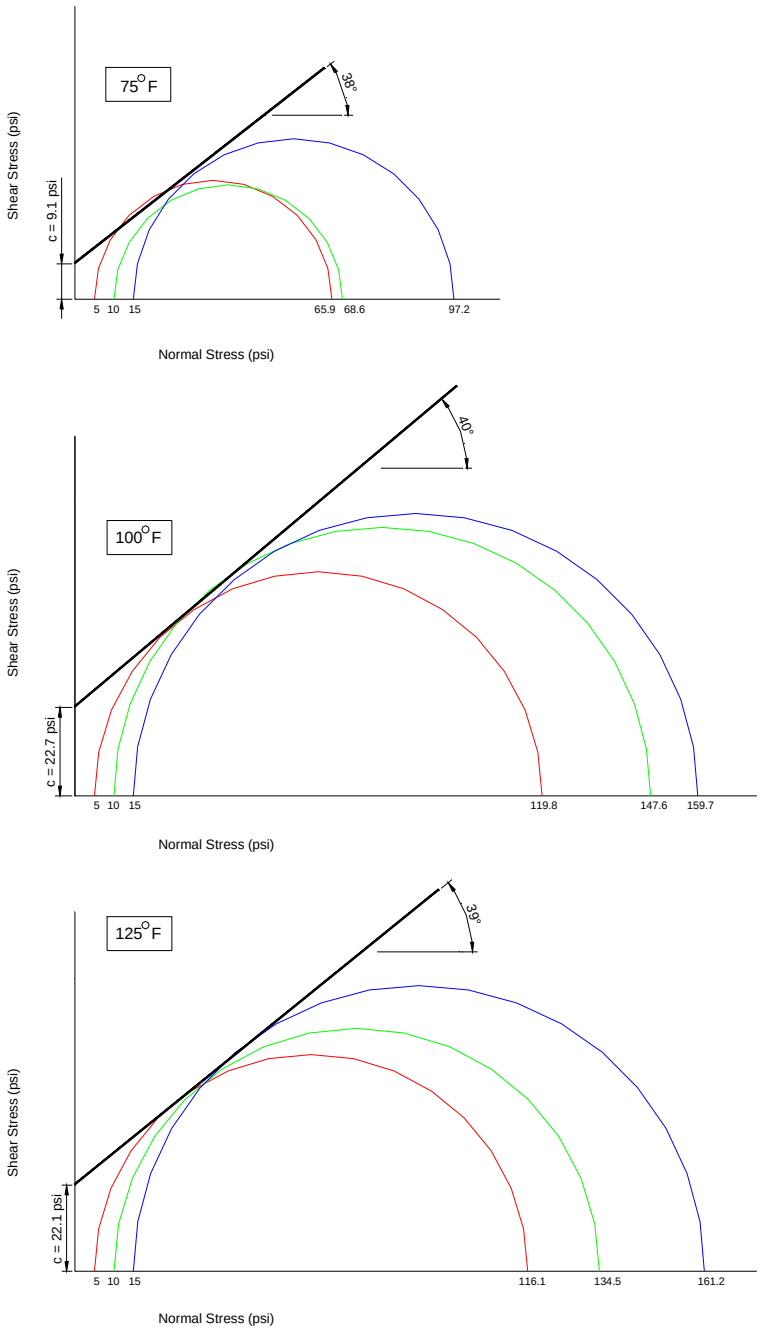

Figure B-7: Mohr-Coulomb Failure Criteria for Tubgrinder RAP Stored for 20 Days at 75°F, 100°F, and 125°F.

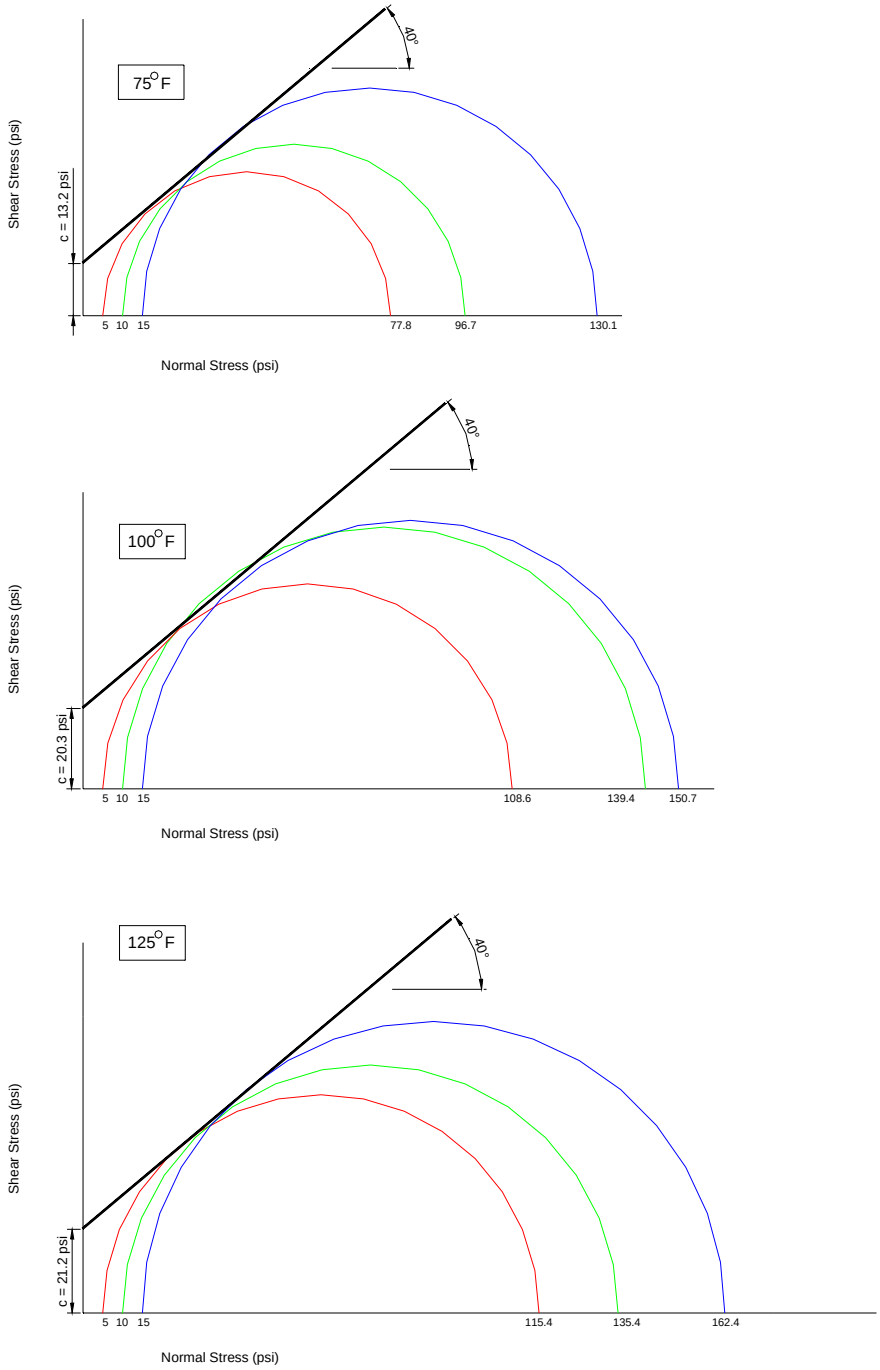

Figure B-8: Mohr-Coulomb Failure Criteria for Tubgrinder RAP Stored for 30 Days at 75°F, 100°F, and 125°F

Field Data

Appendix AA

Subsurface Densities

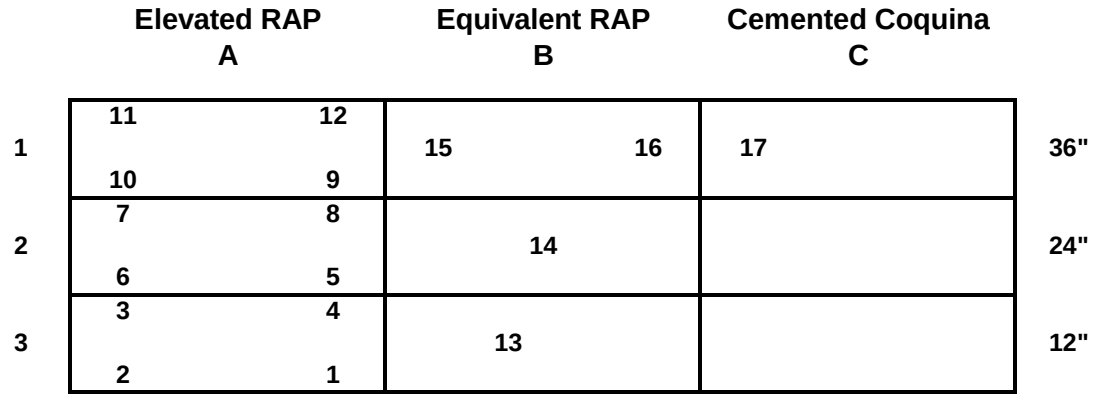

Test No.	Wet Density (pcf)	Speedy Moisture (%)	Dry Density (pcf)
1	127.8	19.3	107.1
2	131.8	15.4	114.2
3	129.0	19.4	108.0
4	120.9	19.3	101.3
5	125.2	19.5	104.8
6	128.8	19.0	108.2
7	118.1	22.7	96.3
8	117.8	23.2	95.6
9	123.9	6.6	116.2
10	115.5	22.1	94.6
11	125.8	12.1	112.2
12	125.9	15.5	109.0
13	121.9	18.6	102.8
14	129.0	19.3	108.1
15	124.2	6.2	116.9
16	116.4	21.8	95.6
17	115.8	21.5	95.3

Figure AA-1: Location and Results of Subsurface Density Tests

Appendix BB
Compaction Energies

	Elevated RAP A	Equivalent RAP B	Cemented Coquina C
36"	A1	B1	C1
24"	A2	B2	C2
12"	A3	B3	C3

Section Location	Total Depth at Location	No. of Passes Per Layer					
		6"	12"	18"	24"	30"	36"
A3	12"	10	8				
B3	12"	4	8				
C3	12"	4	4				
A2	24"	10	8	10	10		
B2	24"	4	8	10	10		
C2	24"	4	4	10	10		
A1	36"	10	8	10	10	10	14
B1	36"	4	8	10	10	10	10
C1	36"	4	4	10	10	10	10

Figure BB-1: Compaction Energy of a Smooth Drum Vibratory Roller Used During Construction of Field Site

Appendix CC
Cone Penetrometer Data

October Data (12 inch Layer)

Location: Elevated RAP
Layer Thickness: 12"

Depth (meters)	Depth (feet)	Tip, Q_c tsf	Friction, F_s tsf	Friction Ratio
0.05	0.16	70.6	0.064	0.09
0.1	0.33	87.7	0.190	0.22
0.15	0.49	107.9	0.275	0.25
0.2	0.66	125.6	0.370	0.29
0.25	0.82	147.9	0.310	0.21
0.3	0.98	157.8	0.386	0.24
0.35	1.15	201.5	0.647	0.32

Location: Equivalent RAP
Layer Thickness: 12"

Depth (meters)	Depth (feet)	Tip, Q_c tsf	Friction, F_s tsf	Friction Ratio
0.05	0.16	38.9	0.020	0.05
0.1	0.33	82.1	0.086	0.10
0.15	0.49	87.9	0.133	0.15
0.2	0.66	104.2	0.224	0.21
0.25	0.82	131.0	0.226	0.17
0.3	0.98	128.7	0.352	0.27
0.35	1.15	152.4	0.434	0.28

October Data (24 inch Layer)

Location: Elevated RAP
Layer Thickness: 24"

Depth (meters)	Depth (feet)	Tip, Q_c tsf	Friction, F_s tsf	Friction Ratio
0.05	0.16	58.9	0.014	0.02
0.1	0.33	82.1	0.189	0.23
0.15	0.49	110.1	0.200	0.18
0.2	0.66	115.2	0.243	0.21
0.25	0.82	150.7	0.259	0.17
0.3	0.98	176.0	0.328	0.19
0.35	1.15	177.4	0.348	0.20
0.4	1.31	207.0	0.371	0.18
0.45	1.48	208.5	0.355	0.17
0.5	1.64	180.5	0.443	0.25
0.55	1.80	175.9	0.537	0.31
0.6	1.97	185.1	0.675	0.36
0.65	2.13	210.2	0.644	0.31

Location: Equivalent RAP
Layer Thickness: 24"

Depth (meters)	Depth (feet)	Tip, Q_c tsf	Friction, F_s tsf	Friction Ratio
0.05	0.16	72.4	0.039	0.05
0.1	0.33	88.1	0.180	0.20
0.15	0.49	116.8	0.196	0.17
0.2	0.66	131.8	0.223	0.17
0.25	0.82	157.5	0.305	0.19
0.3	0.98	157.7	0.360	0.23
0.35	1.15	150.2	0.363	0.24
0.4	1.31	153.5	0.267	0.17
0.45	1.48	169.0	0.371	0.22
0.5	1.64	183.6	0.573	0.31
0.55	1.80	220.9	0.639	0.29
0.6	1.97	228.6	0.508	0.22
0.65	2.13	236.3	0.386	0.16

October Data (36 inch Layer)

Location: Elevated RAP

Layer Thickness: 36"

Depth (meters)	Depth (feet)	Tip, Q_c tsf	Friction, F_s tsf	Friction Ratio
0.05	0.16	60.8	0.064	0.11
0.1	0.33	83.6	0.187	0.22
0.15	0.49	109.0	0.191	0.18
0.2	0.66	120.7	0.222	0.18
0.25	0.82	134.2	0.297	0.22
0.3	0.98	151.4	0.320	0.21
0.35	1.15	143.2	0.280	0.20
0.4	1.31	146.8	0.292	0.20
0.45	1.48	168.7	0.369	0.22
0.5	1.64	188.3	0.406	0.22
0.55	1.80	194.8	0.465	0.24
0.6	1.97	200.4	0.368	0.18
0.65	2.13	211.1	0.372	0.18
0.7	2.30	207.4	0.377	0.18
0.75	2.46	194.1	0.472	0.24
0.8	2.62	183.9	0.292	0.16
0.85	2.79	154.8	0.589	0.38
0.9	2.95	117.9	0.853	0.72
0.95	3.12	103.8	0.850	0.82

Location: Equivalent RAP
Layer Thickness: 36"

Depth (meters)	Depth (feet)	Tip, Q_c tsf	Friction, F_s tsf	Friction Ratio
0.05	0.16	61.9	0.051	0.08
0.1	0.33	96.8	0.097	0.10
0.15	0.49	107.6	0.184	0.17
0.2	0.66	131.8	0.174	0.13
0.25	0.82	181.8	0.322	0.18
0.3	0.98	177.6	0.347	0.20
0.35	1.15	170.3	0.289	0.17
0.4	1.31	187.7	0.339	0.18
0.45	1.48	206.1	0.402	0.20
0.5	1.64	213.6	0.446	0.21
0.55	1.80	199.8	0.394	0.20
0.6	1.97	190.2	0.353	0.19
0.65	2.13	188.1	0.268	0.14
0.7	2.30	190.8	0.455	0.24
0.75	2.46	232.1	0.448	0.19
0.8	2.62	232.5	0.738	0.32
0.85	2.79	203.1	0.925	0.46
0.9	2.95	196.1	0.887	0.45
0.95	3.12	175.7	0.569	0.32

December Data (12 inch Layer)

Location: Elevated RAP
Layer Thickness: 12"

Depth (meters)	Depth (feet)	Tip, Q_c tsf	Friction, F_s tsf	Friction Ratio
0.05	0.16	142.9	0.064	0.04
0.1	0.33	165.3	0.201	0.12
0.15	0.49	204.8	0.291	0.14
0.2	0.66	251.9	0.328	0.13
0.25	0.82	277.2	0.343	0.12
0.3	0.98	281.2	0.386	0.14
0.35	1.15	286.8	0.651	0.23

Location: Equivalent RAP
Layer Thickness: 12"

Depth (meters)	Depth (feet)	Tip, Q_c tsf	Friction, F_s tsf	Friction Ratio
0.05	0.16	101.6	-0.004	0.00
0.1	0.33	150.5	0.052	0.03
0.15	0.49	165.9	0.217	0.13
0.2	0.66	191.3	0.267	0.14
0.25	0.82	223.0	0.357	0.16
0.3	0.98	223.2	0.487	0.22
0.35	1.15	211.2	0.561	0.27

December Data (24 inch Layer)

Location: Elevated RAP
Layer Thickness: 24"

Depth (meters)	Depth (feet)	Tip, Q_c tsf	Friction, F_s tsf	Friction Ratio
0.05	0.16	137.7	0.313	0.23
0.1	0.33	160.7	0.399	0.25
0.15	0.49	182.8	0.446	0.24
0.2	0.66	211.4	0.430	0.20
0.25	0.82	228.4	0.393	0.17
0.3	0.98	253.0	0.431	0.17
0.35	1.15	298.2	0.573	0.19
0.4	1.31	305.5	0.565	0.18
0.45	1.48	285.3	0.698	0.24
0.5	1.64	270.6	0.761	0.28
0.55	1.80	254.2	0.709	0.28
0.6	1.97	275.0	0.738	0.27
0.65	2.13	259.3	0.740	0.29

Location: Equivalent RAP
Layer Thickness: 24"

Depth (meters)	Depth (feet)	Tip, Q_c tsf	Friction, F_s tsf	Friction Ratio
0.05	0.16	159.3	-0.016	-0.01
0.1	0.33	162.0	0.412	0.25
0.15	0.49	200.1	0.482	0.24
0.2	0.66	223.8	0.453	0.20
0.25	0.82	230.9	0.539	0.23
0.3	0.98	229.2	0.491	0.21
0.35	1.15	220.6	0.498	0.23
0.4	1.31	241.0	0.460	0.19
0.45	1.48	257.5	0.460	0.18
0.5	1.64	263.4	0.514	0.20
0.55	1.80	297.0	0.752	0.25
0.6	1.97	324.0	0.787	0.24
0.65	2.13	323.2	0.888	0.27

December Data (36 inch Layer)

Location: Elevated RAP

Layer Thickness: 36"

Depth (meters)	Depth (feet)	Tip, Q_c tsf	Friction, F_s tsf	Friction Ratio
0.05	0.16	127.1	0.176	0.14
0.1	0.33	164.9	0.490	0.30
0.15	0.49	232.8	0.536	0.23
0.2	0.66	241.9	0.647	0.27
0.25	0.82	250.2	0.618	0.25
0.3	0.98	277.0	0.614	0.22
0.35	1.15	263.3	0.588	0.22
0.4	1.31	263.9	0.598	0.23
0.45	1.48	291.5	0.524	0.18
0.5	1.64	278.0	0.591	0.21
0.55	1.80	280.1	0.574	0.20
0.6	1.97	291.6	0.491	0.17
0.65	2.13	304.5	0.483	0.16
0.7	2.30	292.2	0.726	0.25
0.75	2.46	289.5	0.957	0.33
0.8	2.62	237.9	2.238	0.94
0.85	2.79	218.8	2.162	0.99
0.9	2.95	150.9	1.498	0.99
0.95	3.12	164.7	0.710	0.43

Location: Equivalent RAP
Layer Thickness: 36"

Depth (meters)	Depth (feet)	Tip, Q_c tsf	Friction, F_s tsf	Friction Ratio
0.05	0.16	29.9	-0.007	-0.02
0.1	0.33	124.2	-0.013	-0.01
0.15	0.49	168.0	0.005	0.00
0.2	0.66	210.7	0.301	0.14
0.25	0.82	211.2	0.470	0.22
0.3	0.98	250.0	0.517	0.21
0.35	1.15	250.9	0.585	0.23
0.4	1.31	232.5	0.399	0.17
0.45	1.48	235.5	0.378	0.16
0.5	1.64	273.0	0.478	0.18
0.55	1.80	279.9	0.511	0.18
0.6	1.97	261.1	0.421	0.16
0.65	2.13	243.4	0.453	0.19
0.7	2.30	244.0	0.354	0.15
0.75	2.46	222.1	0.205	0.09
0.8	2.62	234.7	0.429	0.18
0.85	2.79	190.0	0.693	0.36
0.9	2.95	172.2	1.354	0.79
0.95	3.12	157.4	1.847	1.17

February Data (12 inch Layer)

Location: Elevated RAP
Layer Thickness: 12"

Depth (meters)	Depth (feet)	Tip, Q_c tsf	Friction, F_s tsf	Friction Ratio
0.05	0.16	250.18	0.394	0.16
0.1	0.33	212.34	0.969	0.46
0.15	0.49	223.47	1.417	0.63
0.2	0.66	296.26	1.435	0.48
0.25	0.82	309.11	1.350	0.44
0.3	0.98	289.14	1.310	0.45
0.35	1.15	267.30	1.229	0.46

Location: Equivalent RAP
Layer Thickness: 12"

Depth (meters)	Depth (feet)	Tip, Q_c tsf	Friction, F_s tsf	Friction Ratio
0.05	0.16	289.40	1.162	0.40
0.1	0.33	295.35	1.327	0.45
0.15	0.49	277.63	1.408	0.51
0.2	0.66	254.60	1.231	0.48
0.25	0.82	221.86	1.129	0.51
0.3	0.98	160.36	0.782	0.49
0.35	1.15	113.94	0.528	0.46

February Data (24 inch Layer)

Location: Elevated RAP
Layer Thickness: 24"

Depth (meters)	Depth (feet)	Tip, Q_c tsf	Friction, F_s tsf	Friction Ratio
0.05	0.16	260.74	0.525	0.20
0.1	0.33	235.29	1.108	0.47
0.15	0.49	304.67	1.289	0.42
0.2	0.66	299.00	0.946	0.32
0.25	0.82	312.98	0.815	0.26
0.3	0.98	294.92	0.798	0.27
0.35	1.15	322.14	1.189	0.37
0.4	1.31	376.93	1.628	0.43
0.45	1.48	367.56	1.416	0.39
0.5	1.64	321.12	1.357	0.42
0.55	1.80	293.35	1.174	0.40
0.6	1.97	274.21	1.080	0.39
0.65	2.13	283.17	1.110	0.39

Location: Equivalent RAP
Layer Thickness: 24"

Depth (meters)	Depth (feet)	Tip, Q_c tsf	Friction, F_s tsf	Friction Ratio
0.05	0.16	240.05	0.073	0.03
0.1	0.33	318.46	1.089	0.34
0.15	0.49	321.77	1.537	0.48
0.2	0.66	339.43	1.584	0.47
0.25	0.82	333.69	1.155	0.35
0.3	0.98	308.30	0.716	0.23
0.35	1.15	289.25	0.652	0.23
0.4	1.31	295.64	0.661	0.22
0.45	1.48	315.76	0.746	0.24
0.5	1.64	314.15	1.069	0.34
0.55	1.80	322.35	1.485	0.46
0.6	1.97	311.02	1.526	0.49
0.65	2.13	348.01	1.222	0.35

February Data (36 inch Layer)

Location: Elevated RAP

Layer Thickness: 36"

Depth (meters)	Depth (feet)	Tip, Q_c tsf	Friction, F_s tsf	Friction Ratio
0.05	0.16	234.88	0.860	0.37
0.1	0.33	278.12	1.521	0.55
0.15	0.49	351.28	1.574	0.45
0.2	0.66	345.89	1.548	0.45
0.25	0.82	364.05	1.649	0.45
0.3	0.98	376.08	1.604	0.43
0.35	1.15	336.11	1.396	0.42
0.4	1.31	320.10	1.289	0.40
0.45	1.48	313.51	1.266	0.40
0.5	1.64	312.77	1.255	0.40
0.55	1.80	312.23	1.220	0.39
0.6	1.97	320.69	1.164	0.36
0.65	2.13	329.63	1.121	0.34
0.7	2.30	297.07	0.470	0.16
0.75	2.46	256.62	0.886	0.35
0.8	2.62	187.44	1.238	0.66
0.85	2.79	164.16	1.631	0.99
0.9	2.95	139.98	1.606	1.15
0.95	3.12	102.68	1.451	1.41

Location: Equivalent RAP
Layer Thickness: 36"

Depth (meters)	Depth (feet)	Tip, Q_c tsf	Friction, F_s tsf	Friction Ratio
0.05	0.16	172.61	0.064	0.04
0.1	0.33	245.63	0.916	0.37
0.15	0.49	292.69	1.048	0.36
0.2	0.66	306.88	1.259	0.41
0.25	0.82	323.54	1.149	0.36
0.3	0.98	318.16	1.095	0.34
0.35	1.15	288.63	0.902	0.31
0.4	1.31	263.61	0.757	0.29
0.45	1.48	282.32	0.802	0.28
0.5	1.64	290.71	0.913	0.31
0.55	1.80	290.44	0.941	0.32
0.6	1.97	262.22	0.779	0.30
0.65	2.13	250.54	0.638	0.25
0.7	2.30	264.33	1.477	0.56
0.75	2.46	318.03	3.598	1.13
0.8	2.62	603.61	5.584	0.93
0.85	2.79	448.52	9.650	2.15
0.9	2.95	508.83	7.609	1.50
0.95	3.12	268.49	7.161	2.67

April Data (12 inch Layer)

Location: Elevated RAP
Layer Thickness: 12"

Depth (meters)	Depth (feet)	Tip, Q_c tsf	Friction, F_s tsf	Friction Ratio
0.05	0.16	165.6	0.045	0.03
0.1	0.33	156.1	0.515	0.33
0.15	0.49	192.9	0.604	0.31
0.2	0.66	228.1	0.653	0.29
0.25	0.82	235.9	0.532	0.23
0.3	0.98	239.7	0.662	0.28
0.35	1.15	278.6	0.892	0.32

Location: Equivalent RAP
Layer Thickness: 12"

Depth (meters)	Depth (feet)	Tip, Q_c tsf	Friction, F_s tsf	Friction Ratio
0.05	0.16	157.4	0.175	0.11
0.1	0.33	142.5	0.287	0.20
0.15	0.49	150.3	0.351	0.23
0.2	0.66	173.0	0.370	0.21
0.25	0.82	186.0	0.340	0.18
0.3	0.98	192.1	0.449	0.23
0.35	1.15	231.0	0.703	0.30

April Data (24 inch Layer)

Location: Elevated RAP
Layer Thickness: 24"

Depth (meters)	Depth (feet)	Tip, Q_c tsf	Friction, F_s tsf	Friction Ratio
0.05	0.16	249.4	0.427	0.17
0.1	0.33	221.4	0.645	0.29
0.15	0.49	246.5	0.836	0.34
0.2	0.66	236.0	0.743	0.31
0.25	0.82	243.8	0.680	0.28
0.3	0.98	234.5	0.631	0.27
0.35	1.15	256.3	0.654	0.26
0.4	1.31	270.0	0.658	0.24
0.45	1.48	265.8	0.727	0.27
0.5	1.64	288.6	0.948	0.33
0.55	1.80	313.1	1.059	0.34
0.6	1.97	320.9	0.902	0.28
0.65	2.13	325.1	0.854	0.26

Location: Equivalent RAP
Layer Thickness: 24"

Depth (meters)	Depth (feet)	Tip, Q_c tsf	Friction, F_s tsf	Friction Ratio
0.05	0.16	306.3	0.618	0.20
0.1	0.33	265.0	0.819	0.31
0.15	0.49	280.5	1.020	0.36
0.2	0.66	278.8	1.027	0.37
0.25	0.82	263.5	0.930	0.35
0.3	0.98	233.9	0.673	0.29
0.35	1.15	221.7	0.571	0.26
0.4	1.31	240.5	0.444	0.18
0.45	1.48	258.7	0.459	0.18
0.5	1.64	268.9	0.762	0.28
0.55	1.80	307.8	0.996	0.32
0.6	1.97	340.6	1.154	0.34
0.65	2.13	356.2	1.070	0.30

April Data (36 inch Layer)

Location: Elevated RAP

Layer Thickness: 36"

Depth (meters)	Depth (feet)	Tip, Q_c tsf	Friction, F_s tsf	Friction Ratio
0.05	0.16	145.5	0.139	0.10
0.1	0.33	213.3	0.455	0.21
0.15	0.49	252.8	0.600	0.24
0.2	0.66	239.7	0.631	0.26
0.25	0.82	240.9	0.618	0.26
0.3	0.98	241.1	0.667	0.28
0.35	1.15	231.2	0.599	0.26
0.4	1.31	229.1	0.611	0.27
0.45	1.48	252.1	0.556	0.22
0.5	1.64	252.8	0.539	0.21
0.55	1.80	258.9	0.495	0.19
0.6	1.97	258.8	0.664	0.26
0.65	2.13	264.0	0.641	0.24
0.7	2.30	253.7	0.615	0.24
0.75	2.46	267.9	0.703	0.26
0.8	2.62	259.8	0.959	0.37
0.85	2.79	177.4	1.072	0.60
0.9	2.95	169.6	0.916	0.54
0.95	3.12	156.0	0.903	0.58

Location: Equivalent RAP
Layer Thickness: 36"

Depth (meters)	Depth (feet)	Tip, Q_c tsf	Friction, F_s tsf	Friction Ratio
0.05	0.16	71.4	0.012	0.02
0.1	0.33	274.5	0.016	0.01
0.15	0.49	262.6	0.009	0.00
0.2	0.66	264.8	0.399	0.15
0.25	0.82	250.3	0.586	0.23
0.3	0.98	272.4	0.601	0.22
0.35	1.15	270.9	0.679	0.25
0.4	1.31	250.5	0.638	0.25
0.45	1.48	249.1	0.621	0.25
0.5	1.64	262.8	0.552	0.21
0.55	1.80	251.8	0.540	0.21
0.6	1.97	244.4	0.439	0.18
0.65	2.13	229.1	0.574	0.25
0.7	2.30	232.5	0.477	0.21
0.75	2.46	237.2	0.505	0.21
0.8	2.62	264.3	0.445	0.17
0.85	2.79	287.9	1.312	0.46
0.9	2.95	261.7	1.526	0.58
0.95	3.12	283.6	1.461	0.52

June Data (12 inch Layer)

Location: Elevated RAP
Layer Thickness: 12"

Depth (meters)	Depth (feet)	Tip, Q_c tsf	Friction, F_s tsf	Friction Ratio
0.05	0.16	145.1	0.020	0.01
0.1	0.33	182.9	0.035	0.02
0.15	0.49	170.3	0.017	0.01
0.2	0.66	211.6	0.007	0.00
0.25	0.82	229.7	0.008	0.00
0.3	0.98	245.1	0.024	0.01
0.35	1.15	262.3	0.017	0.01

Location: Equivalent RAP
Layer Thickness: 12"

Depth (meters)	Depth (feet)	Tip, Q_c tsf	Friction, F_s tsf	Friction Ratio
0.05	0.16	170.3	0.027	0.02
0.1	0.33	146.4	0.225	0.15
0.15	0.49	151.6	0.249	0.16
0.2	0.66	153.1	0.276	0.18
0.25	0.82	167.3	0.147	0.09
0.3	0.98	192.5	0.347	0.18
0.35	1.15	226.5	0.592	0.26

June Data (24 inch Layer)

Location: Elevated RAP
Layer Thickness: 24"

Depth (meters)	Depth (feet)	Tip, Q_c tsf	Friction, F_s tsf	Friction Ratio
0.05	0.16	153.6	0.031	0.02
0.1	0.33	134.7	0.303	0.22
0.15	0.49	157.5	0.349	0.22
0.2	0.66	191.4	0.383	0.20
0.25	0.82	223.6	0.412	0.18
0.3	0.98	227.1	0.366	0.16
0.35	1.15	224.1	0.452	0.20
0.4	1.31	238.0	0.520	0.22
0.45	1.48	259.3	0.604	0.23
0.5	1.64	263.7	0.622	0.24
0.55	1.80	286.5	0.775	0.27
0.6	1.97	319.4	0.887	0.28
0.65	2.13	321.1	0.939	0.29

Location: Equivalent RAP
Layer Thickness: 24"

Depth (meters)	Depth (feet)	Tip, Q_c tsf	Friction, F_s tsf	Friction Ratio
0.05	0.16	28.2	0.186	0.66
0.1	0.33	132.3	0.255	0.19
0.15	0.49	152.2	0.212	0.14
0.2	0.66	167.1	0.218	0.13
0.25	0.82	186.5	0.246	0.13
0.3	0.98	203.7	0.303	0.15
0.35	1.15	224.7	0.355	0.16
0.4	1.31	240.0	0.365	0.15
0.45	1.48	224.8	0.491	0.22
0.5	1.64	255.1	0.766	0.30
0.55	1.80	295.8	0.852	0.29
0.6	1.97	340.8	0.908	0.27
0.65	2.13	345.7	0.815	0.24

June Data (36 inch Layer)

Location: Elevated RAP

Layer Thickness: 36"

Depth (meters)	Depth (feet)	Tip, Q_c tsf	Friction, F_s tsf	Friction Ratio
0.05	0.16	70.5	0.030	0.04
0.1	0.33	177.0	0.254	0.14
0.15	0.49	148.2	0.400	0.27
0.2	0.66	192.3	0.504	0.26
0.25	0.82	217.6	0.583	0.27
0.3	0.98	238.0	0.624	0.26
0.35	1.15	250.8	0.617	0.25
0.4	1.31	233.3	0.559	0.24
0.45	1.48	229.3	0.588	0.26
0.5	1.64	232.5	0.601	0.26
0.55	1.80	222.3	0.583	0.26
0.6	1.97	220.2	0.525	0.24
0.65	2.13	212.4	0.539	0.25
0.7	2.30	214.8	0.477	0.22
0.75	2.46	221.6	0.489	0.22
0.8	2.62	246.3	0.399	0.16
0.85	2.79	257.2	0.825	0.32
0.9	2.95	240.0	1.323	0.55
0.95	3.12	233.0	1.567	0.67

Location: Equivalent RAP
Layer Thickness: 36"

Depth (meters)	Depth (feet)	Tip, Q_c tsf	Friction, F_s tsf	Friction Ratio
0.05	0.16	153.5	0.034	0.02
0.1	0.33	126.8	0.039	0.03
0.15	0.49	152.3	0.065	0.04
0.2	0.66	177.7	0.051	0.03
0.25	0.82	215.8	0.018	0.01
0.3	0.98	218.7	0.425	0.19
0.35	1.15	208.8	0.394	0.19
0.4	1.31	203.3	0.413	0.20
0.45	1.48	200.0	0.407	0.20
0.5	1.64	186.4	0.364	0.19
0.55	1.80	172.1	0.340	0.20
0.6	1.97	169.2	0.296	0.18
0.65	2.13	176.7	0.241	0.14
0.7	2.30	191.3	0.261	0.14
0.75	2.46	232.2	0.501	0.22
0.8	2.62	217.2	0.756	0.35
0.85	2.79	200.8	0.804	0.40
0.9	2.95	156.3	0.747	0.48
0.95	3.12	115.2	0.713	0.62

Appendix DD

Limerock Bearing Ratio Data

	Elevated RAP A	Equivalent RAP B	Cemented Coquina C
36"	A1	B1	C1
24"	A2	B2	C2
12"	A3	B3	C3

LBR	Total Section	0.1 " Data						
Section	Depth (in)	10/5/99	12/6/99	2/7/99	5/1/00	6/6/00	8/7/00	10/9/00
A3	12	18.4	23.4	31.7	65.2	83.6	61.2	36.4
B3	12	21.6	24.1	40.3	24.8	74.0	40.2	124.0
C3	12	wet cond.	46.1	38.5	117.6	164.8	132.0	123.0
A2	24	13.3	68.8	87.1	45.0	46.2	26.0	85.2
B2	24	15.5	58.3	85.0	44.5	70.0	27.2	89.6
C2	24	wet cond.	37.8	29.5	153.6	144.0	92.0	85.6
A1	36	15.1	69.1	103.0	40.0	74.4	39.7	132.4
B1	36	14.4	61.9	88.2	40.4	66.0	39.0	114.0
C1	36	wet cond.	32.0	49.7	207.6	231.2	137.0	104.0

Appendix EE

Automatic Dynamic Cone Penetrometer Data

Oct-99 Elevated RAP 12" Layer		Dec-99 Elevated RAP 12" Layer		Feb-00 Elevated RAP 12" Layer	
Depth, in	**LBR**	**Depth, in**	**LBR**	**Depth, in**	**LBR**
-0.04	0	0	0	-0.04	0
0.91	36	0.87	69	0.87	66
1.81	51	1.89	84	1.89	71
2.72	51	2.99	102	2.76	151
3.58	54	3.9	137	3.82	80
4.49	51	5.04	77	4.84	111
5.39	51	6.02	146	5.79	168
6.42	58	6.93	144	6.69	168
7.32	92	7.95	111	7.6	160
8.27	81	9.02	147	8.58	137
9.17	81	9.88	185	9.53	200
10.24	55	10.79	107	10.43	128
11.42	60	11.85	97	11.34	96
12.24	73	12.87	84	12.32	102

Oct-99 Elevated RAP 24" Layer		Dec-99 Elevated RAP 24" Layer		Feb-00 Elevated RAP 24" Layer	
Depth, in	**LBR**	**Depth, in**	**LBR**	**Depth, in**	**LBR**
-0.04	0	0	0	0	0
1.02	20	0.98	102	0.98	88
1.85	26	1.77	151	1.89	209
2.91	31	2.72	118	2.8	176
3.98	31	3.7	88	3.86	161
4.84	54	4.65	152	4.76	200
5.75	51	5.75	77	5.63	213
6.57	57	6.73	116	6.54	160
7.48	51	7.6	134	7.64	155
8.66	49	8.46	101	8.7	161
9.76	65	9.45	88	9.76	161
10.79	71	10.47	111	10.75	160
11.73	92	11.3	141	11.81	175
12.68	77	12.28	74	12.76	200

Oct-99 Elevated RAP 36" Layer		Dec-99 Elevated RAP 36" Layer		Feb-00 Elevated RAP 36" Layer	
Depth, in	**LBR**	**Depth, in**	**LBR**	**Depth, in**	**LBR**
-0.04	0	0	0	0	0
0.87	51	0.98	88	1.02	84
1.73	54	1.97	102	2.05	111
2.52	60	3.07	102	3.03	116
3.46	49	4.17	102	4.02	88
4.53	55	5.16	146	4.92	128
5.63	65	6.22	161	5.91	102
6.46	107	7.13	200	6.93	139
7.52	68	8.11	168	7.8	202
8.39	112	9.06	152	8.7	144
9.29	85	10.04	131	9.65	152
10.24	77	11.1	189	10.75	128
11.22	74	11.93	195	11.69	200
12.28	107	12.83	152	12.6	176

Oct-99 Equivalent RAP 12" Layer		Dec-99 Equivalent RAP 12" Layer		Feb-00 Equivalent RAP 12" Layer	
Depth, in	**LBR**	**Depth, in**	**LBR**	**Depth, in**	**LBR**
0	0	0	0	0	0
0.94	23	1.02	45	0.98	47
2.01	31	1.97	107	2.09	65
3.07	43	2.8	85	3.19	102
4.09	45	3.74	81	3.98	124
5.08	47	4.61	85	5.08	80
6.06	47	5.51	96	6.18	102
6.97	66	6.42	81	7.05	134
8.11	51	7.24	90	7.99	122
8.9	77	8.15	96	9.06	107
9.69	60	9.25	77	10.04	116
10.55	54	10.2	122	11.14	168
11.5	36	11.3	65	12.09	122
12.64	40	12.36	68		

Oct-99 Equivalent RAP 24" Layer		Dec-99 Equivalent RAP 24" Layer		Feb-00 Equivalent RAP 24" Layer	
Depth, in	**LBR**	**Depth, in**	**LBR**	**Depth, in**	**LBR**
0.04	0	0	0	-0.04	0
1.02	22	0.98	102	0.94	88
2.05	33	1.97	102	1.97	154
3.03	34	2.95	116	2.95	160
3.9	54	3.82	176	4.06	155
4.69	60	4.8	92	5.12	147
5.83	51	5.75	152	6.1	191
7.01	60	6.65	122	7.13	125
8.11	65	7.64	92	8.11	131
9.17	68	8.62	116	9.17	134
10.2	71	9.65	111	10.16	160
11.3	65	10.71	120	11.14	160
12.32	71	11.57	112	11.97	168
		12.56	63	12.87	134

Oct-99 Equivalent RAP 36" Layer		Dec-99 Equivalent RAP 36" Layer		Feb-00 Equivalent RAP 36" Layer	
Depth, in	**LBR**	**Depth, in**	**LBR**	**Depth, in**	**LBR**
0	0	-0.04	0	-0.04	0
1.02	33	0.91	184	1.1	74
1.93	66	2.05	98	2.01	144
2.76	57	3.07	125	2.99	88
3.86	53	4.09	139	3.94	137
4.65	77	5.08	102	5	107
5.67	58	5.91	177	5.98	116
6.65	102	6.81	144	6.85	176
7.8	86	7.76	184	7.76	151
8.62	124	8.74	131	8.78	154
9.69	80	9.76	139	9.69	209
10.75	93	10.79	154	10.67	175
11.89	98	11.73	184	11.57	184
12.8	112	12.68	152	12.56	122

Appendix FF

Falling Weight Deflectometer Data

FLORIDA TECH FWD DATA (October 1999)

A1								
psi	***lbf***	***Df1***	***Df2***	***Df3***	***Df4***	***Df5***	***Df6***	***Df7***
				7.01				
65.5	7182	16.96	8.54	5.19	3.74	3.11	2.08	1.45
82.1	9009	22.67	11.69	7.24	5.15	4.25	2.87	1.96
107.8	11822	32.48	16.96	10.66	7.59	6.18	4.25	2.87
				7.02				
60.1	6594	21.37	8.54	3.81	2.59	2.44	2.04	1.37
77.8	8533	27.55	11.73	5.7	3.77	3.46	2.87	1.88
106.8	11711	38.34	17.24	8.85	5.7	5.07	4.17	2.67
				7.03				
59.1	6483	21.41	8.22	3.85	2.63	2.59	2.32	1.65
76.5	8390	27.2	11.53	5.7	3.81	3.7	3.26	2.28
107.3	1174	38.11	17.32	8.81	5.62	5.31	4.68	3.26

A2								
psi	***lbf***	***Df1***	***Df2***	***Df3***	***Df4***	***Df5***	***Df6***	***Df7***
				4.01				
67.9	7452	18.77	9.25	5.35	3.58	2.79	1.96	1.29
81.3	8914	24.25	11.81	6.96	4.68	3.62	2.51	1.65
104	11409	34.37	16.65	9.84	6.49	5.03	3.5	2.16
				4.02				
68.9	7563	19.48	8.26	5.19	3.62	2.79	1.88	1.33
82.4	9041	23.81	10.55	6.77	4.64	3.62	2.51	1.61
103.6	11361	32.75	14.76	9.44	6.49	5.03	3.58	2.2
				4.03				
60.8	6673	15.62	7.55	4.6	3.46	2.67	1.85	1.22
80.8	8866	20.98	10.43	6.61	4.96	3.77	2.63	1.69
109.4	11997	33.62	16.77	10.82	8.03	6.06	4.21	2.63

A3								
psi	***lbf***	***Df1***	***Df2***	***Df3***	***Df4***	***Df5***	***Df6***	***Df7***
				1.01				
63.6	6975	17.71	9.48	6.61	4.64	3.34	2.08	1.29
81.8	8977	22.59	11.85	8.42	5.86	4.21	2.71	1.57
107.6	11806	33.26	17.63	12.32	8.62	6.18	3.93	2.28
				1.02				
58.8	6451	19.99	9.64	6.1	3.97	2.83	1.85	1.1
75.7	8310	24.56	11.65	7.55	5.07	3.74	2.36	1.45
100.2	10996	37.99	17.55	11.49	7.87	5.59	3.54	2.12
				1.03				
60.4	6626	20.19	10.74	7.04	4.8	3.34	2.08	1.29
81.5	8946	23.89	12.95	8.66	5.98	4.21	2.59	1.61
111.5	12235	35.98	19.21	12.91	9.05	6.33	3.81	2.28

FLORIDA TECH FWD DATA (October 1999)

B1								
psi	***lbf***	***Df1***	***Df2***	***Df3***	***Df4***	***Df5***	***Df6***	***Df7***
				8.01				
61	6689	22.36	8.7	4.44	3.11	2.91	2.36	1.65
78.4	8596	28.26	11.88	6.45	4.52	4.13	3.34	2.28
107.1	11742	38.66	17.28	9.76	6.81	6.1	4.88	3.34
				8.02				
61.3	6721	26.02	8.38	4.13	2.95	2.67	2.28	1.57
79.4	8707	31.85	11.53	6.1	4.33	3.77	3.18	2.2
105.7	11599	42.12	16.73	9.17	6.41	5.62	4.6	3.14
				8.03				
62	6800	21.69	8.34	4.52	3.54	3.14	2.63	1.85
78.6	8628	27.95	11.49	6.37	4.96	4.37	3.62	2.51
106.9	11726	39.25	17.04	9.48	7.24	6.33	5.31	3.66

B2								
psi	***lbf***	***Df1***	***Df2***	***Df3***	***Df4***	***Df5***	***Df6***	***Df7***
				5.01				
69.7	7643	19.88	8.54	5.43	3.93	3.11	2.24	1.37
84	9216	24.44	10.94	7.04	5.07	3.97	2.87	1.69
104	11409	34.37	16.65	9.84	6.49	5.03	3.5	2.16
				5.02				
71.7	78.65	19.17	8.42	5.23	3.66	2.95	2.16	1.37
85.7	9406	23.34	10.66	6.73	4.72	3.81	2.71	1.77
106	1161	32.59	14.92	9.52	6.77	5.35	3.81	2.44
				5.03				
68.8	7547	21.06	9.52	5.7	3.97	3.14	2.16	1.37
82.3	9025	25.07	11.88	7.24	5.15	3.93	2.71	1.69
103.3	11329	33.03	16.53	10.31	7.28	5.59	3.81	2.36

B3								
psi	***lbf***	***Df1***	***Df2***	***Df3***	***Df4***	***Df5***	***Df6***	***Df7***
				2.01				
59.9	6578	22.32	8.14	4.76	3.42	2.71	1.92	1.1
77.9	8548	25.07	10.19	6.37	4.52	3.5	2.48	1.45
104	11409	35.82	15.62	9.96	7.08	5.39	3.74	2.12
				2.02				
59.1	6483	23.3	10.62	6.53	4.37	3.14	2.12	1.29
77.6	8517	27.44	12.95	8.3	5.7	4.25	2.87	1.73
104.4	11456	41.41	19.84	12.99	8.74	6.37	4.21	2.44
				2.03				
59.7	6546	23.77	13.22	8.66	5.78	4.05	2.44	1.33
78.8	8644	26.33	14.88	9.92	6.73	4.88	3.03	1.77
107.9	11838	40.82	22.12	14.96	10.31	7.32	4.48	2.48

FLORIDA TECH FWD DATA (October 1999)

C1								
psi	***lbf***	***Df1***	***Df2***	***Df3***	***Df4***	***Df5***	***Df6***	***Df7***
				9.01				
50.4	5529	98.22	65.27	41.25	19.52	8.38	1.85	1.1
68.5	7516	118.81	82.24	55.86	29.72	12.99	2.59	1.33
99.4	10900	101.37	111.57	81.06	48.54	21.45	3.46	1.22
				9.02				
52.8	5799	1077.75	70.59	46.53	27.24	13.11	4.25	2.12
71.4	7833	113.03	93.34	63.07	38.62	19.8	6.29	1.69
97.6	10709	100.94	121.96	93.74	61.02	31.96	9.44	1.49
				9.03				
51.1	5609	122.28	77.55	50.43	27	11.61	3.5	1.22
69.1	7579	99.52	101.29	69.6	38.25	17.48	4.92	1.18
96.3	10566	105.15	116.92	101.14	59.48	27.32	7	0.98

C2								
psi	***lbf***	***Df1***	***Df2***	***Df3***	***Df4***	***Df5***	***Df6***	***Df7***
				6.01				
56.2	6165	71.02	49.52	32	13.93	3.26	3.18	1.02
72.4	7945	89.88	63.03	41.77	17.63	4.37	3.97	1.14
104.9	11504	103.46	81.81	55.62	24.48	6.02	4.84	1.06
				6.02				
61	6689	83.42	34.68	18.81	6.1	1.49	1.49	1.45
75.7	8310	73.34	42.63	24.64	9.44	2.71	1.81	1.81
105.9	11615	95.62	58.26	34.48	15.11	5.15	2.44	2.4
				6.03				
56.3	6181	97.99	56.57	31.53	12.79	4.76	1.1	1.29
71.5	78.49	99.76	68.46	40.9	17.87	5.86	0.98	1.73
96.5	10582	100.66	107.44	60.11	27.95	9.68	1.53	2.16

C3								
psi	***lbf***	***Df1***	***Df2***	***Df3***	***Df4***	***Df5***	***Df6***	***Df7***
				3.01				
65.7	7214	44.4	26.88	15.94	10.39	5.31	2.83	1.81
86.8	9518	50.9	31.22	20.03	16.25	7.04	3.5	2.08
120.1	13172	66.25	42.63	31.14	21.88	10.23	5.03	2.87
				3.02				
54.9	6022	57.32	32.99	11.77	2.75	2.48	2.04	1.18
77.5	8501	46.96	30.51	14.92	5.59	4.17	2.83	1.69
110.4	12108	60.07	40.9	23.7	10.94	6.85	3.93	2.51
				3.03				
58.1	6371	48.22	36.92	18.74	10.03	4.21	3.18	1.81
81.7	8962	44.48	33.85	20.94	13.66	5.51	3.7	2.2
114.3	12537	52.71	43.89	28.26	19.99	8.34	5.27	3.11

FLORIDA TECH FWD DATA (December 1999)

A1								
psi	***lbf***	***Df1***	***Df2***	***Df3***	***Df4***	***Df5***	***Df6***	***Df7***
				7.01				
59.4	6514	11.53	6.96	4.84	3.22	2.4	1.57	0.88
76.5	8390	13.77	6.22	5.94	4.13	3.11	2.16	1.29
100.7	11043	19.84	11.77	8.77	6.1	4.64	3.3	1.96
				7.02				
57.2	6276	17.79	7.63	4.68	3.18	2.44	1.73	1.02
72.4	7945	19.13	9.4	5.78	4.13	3.22	2.36	1.45
96.8	10614	26.65	13.07	8.54	6.22	4.88	3.54	2.2
				7.03				
56	6149	15.19	6.18	3.74	2.87	2.48	1.92	1.25
71.5	7849	17	7.95	5.15	3.89	3.34	2.59	1.73
96.8	10614	24.44	11.73	7.67	5.82	4.96	3.89	2.51

A2								
psi	***lbf***	***Df1***	***Df2***	***Df3***	***Df4***	***Df5***	***Df6***	***Df7***
				4.01				
61.7	6769	9.48	6.73	4.44	3.26	2.48	1.57	0.94
83.6	9168	11.96	8.5	5.78	4.25	3.34	2.16	1.29
111.4	12219	17.63	12.28	8.46	6.29	4.88	3.18	1.92
				4.02				
60.4	6626	11.69	7.12	4.52	3.26	2.51	1.61	0.86
80	8771	14.4	8.5	5.51	4.05	3.22	2.16	1.29
104	11456	21.14	11.92	7.75	5.9	4.64	3.14	1.77
				4.03				
29.5	6530	15.07	7.28	5.15	3.62	2.71	1.73	0.82
78.5	8612	18.07	6.93	6.37	4.6	3.54	2.26	1.29
102.6	11250	26.29	12.71	9.13	6.73	5.11	3.38	1.85

A3								
psi	***lbf***	***Df1***	***Df2***	***Df3***	***Df4***	***Df5***	***Df6***	***Df7***
				1.01				
64	7023	14.68	7.79	5.11	3.74	2.71	1.69	0.82
81.8	8977	19.29	9.4	6.45	4.8	3.62	2.28	1.18
105.7	11599	27.4	13.89	9.72	7.16	5.35	3.42	1.85
				1.02				
62	6800	15.43	8.54	5.9	4.09	2.95	1.81	0.94
82.6	9057	19.29	10.35	7.16	5.03	3.74	2.32	1.25
107.3	11774	29.96	14.84	10.47	7.51	5.59	3.46	1.88
				1.03				
64.7	7102	12.2	7.99	5.94	4.09	2.95	1.77	1.02
85.2	9343	15.07	8.74	6.57	5.27	3.93	2.51	1.23
111.8	12267	23.22	13.22	10.07	7.95	5.9	3.58	1.85

FLORIDA TECH FWD DATA (December 1999)

B1								
psi	***lbf***	***Df1***	***Df2***	***Df3***	***Df4***	***Df5***	***Df6***	***Df7***
				8.01				
56.2	6165	12.79	6.49	4.13	3.22	2.71	2	1.25
72.4	7945	15.86	8.22	5.43	4.29	3.58	2.67	1.73
96.3	10566	22.34	12.32	8.3	6.41	5.35	3.97	2.51
				8.02				
57.5	6308	15.07	7.04	4.01	3.03	2.48	1.88	1.18
73.9	8103	17.16	8.22	5.03	4.05	3.38	2.59	1.69
96.5	10582	23.85	11.96	7.63	5.98	4.99	3.81	2.44
				8.03				
59.1	6483	12.28	6.29	4.01	3.14	2.59	2	1.29
76	8342	15.31	7.95	5.35	4.25	3.58	2.79	1.81
98.9	10852	22.12	11.57	7.91	6.25	2.27	4.05	2.63

B2								
psi	***lbf***	***Df1***	***Df2***	***Df3***	***Df4***	***Df5***	***Df6***	***Df7***
				5.01				
63.4	6959	18.22	9.17	5.78	3.42	2.51	1.73	0.98
82.4	9041	20.35	10.98	7.12	4.4	3.03	2.28	1.14
106.5	11679	26.77	13.62	8.85	6.25	4.84	3.34	1.88
				5.02				
63.7	6991	14.56	8.18	5.27	3.62	2.63	1.69	0.86
86.6	9502	18.74	9.8	6.25	4.44	3.38	2.2	1.25
113	12394	26.65	14.01	9.09	6.53	4.99	3.3	1.81
				5.03				
60.5	6642	14.99	6.25	4.17	3.26	2.44	1.69	0.59
80.1	8787	17.55	8.54	5.78	4.25	3.3	2.24	1.25
105	11520	24.68	11.92	8.11	6.14	4.76	3.26	1.73

B3								
psi	***lbf***	***Df1***	***Df2***	***Df3***	***Df4***	***Df5***	***Df6***	***Df7***
				2.01				
64.4	7071	14.96	7.67	5.23	3.77	2.91	1.92	0.94
86.3	9470	18.89	7.95	5.23	4.48	3.74	2.36	1.18
114.6	12569	27.99	13.5	9.05	7	5.43	3.54	1.57
				2.02				
63.6	6975	17.55	9.13	5.9	4.21	2.95	1.92	0.98
87.2	9565	21.49	11.77	7.87	5.47	4.01	2.55	1.37
118.2	12966	32.95	17.24	11.85	8.34	6.06	3.77	1.92
				2.03				
62.1	6816	20.31	10.15	7.16	4.92	3.46	2.04	1.1
83.4	9152	26.49	12.55	8.7	6.02	4.29	2.51	1.29
111	12171	41.14	18.97	12.95	9.17	6.53	3.89	2

FLORIDA TECH FWD DATA (December 1999)

C1								
psi	***lbf***	***Df1***	***Df2***	***Df3***	***Df4***	***Df5***	***Df6***	***Df7***
				9.01				
53.9	5911	51.45	16.18	8.07	4.68	3.34	2.28	1.45
75.9	8326	42.87	20.51	11.22	6.69	4.72	3.18	2
104.2	11425	51.85	29.72	17.67	10.82	7.44	4.8	3.03
				9.02				
58.1	6371	37.63	11.49	6.61	4.37	3.34	2.16	1.37
79.4	8707	33.66	14.56	9.6	6.18	4.76	3.22	1.96
108.1	11854	46.65	22.48	14.68	10.07	7.51	4.99	3.03
				9.03				
52.8	5799	46.65	15.03	6.41	4.76	3.26	1.96	0.66
73.9	8103	37.79	19.13	10.82	6.37	4.21	2.71	1.73
101.4	11123	54.13	28.62	17.51	10.62	6.73	4.25	2.63

C2								
psi	***lbf***	***Df1***	***Df2***	***Df3***	***Df4***	***Df5***	***Df6***	***Df7***
				6.01				
55.3	6070	38.42	17.63	7.67	4.09	2.59	1.53	0.94
74.7	8199	35.31	21.45	9.64	5.11	3.22	1.96	1.25
102	11186	45.82	26.69	14.64	7.99	4.88	2.91	1.69
				6.02				
54.9	6022	31.49	12.24	6.45	3.74	2.44	1.49	0.78
73	8008	28.85	15.55	9.13	4.8	3.18	1.85	1.25
98.4	10789	38.5	20.9	13.22	7.36	4.68	2.79	1.88
				6.03				
54	5927	41.45	14.4	9.09	5.86	4.05	2.48	0.98
76	8342	39.25	18.77	12.2	7.91	5.51	3.46	1.92
104.3	11440	87.99	28.54	19.21	12.79	8.77	5.35	2.87

C3								
psi	***lbf***	***Df1***	***Df2***	***Df3***	***Df4***	***Df5***	***Df6***	***Df7***
				3.01				
56.5	6197	46.18	17	9.29	5.59	4.21	2.63	1.33
80.7	8850	36.73	18.46	11.02	6.61	4.96	3.18	1.45
111	12171	48.5	29.48	16.88	10.23	7.4	4.6	2.2
				3.02				
54.9	6022	63.66	14.44	8.46	5.23	3.62	2.2	0.98
76.5	8390	37.51	15.35	9.76	6.18	4.52	2.87	1.45
104.6	11472	46.65	21.41	14.44	9.4	6.85	4.21	2.2
				3.03				
58.5	6419	16.69	9.4	6.77	4.68	3.46	2.2	1.1
83.4	9152	21.25	10.47	7.48	5.86	4.6	2.99	1.41
117.2	12855	31.14	16.88	12.59	8.89	6.53	4.13	2.04

FLORIDA TECH FWD DATA (February 2000)

A1								
psi	***lbf***	***Df1***	***Df2***	***Df3***	***Df4***	***Df5***	***Df6***	***Df7***
				7.01				
62.8	6896	9.52	5.47	3.77	2.87	2.36	1.69	1.02
81.1	8898	11.81	7.12	5.03	3.93	3.3	2.08	1.37
103.6	11361	16.14	9.88	7.12	5.59	4.6	3.07	1.96
				7.02				
58.9	6467	12.44	5.51	3.54	2.91	2.24	1.57	0.94
76	8432	14.6	6.96	4.64	3.77	2.95	2.16	1.33
96.9	10630	19.6	9.8	6.65	5.19	4.17	3.07	1.77
				7.03				
56.8	6228	11.92	5.23	3.58	2.83	2.48	2	1.41
73.3	8040	14.09	6.73	4.68	3.74	3.26	2.59	1.81
94.3	10344	19.44	9.6	6.81	5.35	4.68	3.7	2.51

A2								
psi	***lbf***	***Df1***	***Df2***	***Df3***	***Df4***	***Df5***	***Df6***	***Df7***
				4.01				
62.7	6880	9.13	5.51	4.01	3.03	2.28	1.45	0.74
85.5	9375	11.69	7.2	5.23	4.01	3.14	2	1.22
111.8	12267	16.81	10.27	7.63	5.82	4.56	2.99	1.69
				4.02				
64.9	7118	12.4	5.9	4.37	3.03	2.44	1.61	1.14
84.4	9263	15.27	7.59	4.99	4.37	3.22	2.04	1.06
106.2	11647	20.55	10.39	7.4	5.7	4.52	3.03	1.77
				4.03				
64.7	7102	12.28	6.29	4.56	3.46	2.67	1.73	0.98
84.3	9248	15.11	7.99	5.86	4.4	3.42	2.2	1.25
106.9	11726	21.22	11.41	8.42	6.29	4.92	3.26	1.81

A3								
psi	***lbf***	***Df1***	***Df2***	***Df3***	***Df4***	***Df5***	***Df6***	***Df7***
				1.01				
64.6	7087	14.6	7.16	5.19	3.7	2.79	1.77	0.98
86.8	9518	21.1	9.52	7	5.19	3.85	2.4	1.37
110.5	12124	29.17	13.93	10.31	7.91	5.7	3.38	1.96
				1.02				
65.7	7214	13.42	7.08	5.31	3.85	2.83	1.81	1.06
85.7	9406	17.24	8.81	6.57	4.84	3.62	2.24	1.29
110	12060	23.93	12.79	9.56	7.28	5.27	3.18	1.81
				1.03				
63	6912	18.93	8.89	6.57	4.4	3.18	2.08	1.02
84.6	9279	19.48	10.82	7.99	5.51	3.97	2.55	1.25
107.9	11838	27.16	15.43	11.1	8.07	5.94	3.5	1.85

FLORIDA TECH FWD DATA (February 2000)

B1								
psi	***lbf***	***Df1***	***Df2***	***Df3***	***Df4***	***Df5***	***Df6***	***Df7***
				8.01				
59.2	6499	12.2	5.15	3.7	2.95	2.51	1.73	1.18
76.9	8437	14.33	6.53	4.84	3.85	3.3	2.36	1.57
99.2	10884	19.44	9.29	6.96	5.62	4.72	3.42	2.28
				8.02				
57.3	6292	10.39	5.62	3.81	2.91	2.48	1.88	1.25
73.4	8056	12.75	7.08	4.92	3.77	3.22	2.44	1.61
94.7	10392	17.83	9.99	7.04	5.47	4.64	3.5	2.28
				8.03				
57.1	6260	10.9	5.47	4.01	3.18	2.67	1.77	1.25
74.4	8167	13.38	6.69	5.15	4.09	3.42	2.51	1.69
97.1	10646	19.05	9.99	7.51	6.02	4.99	3.7	2.44

B2								
psi	***lbf***	***Df1***	***Df2***	***Df3***	***Df4***	***Df5***	***Df6***	***Df7***
				5.01				
66.5	7293	10.78	6.45	4.17	3.11	2.48	1.73	0.98
87.8	9629	13.74	8.46	5.55	4.21	3.38	2.16	1.29
112.3	12314	19.56	11.81	7.87	5.78	4.56	3.26	1.73
				5.02				
59.2	6499	52.83	8.46	4.48	3.03	2.36	1.49	0.98
79.8	8755	27.48	10.15	5.47	3.62	2.91	2.04	1.18
103.1	11313	34.33	13.7	7.87	5.27	4.17	3.03	1.77
				5.03				
62.3	6832	9.88	5.94	4.13	3.34	2.51	1.57	0.98
81.3	8914	12.63	7.75	5.31	4.44	3.42	2.08	1.33
104	11409	17.59	10.74	7.51	6.06	4.72	2.95	1.77

B3								
psi	***lbf***	***Df1***	***Df2***	***Df3***	***Df4***	***Df5***	***Df6***	***Df7***
				2.01				
64.2	7039	11.1	6.02	4.09	3.07	2.36	1.73	0.86
84.7	9295	15.07	8.22	5.74	4.33	3.46	2.32	1.29
108.8	11933	22	12	8.54	6.41	5.07	3.42	1.85
				2.02				
65.2	7150	30.94	8.89	6.29	4.56	3.34	2.12	1.1
90.7	9947	20.66	11.06	7.99	5.9	4.4	2.79	1.37
119.4	13093	29.96	16.14	11.81	8.74	6.49	4.13	2.08
				2.03				
59.8	6562	13.74	9.09	6.65	4.92	3.62	2.16	1.14
80.5	8834	17.16	11.37	8.38	6.29	4.68	2.71	1.45
106.2	11647	24.68	16.06	11.88	8.89	6.57	3.93	1.92

FLORIDA TECH FWD DATA (February 2000)

C1								
psi	***lbf***	***Df1***	***Df2***	***Df3***	***Df4***	***Df5***	***Df6***	***Df7***
				9.01				
53.9	5911	45.27	14.56	7.91	4.84	3.58	2.36	1.45
74.3	8151	45.19	18.74	11.18	6.65	4.72	3.11	1.88
99.4	10900	61.81	28.5	16.61	10.27	7.04	4.48	2.79
				9.02				
58.6	6435	16.14	7.51	4.76	3.66	2.91	2.04	1.22
82	8993	21.1	11.1	7.08	5.27	4.21	3.03	1.81
110	12060	35.03	17.12	11.14	8.26	6.49	4.44	2.71
				9.03				
55.5	6085	27.87	8.07	4.72	3.3	2.63	1.96	1.33
75.2	8247	31.1	11.45	6.88	4.52	3.58	2.55	1.73
100.4	11011	44.48	17.95	10.94	7	5.35	3.77	2.48

C2								
psi	***lbf***	***Df1***	***Df2***	***Df3***	***Df4***	***Df5***	***Df6***	***Df7***
				6.01				
58.5	6419	23.42	7.71	5.03	3.54	2.71	1.81	0.86
81.7	8962	25.66	10.23	6.73	4.72	3.58	2.36	1.29
109.1	11965	34.96	15.59	10.03	6.92	5.11	3.34	1.85
				6.02				
56.9	6244	31.73	8.22	5.27	3.46	2.55	1.77	1.06
77.5	8501	26.85	10.59	6.88	4.56	3.26	2.28	1.33
101.7	11154	32.48	15.51	10.35	6.88	4.8	3.3	2
				6.03				
57.3	6292	23.77	7.16	4.68	3.46	2.91	2.16	1.25
77.3	8485	26.81	10.47	6.92	4.88	3.97	2.87	1.73
102.4	11234	39.4	16.49	10.94	7.63	6.02	4.33	2.51

C3								
psi	***lbf***	***Df1***	***Df2***	***Df3***	***Df4***	***Df5***	***Df6***	***Df7***
				3.01				
55.6	6101	24.99	10.11	7.2	5.66	3.5	2	0.66
83.3	9136	30.19	14.6	9.96	6.88	5.19	3.26	1.61
115	12616	42.55	22.12	14.92	10.15	7.59	4.68	2.24
				3.02				
55.5	6085	18.18	10.78	7.24	4.99	3.85	2.4	1.22
81.8	8977	24.96	13.81	9.4	6.49	5.03	3.34	1.65
112.4	12330	36.49	20.43	13.7	9.44	7.28	4.64	2.36
				3.03				
56.2	6165	26.37	11.33	8.42	5.82	3.93	2.24	1.14
80.4	8819	26.73	14.01	10.23	7.08	4.68	2.63	1.49
110	12060	34.05	20.35	14.68	10.07	6.57	3.7	1.96

FLORIDA TECH FWD DATA (April 2000)

A1								
psi	***lbf***	***Df1***	***Df2***	***Df3***	***Df4***	***Df5***	***Df6***	***Df7***
7.01								
62.1	6816	9.01	4.84	3.07	2.2	1.81	1.29	0.82
83.9	9200	12.16	6.49	4.21	3.11	2.48	1.81	1.18
107.8	11822	17.4	9.33	6.14	4.56	3.62	2.59	1.69
7.02								
59.4	6514	11.06	5.78	3.18	2.08	1.81	1.61	1.06
85.5	9375	15.19	7.36	4.68	3.18	2.36	1.73	1.22
114.7	12585	24.68	11.14	6.88	4.76	3.77	2.71	1.73
7.03								
54	5927	11.45	4.68	3.34	2.55	2.08	1.61	1.22
71.8	7881	13.81	5.9	4.64	3.7	2.51	2	1.53
93.1	10217	19.33	8.85	6.61	5.19	3.85	3.07	2.24

A2								
psi	***lbf***	***Df1***	***Df2***	***Df3***	***Df4***	***Df5***	***Df6***	***Df7***
4.01								
67.5	7404	12.16	5.7	3.77	2.67	2	1.29	0.82
84.7	9295	14.13	6.77	4.48	3.3	2.55	1.77	1.1
103.9	11393	18.7	8.93	6.02	4.4	3.42	2.32	1.45
4.02								
63.7	6991	11.73	6.57	4.29	2.87	2.12	1.49	0.82
82.4	9041	15.11	7.83	5.59	3.5	2.75	1.69	1.25
101.1	11091	19.68	10.31	7.36	4.68	3.5	2.2	1.57
4.03								
64.7	7102	11.06	5.66	3.81	2.75	2.12	1.33	0.78
82	8993	13.7	7.2	4.99	3.66	2.71	1.73	1.06
101	11075	17.95	9.6	6.73	4.96	3.74	2.4	1.41

A3								
psi	***lbf***	***Df1***	***Df2***	***Df3***	***Df4***	***Df5***	***Df6***	***Df7***
1.01								
58.5	7277	15.27	6.06	4.99	3.42	2.55	1.57	0.94
86.2	9248	18.22	8.93	6.14	4.21	3.18	2	1.14
112.3	11854	24.76	11.81	8.77	5.94	4.48	2.91	1.61
1.02								
61.3	6721	13.14	7.67	5.11	3.58	2.63	1.69	1.1
83.7	9184	16.37	9.8	6.53	4.48	3.18	1.96	1.06
107.2	11758	22.91	12.95	8.46	5.98	4.29	2.67	1.57
1.03								
64.6	7087	17	8.14	5.51	3.81	2.79	1.81	1.06
87.6	9613	23.58	10.11	6.77	4.68	3.34	2.16	1.25
110.2	12092	29.88	12.59	8.38	6.02	4.48	2.79	1.57

FLORIDA TECH FWD DATA (April 2000)

B1								
psi	***lbf***	***Df1***	***Df2***	***Df3***	***Df4***	***Df5***	***Df6***	***Df7***
				8.01				
53.9	5911	11.1	4.92	3.3	2.51	2.04	1.49	1.06
72.7	7976	13.97	6.57	4.44	3.42	2.91	2.12	1.45
95.2	10439	19.29	9.48	6.49	4.99	4.21	3.14	2.16
				8.02				
54	5927	11.73	5.03	3.07	2.36	2	1.29	1.25
75.3	8262	15.03	6.61	4.4	3.34	2.71	2	1.41
97.6	10709	21.06	9.64	6.49	4.92	4.05	2.99	2.08
				8.03				
54.6	5990	11.69	4.29	3.74	2.4	1.61	1.18	0.86
74	8119	15.03	6.25	4.21	3.3	2.75	2.08	1.49
96.5	10582	21.14	8.85	6.92	4.92	3.74	2.87	1.96

B2								
psi	***lbf***	***Df1***	***Df2***	***Df3***	***Df4***	***Df5***	***Df6***	***Df7***
				5.01				
68.6	7531	12.63	6.37	3.89	2.67	2.04	1.45	0.82
86.3	9470	15.19	7.67	4.88	3.46	2.71	1.96	1.22
104.4	11456	19.48	10.07	6.49	4.72	3.7	2.63	1.61
				5.02				
69.8	7659	11.49	6.22	4.29	3.07	2.4	1.49	0.94
89.4	9804	14.29	7.63	5.39	3.77	2.87	1.81	1.06
110.8	12155	19.64	10.07	7.08	5.15	3.81	2.28	1.37
				5.03				
62.1	6816	13.22	5.55	3.7	2.63	2.36	1.33	0.55
81.5	8946	15.86	6.65	4.96	3.5	2.59	1.81	1.29
103.4	11345	21.22	9.17	6.81	4.84	3.22	2.4	1.69

B3								
psi	***lbf***	***Df1***	***Df2***	***Df3***	***Df4***	***Df5***	***Df6***	***Df7***
				2.01				
62.8	6896	12.2	7.24	4.72	3.34	2.67	1.73	1.06
88.2	9677	15.62	9.01	6.18	4.33	3.11	2.04	1.06
116.2	12743	22.55	12.83	9.05	6.25	4.37	2.99	1.57
				2.02				
58.6	6435	12.55	8.3	5.47	3.74	2.71	1.77	0.98
82.7	9073	17.32	10.31	6.92	4.64	3.5	2.2	1.25
108.8	11933	22.2	13.46	9.01	6.18	4.6	2.91	1.57
				2.03				
60.4	66.26	14.52	8.22	5.78	4.25	3.03	1.96	1.06
79.2	8691	17.28	9.72	6.81	4.92	3.62	2.24	1.18
101.7	11154	24.48	12.83	8.97	6.61	4.84	3.03	1.57

FLORIDA TECH FWD DATA (April 2000)

C1								
psi	***lbf***	***Df1***	***Df2***	***Df3***	***Df4***	***Df5***	***Df6***	***Df7***
				9.01				
53.3	5847	18.11	5.94	3.58	2.71	2.12	1.49	0.98
75.7	8310	22.24	8.93	5.43	4.13	3.18	2.28	1.45
102.1	11202	33.38	14.44	8.74	6.53	4.96	3.5	2.16
				9.02				
55.3	6070	17.16	3.22	2.28	1.88	1.65	1.33	0.94
79.5	8723	12.75	4.88	3.42	2.83	2.51	2	1.41
108.8	11933	17.36	7.67	5.39	4.44	3.85	3.03	2.08
				9.03				
53.4	5863	7.12	2.28	1.85	1.57	1.49	1.25	0.86
77.5	8501	11.14	3.58	2.91	2.48	2.24	1.85	1.33
106.6	11695	23.3	5.78	4.56	3.81	3.38	2.71	1.96

C2								
psi	***lbf***	***Df1***	***Df2***	***Df3***	***Df4***	***Df5***	***Df6***	***Df7***
				6.01				
66.3	7277	7.36	3.42	2.51	2.12	1.81	1.33	0.82
89.8	9851	8.97	4.37	3.3	2.75	2.44	1.81	1.14
113.6	12457	12.51	6.29	4.72	3.89	3.38	2.55	1.61
				6.02				
65.6	7198	11.45	2.67	2.2	1.88	1.65	1.22	0.78
88.6	9724	8.93	3.85	3.14	2.67	2.36	1.81	1.25
113	12394	11.65	5.59	4.37	3.66	3.14	2.44	1.65
				6.03				
62.8	6896	7.87	3.38	2.91	2.48	2.12	1.61	1.1
84.7	9295	9.13	4.84	4.13	3.54	3.03	2.32	1.53
109.4	11997	12.48	7.04	5.86	4.96	4.21	3.18	2

C3								
psi	***lbf***	***Df1***	***Df2***	***Df3***	***Df4***	***Df5***	***Df6***	***Df7***
				3.01				
59.7	6546	10.27	6.37	4.84	3.97	3.66	2	1.61
86.3	9470	14.4	8.58	6.41	5.27	4.29	2.79	1.61
119.9	13157	21.49	13.22	9.99	8.14	6.45	4.25	2.28
				3.02				
58.5	6419	5.19	4.44	3.93	3.42	2.67	1.88	1.06
74.2	8135	6.85	5.78	4.99	4.33	3.38	2.32	1.33
91.1	9994	10.27	8.14	6.88	5.86	4.6	3.26	1.88
				3.03				
51.3	5625	15.98	8.11	6.06	4.13	2.95	1.81	0.94
76	8342	22.16	10.98	8.22	5.51	3.89	2.32	1.22
104	11409	32.48	16.29	12.83	7.08	5.03	3.03	1.61

FLORIDA TECH FWD DATA (June 2000)

A1								
psi	***lbf***	***Df1***	***Df2***	***Df3***	***Df4***	***Df5***	***Df6***	***Df7***
				7.01				
61	6689	11.81	4.68	3.22	2.44	2.04	1.49	1.02
85	9327	18.3	7.2	4.99	3.77	3.14	2.32	1.53
105.9	11615	24.33	9.56	6.61	5.03	4.17	3.03	2
				7.02				
58.8	6451	12.83	5.31	3.62	2.63	2.16	1.57	1.06
82.3	9025	19.84	8.11	5.59	4.09	3.34	2.44	1.57
104.2	11425	26.33	10.74	7.44	5.43	4.4	3.18	2.04
				7.03				
59.4	6514	12.59	4.88	3.5	2.75	2.36	1.85	1.33
81.5	8945	19.21	7.4	5.35	4.13	3.54	2.79	1.96
106.8	11711	25.55	9.8	7.12	5.55	4.64	3.62	2.59

A2								
psi	***lbf***	***Df1***	***Df2***	***Df3***	***Df4***	***Df5***	***Df6***	***Df7***
				4.01				
61.4	6737	12.2	4.88	3.42	2.48	2	1.33	0.78
84.4	9263	18.54	7.4	5.23	3.85	2.99	2.04	1.25
106.2	11647	23.93	9.6	6.81	4.99	3.89	2.63	1.57
				4.02				
58.1	6371	13.93	6.1	3.93	2.79	2.16	1.53	0.98
80.5	8834	21.41	9.44	6.06	4.21	3.3	2.36	1.41
106.5	11679	28.38	12.59	8.07	5.47	4.13	3.07	1.85
				4.03				
61.1	6705	12.91	5.39	3.74	2.67	2.08	1.41	0.86
87.6	9613	20.35	8.22	5.74	4.21	3.26	2.2	1.33
105.7	11599	26.88	10.98	7.67	5.59	4.37	2.95	1.81

A3								
psi	***lbf***	***Df1***	***Df2***	***Df3***	***Df4***	***Df5***	***Df6***	***Df7***
				1.01				
	6419	13.03						
	9454	19.72						
	12314	25.55						
				1.02				
60.1	6594	14.52	6.92	5.07	3.58	2.63	1.61	0.86
80.8	8866	22.95	10.35	7.59	5.35	3.93	2.4	1.33
106.8	11711	30.23	13.5	9.99	7.12	5.19	3.18	1.77
				1.03				
61.7	6769	12.44	6.06	4.33	3.14	2.36	1.49	0.86
85.6	9391	20.11	9.17	6.57	4.8	3.62	2.28	1.33
105.5	11568	26.49	12.04	8.58	6.29	4.8	3.11	1.77

FLORIDA TECH FWD DATA (June 2000)

B1								
psi	***lbf***	***Df1***	***Df2***	***Df3***	***Df4***	***Df5***	***Df6***	***Df7***
				8.01				
58.4	6403	12.55	5.23	3.74	2.87	2.36	1.81	1.29
81.4	8930	19.37	7.95	5.74	4.44	3.58	2.71	1.88
106.6	11695	25.86	10.66	7.67	5.86	4.8	3.62	2.51
				8.02				
60.1	6594	15.07	5.62	3.77	2.79	2.4	1.73	1.18
83.3	9136	23.58	8.74	5.82	4.37	3.66	2.63	1.77
105	11520	34.88	11.73	7.87	5.78	4.84	3.5	2.32
				8.03				
59.1	6483	13.66	5.15	3.62	2.83	2.36	1.85	1.29
81.8	8977	21.37	7.91	5.55	4.33	3.62	2.83	1.96
105.3	11552	28.46	10.47	7.44	5.7	4.84	3.7	2.59

B2								
psi	***lbf***	***Df1***	***Df2***	***Df3***	***Df4***	***Df5***	***Df6***	***Df7***
				5.01				
60.8	6673	11.53	5.07	3.5	2.51	2	1.41	0.86
82.3	9025	18.07	7.75	5.39	3.89	3.11	2.2	1.41
106.8	11711	24.01	10.15	7.04	5.07	4.05	2.91	1.81
				5.02				
56.8	6228	15.39	6.81	4.37	2.83	2.08	1.37	0.78
81.3	8914	24.29	10.55	6.81	4.4	3.14	2.12	1.25
106.6	11695	31.25	13.58	8.77	5.62	4.01	2.83	1.65
				5.03				
57.8	6340	13.26	4.64	3.34	2.51	2	1.41	0.94
81.4	8930	21.25	7.28	5.15	3.85	3.03	2.16	1.37
106.6	11695	27.83	9.76	6.88	5.07	4.01	2.83	1.81

B3								
psi	***lbf***	***Df1***	***Df2***	***Df3***	***Df4***	***Df5***	***Df6***	***Df7***
				2.01				
	6213	11.02						
	9168	17.16						
	11901	22.99						
				2.02				
	6213	14.13						
	8882	22						
	11726	29.25						
				2.03				
55.7	6117	16.1	7.24	5.47	3.81	2.51	1.81	0.98
82	8993	25.31	10.9	7.99	5.62	3.7	2.59	1.37
107.5	11790	32.87	14.33	10.27	7.28	4.99	3.38	1.85

FLORIDA TECH FWD DATA (June 2000)

C1								
psi	***lbf***	***Df1***	***Df2***	***Df3***	***Df4***	***Df5***	***Df6***	***Df7***
				9.01				
62	6800	6.14	2.67	2.2	1.96	1.73	1.45	1.1
88.4	9693	11.02	4.48	3.54	3.11	2.75	2.28	1.65
110.7	12140	15.55	6.18	4.84	4.25	3.74	3.07	2.16
				9.02				
66	7245	4.96	2.28	2.16	1.96	1.53	1.41	1.25
94.2	10328	10.15	3.89	3.42	3.14	2.48	2.2	1.88
117.8	12918	15.03	5.43	4.6	4.13	3.54	3.03	2.32
				9.03				
59.4	6514	4.33	1.88	1.73	1.57	1.49	1.29	1.02
83.9	9200	6.45	3.03	2.71	2.51	2.32	2	1.53
109.4	11997	8.46	4.21	3.74	3.42	3.14	2.67	2.04

C2								
psi	***lbf***	***Df1***	***Df2***	***Df3***	***Df4***	***Df5***	***Df6***	***Df7***
				6.01				
68.4	7500	3.11	1.88	1.85	1.57	1.45	1.14	0.94
100.1	10980	5.23	3.03	2.71	2.48	2.24	1.85	1.33
126.6	13888	7.87	4.13	3.7	3.34	2.99	2.44	1.69
				6.02				
62.3	6832	3.22	1.88	1.73	1.61	1.49	1.22	0.86
94.4	10360	6.22	3.11	2.75	2.51	2.36	1.88	1.41
119.2	13077	8.74	4.09	3.89	3.54	3.14	2.51	1.88
				6.03				
61.7	6769	3.03	2.24	2.08	1.92	1.77	1.45	1.1
88.6	9724	5.19	3.58	3.3	3.03	2.71	2.24	1.61
111.7	12251	7.95	4.84	4.72	4.09	3.66	2.79	2.24

C3								
psi	***lbf***	***Df1***	***Df2***	***Df3***	***Df4***	***Df5***	***Df6***	***Df7***
				3.01				
	6848	5.19						
	9756	8.58						
	12124	11.77						
				3.02				
	7214	4.96						
	10280	8.3						
	12902	11.57						
				3.03				
68.1	7468	9.72	5.86	4.68	3.7	2.95	1.88	1.02
95.9	10519	16.37	8.89	7.04	5.51	4.21	2.79	1.41
119.4	13093	20.47	11.29	9.13	7.24	5.51	3.7	1.88

FLORIDA TECH FWD DATA (August 2000)

A1								
psi	***lbf***	***Df1***	***Df2***	***Df3***	***Df4***	***Df5***	***Df6***	***Df7***
7.01								
63.6	6975	11.73	5.03	3.58	2.67	2.2	1.61	1.06
82.7	9073	16.29	7.08	5.03	3.77	3.11	2.28	1.45
96.8	10614	20.11	8.81	6.25	4.68	3.81	2.83	1.85
7.02								
59.8	6562	11.45	6.45	4.21	2.83	2.24	1.61	1.33
82.7	9073	17.04	9.13	5.94	4.05	3.22	2.32	1.73
99.1	10868	22.12	11.25	7.4	5.03	4.01	2.99	1.96
7.03								
62.6	6864	12.44	5.35	3.7	2.87	2.44	1.92	1.33
80.4	8819	16.96	7.44	5.19	3.97	3.38	2.63	1.85
96	10535	20.55	9.4	6.53	4.96	4.17	3.26	2.28

A2								
psi	***lbf***	***Df1***	***Df2***	***Df3***	***Df4***	***Df5***	***Df6***	***Df7***
4.01								
62	6800	10.27	5.43	3.66	2.63	2.04	1.37	0.82
82.1	9009	15.15	7.59	5.07	3.7	2.83	1.92	1.18
96.8	10614	19.72	9.09	6.29	4.6	3.54	2.4	1.49
4.02								
60.1	6594	14.21	6.73	4.48	2.95	2.2	1.49	0.94
77.8	8533	19.88	9.4	6.29	4.13	3.03	2.04	1.29
94.2	10328	24.25	11.57	7.75	5.07	3.74	2.55	1.61
4.03								
61.4	6737	12.75	5.82	4.05	2.87	2.24	1.49	0.86
82.8	9089	17.83	8.26	5.82	4.13	3.22	2.16	1.29
99.2	10884	22.55	10.31	7.32	5.23	4.01	2.67	1.57

A3								
psi	***lbf***	***Df1***	***Df2***	***Df3***	***Df4***	***Df5***	***Df6***	***Df7***
1.01								
64	7023	15.11	7.4	5.03	3.38	2.48	1.49	0.82
84.7	9295	21.06	9.6	6.57	4.52	3.38	2.04	1.14
111.8	12267	27.95	12.99	8.81	6.06	4.48	2.83	1.61
1.02								
61.5	6753	14.17	7.83	5.55	3.81	2.67	1.61	1.14
80.7	8850	19.56	10.55	7.28	4.96	3.5	2.12	1.33
94	10312	22.79	13.07	8.97	6.25	4.4	2.71	1.49
1.03								
60.8	6673	14.09	6.45	4.52	3.42	2.48	1.53	0.94
78.8	8644	20.27	8.97	6.25	4.72	3.46	2.24	1.22
93.6	10265	24.92	11.06	7.75	5.78	4.21	2.71	1.53

FLORIDA TECH FWD DATA (August 2000)

B1								
psi	***lbf***	***Df1***	***Df2***	***Df3***	***Df4***	***Df5***	***Df6***	***Df7***
				8.01				
61.7	6769	14.56	5.82	4.01	3.07	2.55	1.88	1.33
80	8771	20.19	8.18	5.66	4.33	3.54	2.59	1.81
94.9	10408	24.76	10.11	7.08	5.43	4.44	3.3	2.24
				8.02				
64.2	7039	14.37	6.49	4.33	3.07	2.44	1.77	1.14
85.6	9391	20.39	9.17	6.1	4.29	3.42	2.48	1.65
101.8	11170	24.92	11.41	7.63	5.31	4.21	3.11	2.04
				8.03				
63.6	6975	12.36	5.55	3.85	2.87	2.4	1.88	1.33
81.7	8962	16.96	7.75	5.43	4.01	3.338	2.59	1.85
95.9	10519	20.66	9.68	6.77	5.07	4.21	3.26	2.28

B2								
psi	***lbf***	***Df1***	***Df2***	***Df3***	***Df4***	***Df5***	***Df6***	***Df7***
				5.01				
60.7	6657	10.35	5.43	3.89	2.83	2.24	1.61	0.98
79.2	8691	14.6	7.51	5.35	3.85	3.03	2.12	1.25
95.7	10503	18.11	9.33	6.57	4.76	3.77	2.63	1.57
				5.02				
63.1	6928	14.01	7.51	4.88	3.22	2.32	1.45	0.86
82.3	9025	20.9	10.47	6.73	4.44	3.22	2.04	1.22
96.8	10614	25.66	13.03	8.3	5.51	3.97	2.59	1.53
				5.03				
62.1	6816	12.04	5.35	3.74	2.67	2.08	1.45	0.86
82.8	9089	16.73	7.59	5.35	3.81	2.95	2.08	1.25
97.9	10741	20.7	9.44	6.61	4.76	3.66	2.55	1.57

B3								
psi	***lbf***	***Df1***	***Df2***	***Df3***	***Df4***	***Df5***	***Df6***	***Df7***
				2.01				
67.1	7357	12.2	6.49	4.72	3.46	2.48	1.61	1.02
84.9	9311	16.85	8.58	6.29	4.64	3.34	2.08	1.33
108.4	11885	22.59	11.49	8.38	6.14	4.48	2.87	1.73
				2.02				
59.8	6562	13.14	7.55	5.35	3.77	2.79	1.81	0.98
74.3	8151	17.95	9.6	6.85	4.8	3.58	2.24	1.22
92.3	10122	23.26	12.36	8.77	6.14	4.6	2.95	1.53
				2.03				
64.4	7071	16.33	8.77	5.94	4.09	2.91	1.81	1.02
87.5	9597	22.08	11.65	7.91	5.47	3.93	2.4	1.33
103.6	11361	26.65	14.21	9.56	6.61	4.8	2.95	1.65

FLORIDA TECH FWD DATA (August 2000)

C1								
psi	***lbf***	***Df1***	***Df2***	***Df3***	***Df4***	***Df5***	***Df6***	***Df7***
				9.01				
62.7	6880	12.36	3.97	3.26	2.67	2.36	1.81	1.25
84.9	9311	16.77	6.06	4.72	3.89	3.34	2.51	1.69
102.4	11234	20.35	8.18	6.18	5.07	4.21	3.18	2.12
				9.02				
68.6	7531	6.02	2.79	2.4	2	1.81	1.53	1.18
91.8	10074	9.09	4.17	3.5	2.91	2.63	2.24	1.61
110.1	12076	11.77	5.43	4.48	3.74	3.34	2.79	2
				9.03				
64.9	7118	5.78	2.36	2.12	1.96	1.69	1.37	1.18
87.6	9613	8.26	3.5	3.07	2.67	2.44	2	1.61
106.5	11679	10.23	4.56	3.93	3.42	3.14	2.55	1.96

C2								
psi	***lbf***	***Df1***	***Df2***	***Df3***	***Df4***	***Df5***	***Df6***	***Df7***
				6.01				
65.3	7166	5.23	3.03	2.63	2.32	2	1.53	1.02
88.8	9740	9.92	4.37	3.77	3.26	2.79	2.12	1.37
107.8	11822	12.24	5.82	4.84	4.13	3.5	2.63	1.73
				6.02				
68.5	7516	4.44	2.48	2.24	2	1.77	1.41	1.02
95.2	10439	7.16	3.89	3.3	2.95	2.59	2.04	1.41
113.1	12410	9.96	5.27	4.29	3.77	3.34	2.59	1.77
				6.03				
61.4	6737	8.81	3.22	2.83	2.48	2.2	1.73	1.18
81.8	8977	10.59	4.76	4.17	3.62	3.18	2.44	1.61
97.9	10741	12.48	6.18	5.35	4.6	4.01	3.07	2.04

C3								
psi	***lbf***	***Df1***	***Df2***	***Df3***	***Df4***	***Df5***	***Df6***	***Df7***
				3.01				
68.8	7547	11.85	6.53	5.39	4.21	3.26	2.51	1.57
91	9979	15.94	9.17	7.28	5.78	4.44	3.34	2
113.3	12489	20.43	13.22	9.88	7.71	5.98	4.4	2.55
				3.02				
74.2	8135	9.05	5.39	4.56	3.81	3.3	2.28	1.29
90.8	9963	11.49	6.88	5.86	4.84	4.09	2.83	1.57
108.1	11856	14.72	8.89	7.63	6.22	5.27	3.58	2
				3.03				
61.5	6753	10.03	6.49	5.19	4.01	2.95	1.96	1.1
87.2	9565	14.68	9.09	7.16	5.51	4.01	2.55	1.41
108.8	11933	18.38	11.25	9.01	6.88	4.92	3.14	1.81

FLORIDA TECH FWD DATA (October 2000)

A1								
psi	***lbf***	***Df1***	***Df2***	***Df3***	***Df4***	***Df5***	***Df6***	***Df7***
7.01								
62.6	6853	8.46	6.17	4.23	3.08	2.45	1.79	1.15
88.2	9666	12.12	8.69	6.09	4.35	3.5	2.59	1.6
115.1	12606	16.43	11.68	8.18	5.85	4.7	3.44	2.19
7.02								
68.3	7484	7.98	4.97	3.66	2.8	2.33	1.5	1.21
96.2	10540	11.99	7.54	5.6	4.22	3.46	2.59	1.64
123	13475	16.24	10.1	7.56	5.65	4.6	3.57	2.11
7.03								
63.3	6936	8.4	5.46	4.04	3.03	2.54	2.02	1.29
88.4	9690	11.85	7.76	5.73	4.28	3.58	2.81	1.84
115.6	12665	15.87	10.47	7.74	5.73	4.79	3.76	2.41

A2								
psi	***lbf***	***Df1***	***Df2***	***Df3***	***Df4***	***Df5***	***Df6***	***Df7***
4.01								
70.8	7754	9.31	6.04	4.07	2.9	2.31	1.63	1
94.3	10333	12.66	8.28	5.66	4.01	3.22	2.31	1.41
118	12927	16.64	10.85	7.44	5.38	4.31	3.06	1.88
4.02								
62.2	6817	10.74	6.64	4.76	3.34	2.63	1.84	1.06
87.4	9574	15.98	9.44	6.76	4.71	3.71	2.61	1.51
113.7	12455	21.09	12.65	9.05	6.27	4.93	3.48	2.02
4.03								
65.6	7182	9.43	6.07	4.44	3.24	2.56	1.8	0.99
93.2	10206	13.47	8.8	6.43	4.66	3.67	2.59	1.52
119.5	13090	17.96	11.86	8.66	6.3	4.94	3.48	2.04

A3								
psi	***lbf***	***Df1***	***Df2***	***Df3***	***Df4***	***Df5***	***Df6***	***Df7***
1.01								
62.2	6814	10.82	7.13	5.1	3.75	2.85	1.81	1.06
87.6	9598	15.08	9.86	7.13	5.19	3.97	2.58	1.47
115.2	12617	20.3	13.17	9.53	6.92	5.3	3.45	1.96
1.02								
61.6	6750	12.31	7.87	5.94	4.26	3.22	1.95	0.99
85.9	9407	17.21	11.24	8.44	6.02	4.5	2.81	1.47
113.8	12463	23.31	15.26	11.43	8.14	6.06	3.82	1.98
1.03								
64.1	7020	12.2	7.52	5.48	3.93	3.06	1.94	1.01
87.2	9555	17.06	10.62	7.73	5.56	4.33	2.77	1.52
112.1	12283	22.91	14.22	10.31	7.42	5.79	3.74	2.01

FLORIDA TECH FWD DATA (October 2000)

B1								
psi	***lbf***	***Df1***	***Df2***	***Df3***	***Df4***	***Df5***	***Df6***	***Df7***
				8.01				
62.9	6896	9.23	5.9	4.35	3.15	2.65	1.97	1.31
89	9753	13.19	8.44	6.22	4.52	3.78	2.81	1.85
115.3	12633	17.56	11.32	8.31	6.09	5.02	3.75	2.48
				8.02				
62.7	6873	10.17	6.07	4.39	3.22	2.61	1.98	1.32
88.1	9653	14.44	8.73	6.33	4.62	3.71	2.8	1.84
115.6	12669	19.48	11.92	8.67	6.28	5.01	3.75	2.47
				8.03				
62.8	6877	8.94	5.28	3.94	3.06	2.58	2.02	1.26
88.4	9690	12.75	7.68	5.74	4.39	3.68	2.83	1.79
116.2	12733	17.21	10.54	7.89	6.04	5	3.79	2.43

B2								
psi	***lbf***	***Df1***	***Df2***	***Df3***	***Df4***	***Df5***	***Df6***	***Df7***
				5.01				
64	7016	8.59	5.75	4.43	3.21	2.5	1.75	1.06
87.8	9621	12.33	8.04	6.18	4.48	3.51	2.47	1.52
114.9	12593	16.22	10.72	8.21	5.96	4.65	3.29	1.99
				5.02				
62.3	6825	10.17	6.91	4.72	3.26	2.53	1.8	1
87.6	9602	14.7	9.69	6.6	4.56	3.52	2.48	1.5
114.8	12582	19.83	13	8.88	6.07	4.7	3.36	1.94
				5.03				
63.2	6920	8.78	5.8	4.35	3.11	2.46	1.69	1.03
88.5	9693	12.19	8.19	6.14	4.37	3.48	2.44	1.39
115	12601	16.68	11	8.23	5.89	4.67	3.24	1.94

B3								
psi	***lbf***	***Df1***	***Df2***	***Df3***	***Df4***	***Df5***	***Df6***	***Df7***
				2.01				
65.9	7222	8.36	5.77	4.52	3.25	2.65	1.84	0.93
87.7	9610	11.73	8.06	6.33	4.69	3.76	2.6	1.42
114.5	12542	15.9	10.94	8.61	6.37	5.13	3.54	1.9
				2.02				
65.3	7155	11.66	7.83	5.74	4.04	3.27	2.2	1.08
89	9753	16.96	10.95	8.03	5.72	4.51	2.92	1.61
113.5	12439	22.61	14.52	10.68	7.67	6.04	3.99	2.13
				2.03				
64.5	7071	11.43	7.91	5.94	4.22	3.16	2.04	12.11
91.1	9976	16.19	11.37	8.5	6.07	4.5	2.88	1.65
117.1	12828	21.86	15.5	11.46	8.19	6.02	3.69	2.34

FLORIDA TECH FWD DATA (October 2000)

C1								
psi	***lbf***	***Df1***	***Df2***	***Df3***	***Df4***	***Df5***	***Df6***	***Df7***
				9.01				
62.6	6861	17.48	7.45	5.28	3.99	3.39	2.64	1.46
87.1	9542	25.98	11.09	7.7	5.81	4.9	3.76	2.14
111.1	12172	35.32	15.54	10.6	7.92	6.69	5	2.93
				9.02				
63.9	7000	10.94	5.88	4.4	3.61	3.22	2.53	1.52
89.2	9773	16.66	9	6.59	5.31	4.69	3.63	2.24
113	12383	23.2	12.74	9.14	7.24	6.36	5.02	2.93
				9.03				
63.2	6920	11.03	4.22	3.3	2.76	2.43	2	1.37
88.2	9666	17.26	6.56	4.87	3.97	3.5	2.91	2.03
112.2	12288	23.33	9.35	6.79	5.44	4.74	3.91	2.7

C2								
psi	***lbf***	***Df1***	***Df2***	***Df3***	***Df4***	***Df5***	***Df6***	***Df7***
				6.01				
64.3	7047	9.8	5.55	4.15	3.22	2.73	1.95	1.15
89.3	9780	14.56	8	5.89	4.48	3.81	2.74	1.6
114.1	12498	19.71	10.93	7.89	5.88	5	3.65	2.14
				6.02				
59.5	6523	9.44	5.29	3.95	3.17	2.74	1.91	1.46
88.8	9725	16.7	9.39	6.44	4.85	4.04	2.98	1.84
113.4	12426	23.39	13.2	8.81	6.45	5.28	3.98	2.48
				6.03				
62.9	6888	14.15	5.47	4.3	3.5	3.02	2.36	1.46
86.5	9475	20.22	8.52	6.6	5.28	4.5	3.37	2.12
110.2	12076	27.59	12.59	9.38	7.3	6.25	4.63	2.87

C3								
psi	***lbf***	***Df1***	***Df2***	***Df3***	***Df4***	***Df5***	***Df6***	***Df7***
				3.01				
63.7	6976	14.39	9.08	6.48	4.89	3.88	2.58	1.37
87.2	9558	19.83	12.81	9.1	6.79	5.42	3.65	1.92
112.6	12331	26.63	17.28	12.11	8.98	7.13	4.77	2.53
				3.02				
59.7	6539	14.28	7.93	5.86	4.52	3.61	2.37	1.35
85.9	9415	19.99	11.18	8.38	6.49	5.28	3.46	1.91
114.9	12590	27.17	15.42	11.42	8.8	7.06	4.71	2.55
				3.03				
58.5	6404	19.92	8.7	6.36	4.65	3.52	2.17	1.18
82.9	9078	25.33	12	8.8	6.44	4.8	2.98	1.64
108.9	11926	32.38	15.97	11.74	8.67	6.62	4.02	2.23

Appendix GG
Comparison Graphs

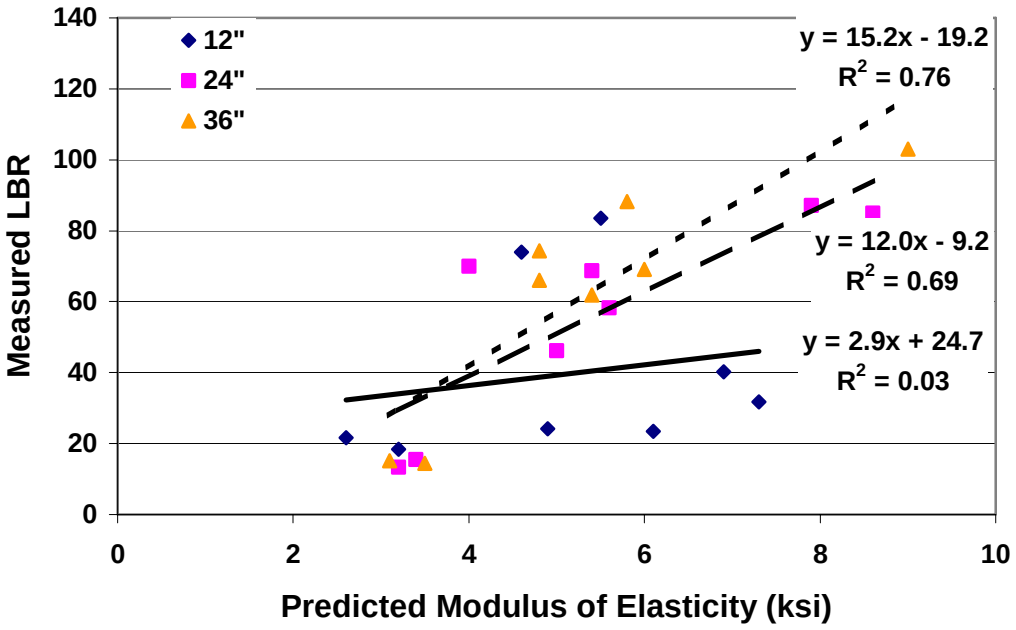

Figure G-1: Predicted Modulus of Elasticity, E_s vs. LBR

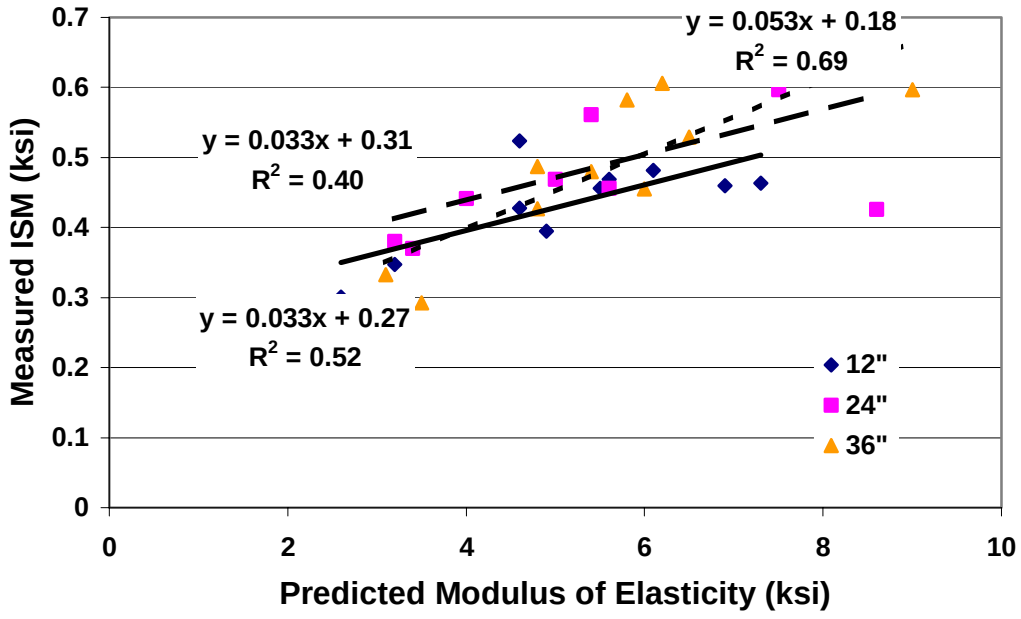

Figure G-1: Predicted Modulus of Elasticity, E_s vs. ISM

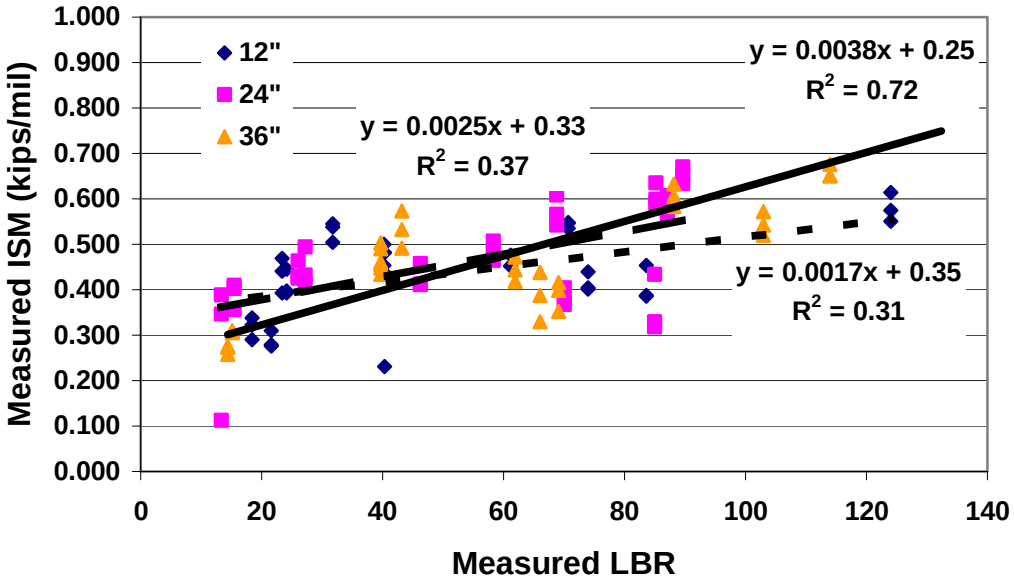

Figure G-1: LBR vs. RAP ISM's of Middle FWD Tests

References

American Road and Transportation Builders Association. *Stabilization and Pavement Recycling.* Washington, DC: Author.

American Society of Testing and Materials. *Annual Book of ASTM Standards.* Philadelphia: 1994.

Asphalt Institute. (1989). *The Asphalt Handbook.* National Stone Association, Washington, D. C.

Barksdale, R.D. *The Aggregate Handbook.* Washington D.C.: National Stone Association, 1991.

Bishop, A.W. and Henkel, D.J. *Soil Properties in the Triaxial Test.* London: Edward Arnold Publishers Ltd., 1964.

Bosso, Massimo. Effects of Waste Glass Content on the Shear and Deformation Characteristics of Conventional Florida Highway Aggregate. M.S. Thesis in Civil Engineering. Florida Institute of Technology, 1995. Melbourne, FL.

Bush, A.J. & Thompson, M.R., (1990). *Predicting Capacities of Low Volume Airfield Pavements,* Third International Conference on Bearing Capacities of Roads and Airfields. 1071-1080.

Ciesielski, S.K. "Using Waste Material in Paving Projects." *Pavement Maintenance.* Vol. 10, no. 7 (1995): 424-429.

Coduto, D.P. (2001). Foundation Design, 2nd ed. Prentice-Hall, Inc, Upper SaddleRiver, New Jersey.

Collins, R.J. and Ciesielski, S.K. "Recycling and use of Waste Materials and By-Products in Highway Construction – A Synthesis of Highway Practice." *Transportation Research Board – National Research Council.* no. 199 (1994): 3-7.

Cosentino, P.J., (1987). Pressuremeter Moduli for Airport Pavement Design. Doctoral Dissertation, Texas A&M University Department of Civil Engineering. College Station, Texas.

Das, Braja M. *Principles of Geotechnical Engineering.* Boston: PWS Publishing Company, 1994.

DeGroot, D., Shelbourne, W., & Switzenbaum, M., (1995, August). Use of Recycled Materials and Recycled Products in Highway Construction. University of Massachusetts Transportation Center. Amherst, Massachusetts.

Doig, B., A.

Dynatest Model 8000 Falling Weight Deflectometer Test System Specifications,. Dynatest International A/S (2000).

Florida Department of Transportation. *Standard Specifications for Road and Bridge Construction.* Tallahassee, FL.: 1999.

FHWA, *Participant's Notebook,* Techniques for Pavement Rehabilitation (1987). US Department of Transportation 95-142.

Fwa, T.F., Low, B.H., and Tan, S.A. "Compaction of Asphalt Mixtures for Laboratory Testing: Evaluation Based on Density Profile." *Journal of Testing and Evaluation.* Vol. 21, no. 5 (1993): 414-421.

Fwa, T.F., Low, B.H., and Tan, S.A. "Behavior Analysis of Asphalt Mixtures and the Relationship to their Performance." *ASTM STP* 1265 (1995): 97-110.

Garg, N., and Thompson, M.R. "Lincoln Avenue Reclaimed Asphalt Pavement Base Project." *Transportation Research Record.* no. 1547 (1996): 89-95.

Highter, W.H., Clary, J.A., and DeGroot, D.J. Structural Numbers for Reclaimed Asphalt Pavement Base and Subbase Course Mixes. Final Report. University of Massachusets Amherst, 1997. Amherst, MA.

Ho, R.H. Personal Communication: 2000.

Holmes, A.J. "Recycling vs. Reconstruction." *Highways and Transportation.* Vol. 38, no. 4 (1991): 17 – 21.

Holt, F.B. (2000), Vice President Business Development, Dynatest International A/S. (Personal Communication).

Holtz, R.D., and Kovacs, W.D. *An Introduction to Geotechnical Engineering.* Englewood Cliffs, New Jersey: Prentice Hall, 1981.

Huang, Yang H. *Pavement Analysis and Design.* Englewood Cliffs, New Jersey: Prentice Hall, 1993.

Jester, Robert N. *Progress of SUPERPAVE (Superior Performing Asphalt Pavement).* West Conshohocken, PA.: ASTM Publication, 1997.

Lambe, T.W., and Whitman, R.V. *Soil Mechanics.* New York, NY: John Wiley and Sons Inc, 1969.

MacGregor, J.A., Highter, W.H., and DeGroot, D.J. "Strutural Numbers for Reclaimed Asphalt Pavement Base and Subbase Course Mixes." *Transportation Research Record.* no. 1687 (1999): 22-28.

Maher, M.H., Gucunski, N, and Papp Jr., W.J. "Recycled Asphalt Pavement as a Base and Sub-base Material." *Testing Soil Mixed with Waste or Recycled Materials.* ASTM STP 1275 (1997): 42-53.

Mauer, M.C. & deBeer, M. (1988). Computer Programs to Plot DCP Data – Users Manual. Division of Roads and Transport Technology, Pretoria, South Africa.

McCaulley, D.B., Mittelacher, M., Mross, J.L., Roebuck, J.P., and Winemberg, R. *Florida Aggregates in Construction - Their Characteristics and Performance. Technical Report 90-01* . Florida: Florida Concrete and Products Association and the Concrete Materials Engineering Council, 1990.

Michalak, Chester H., & Scullion, Tom (1995). Modulus 5.0: User's Manual, Texas DOT, Research Report 1987-1.

Montemayor, Tomas. Compaction and Strength- Deformation Characteristics of Reclaimed Asphalt Pavement. M.S. Thesis in Civil Engineering. Florida Institute of Technology, 1998. Melbourne, FL.

Marek, C.R. (1991) Basic Properties of Aggregate. In R.D. Barksdale (Ed.), *The Aggregate Handbook.* Washington, D.C.: National Stone Association.

Munzenmaier, A.M. "City Saves by Using Recycled Asphalt Pavement as a Base." *Public Works.* (1994): 62-63.

National Asphalt Pavement Association (1996). *Recycling Hot Mix Asphalt Pavements.* (Information Series 123). Lanham, MD

National Center for Asphalt Technology, Auburn University, and U.S. Department of Transportation, Federal Highway Administration. *Pavement Recycling Guidelines for State and Local Governments - Participants Reference Book.* Auburn, AL.: 1998.

Palise, Frank. "Performance Evaluation of Reclaimed Asphalt Pavement (RAP) as a Dense Graded Aggregate Base Course (DGABC)." *Laboratory Investigation 92-2 (file #59-R-332) – Civil and Environmental Engineering at Rutgers University.* (1994).

Papp, W.J. Jr., Maher, M.H., Bennert, T.A., and Gucunski, N. "Behavior of Construction and Demolition Debris in Base and Subbase Applications." *Recycled Materials in Geotechnical Applications.* Vol. 79 (1998): 122-136.

Parker, Frazier, Mammons, Mike & Hall, Jim (1998). Development of Automated Dynamic Cone Penetrometer for Evaluating Soils and Pavement Materials. (Available from {Highway Research Center, Harbert Engineering Center, Auburn University, Alabama}).

Ping, W.V., & Yu, Z. (1994). *Evaluation of Laboratory Limerock Bearing Ratio Test on Pavement Soils in Florida*, Journal of American Society of Civil Engineers. 223-230.

Porter, O.J. (1949). *Development of the Original Method for Highway Design*, Journal of American Society of Civil Engineers. No. 2406. 461-467.

Prokopy, Steven. "Recycle & Reclaim." *Rock Products*. Vol. 98 (1995): 44-56.

Roads and Bridges. "State of the Practice for Use of RAP in Hot-Mix Asphalt." *Roads and Bridges.* Vol. 37, no. 1 (1999): 48-54.

Robertson, P.K., & Campanella, R.G., (1983). *Interpretation of Cone Penetration Tests. Part I: Sand*, Canadian Geotechnical Journal. Vol 20, 718-733.

Rodriguez, D., C.,

Sayed, S.M., Pulsifier, J.M., and Schmitt, R.C. "Construction and Performance of Shoulders Using UNRAP Base." *Journal of Materials in Civil Engineering.* Vol 5, no. 3 (1993): 321-338.

Scherocman, J.A. Pavement Recycling. Stabilization and Pavement Recycling (pp. 23-27). Washington, DC: American Road and Transportation Builders Association.

Schmertman, J.H. (1970). *Static Cone to Compute Settlement Over Sand*, Journal of Soil Mechanics and Foundation Division, ASCE. Vol 96, No SM3, 1011-1043.

Schmertman, J.H. & Hartman, J.P., (1978). *Improved Strain Influence Factor Diagrams*, Journal of Geotechnical Engineering Division, ASCE. Vol 104, No. GT8, 1131-1135.

Schmidt, W., Hoenstine, R.W., Knapp, M.S., Lane, E., Ogden, G.M., and Scott, T.M. *The Limestone, Dolomite and Coquina Resources of Florida*. Florida: State of Florida Department of Natural Resources, 1979.

Smith, L.L. "Wasting No Time. – Florida's History of Succesful Recycling for Transportation." *TR News.* no. 184 (1996): 4-7.

Taha, Ramzi., Ali, Galal., Basma, Adnan., and Al-Turk, Omar. "Evaluation of Reclaimed Asphalt Pavement in Aggregate Road Bases and Subbases." *Transportation Research Record.* no. 1652 (1999): 264-269.

Tan, S.A., Low, B.H., and Fwa, T.F. "Behavior of Asphalt Concrete Mixtures in Triaxial Compression." *Journal of Testing and Evaluation.* Vol. 22, no. 3 (1994): 195-203.

Warren, J., (1998, Winter). *Using RAP in Superpave - Florida's Experience*, Hot Mix Asphalt Technology (HMAT), Vol 3, No 4. 17-19.